COLOR ATLAS OF

Infectious Disease

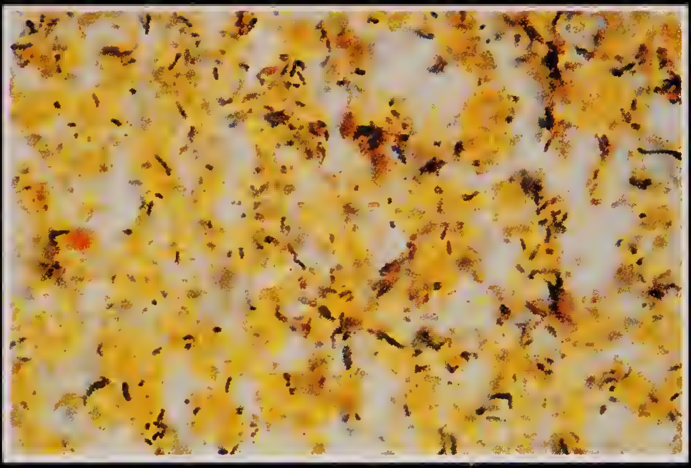

VOLUME 3 OF 3

RC
111
.C56
1995
v. 3

Barcode: 779

Color Atlas of Infectious Disease

Volume 3 of 3

Romelle Belmonte, MD
Joseph Bikowski, MD
Dennis A. Clements, MD, PhD
Christine Finck, MD
John L. Guarisco, MD
Boris Gueft, MD
J. Steven Hata, MD
Jason Lazar, MD
Prashant K. Rohatgi, MD
Lawrence Stack, MD
Bruce H. Thiers, MD
Michael P. Vrabec, MD, FACS

Property Of
Hickey College
Library- Vet Tech
Institute

Clinical Communications Inc.
Greenwich, CT

FEB - '08

Acknowledgement

Grateful acknowledgement is made to the following for their generosity in providing illustrations for this series: F. Battastini, E.N. Beckman, F. Beltran, F. Ciferri, L.W. Dewhirst, F. Etges, L. Garcia, C. Hockman, R.B. Holliman, L.A. Jensen, M. King, R.E. Kuntz, T.J. Lau, M. Louderbeck, L. Milliman, W.L. Moore, H. Nagata, R.D. Pearson, R. Reinecke, W. Rogers, and H. Zaiman.

© 1995 Clinical Communications Inc.

All rights reserved. No part of this book may be reproduced or transmitted in any form or by any means, electronic or mechanical, including photocopying, recording, or by any information storage and retrieval system, without permission in writing from the publisher.

Clinical Communications Inc.
Greenwich Office Park #6
Greenwich, CT 06830

ISBN: 1-57013-041-8

Printed in Hong Kong

Introduction

Infection continues to present a diagnostic challenge in clinical medicine, despite increased understanding of the cellular basis of infectious processes. Newer imaging techniques (eg, computed tomography, magnetic resonance imaging) have proved invaluable in diagnosing various infections, although older methods (eg, cultures, radiography) continue to be important diagnostic tools. Infectious diseases are suited to visual presentation, and an atlas can be a valuable educational resource.

This book, which is the last of the three volumes in this series, is intended to assist the clinician rather than the microbiologist. Thus it takes an anatomical approach based on major organs or groups of organs. For the most part, only those infections that the clinician is likely to see in practice are illustrated; however, a few unusual or exotic infections are shown. Whenever possible, several different images are used to illustrate the different manifestations of an infection. The captions are focused on the images and their interpretation rather than on the etiology and management of the particular disease.

Volume 3 of this atlas is divided into four parts: cardiovascular, lower respiratory tract, skin/soft tissue, and bone/joint. It is hoped that this book will be useful to the practitioner of clinical medicine.

Digitized by the Internet Archive
in 2018 with funding from
Kahle/Austin Foundation

https://archive.org/details/coloratlasofinfe0000unse

Cardiovascular

Aorta

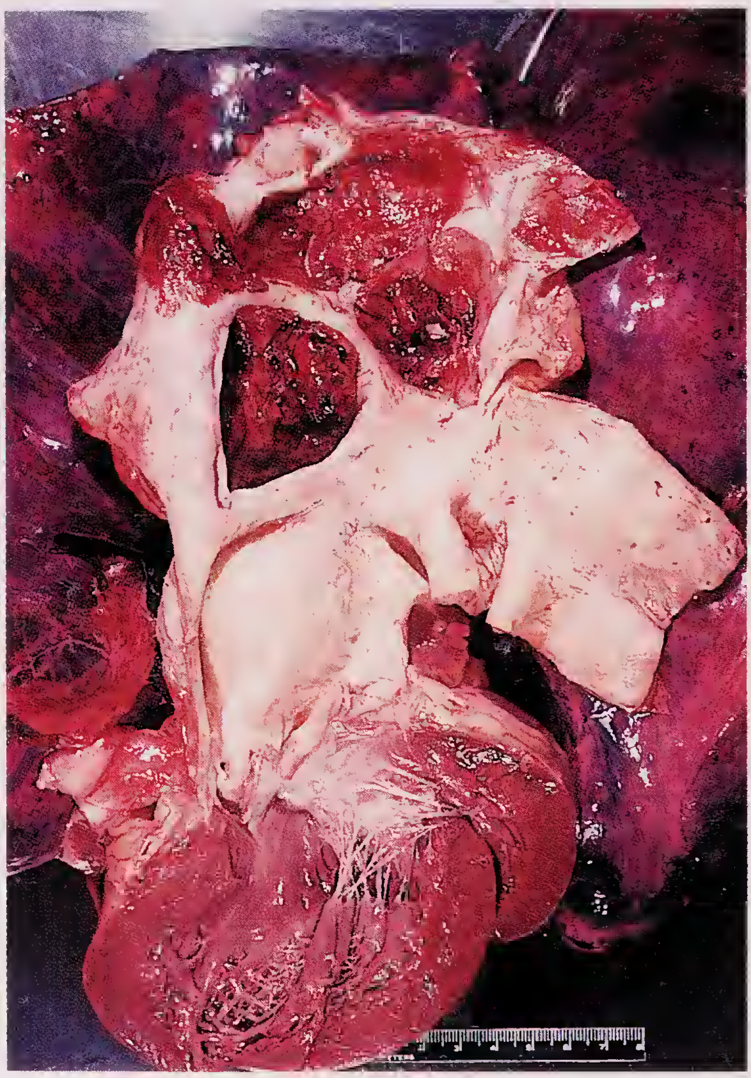

1

1 ♦ Luetic aneurysm (syphilitic) in a middle-aged man.

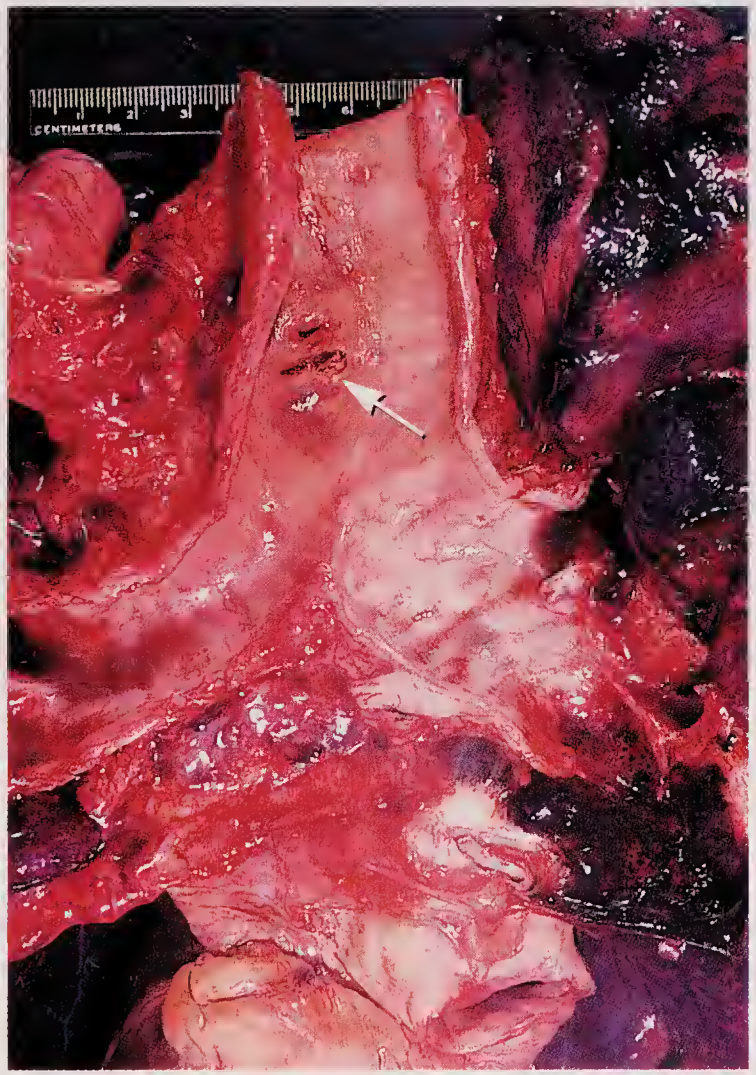

2

2 ♦ Luetic aneurysm in the patient in 1. The aneurysm has ruptured into the trachea (arrow at rupture site), causing spectacular fatal tracheal hemorrhage.

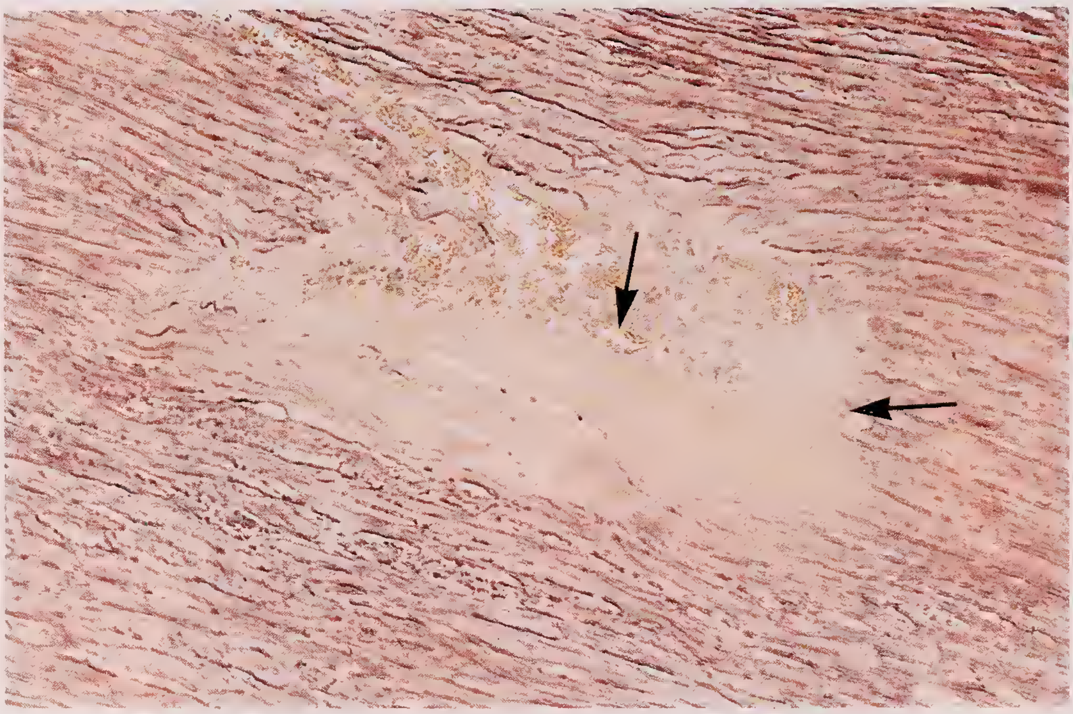

3

3 ◆ Luetic mesaortitis. The destruction (arrows) of elastic fibers is shown in the center of the photograph of the aorta, which is stained for elastic tissue.

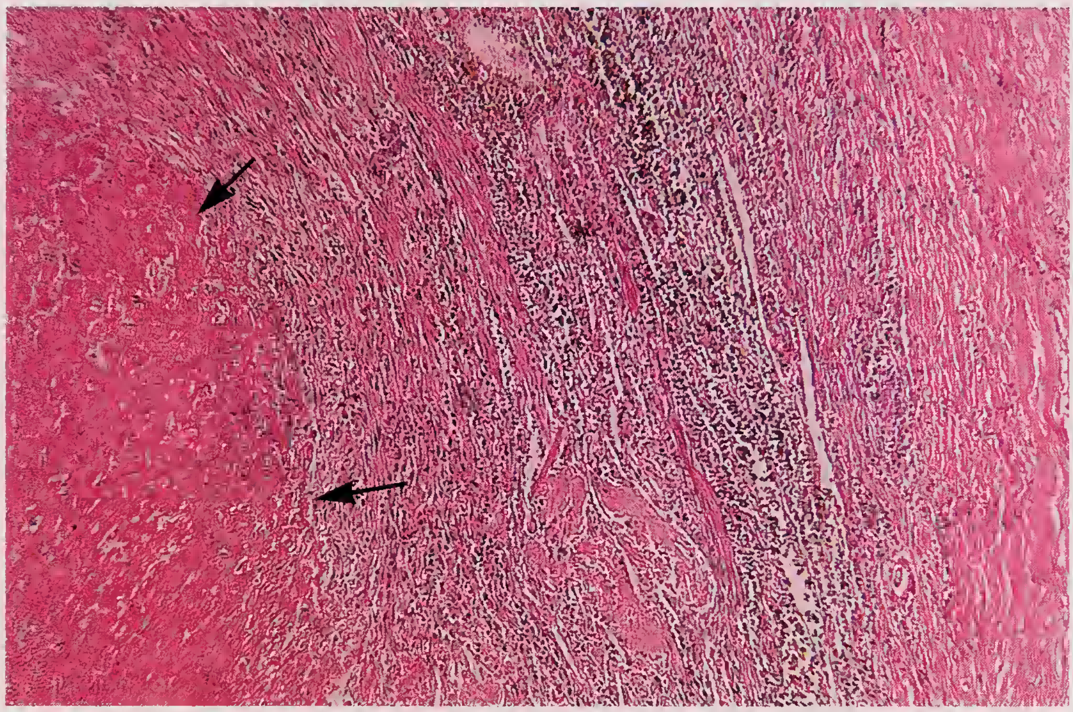

4

4 ◆ Chronic mesaortitis in syphilis with chronic inflammation. A large fibrin thrombus (arrows) is also present.

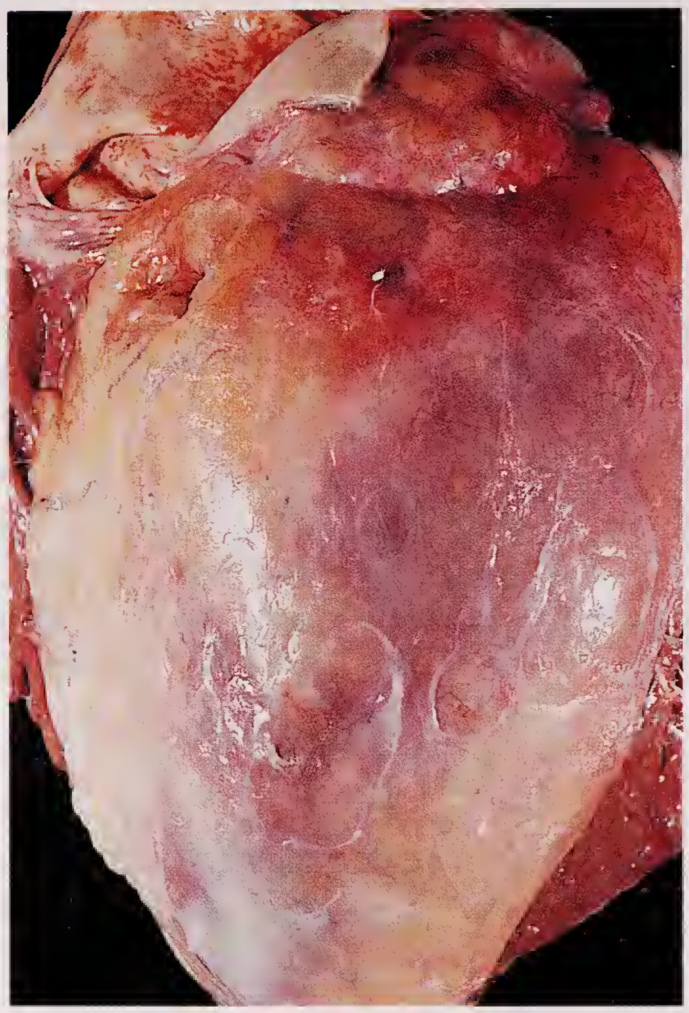

5

5♦ Acute pneumococcal pericarditis found at autopsy in a woman who died with a severe pneumococcal lobar pneumonia shortly after being admitted to the hospital. Delicate, gray deposits of fibrin are apparent on the pericardium; they are easily removed with forceps.

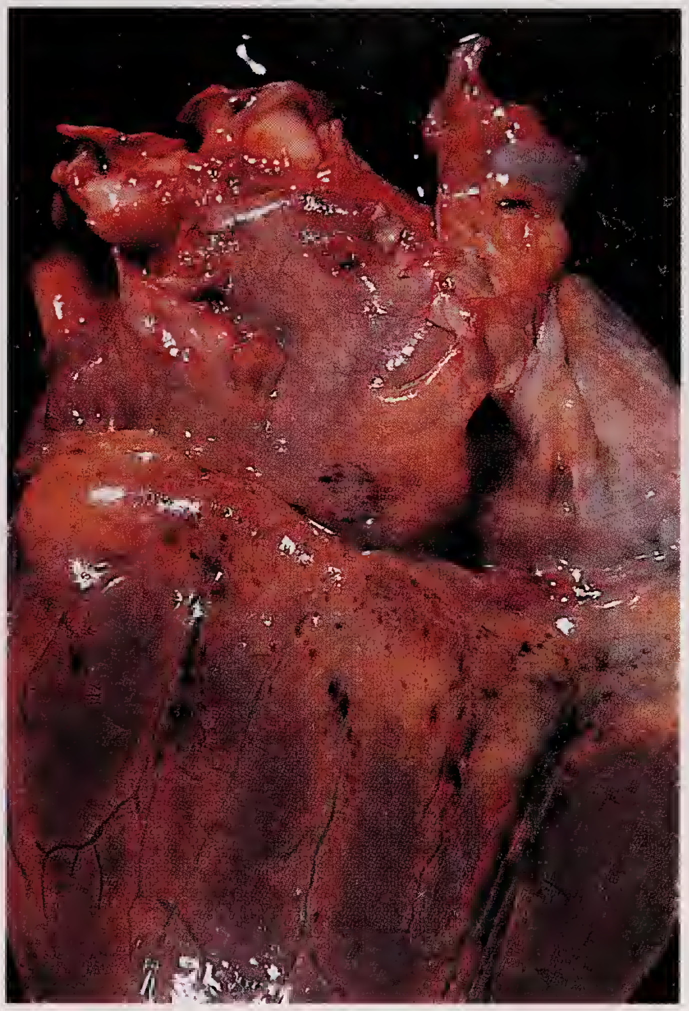

6

6 ♦ *Staphylococcus aureus* sepsis arising from suppurative pyelonephritis in an elderly man. Petechiae are seen on the pericardium.

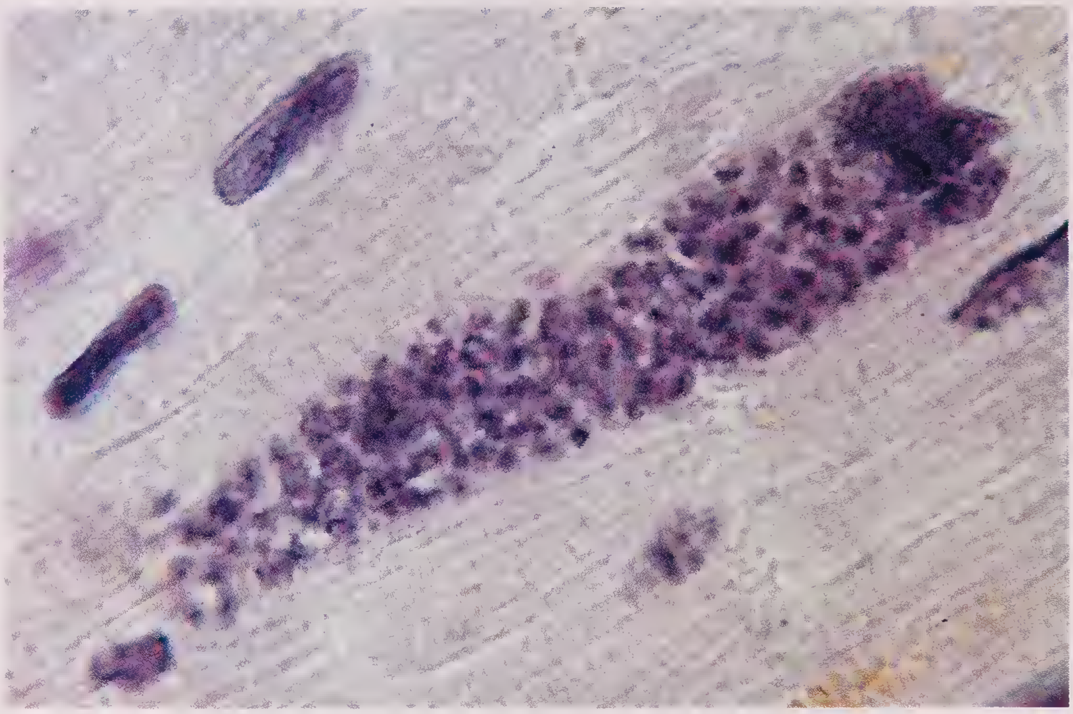

7

7 ♦ Myocardium of a middle-aged man with severe Hodgkin's lymphoma. Toxoplasmosis is common and serious in any immunodeficiency syndrome. The trophozoites invade cells and destroy them. Each tiny organism contains bluish nuclear material and a pink kinetoplast.

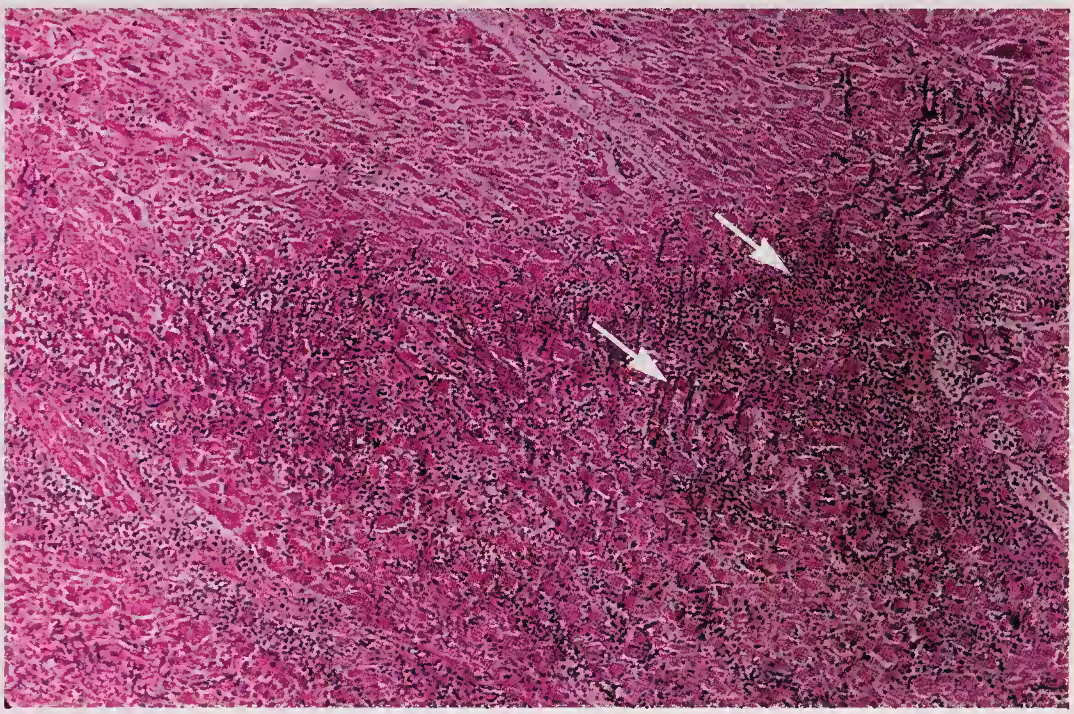

8

8 ♦ Chronic myelocytic leukemia with fungal infection in a section of myocardium from an elderly man. Severe, acute inflammation and necrosis of the heart muscle are present. The hyphae of *Aspergillus* (arrows) stream from the periphery of the lesion.

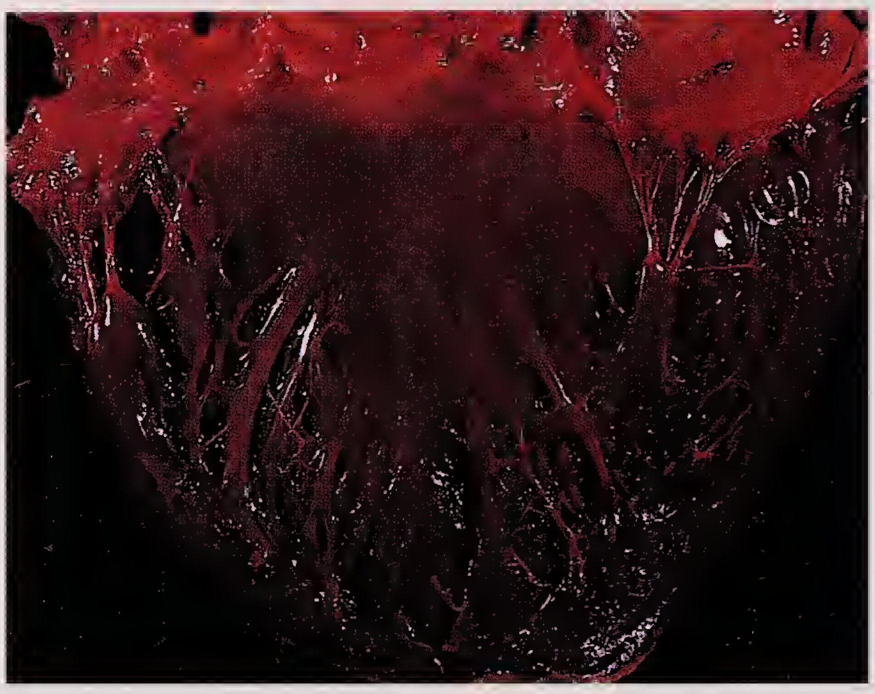

9

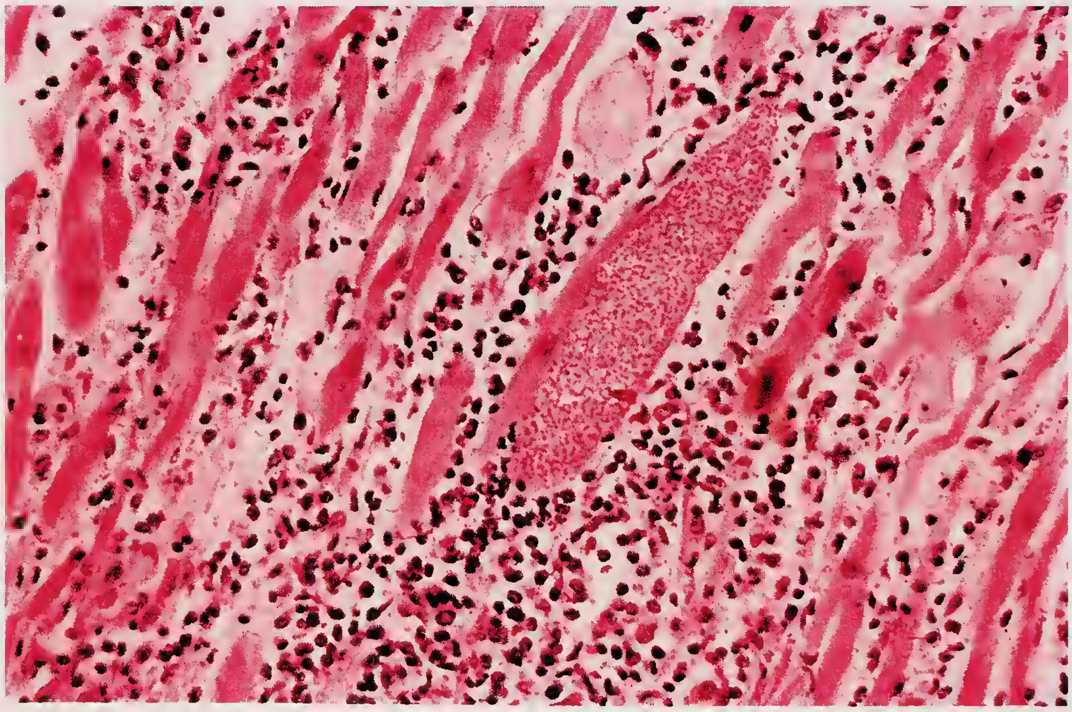

10

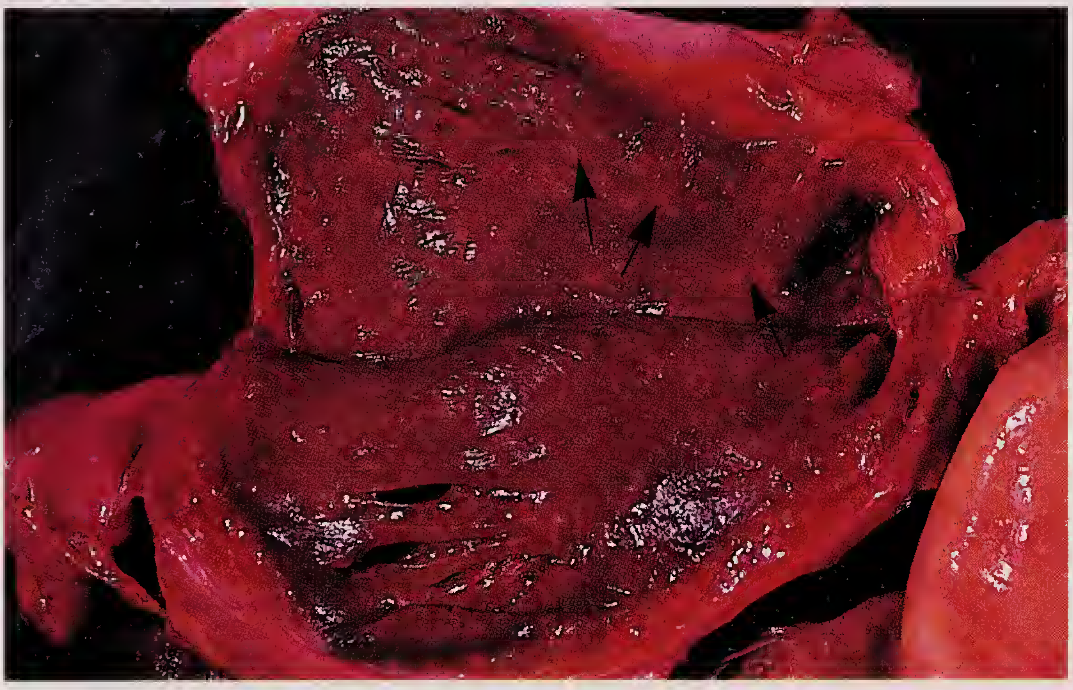

11

9 ♦ Acute myocarditis, which was diagnosed at autopsy in a man who had died shortly after being admitted for pneumococcal pneumonia. It was noted that the opened heart was remarkably soft; when placed on the photograph stand, the left ventricle lay flat, as if compressed. Severe foci of cardiac muscle degeneration with inflammation were noted microscopically.

10 ♦ Photomicrograph showing severe inflammation of the myocardium in Chagas' disease (also known as South American trypanosomiasis). The visceral lesions contain the intracellular parasite without flagella.

11 ♦ Acute myocarditis, which is the result of bacterial embolization from an advanced necrotic mass containing adenocarcinoma and Gram-negative bacilli. The myocardium is studded with small, dull, yellow spots, which are early abscesses containing bacterial colonies (arrows).

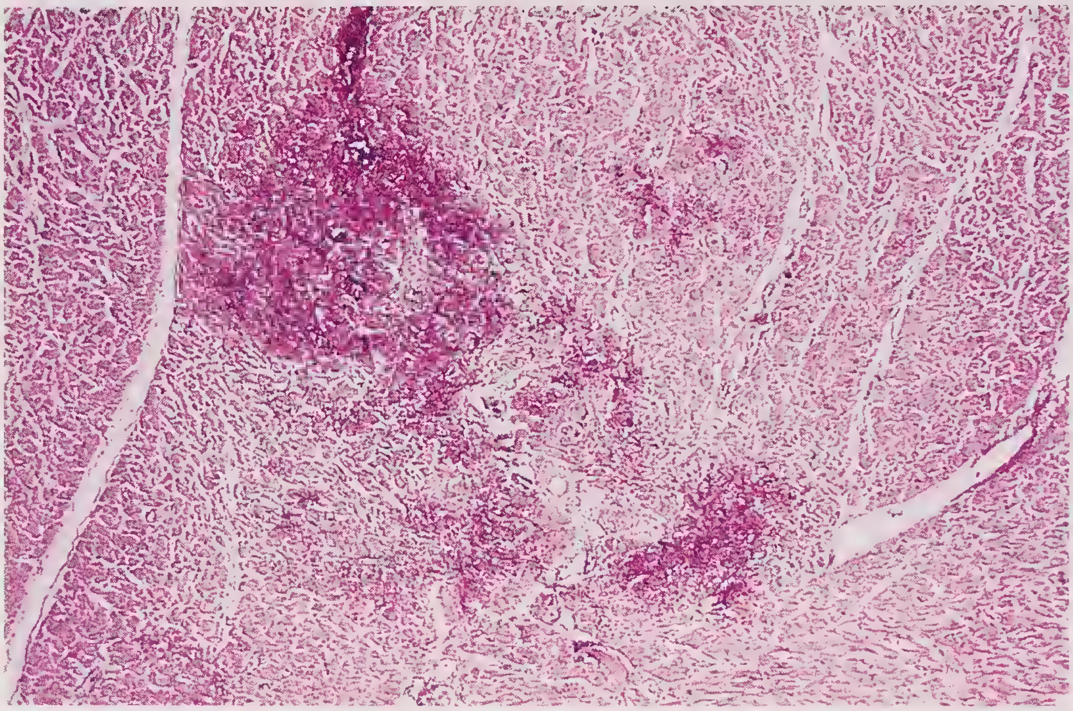

12

12 ♦ Coxsackievirus infection in an infant, which was proved by virus isolation before death. The calcification results from severe myocarditis with necrosis.

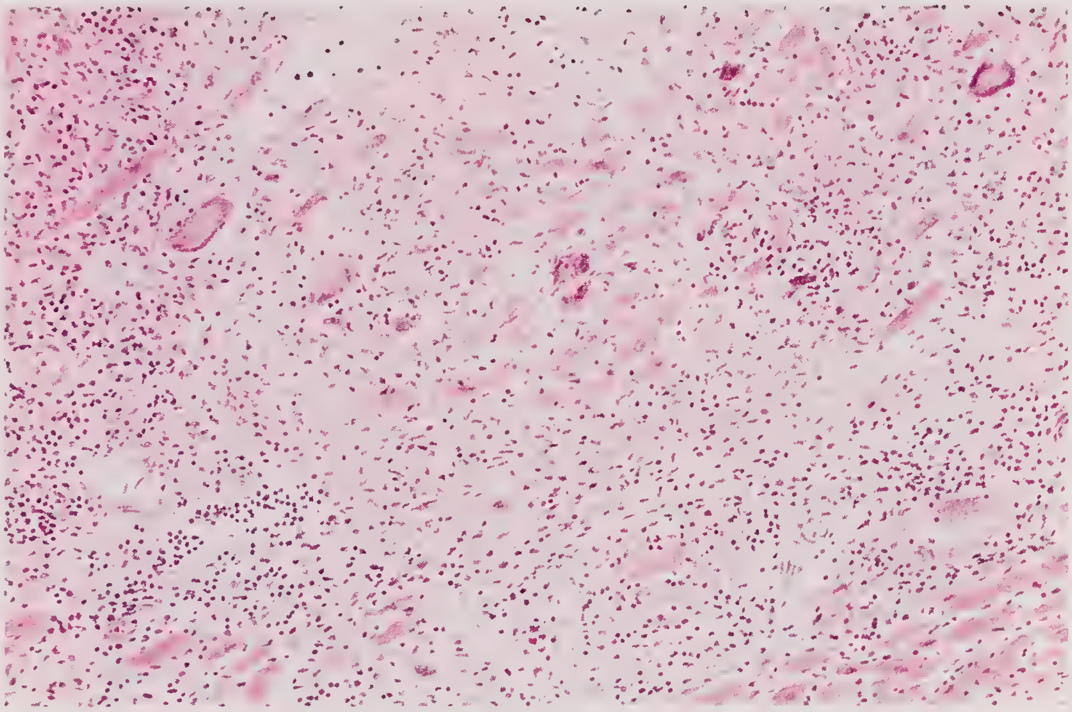

13

13 ◆ Gummatous inflammation of myocardium in syphilis, with necrosis, severe chronic inflammation, and some giant cells. Degenerating myocardial fibers are present in the background.

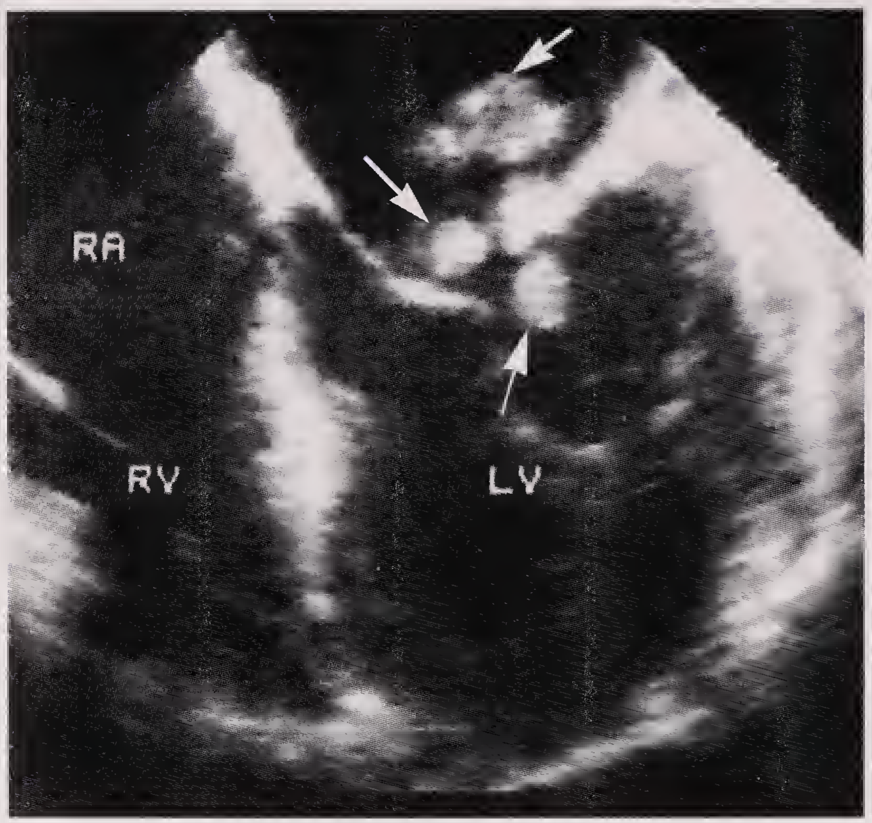

14

14 ♦ Transesophageal echocardiogram after pacemaker replacement in a patient who subsequently developed fever, chills, and night sweats. Multiple, large, rounded echodensities (arrows) diagnostic of mitral valve endocarditis are present.

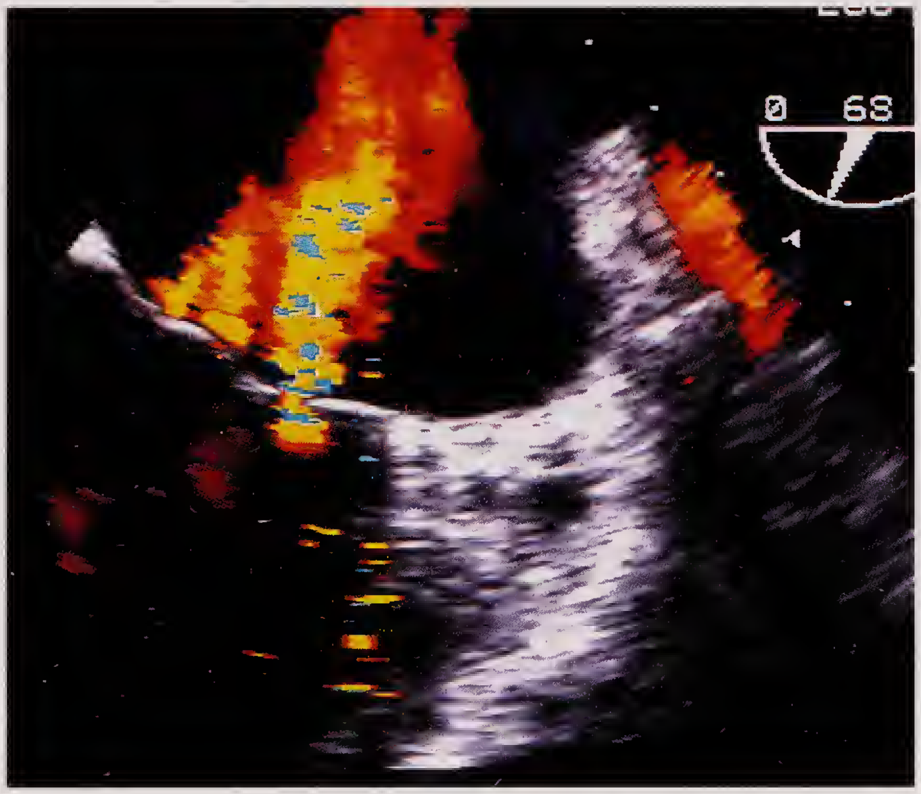

15

15 ♦ Transesophageal echocardiogram of a patient with mitral valve endocarditis, resulting in severe mitral regurgitation. The scan shows a yellow and red jet of blood flow from the left ventricle into the left atrium during systole. A red jet of flow reversal from the left atrium to the left upper pulmonary vein is also present.

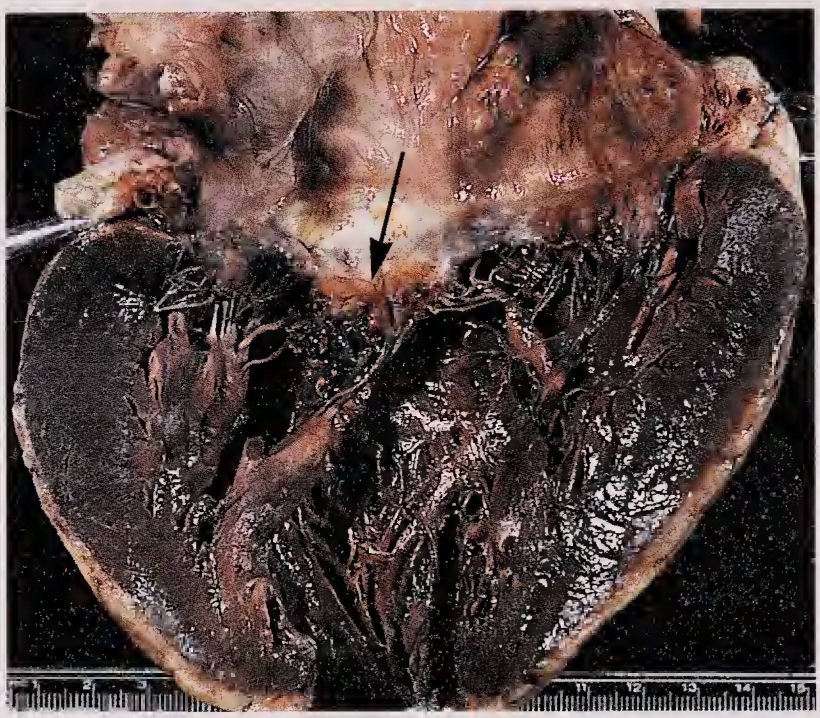

16

16 ◆ Subacute bacterial endocarditis of the mitral valve as a result of extensive dental work with tooth extraction and reparative gum surgery. Postmortem culture showed penicillin-sensitive *Streptococcus viridans*. There were emboli to the kidneys, spleen, liver, brain, and heart. Nodular vegetation can be seen (arrow).

17 ◆ Section of inflamed mitral valve vegetation, showing severe, acute endocarditis.

18 ◆ Mitral valve in acute staphylococcal endocarditis, showing a bacterial colony and acute inflammation.

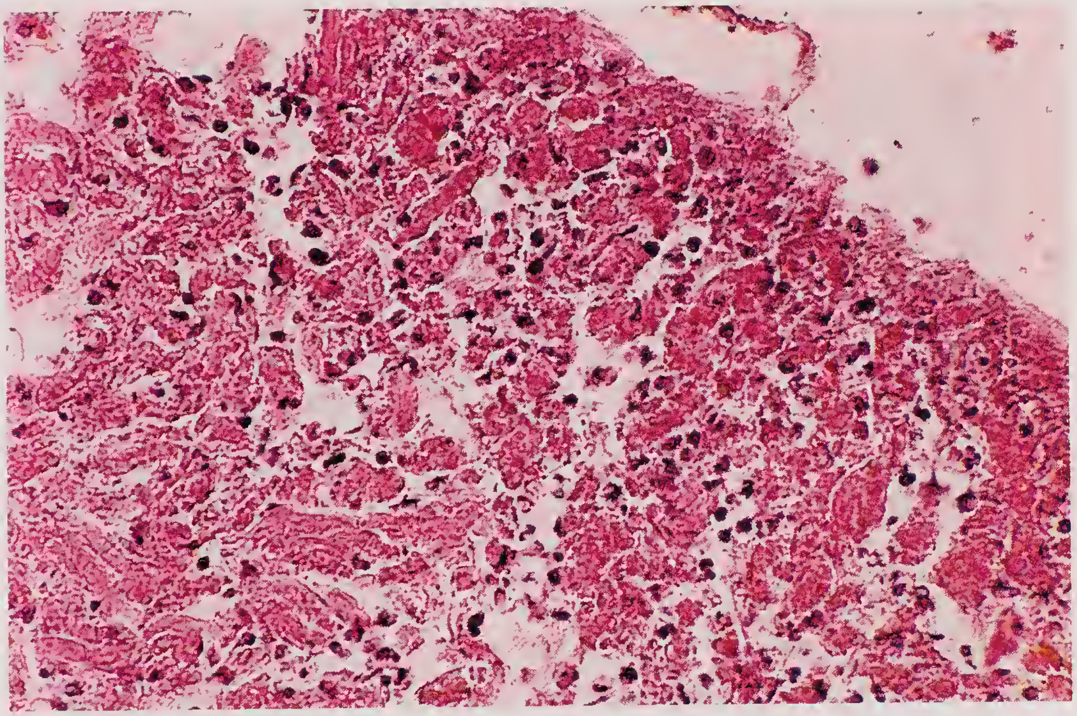

17

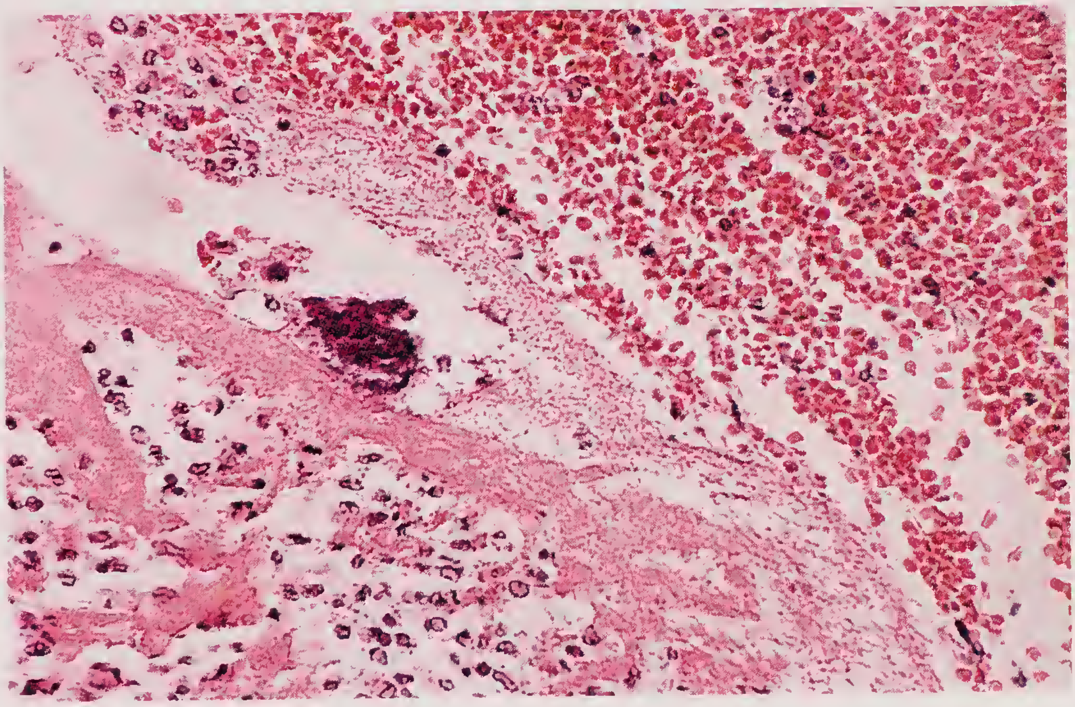

18

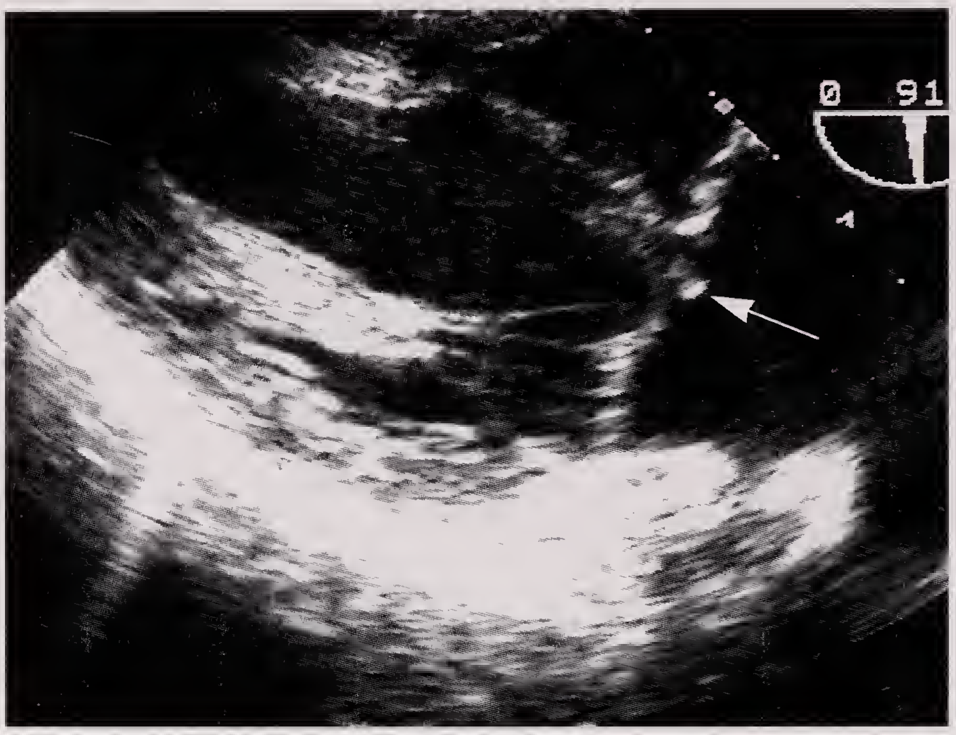

19

19 ♦ Transgastric long-axis views of the mitral valve, with the chordae tendineae inserting upon the ventricular aspect of the valve. On the right side of the photograph is a small echodensity (arrow), which is consistent with a vegetation of the anterior leaflet of the mitral valve.

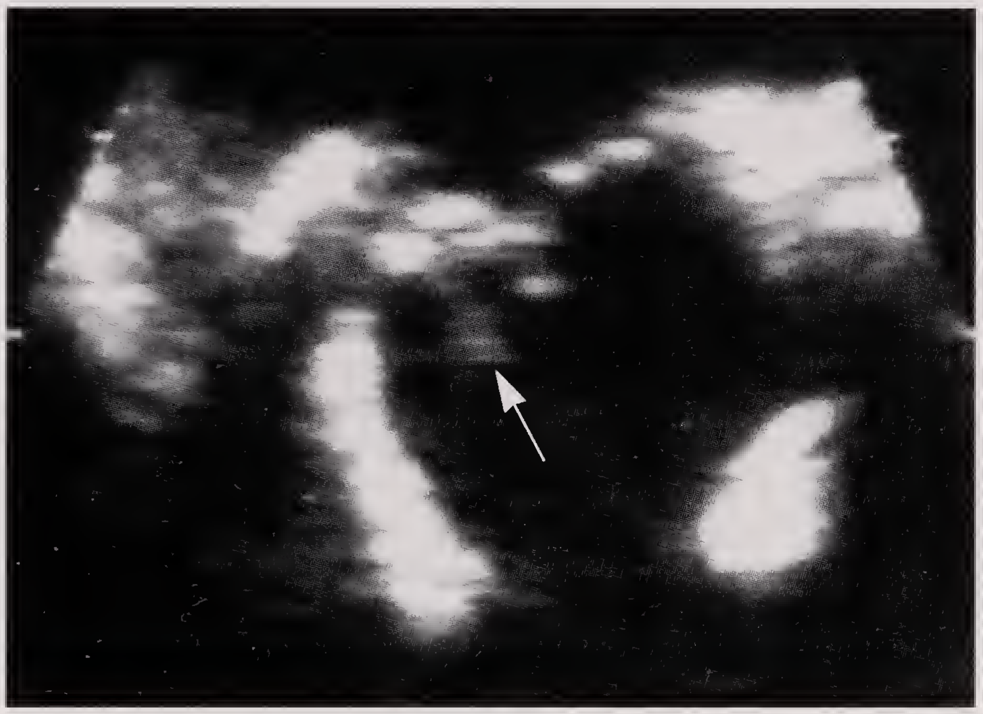

20

20 ♦ Transesophageal echocardiogram after a mitral valve replacement for suspected endocarditis, which revealed a vegetation on the ventricular aspect of the anterior leaflet of the prosthetic valve (arrow).

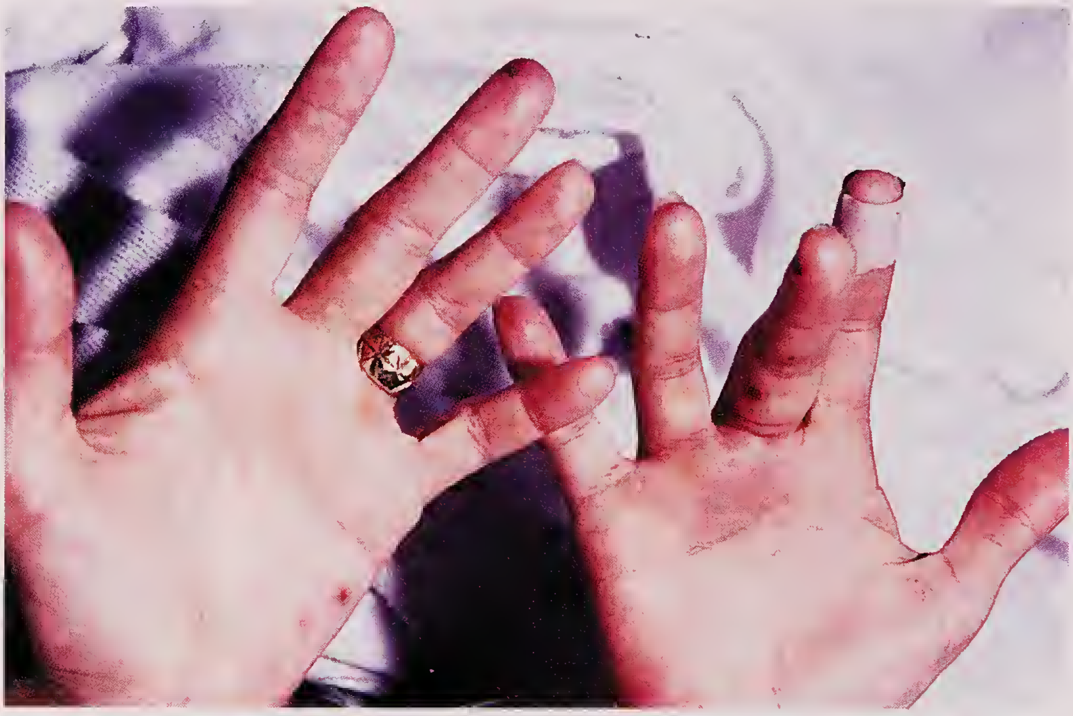

21

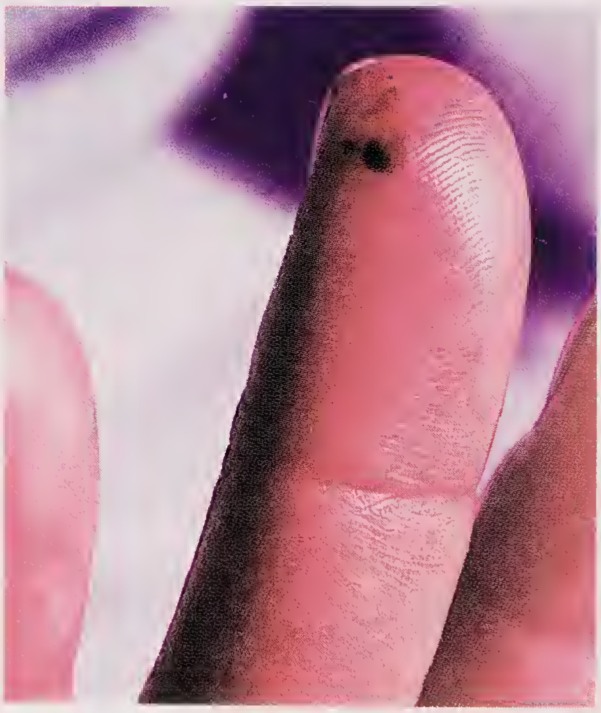

22

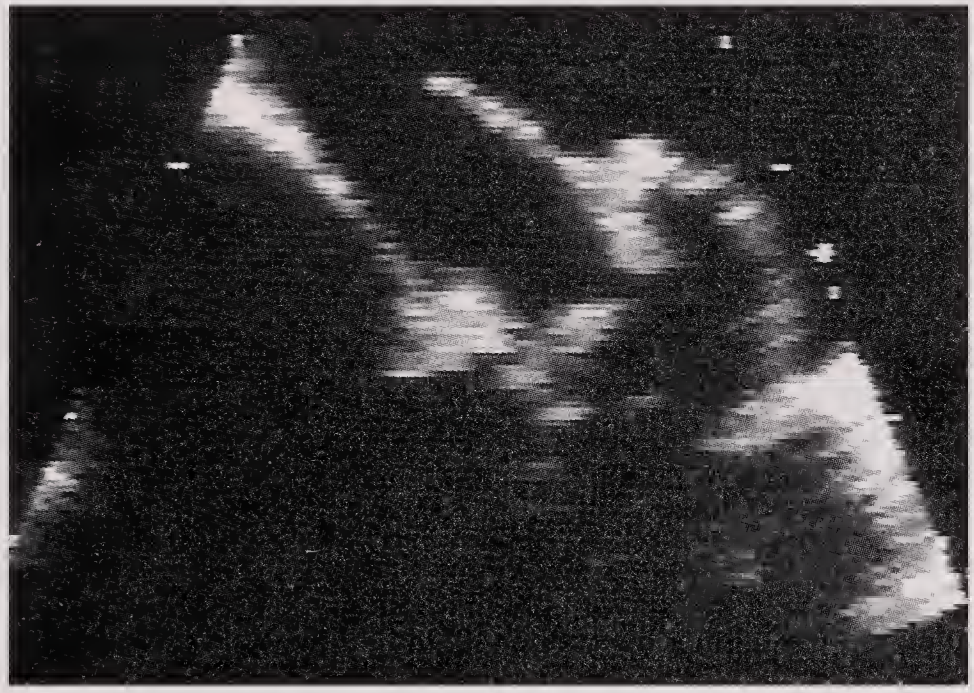

23

21-22 ♦ Janeway lesions on the hands and fingertip of a patient with mitral valve endocarditis. The erythematous, macular lesions on the fingertips are painless and nontender. The presence of these lesions is considered a hallmark of bacterial endocarditis.

23 ♦ Echocardiogram of a patient with a history of mitral valve prolapse who presents with a 2-month history of shortness of breath. Blood cultures are positive. The posterior leaflet of the mitral valve is flail and is displaced into the left atrium during systole due to disruption of the chordae tendineae.

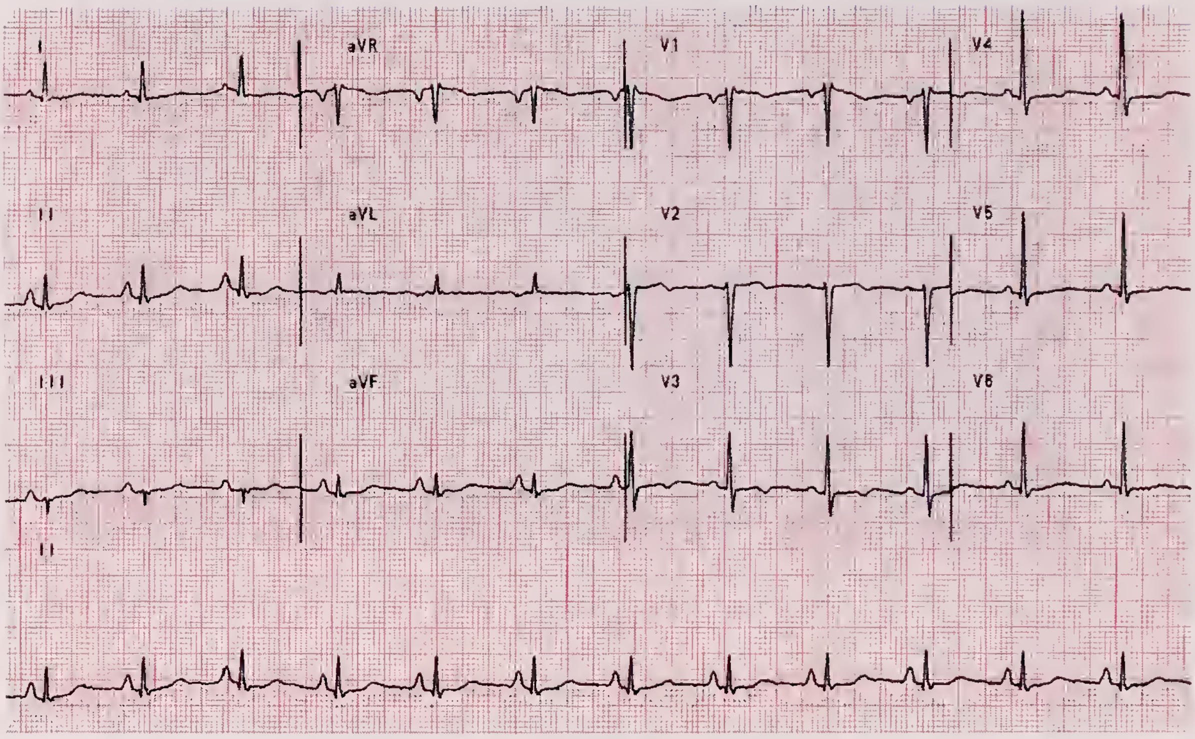
I
aVR
V1
V4
II
aVL
V2
V5
III
aVF
V3
V6
II

24

24 ♦ Electrocardiogram (ECG) of a patient with tricuspid valve endocarditis due to *Staphylococcus epidermidis*, resulting in severe tricuspid regurgitation. The ECG shows sinus rhythm with right atrial enlargement and a right ventricular conduction delay.

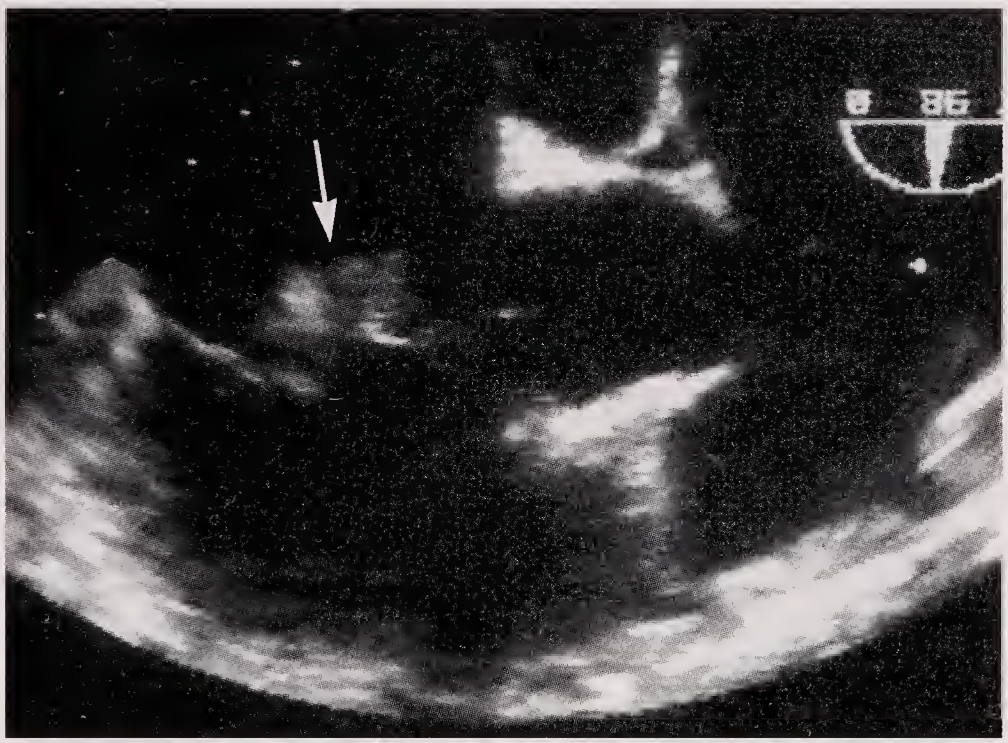

25

25 ♦ Transesophageal echocardiogram of an intravenous drug user, showing a large vegetation (arrow) on the tricuspid valve. *Staphylococcus aureus* was isolated on blood cultures.

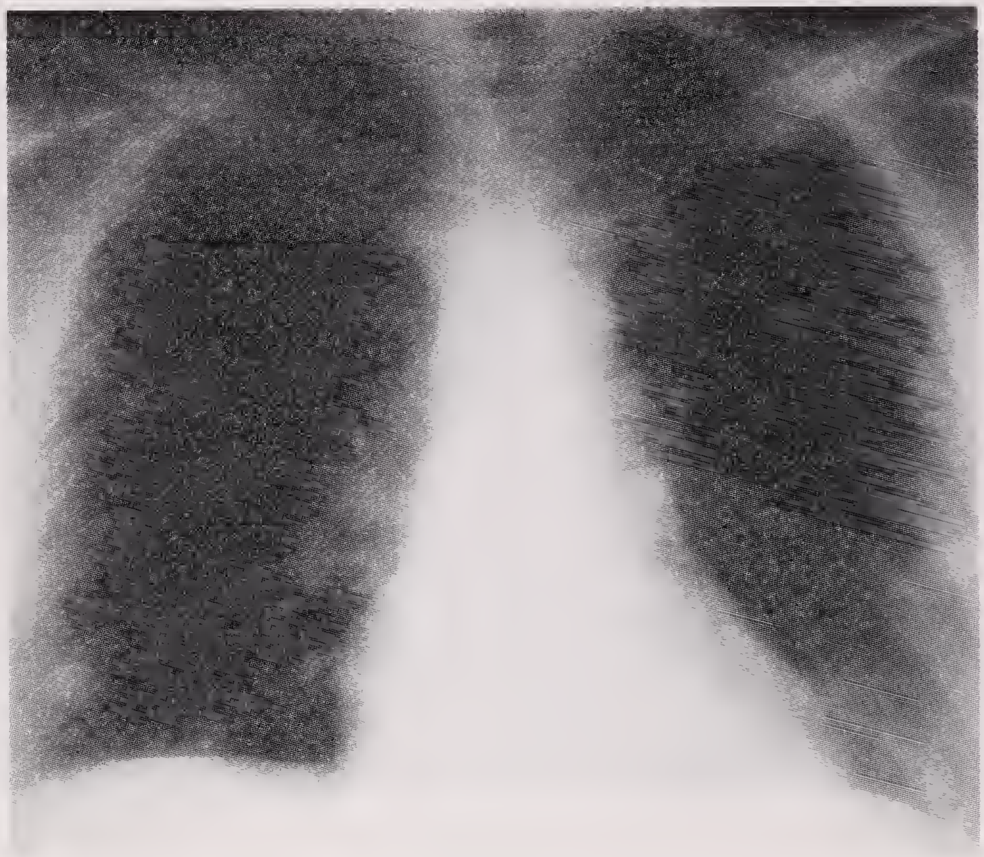

26

26 ◆ Chest radiograph of a patient with tricuspid valve endocarditis, resulting in septic emboli in the lungs. Multiple, rounded infiltrates are present bilaterally.

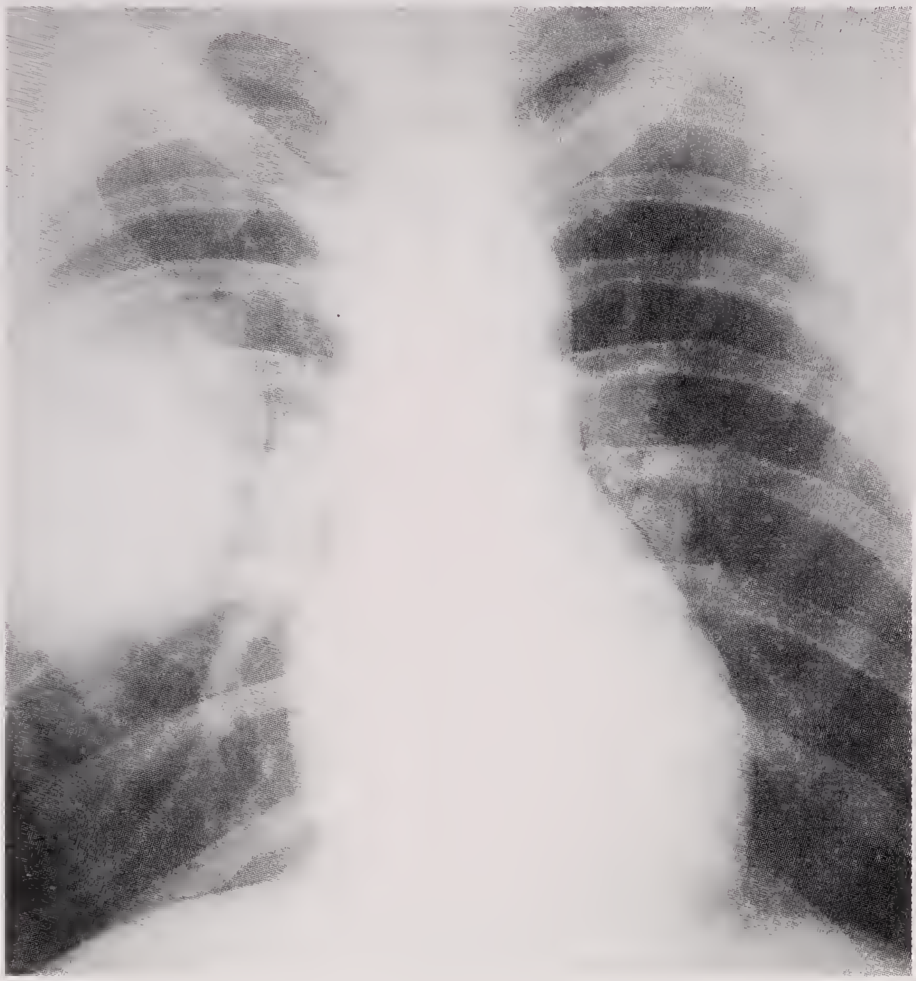

27

27 ♦ Chest radiograph of a patient with tricuspid valve endocarditis, which shows a very large infiltrate of the right upper lobe with an air-fluid level consistent with a pyogenic lung abscess.

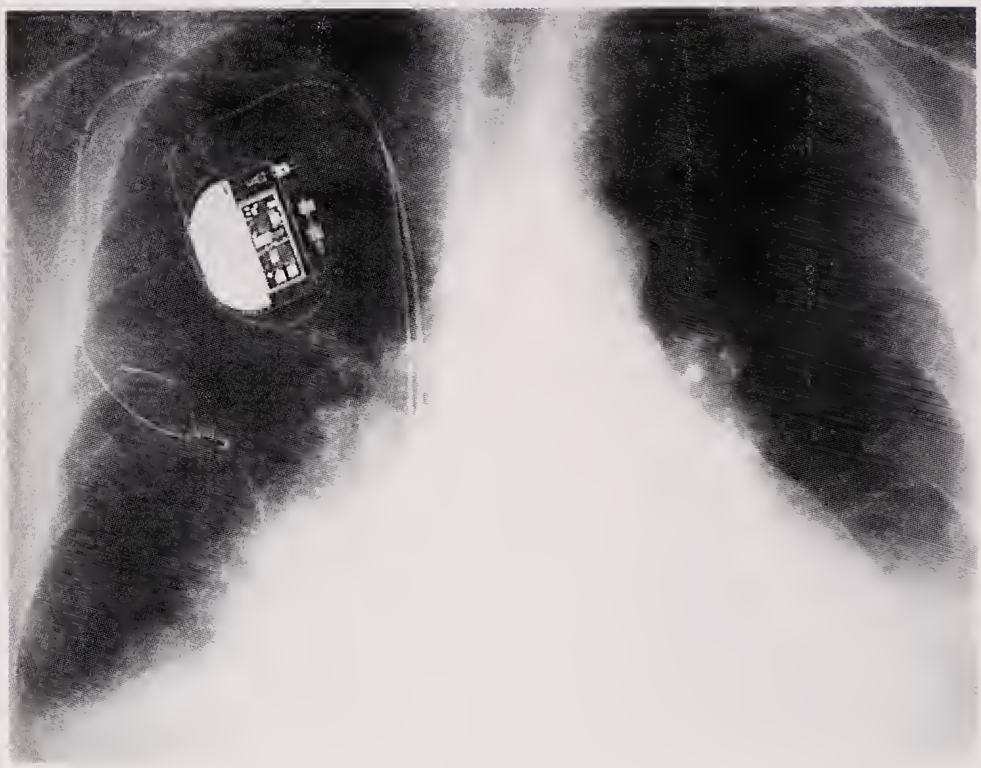

28

28 ♦ Chest radiograph of a patient with aortic valve endocarditis, leading to severe aortic insufficiency as a complication of a pacemaker infection. Cardiomegaly and diffuse pulmonary infiltrates consistent with pulmonary edema are present.

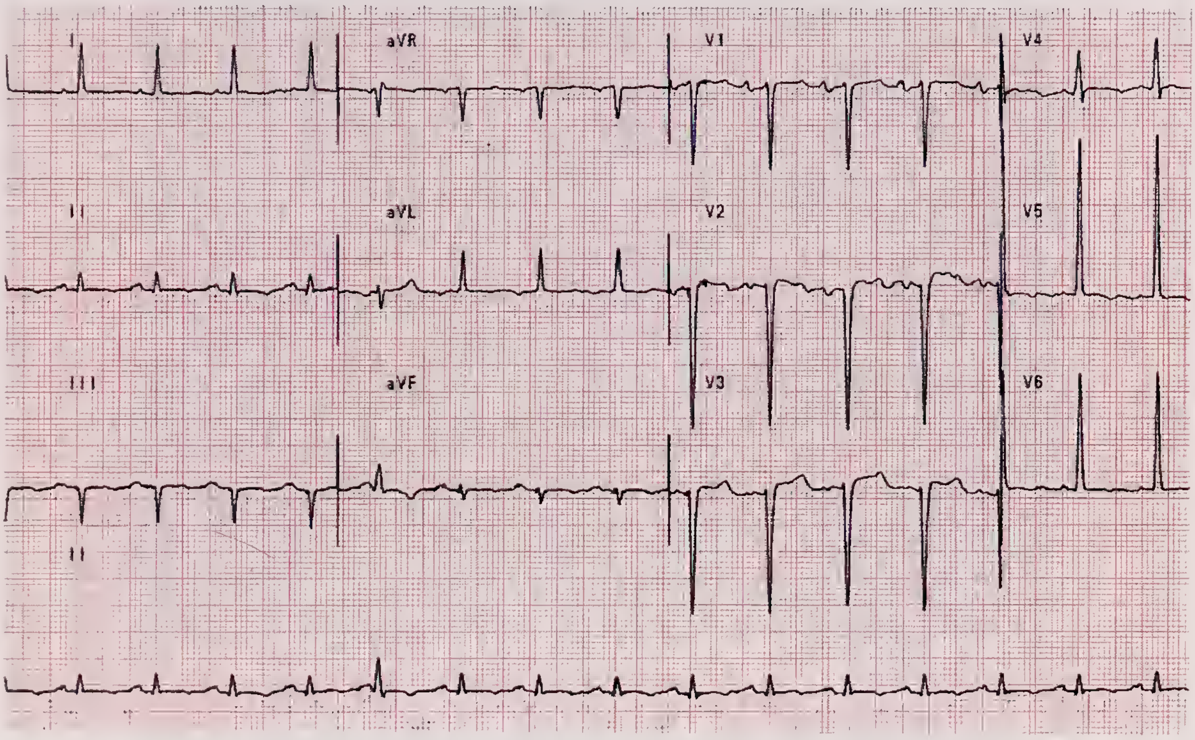
I
aVR
V1
V4
II
aVL
V2
V5
III
aVF
V3
V6
II

29

29 ◆ Electrocardiogram (ECG) of a patient with an aortic valve endocarditis, resulting in severe aortic insufficiency with a dilated left atrium and left ventricle. The ECG shows sinus tachycardia, left ventricular hypertrophy, and left atrial abnormality.

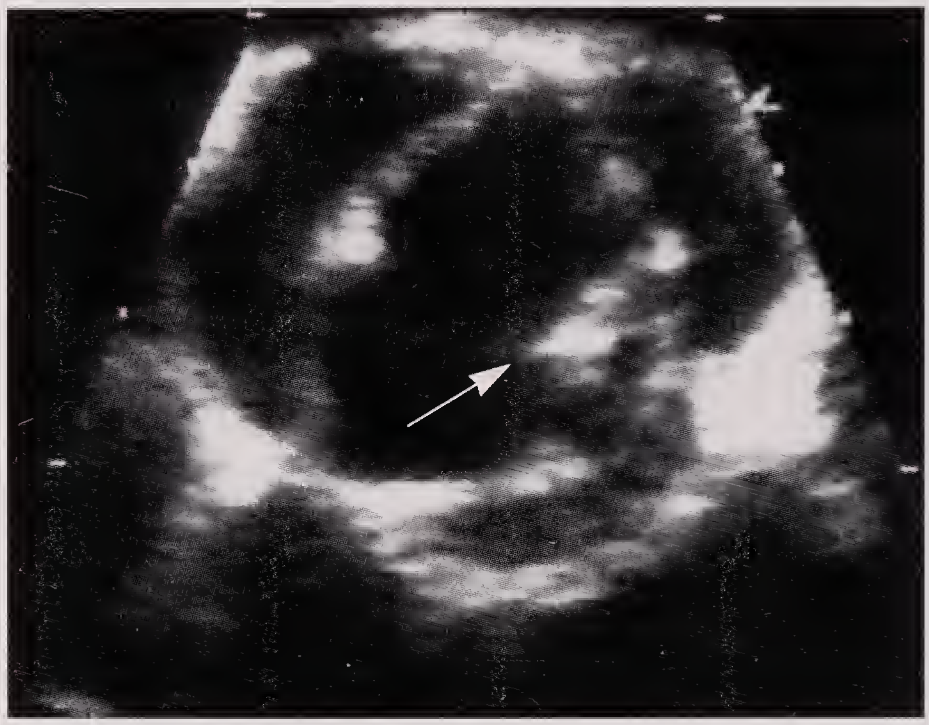

30

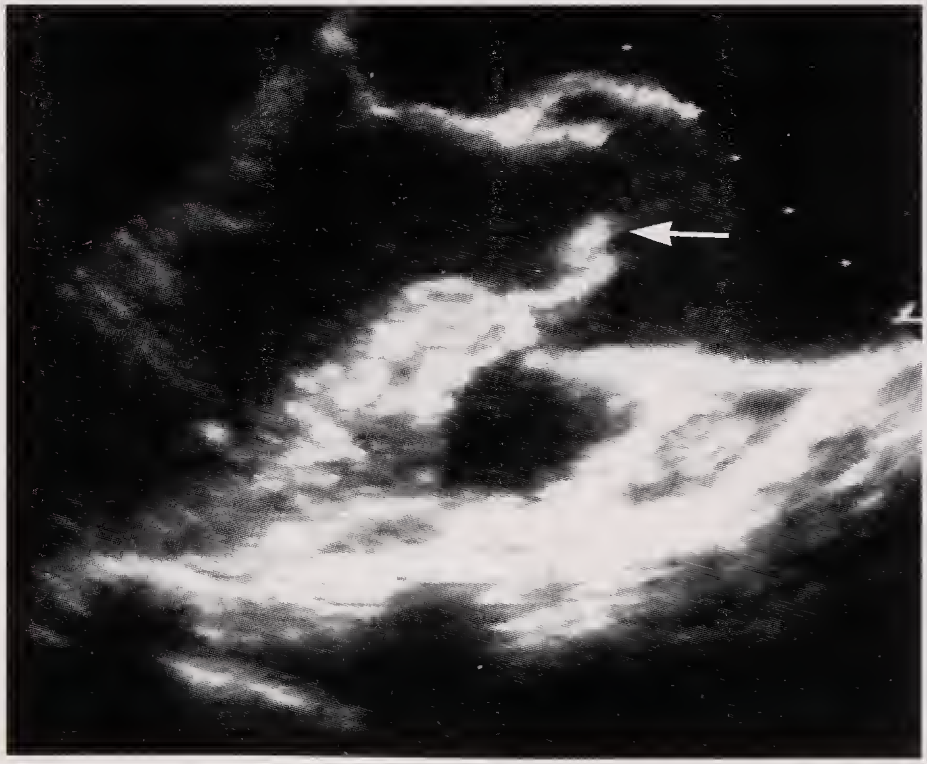

31

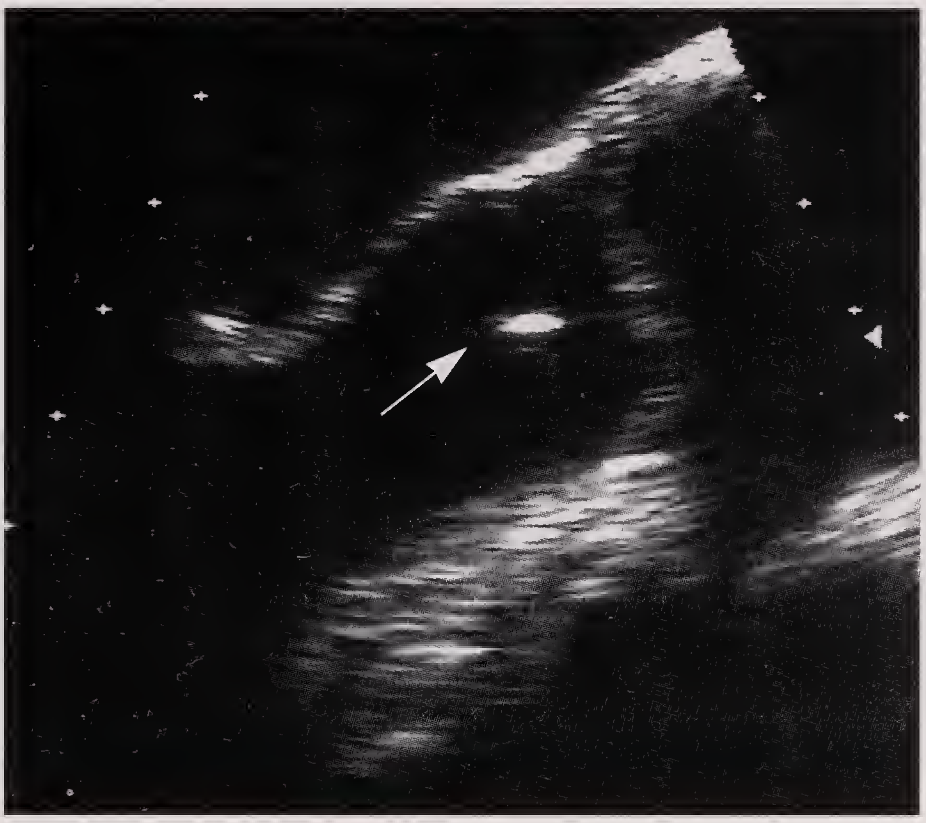

32

30-31 ♦ Transesophageal echocardiograms of a patient with *Streptococcus pneumoniae* endocarditis of a bicuspid aortic valve. 30 is a short-axis view of the two leaflets, and 31 is a long-axis view of the leaflets and vegetation. The arrows point to the vegetation.

32 ♦ Transesophageal echocardiogram in a patient with *Streptococcus viridans* bacteremia, which reveals a small vegetation (arrow) on the ventricular aspect of the aortic valve.

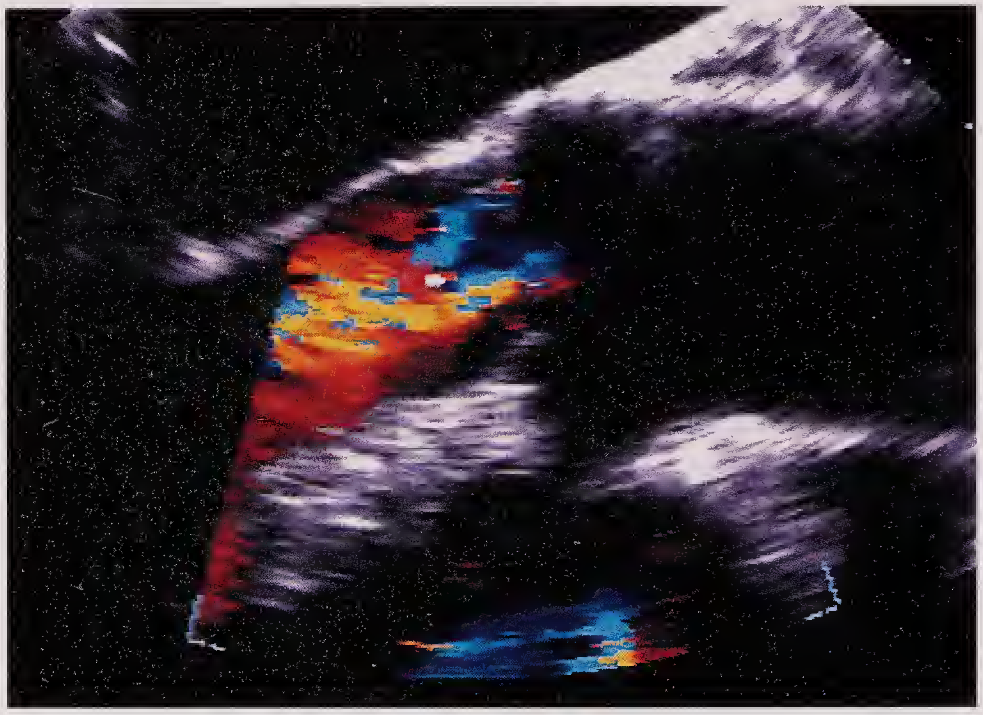

33

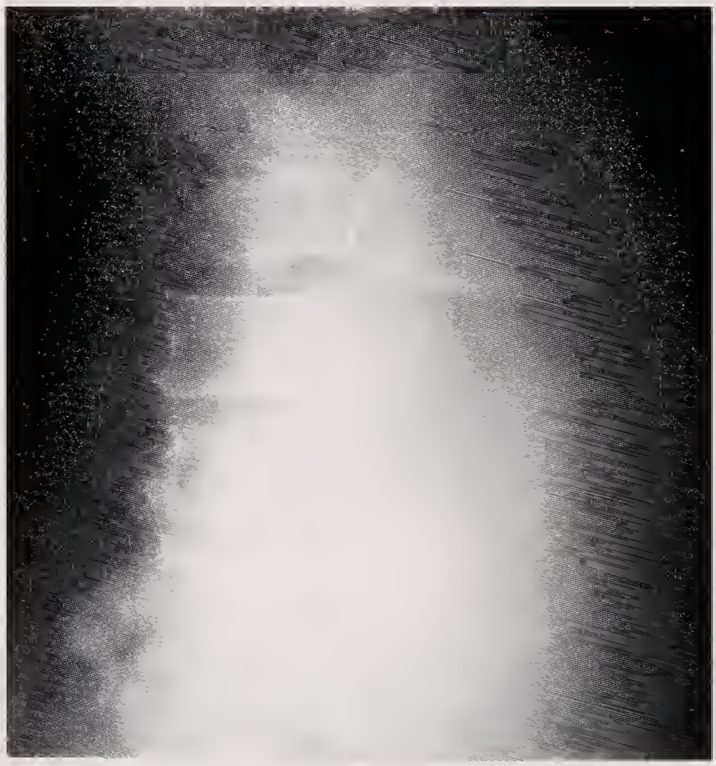

34

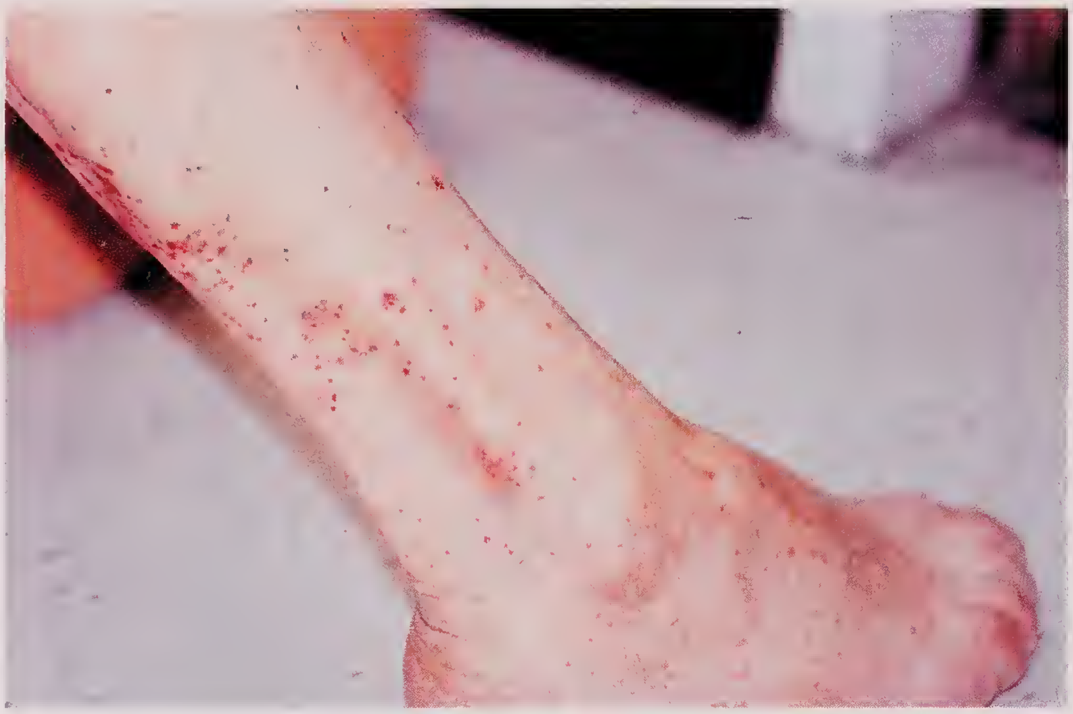

35

33 ♦ Transesophageal echocardiogram with color Doppler flow of the patient in 32, showing a jet of aortic insufficiency (yellow).

34 ♦ Abdominal radiograph of a patient with aortic valve endocarditis due to *Staphylococcus aureus*. Over one half of individuals with left-sided endocarditis have splenomegaly, which is massive in this case. The radiographic shadow in the left upper quadrant represents the splenomegaly.

35 ♦ Lower extremity of an individual with aortic valve endocarditis. The multiple purpuric lesions are palpable; they represent septic emboli from vegetations.

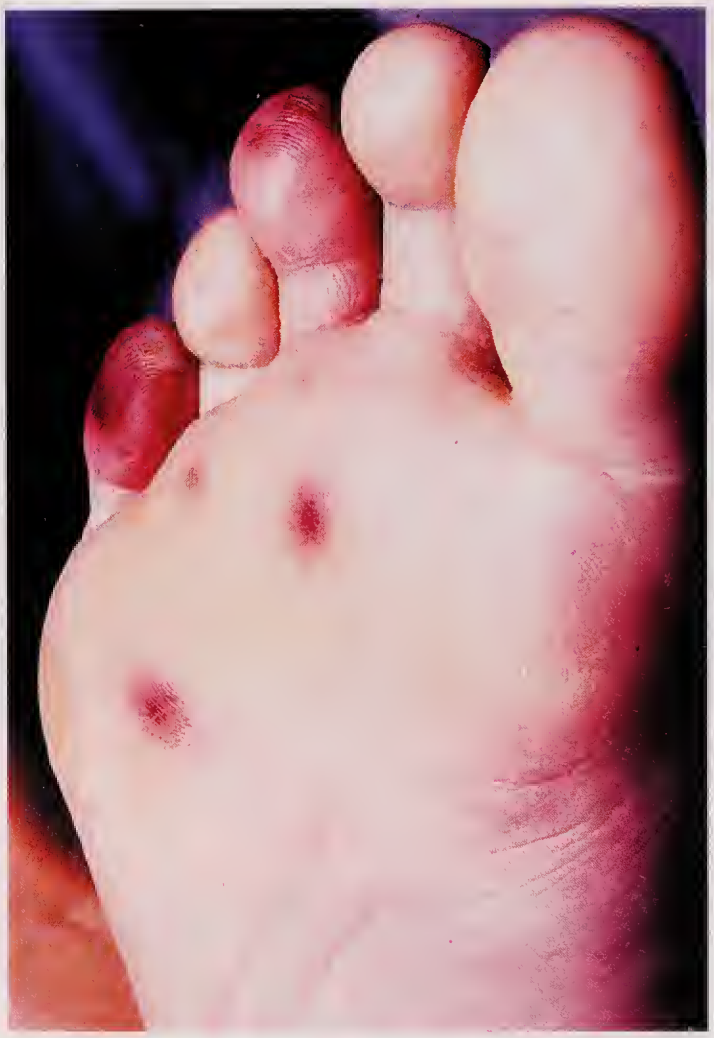

36

36 ♦ Sole of the foot of an individual with aortic valve endocarditis. The hemorrhagic nodule lesions are painless. The presence of Janeway spots is considered a hallmark of bacterial endocarditis.

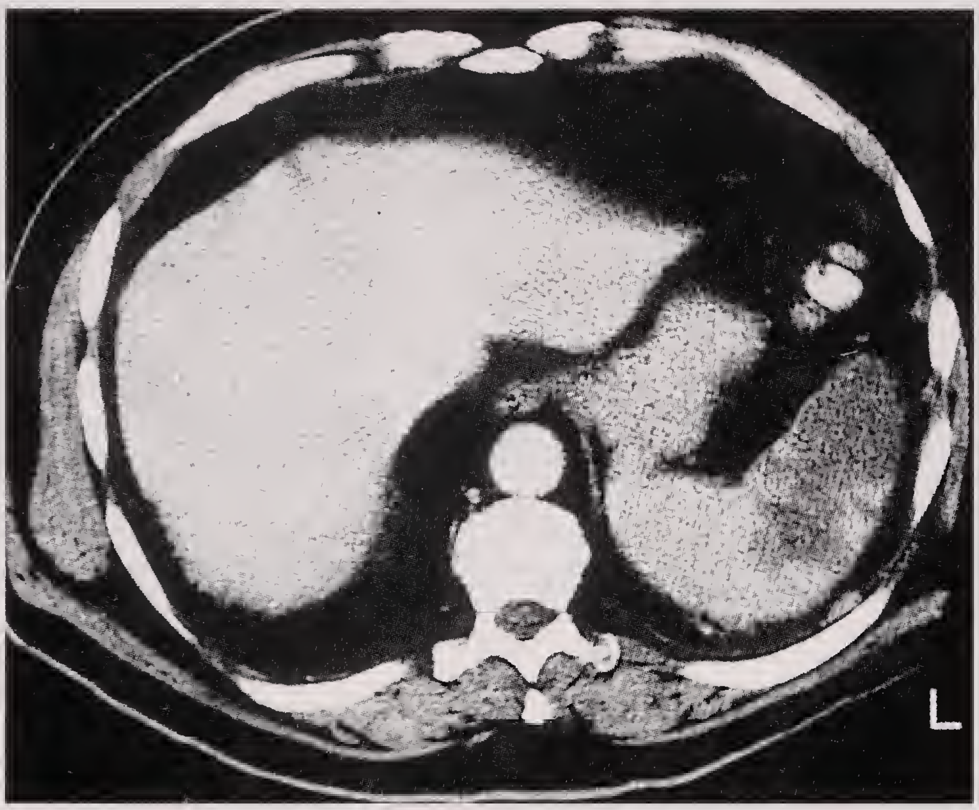

37

37 ♦ Abdominal computed tomography scan of an individual with aortic valve endocarditis, showing large, low-density lesions within the spleen, which are consistent with splenic infarcts.

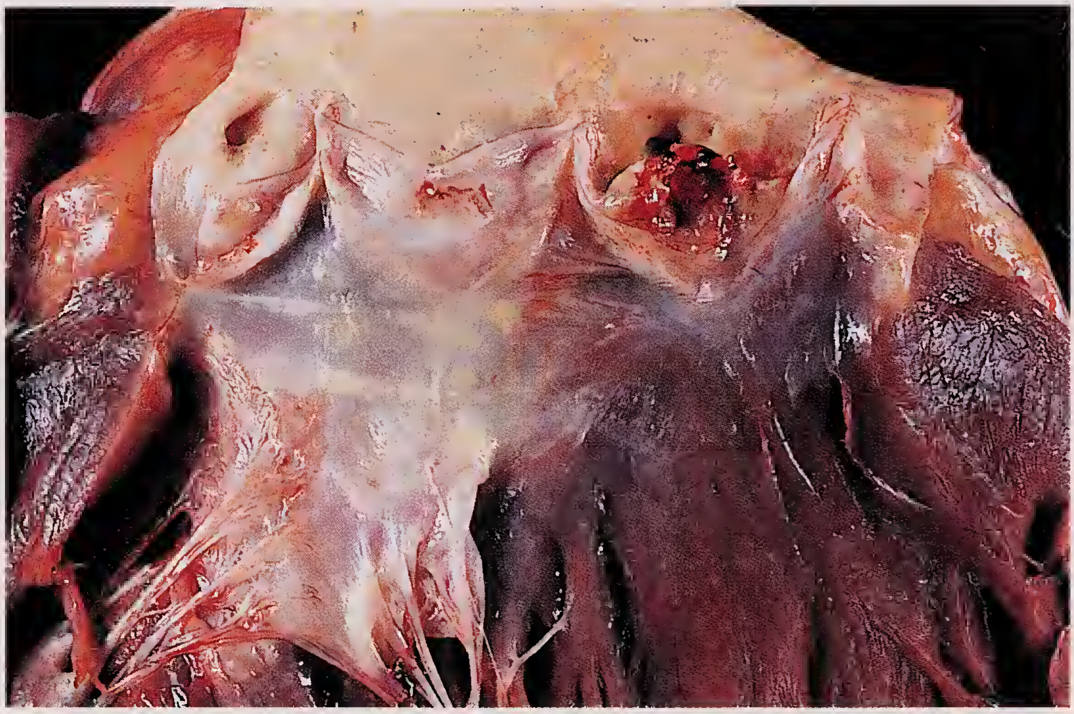

38

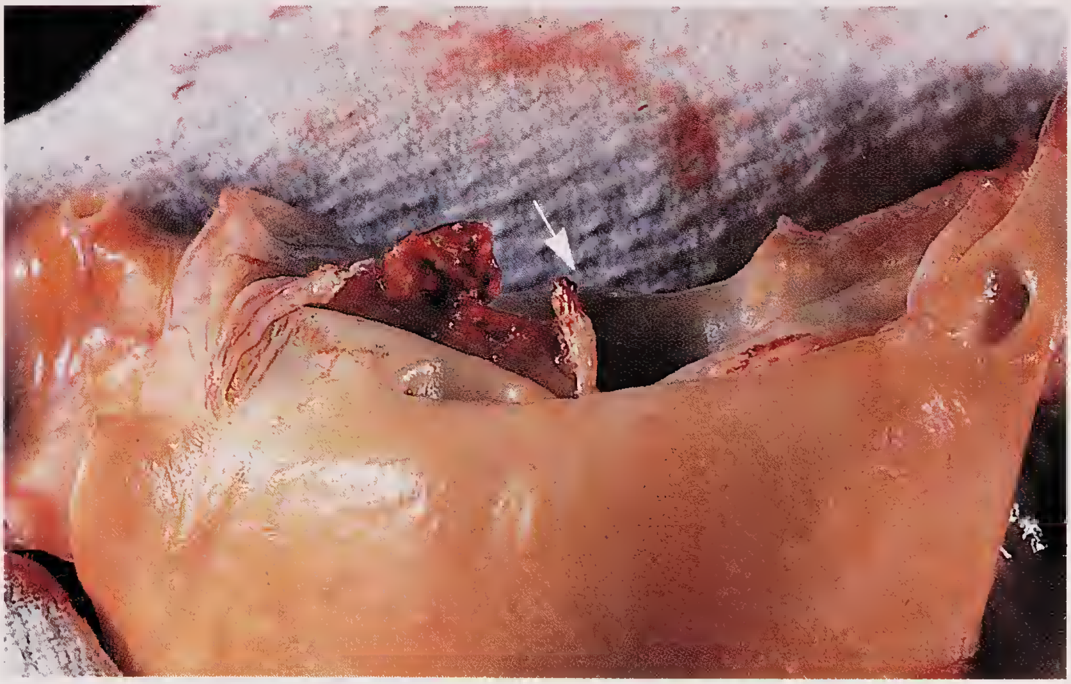

39

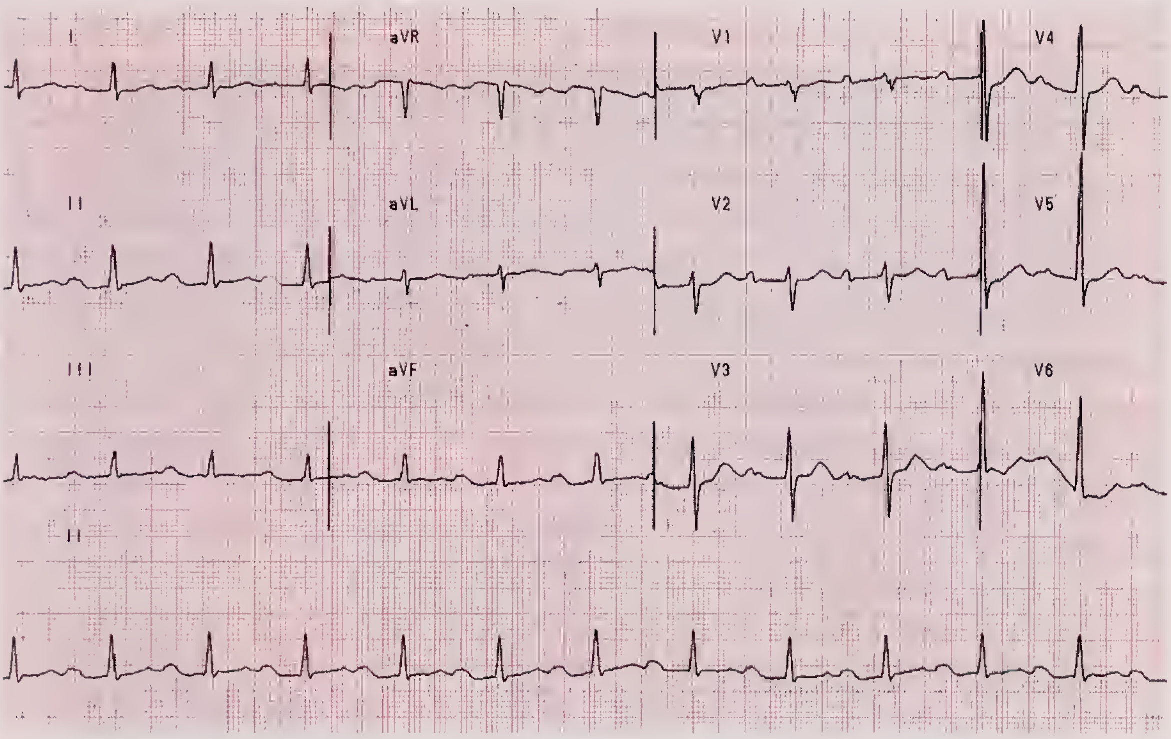

40

38 ♦ Subacute endocarditis with loud murmurs of an aortic valve insufficiency. The right aortic leaflet is partly destroyed by a hemorrhagic vegetation. Blood cultures are positive for an enterococcal species.

39 ♦ Subacute endocarditis. The tear in 38 is shown more clearly when photographed from above (arrow).

40 ♦ Electrocardiogram (ECG) of a patient with aortic valve endocarditis, resulting in an aortic abscess. The ECG shows sinus rhythm with first-degree atrioventricular block. Prolongation of the PR interval is strong evidence of abscess formation.

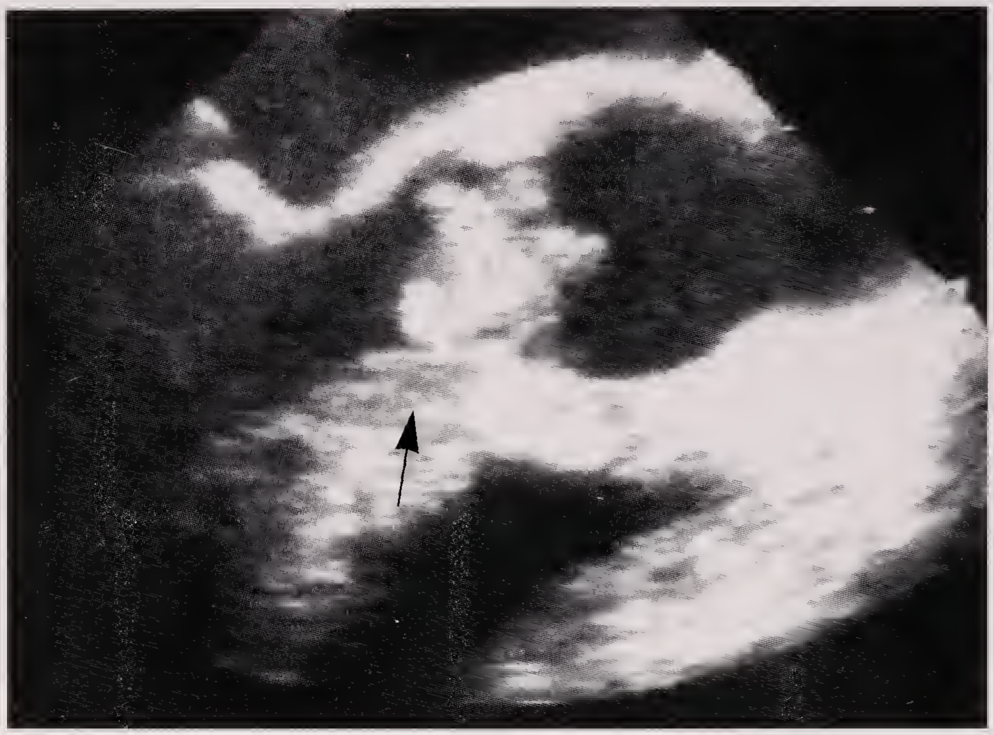

41

41 ♦ Transesophageal echocardiogram of the aortic valve in an intravenous drug user. The scan shows a very large vegetation of the aortic valve (arrow) that resulted in severe aortic insufficiency, subsequently requiring aortic valve replacement.

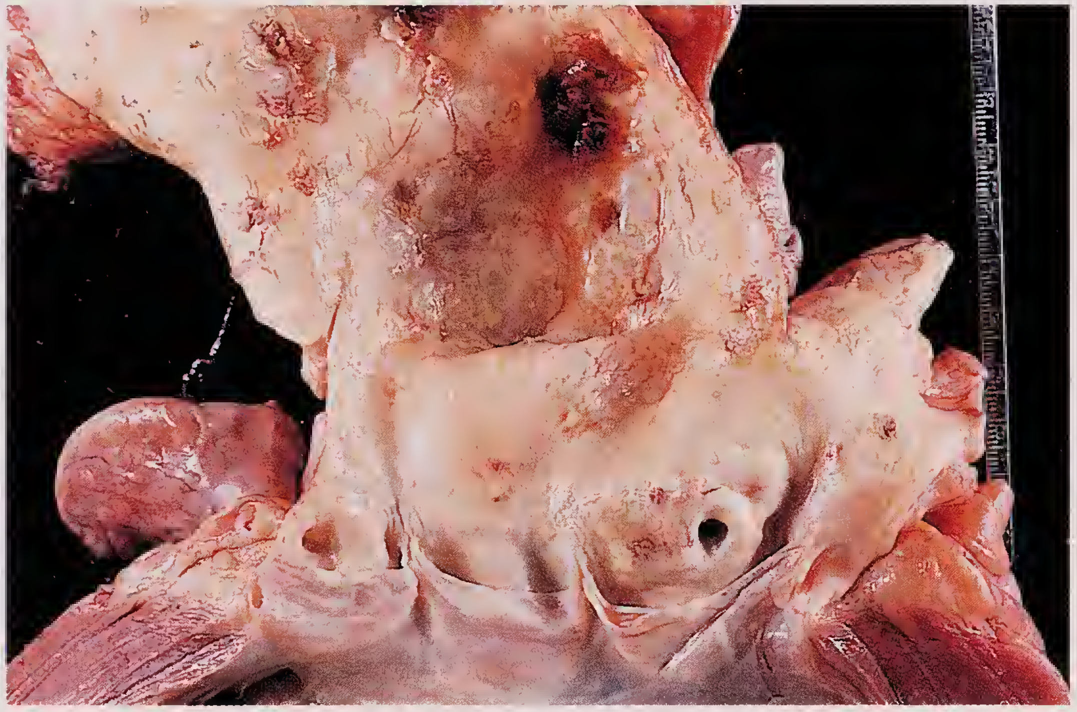

42

42 ♦ Dilated, syphiliti, sagging aortic valve with exposed coronary ostia and moderately advanced aortic aneurysm.

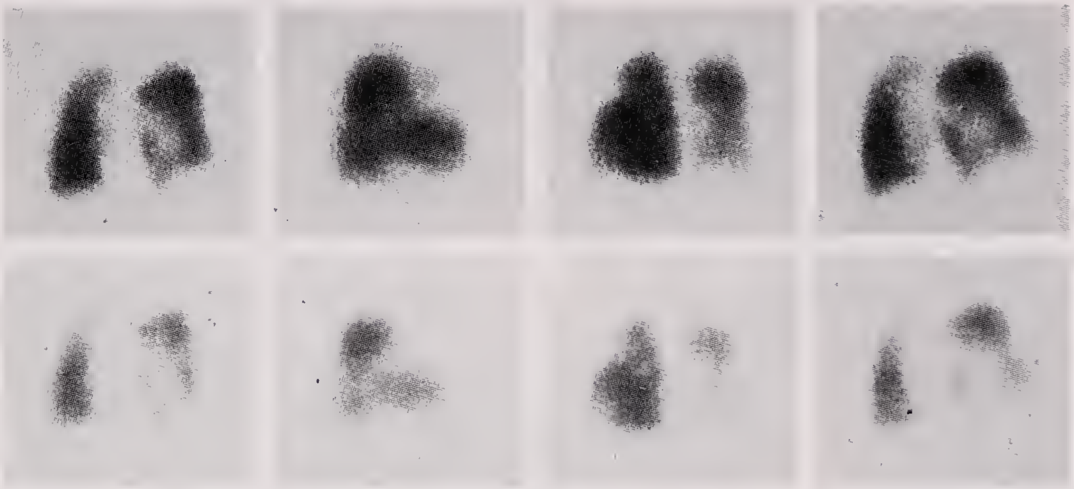

43

43 ♦ Lung perfusion scan of a patient with right-sided endocarditis, which shows multiple, bilateral segmental and subsegmental perfusion defects, suggesting a high probability for septic pulmonary emboli.

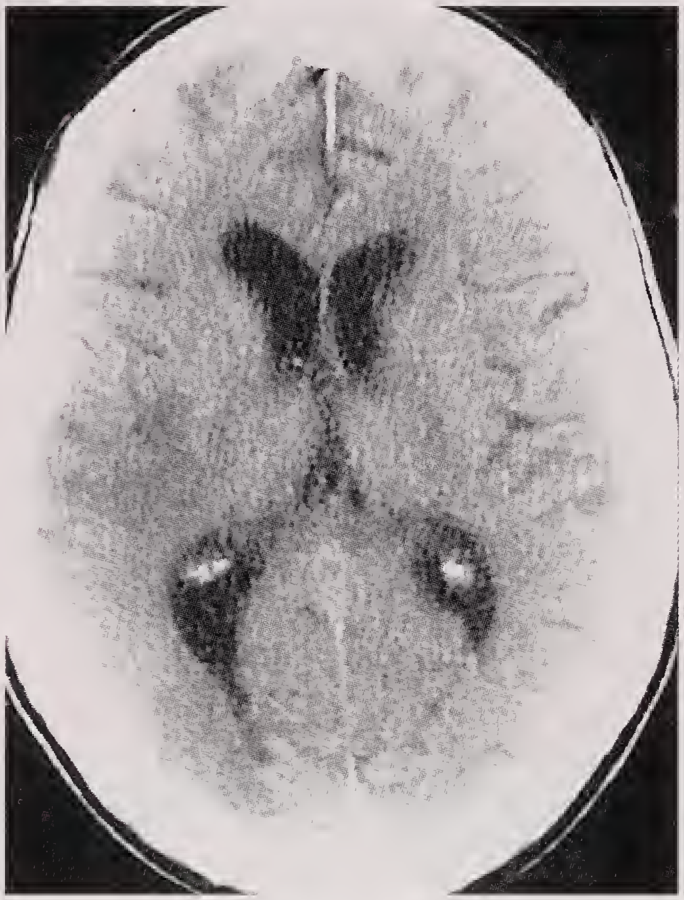

44

44 ♦ Computed tomography scan of the brain of a patient with prosthetic valve endocarditis who developed left-sided hemiparesis. A low-density lesion in the right parietal region is most compatible with a nonhemorrhagic infarct. The clinical history suggests that this finding represents a septic embolus.

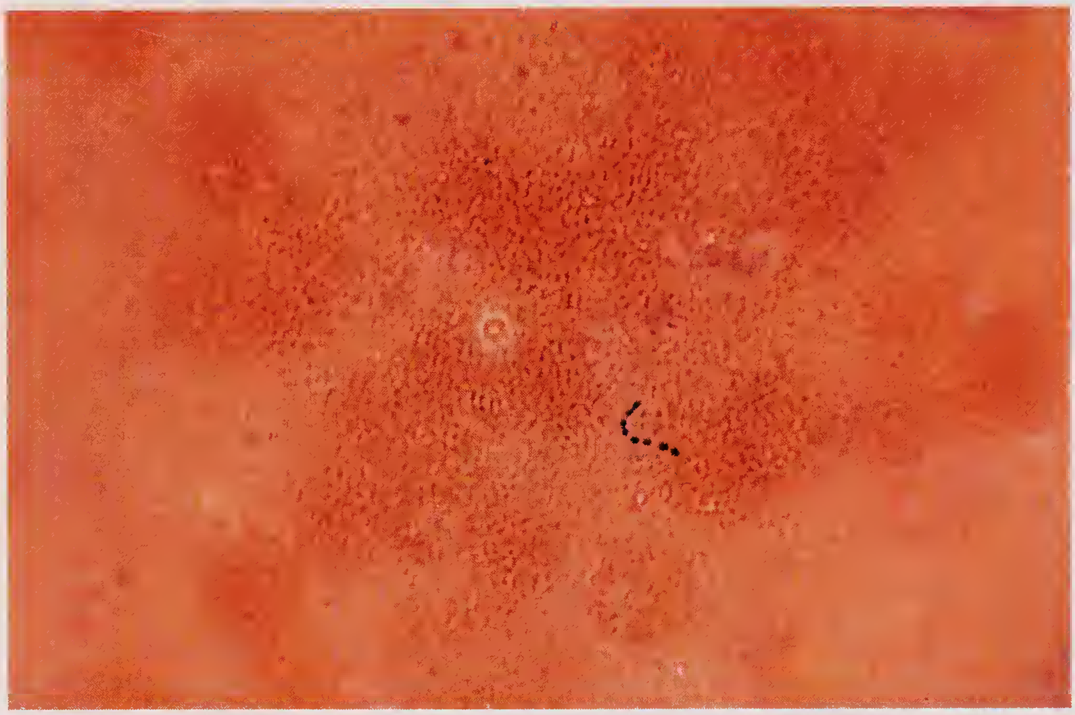

45

45 ♦ Gram-stained smear from mitral valve endocarditis, showing a chain of Gram-positive cocci.

46 ♦ Chronic active myocarditis from the patient in 45.

47 ♦ A 58-year-old man with serologic testing positive for syphilis and inadequate therapy, showing a classical proximal aortic aneurysm and dilated aortic valve ring with insufficient valve. A dilated, hypertrophic, failing left ventricle and a thickened left ventricular endocardium due to turbulent flow can also be seen. In addition, exaggerated aortic atherosclerosis is present.

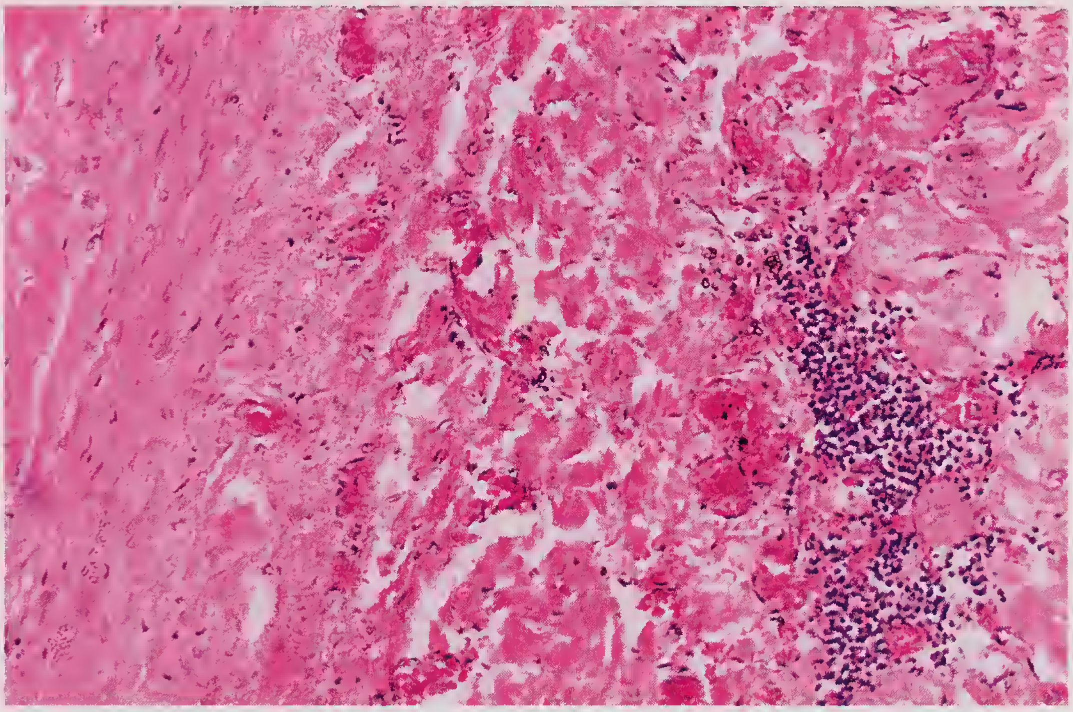

46

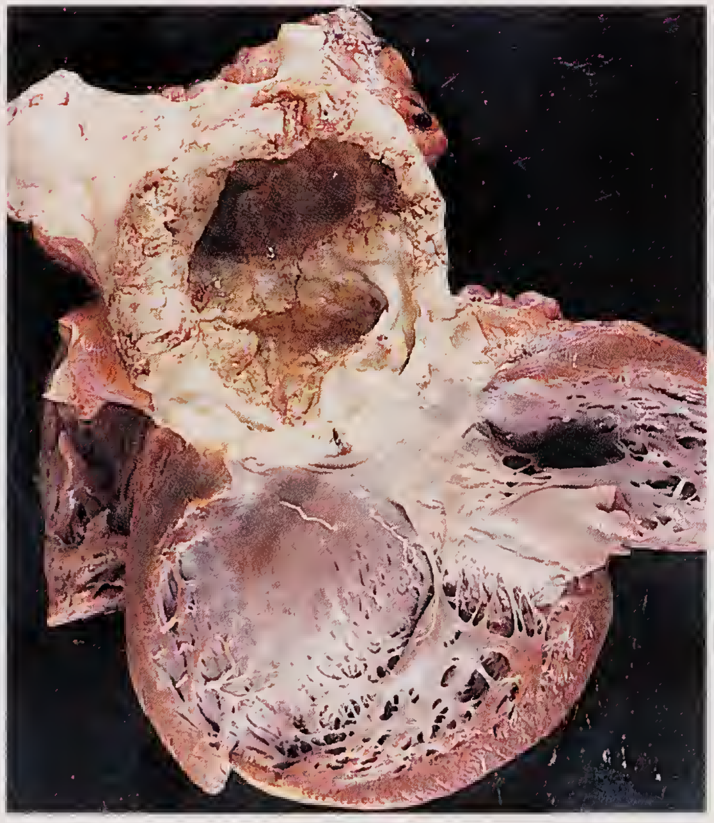

47

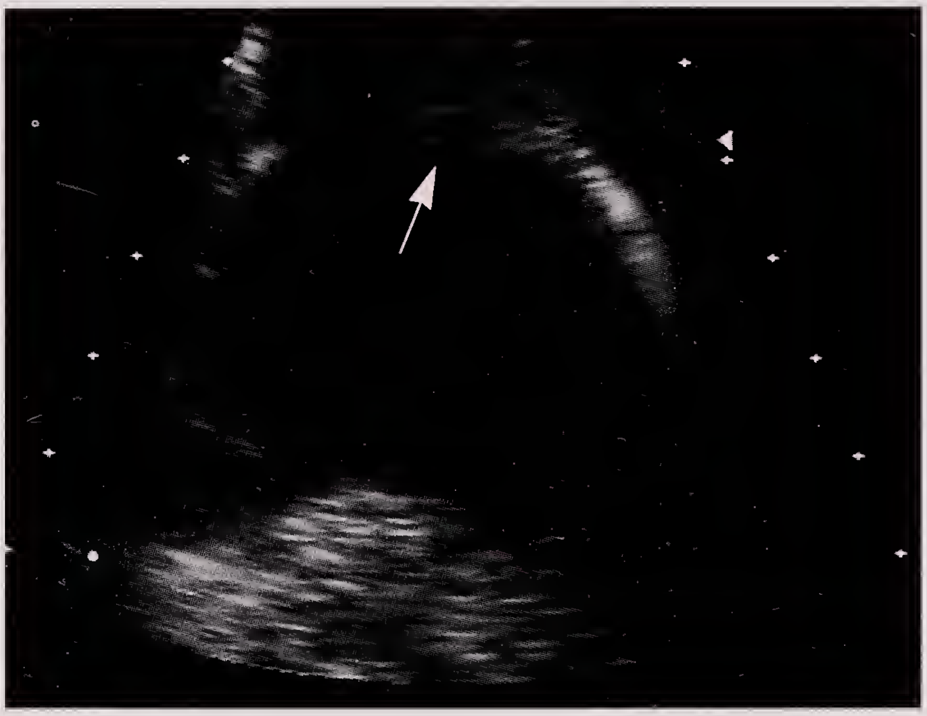

48

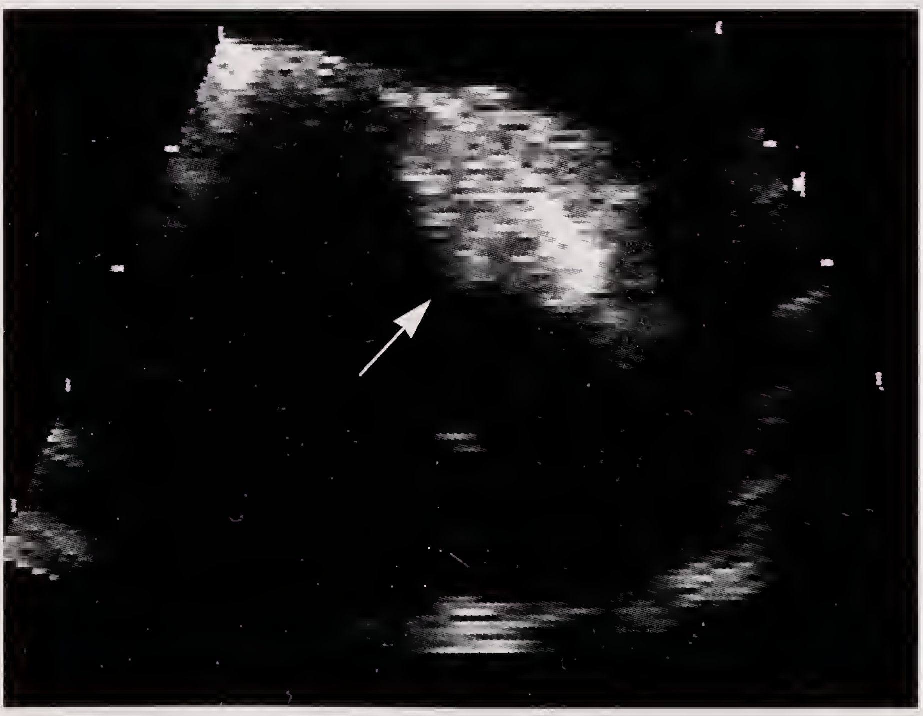

49

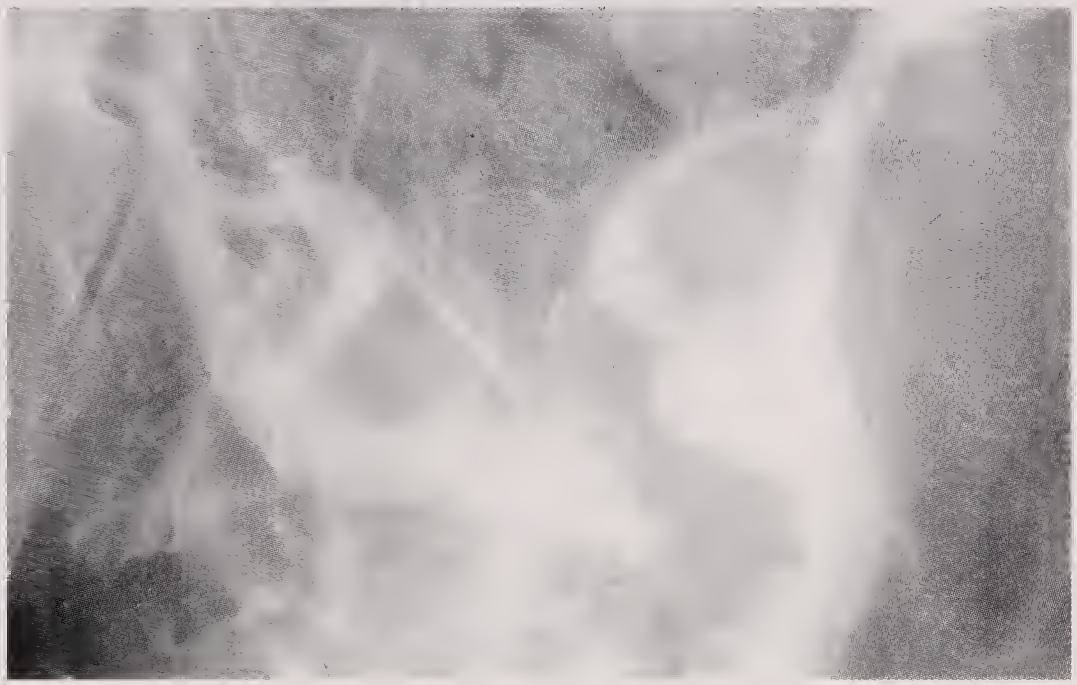

50

48-49 ♦ Transesophageal echocardiograms in a patient with *Staphylococcus aureus* bacteremia, which represent two views of a large vegetation (arrows) on a pacemaker wire in the right atrium.

50 ♦ Peripheral arteriogram showing a mycotic aneurysm of the right common iliac artery.

Lower Respiratory Tract

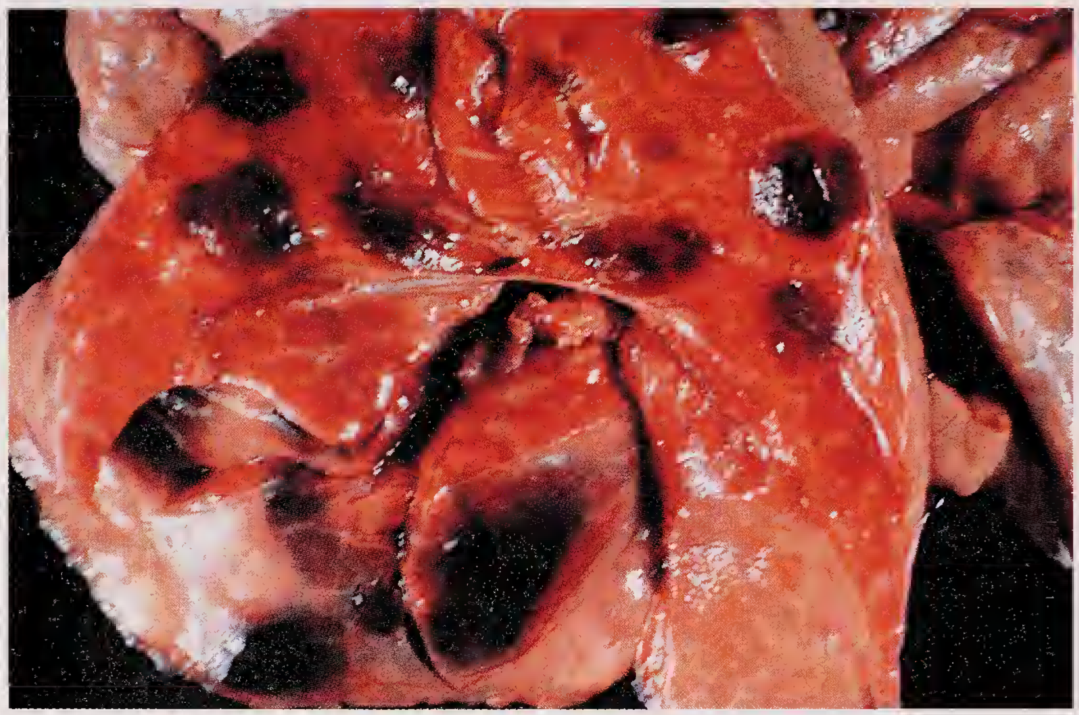

51

51 ◆ Autopsy specimen showing multiple pulmonary abscesses/ areas of infarction associated with *Staphylococcus aureus* pneumonia/sepsis.

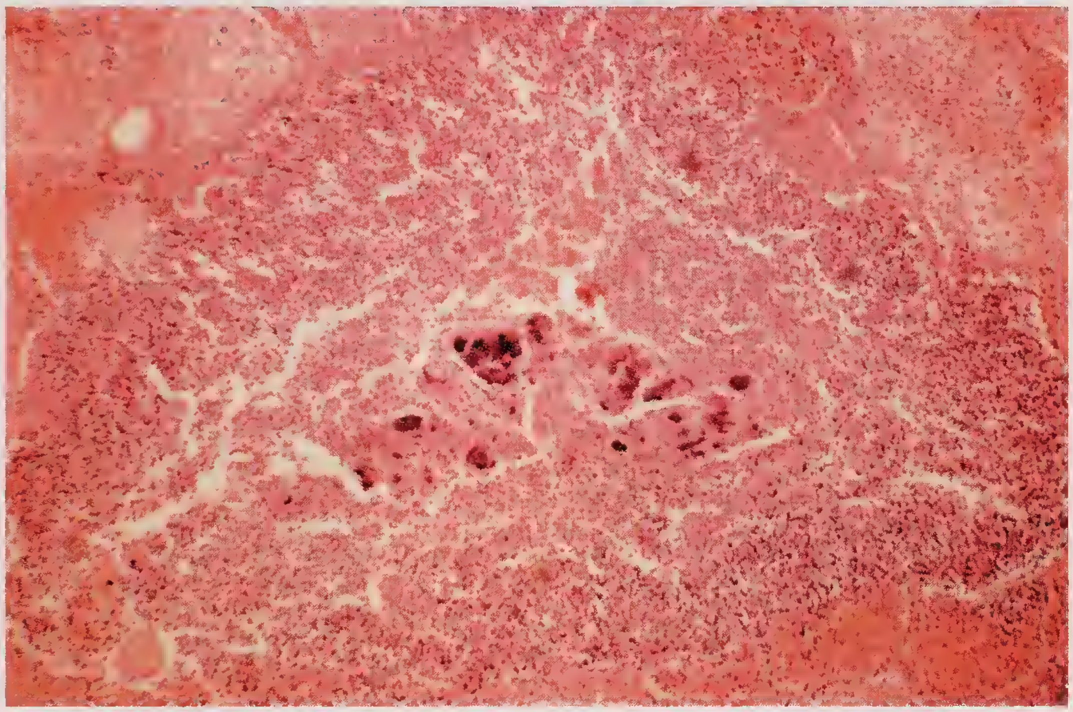

52

52 ♦ Photomicrograph of lung tissue, depicting a microabscess within the pulmonary parenchyma in *Staphylococcus aureus* pneumonia (hematoxylin-eosin stain). The inflammatory cell infiltrate is quite prominent, and spontaneous drainage of necrotic material can lead to cavitation.

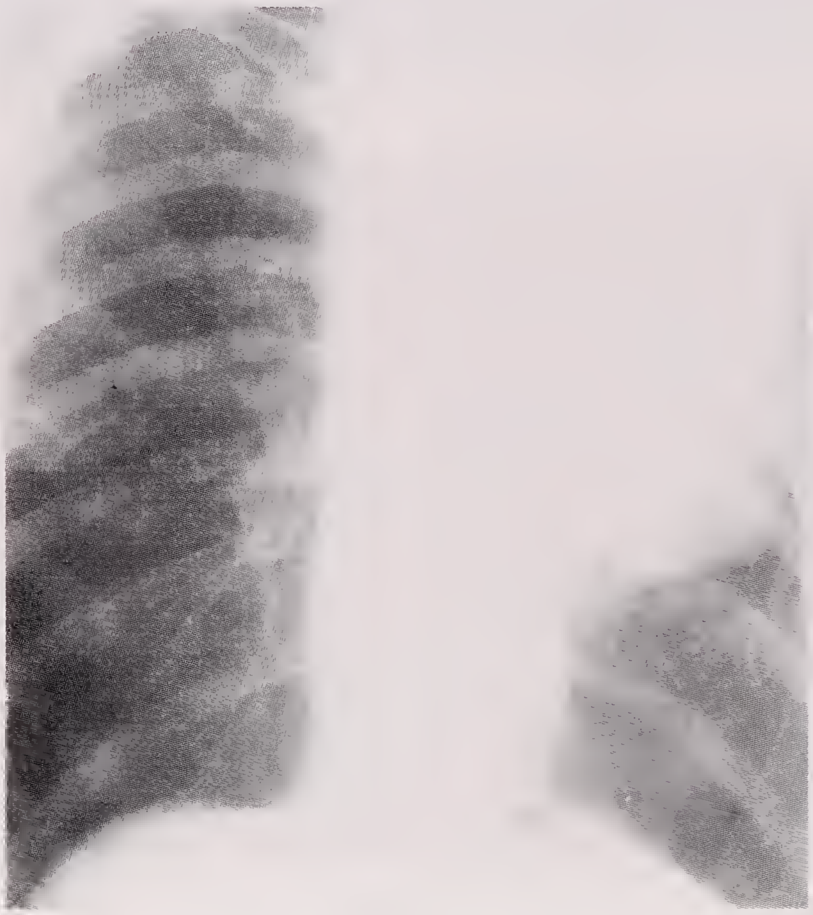

53

53 ♦ Chest radiograph of an individual with *Staphylococcus aureus* infection, which shows diffuse left upper lung alveolar infiltrate. No classic radiographic pattern is found in the lung. Affected patients can present with a lobar or diffuse pneumonia, single or multiple lung abscesses, and pleural effusions. Thus, a chest radiograph alone is not sufficient to diagnose *S aureus* pneumonia.

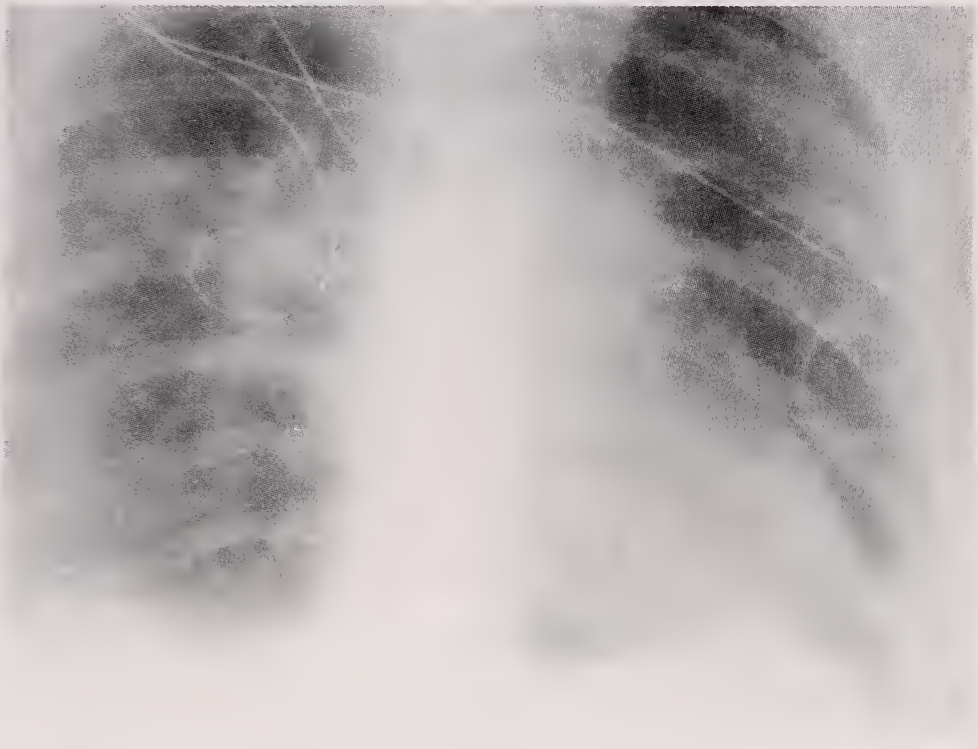

54

54 ♦ Chest radiograph of an individual with *Staphylococcus aureus* pneumonia, showing pneumatocoeles. These thin-walled, cystic lesions in the pulmonary parenchyma appear more commonly in infants than adults with this disease.

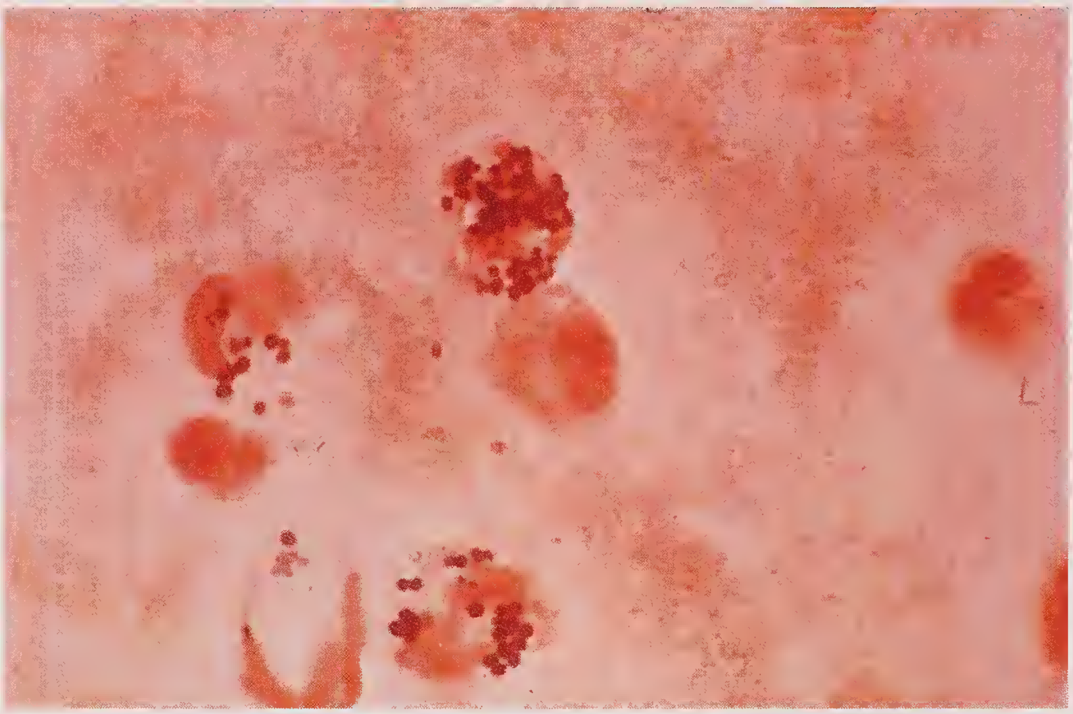

55

55 ♦ Bronchoalveolar lavage specimen showing associated intracellular *Staphylococcus aureus* in *S aureus* pneumonia. Bronchoalveolar lavage of the involved bronchopulmonary segment combined with protected brush catheter biopsy for quantitative bacterial cultures and fiberoptic bronchoscopy, can provide improved sensitivity in the diagnosis of pneumonia.

56-57 ♦ Chest radiographs of an individual with lobar pneumonia due to *Streptococcus pneumoniae.* The lobar or segmental infiltrate on chest radiographs is an often touted "classic pattern" of presentation, although it may not appear consistently in all patients. Subsegmental or less homogenous patterns seem to be more common, particularly in patients with underlying chronic lung disease.

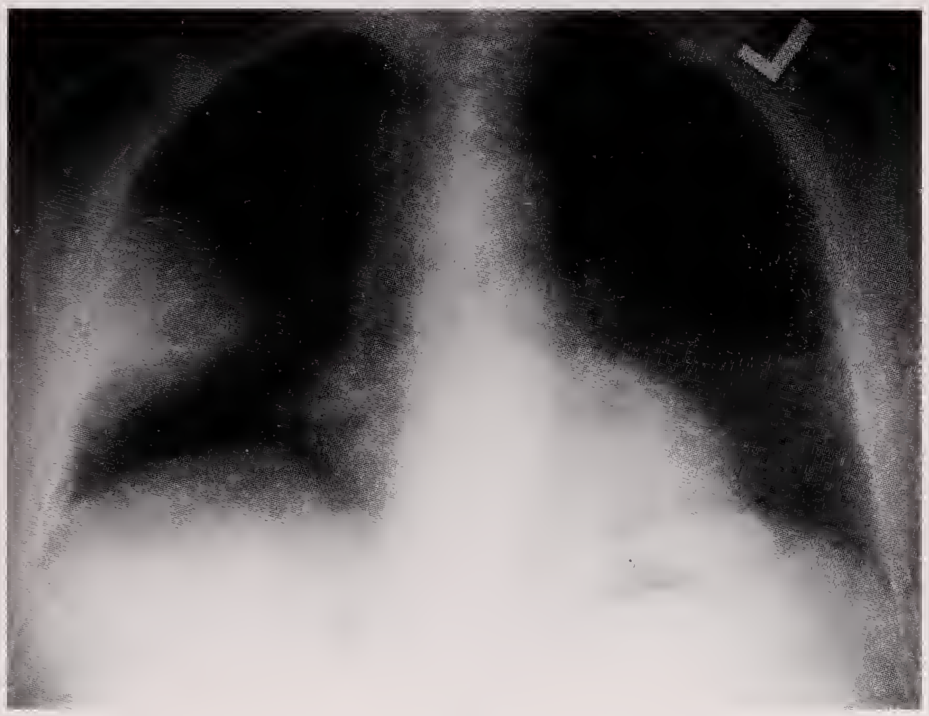

56

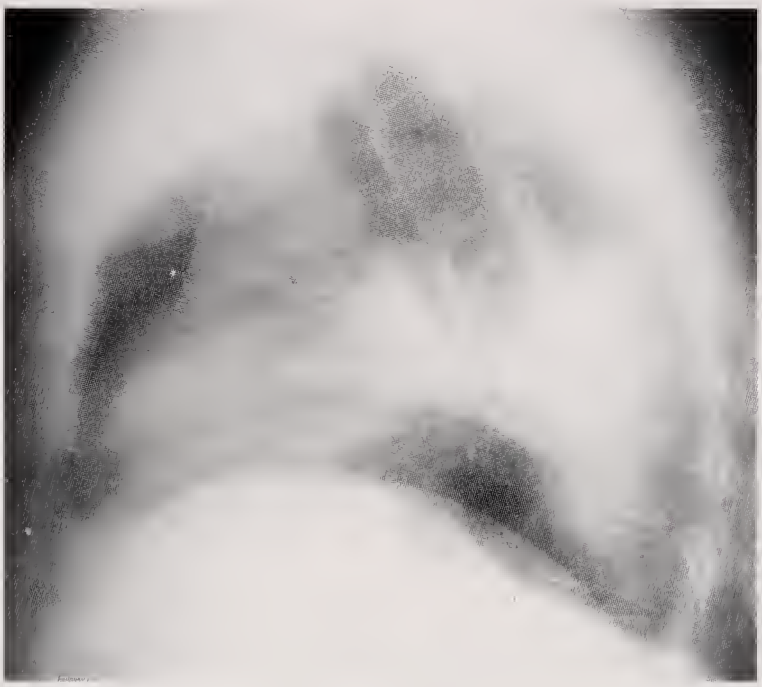

57

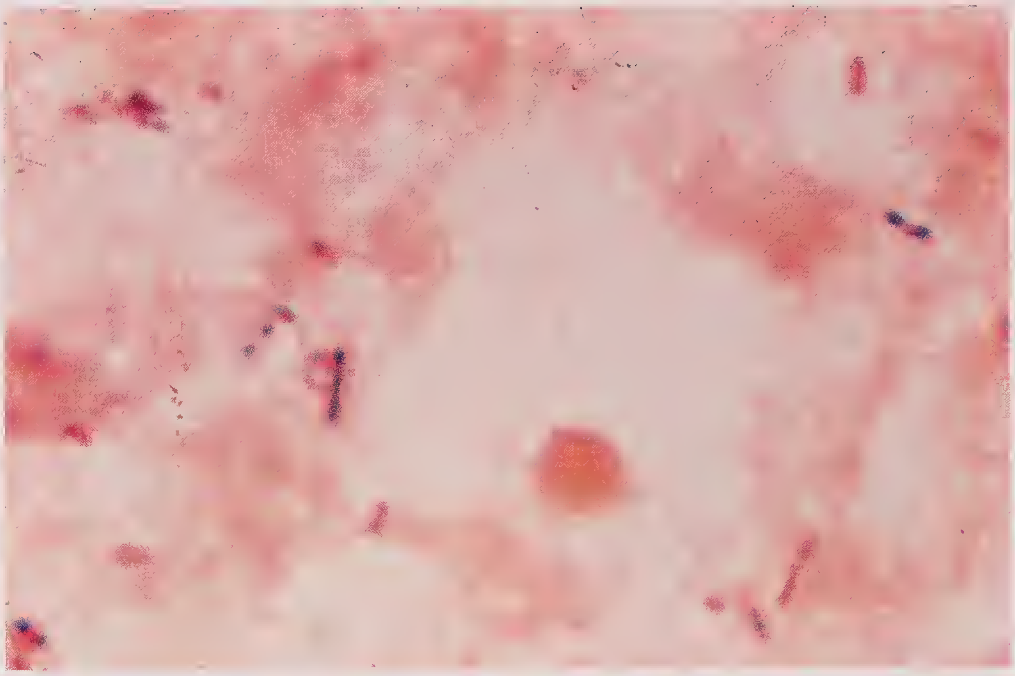

58

58 ♦ Gram's stain emphasizing the capsule of *Streptococcus pneumoniae.* The Gram-positive, aerobic bacterium appears as diplococci or chains, typically surrounded by inflammatory cells, on sputum examination. Gram staining is strongly suggestive of the diagnosis of pneumonia in the presence of a significant number of leukocytes and an insignificant number of oral epithelial cells.

59 ♦ Chest radiograph showing right upper lobe consolidation due to *Klebsiella pneumoniae.* This bacterium colonizes the supralaryngeal airways of alcoholic individuals and elderly persons with debilitating disease. The radiographic appearance, which is variable, includes massive lobar consolidation with frequent tendency for abscess formation.

60 ♦ Chest radiograph of an individual with *Pseudomonas aeruginosa* pneumonia, showing diffuse airspace involvement. The patient with *P aeruginosa* pneumonia to such a degree typically appears extremely toxic. The pneumonia is often bilateral, with diffuse airspace involvement on chest radiograph.

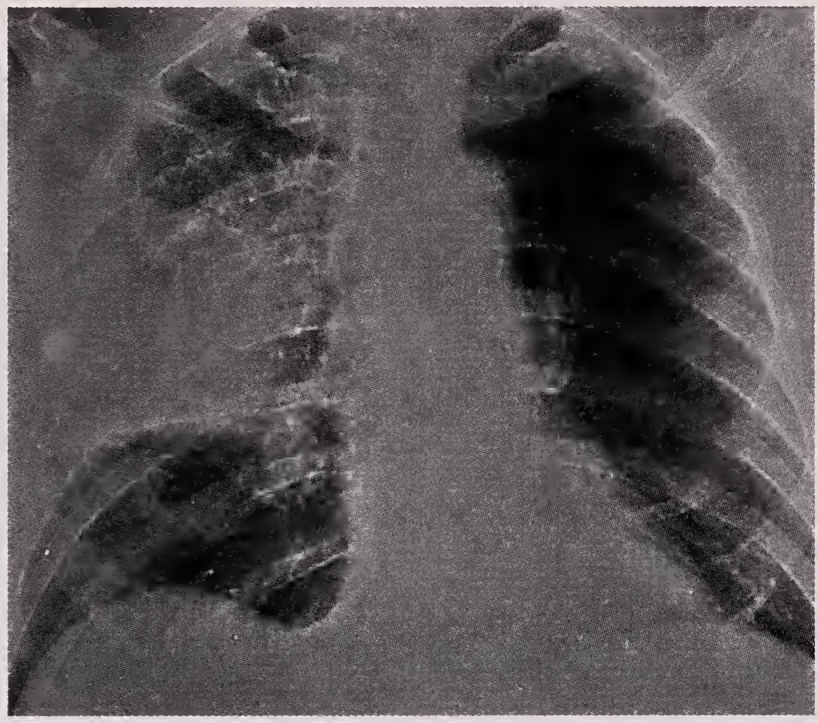

59

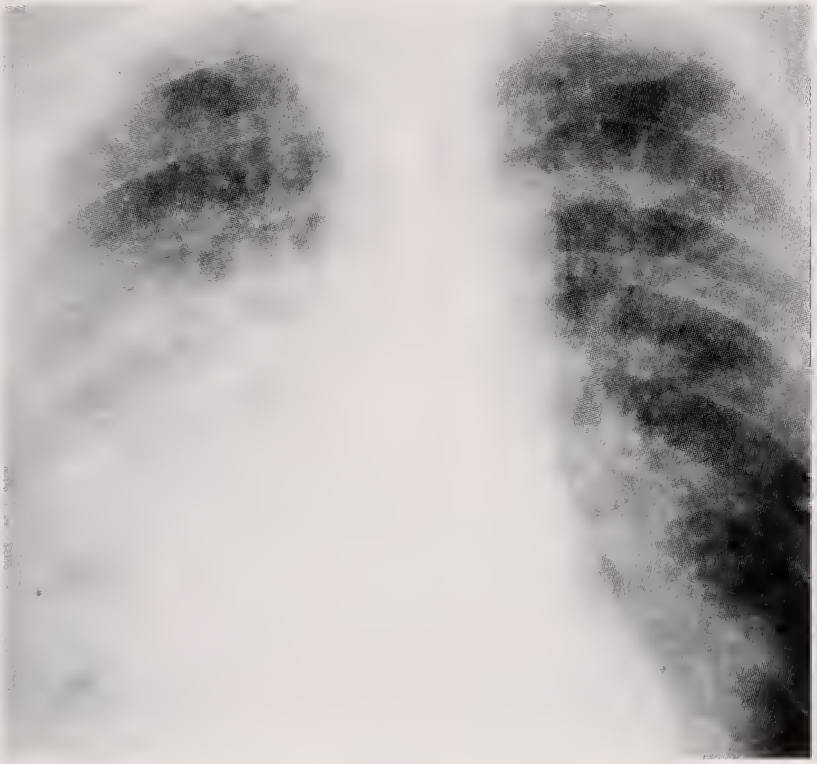

60

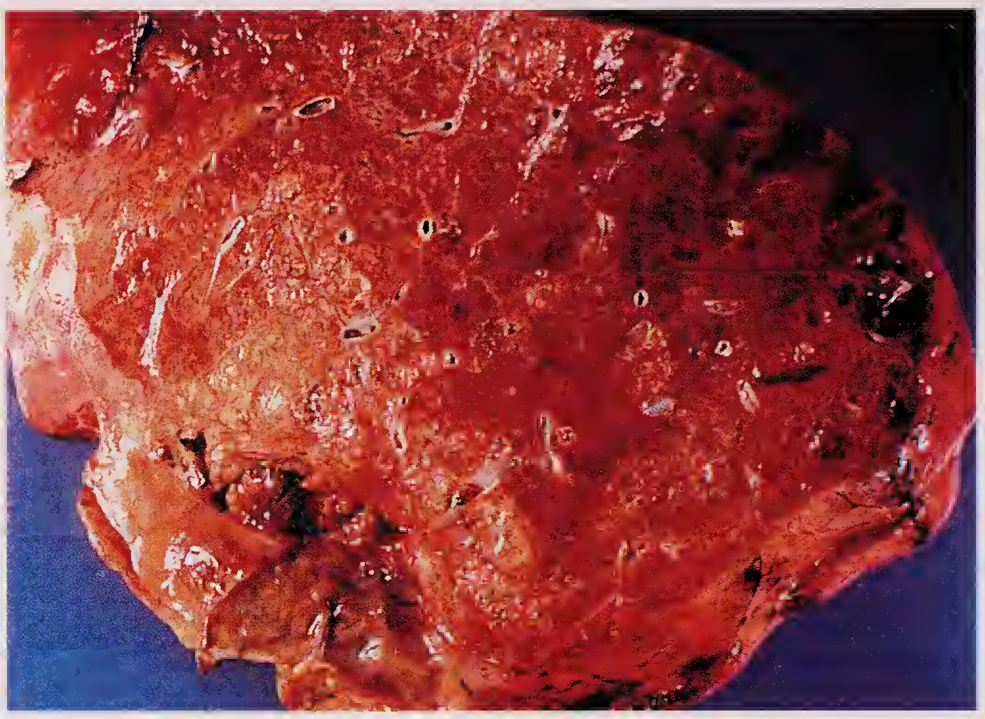

61

61 ◆ Autopsy specimen showing diffuse, hemorrhagic, parenchymal changes of *Pseudomonas aeruginosa* pneumonia. The lung lesions can appear as poorly localized, hemorrhagic areas, with microscopic intra-alveolar hemorrhage and alveolar necrosis. Lung abscesses, necrotic nodules with significant leukocyte invasion, and bacterial invasion of blood vessel walls are also depicted.

62 ◆ Autopsy specimen of a lung, showing diffuse *Pseudomonas aeruginosa* pneumonia. This photograph is notable for the nodular, lobular appearance of this multicentered infection.

63 ◆ Autopsy specimen of a large *Pseudomonas aeruginosa* lung abscess.

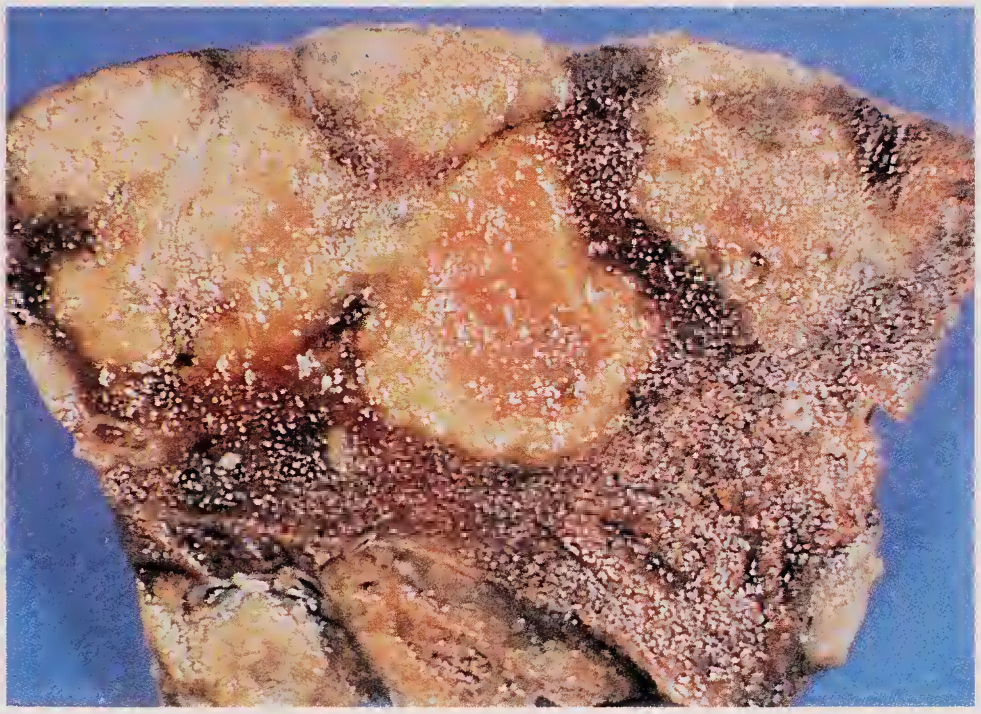

62

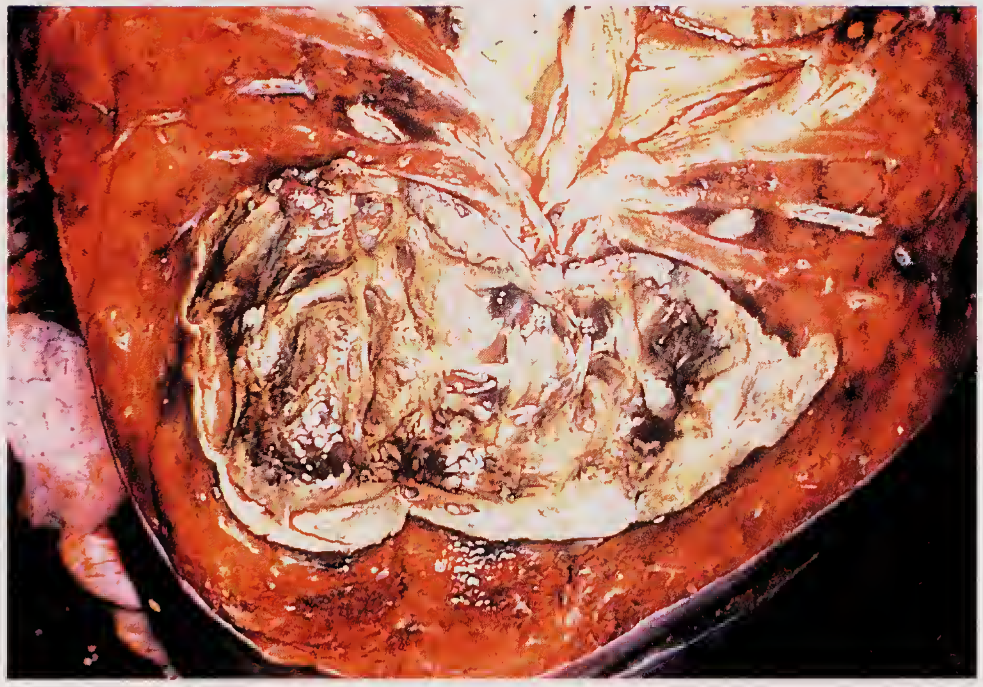

63

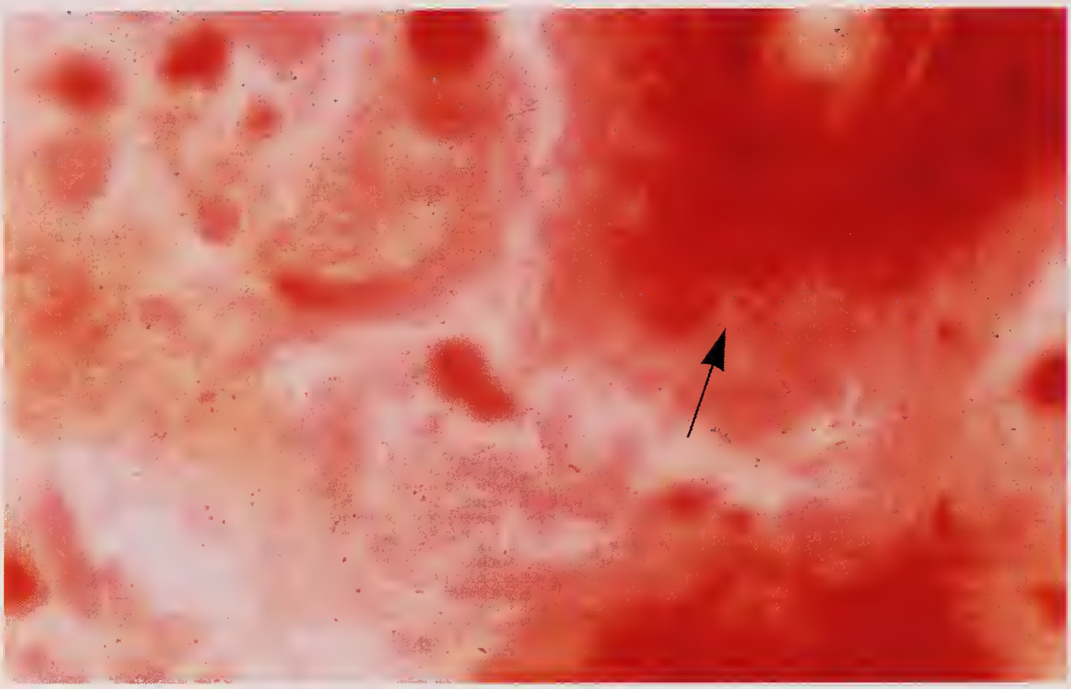

64

64 ♦ Histologic section depicting *Pseudomonas* vasculitis of the lung. Gram-negative rods can be seen juxtaposed to the vessel wall (arrow). This can be seen with bacteremia-induced *P aeruginosa* pneumonia.

65-66 ♦ Microscopic appearance of actinomycotic sulfur granules and inflammatory cells (Gomori's methenamine silver stain). The identification of sulfur granules with bacteriologic culture of a species of *Actinomyces* strongly supports the diagnosis of actinomycosis. In another microscopic view, in 66, the sulfur granules are seen in the center as delicate, black staining, branching filaments of actinomycosis. The less distinct, peripheral portions of the filaments appear "clubbed," because they are covered by polysaccharide-protein complex produced by the host. Sulfur granules have been described with other organisms, including staphylococcus (botryomycosis), *Nocardia, Streptomyces*, and various fungi; however, they all lack the characteristic peripheral "clubbing."

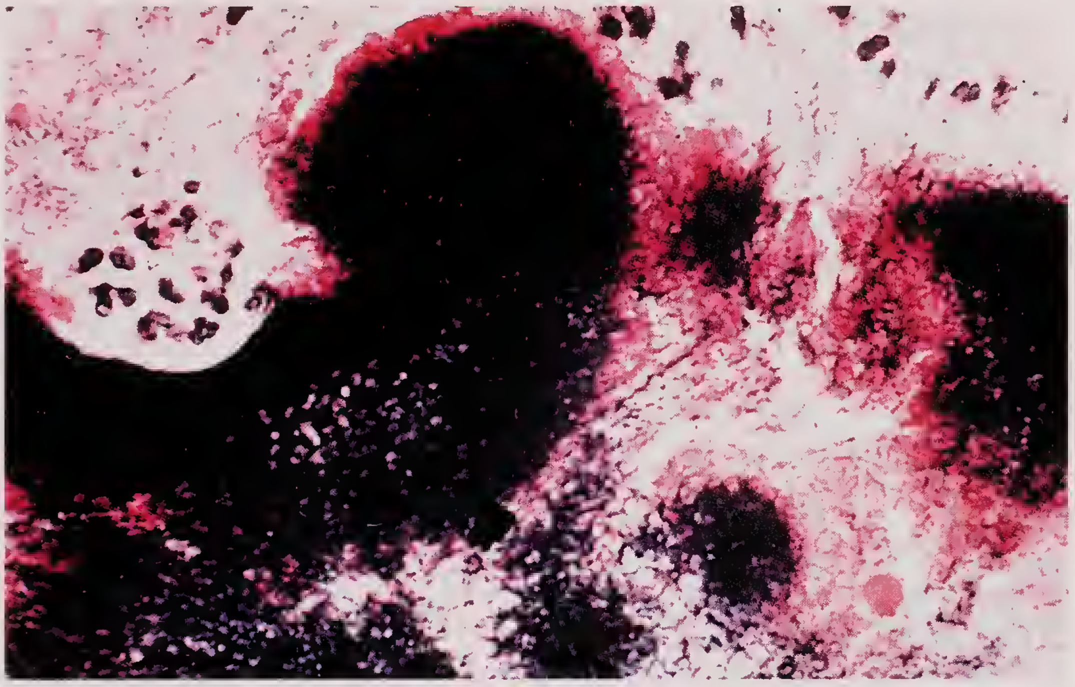

65

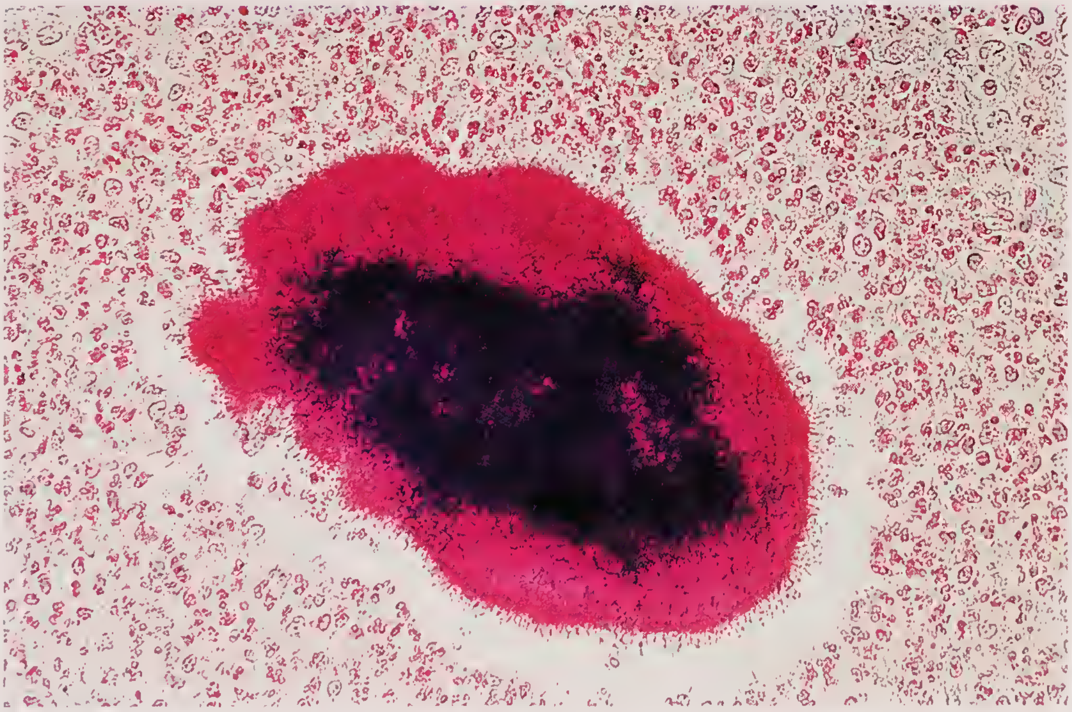

66

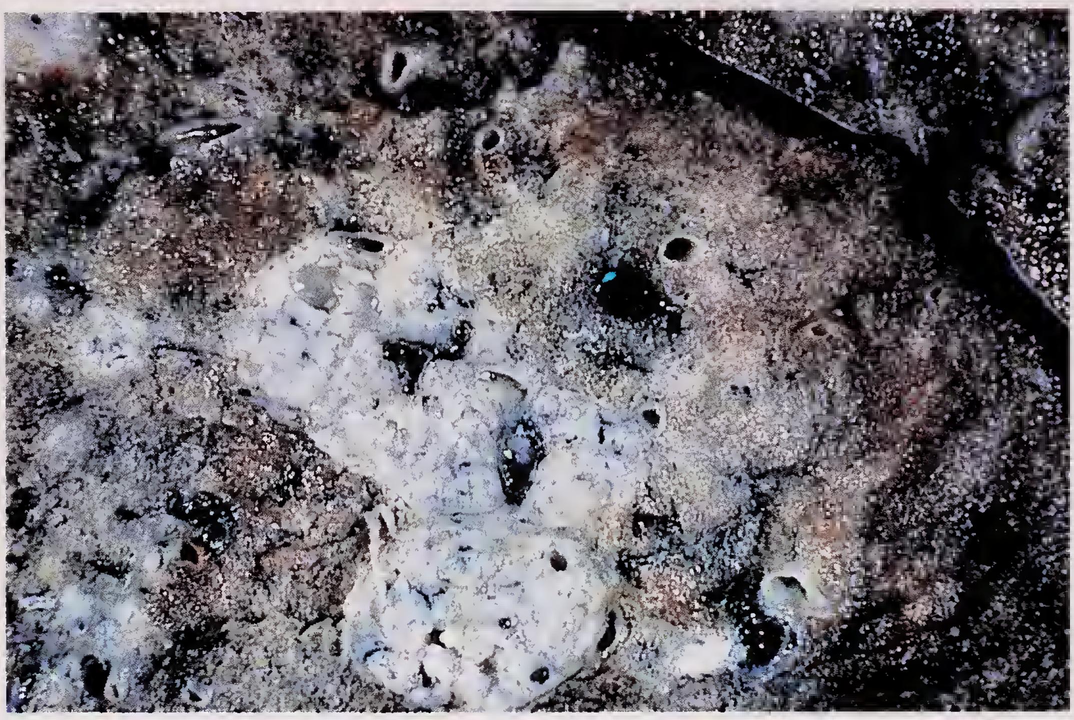

67

67 ♦ Pulmonary parenchymal cavity secondary to chronic *Nocardia* infection. Chest radiographic findings are variable. Confluent parenchymal infiltrates, thin-walled cavities, pulmonary nodules, pleural effusion, and single or multiple abscesses have been reported. Pulmonary disease is typically caused by *N asteroides*, infecting the lung through inhalation.

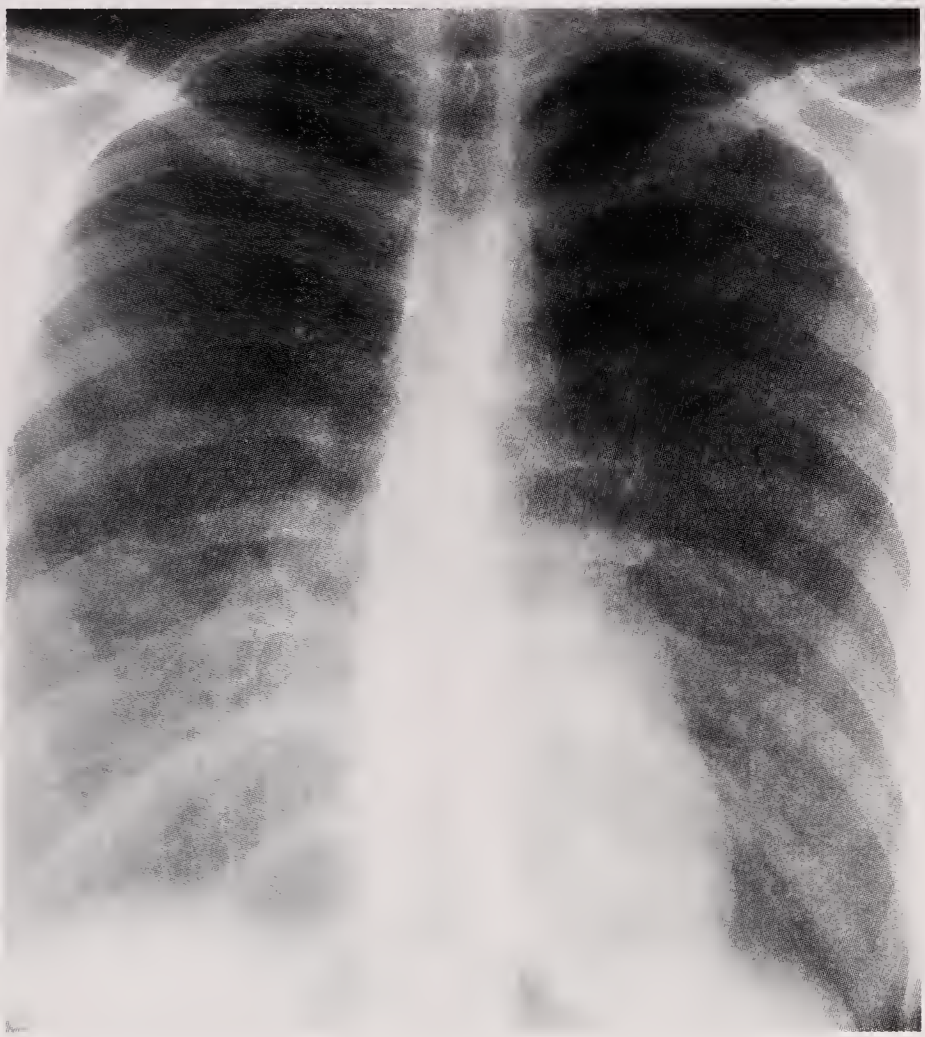

68

68 ♦ Chest radiograph of an individual with pneumonia caused by *Mycoplasma pneumoniae*, which is believed to be the major cause of atypical pneumonia syndromes. The appearance of the radiograph is variable, with interstitial findings with or without concomitant airway opacities.

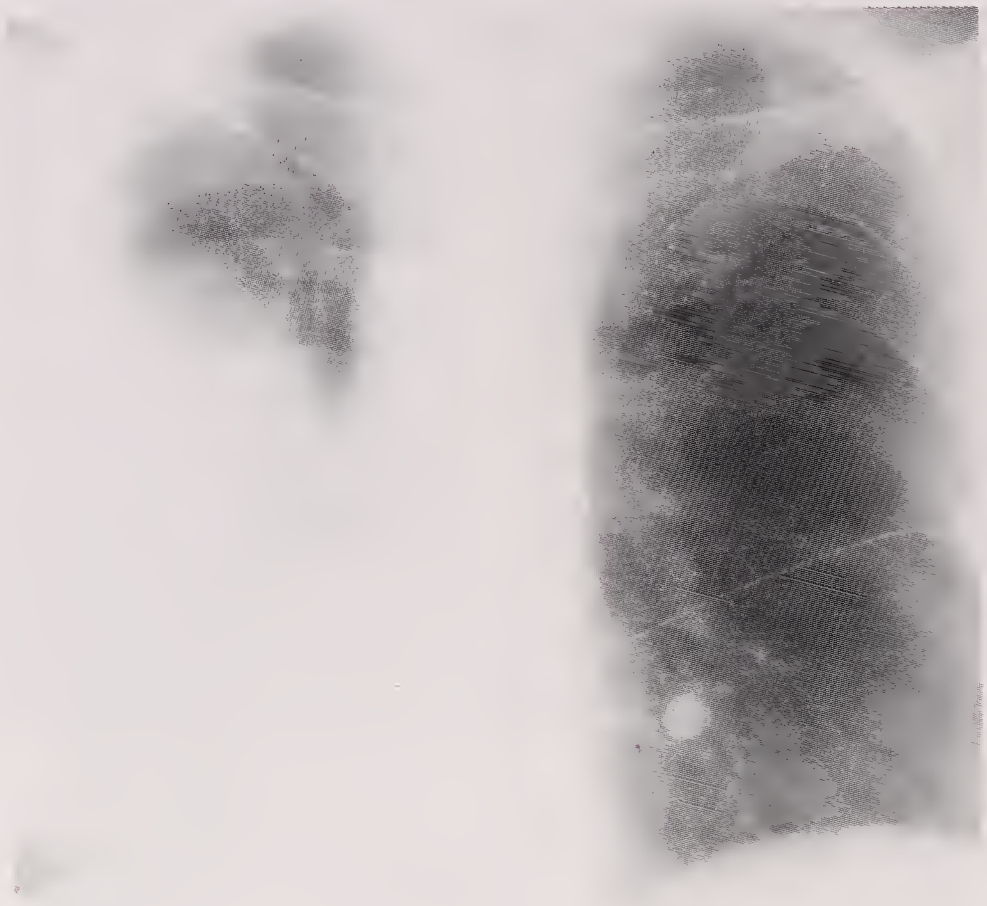

69

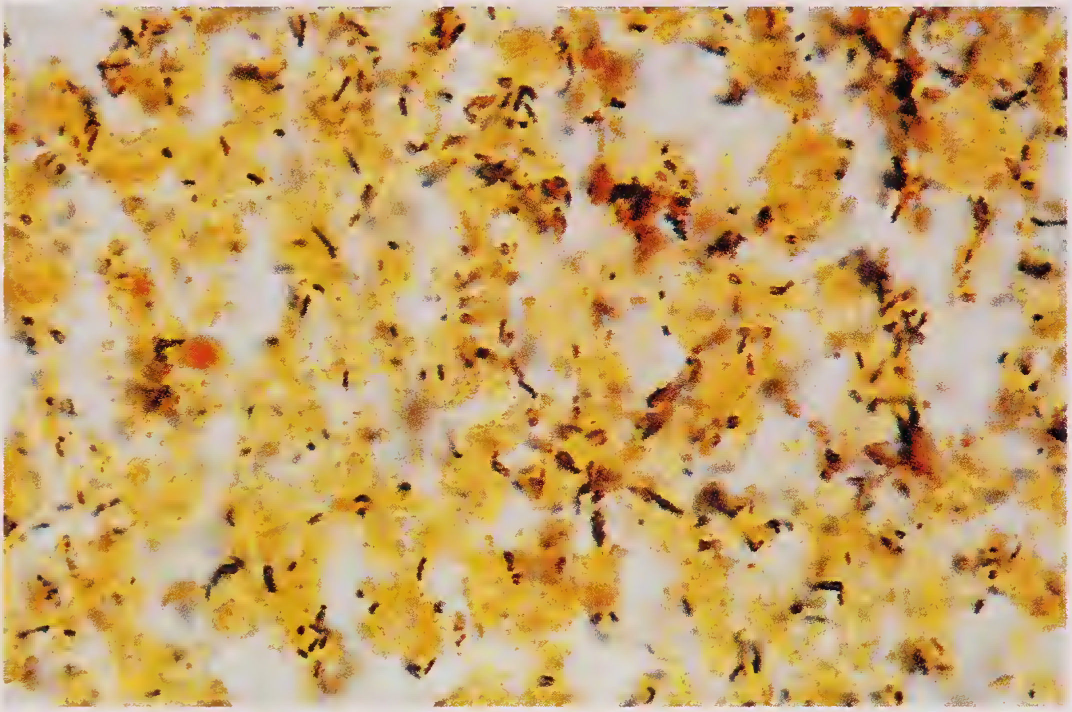

70

69-70 ♦ *Legionella pneumophila* pneumonia. The appearance of the chest radiograph in 69 is generally described as airspace consolidation, usually unilateral in presentation. The disease can progress with bilateral involvement with a tendency to affect the lower lobes. Lymph node enlargement in the hilum and mediastinum is not characteristic. Pleural effusion reportedly occurs.

Gram's stains of sputum in 70 fail to show *L pneumophila* organisms. However, the organisms can be seen clearly with modified Dieterle's silver-impregnation stain.

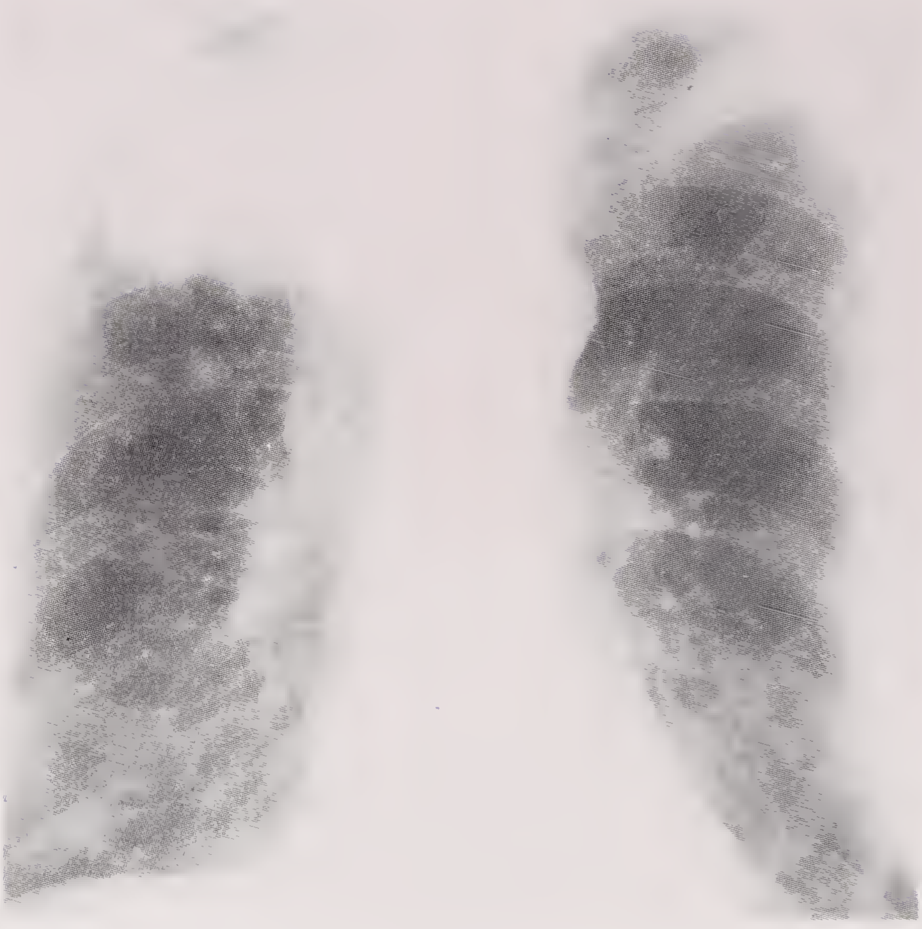

71

71 ♦ Chest radiograph with lobar consolidation of the right upper lobe.

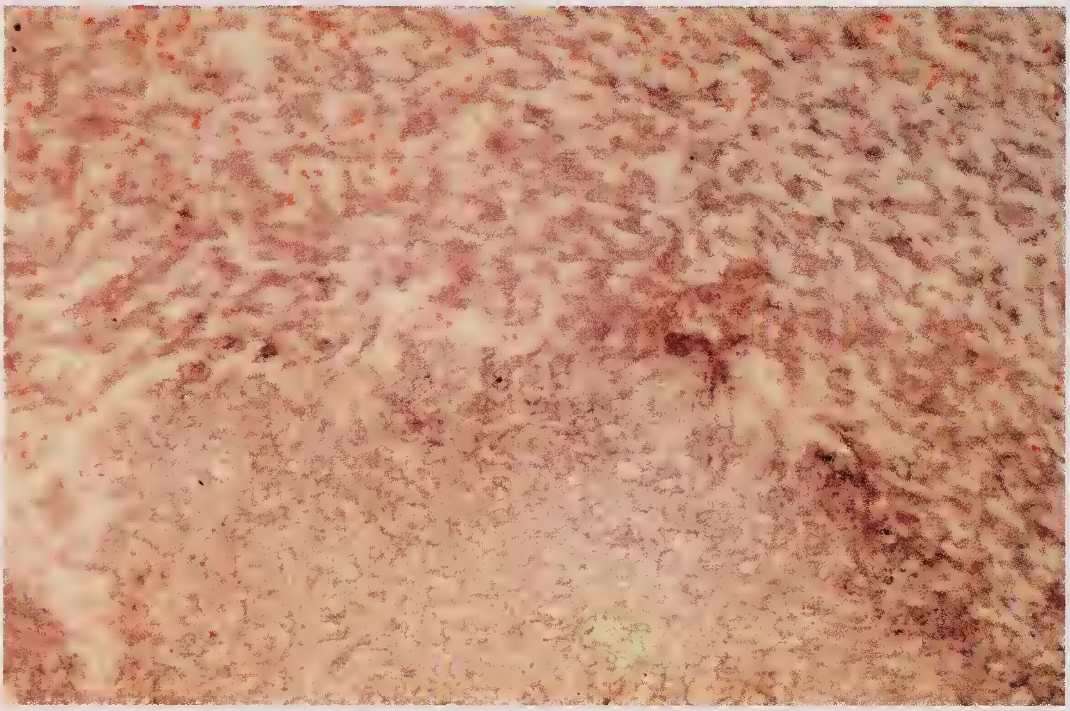

72

72 ♦ Mass of mycelial elements from an aspergilloma (Grocott-Gomori stain). Aspergillomas are masses of *Aspergillus* organisms growing inside existing lung cavities. An intense inflammatory reaction may occur around the cavity, but the fungus does not invade the walls.

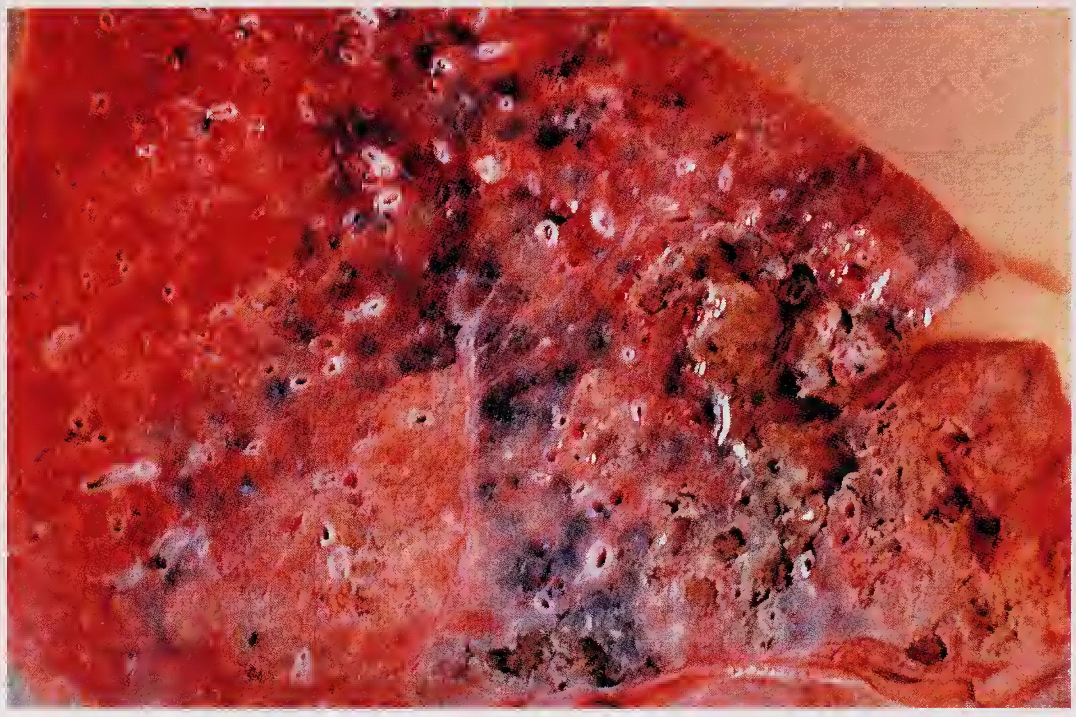

73

73 ♦ Lung section with a necrotizing bronchopneumonia due to invasive aspergillosis. Chronic necrotizing aspergillosis is a fibrocavitary lung disease that occurs in structurally abnormal lungs.

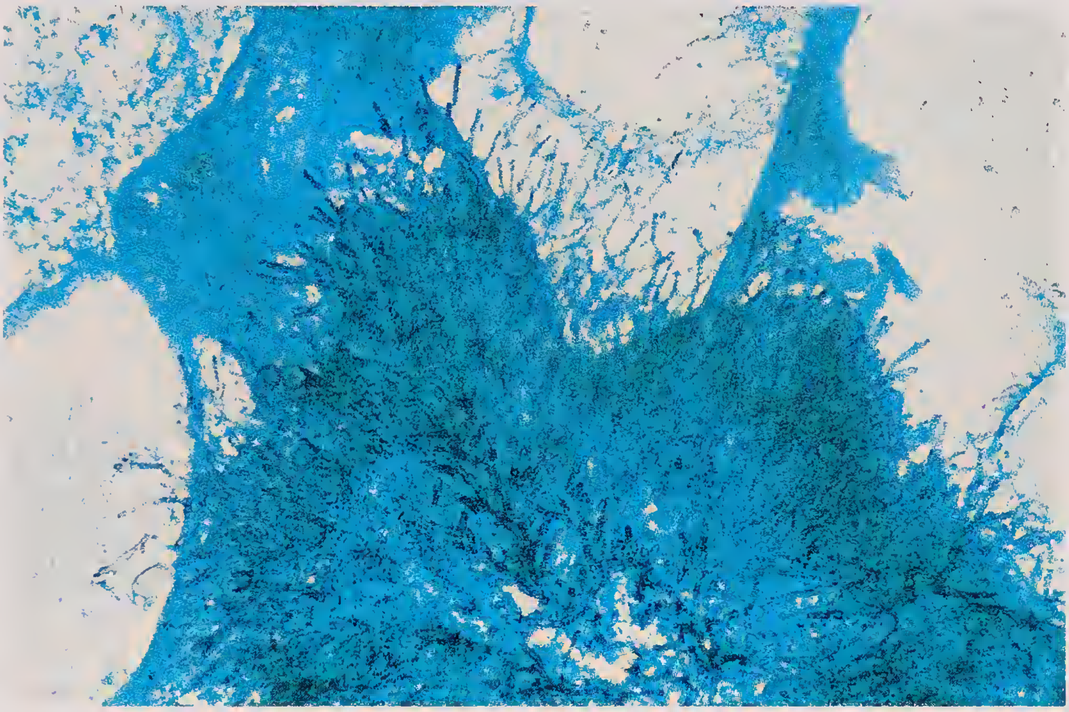

74

74 ◆ Lung tissue with cluster of *Aspergillus* hyphae (Grocott-Gomori stain). These narrow, septate hyphae branch at acute angles, unlike the broad, nonseptate, right-angle branching hyphae in mucormycosis. Evidence of tissue invasion by *Aspergillus* hyphae is diagnostic for invasive disease. *Aspergillus* hyphae can also be found in the mucous plugs of allergic bronchopulmonary aspergillosis and the intracavitary mass or aspergilloma.

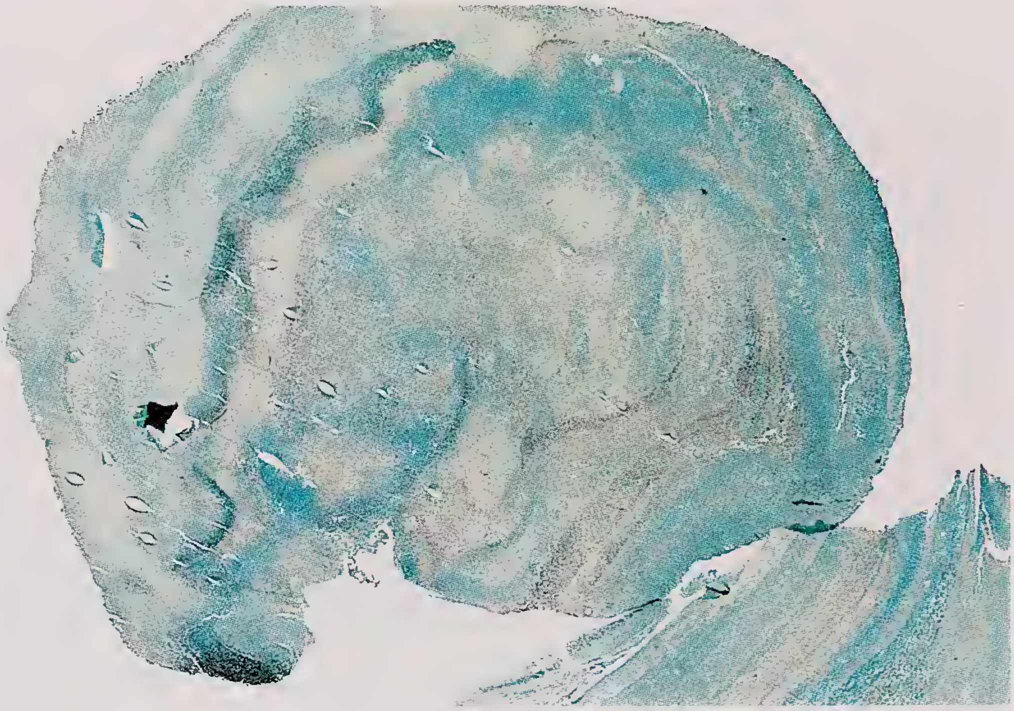

75

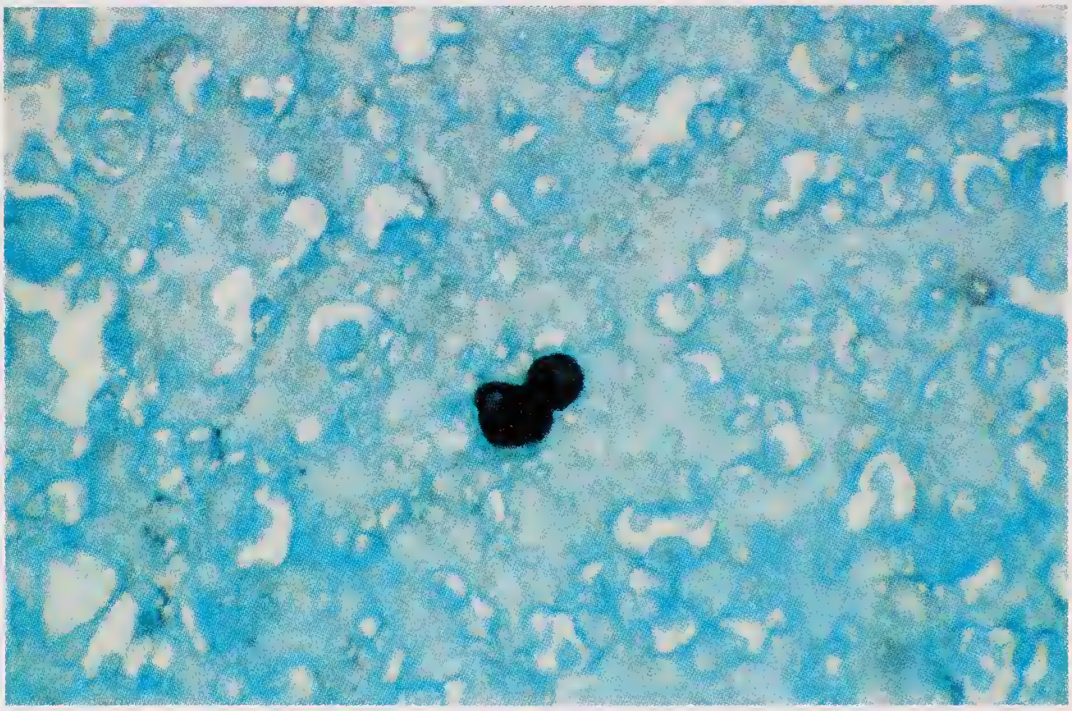

76

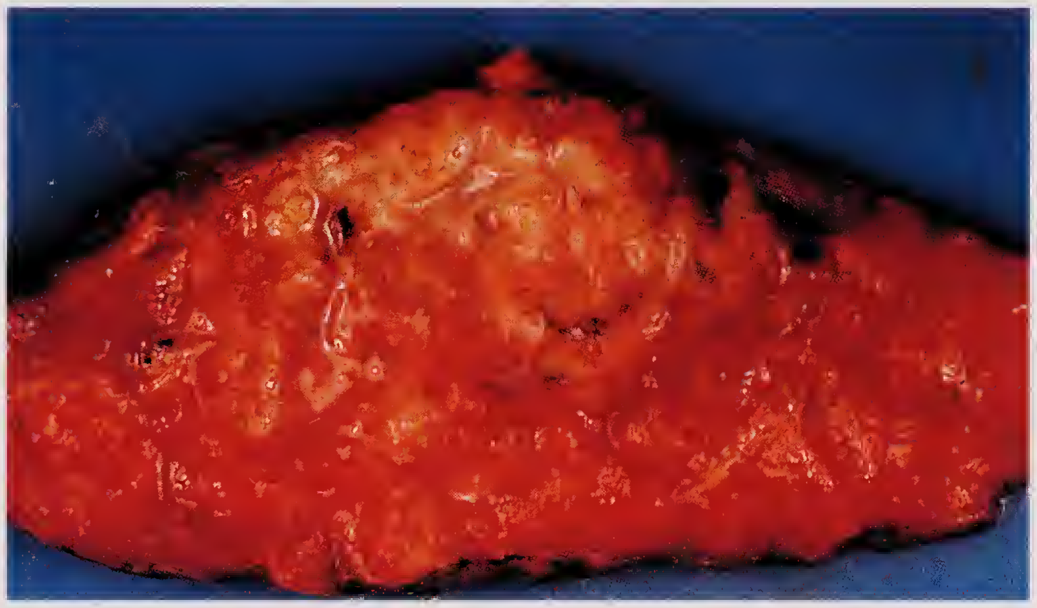

77

75 ♦ Low-power microscopic view of a fungus ball showing characteristic laminated appearance in aspergilloma. Aspergillomas or fungus balls are composed of a tangled mass of *Aspergillus* mycelia and cellular debris from the host. On microscopic examination, one sees zones of mycelial elements alternating with layers of pyknotic cellular debris. Classically, they form in preexisting pulmonary cavities that communicate with the bronchial tree. Tuberculous cavities and fibrocystic spaces of chronic sarcoidosis are involved most frequently.

76 ♦ Blastomycosis (Grocott-Gomori stain).

77 ♦ Lung section demonstrating pulmonary candidiasis with a necrotizing bronchopneumonia and abscess formation.

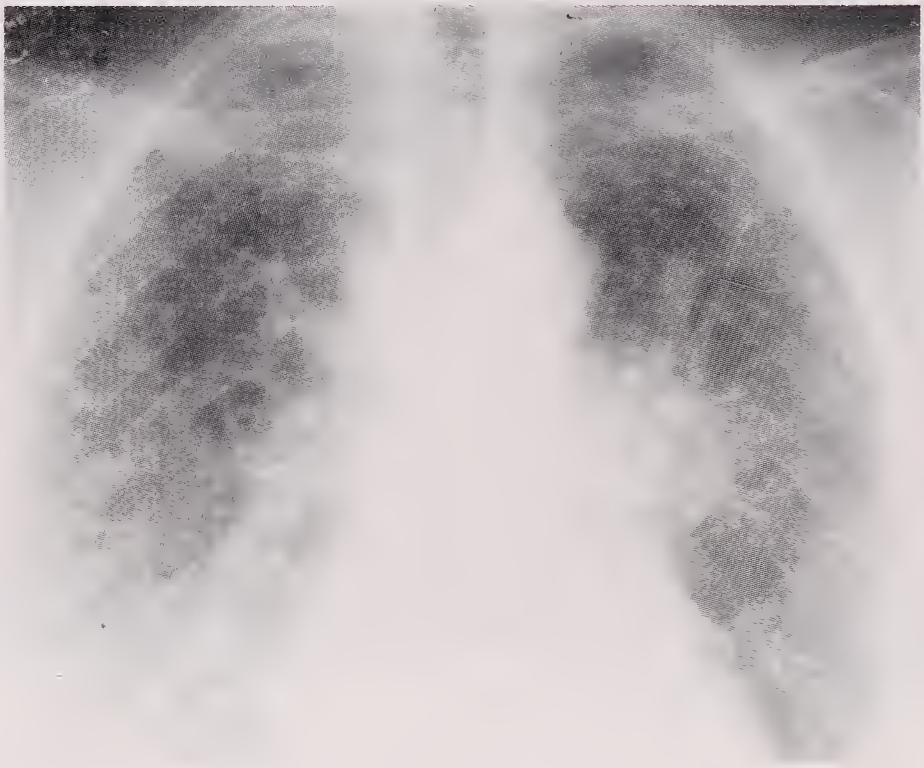

78

78 ♦ Chest radiograph of an individual with disseminated candidiasis, with diffuse, patchy, airspace consolidation. The characteristic radiographic appearance of this type of candidiasis is bilateral, patchy, and homogenous, with poorly defined areas of airspace consolidation. A diffuse nodular pattern, cavitation, and mycetoma formation are also reported.

79 ♦ Colonies of *Candida albicans* in lung tissue. Culture results may not be reliable for diagnosis, because the fungus is part of the normal human flora.

80 ♦ *Candida* yeast and hyphae in lung tissue. Diagnosis is usually made by demonstration of invasive organisms on tissue biopsy. Many cases are not diagnosed until autopsy.

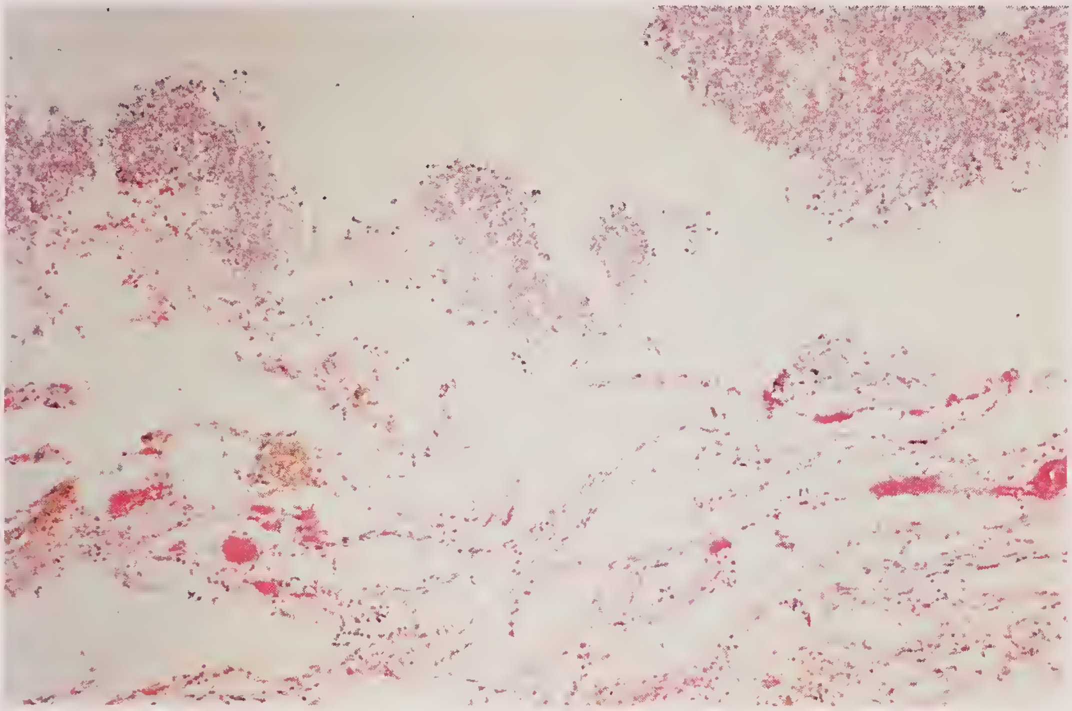

79

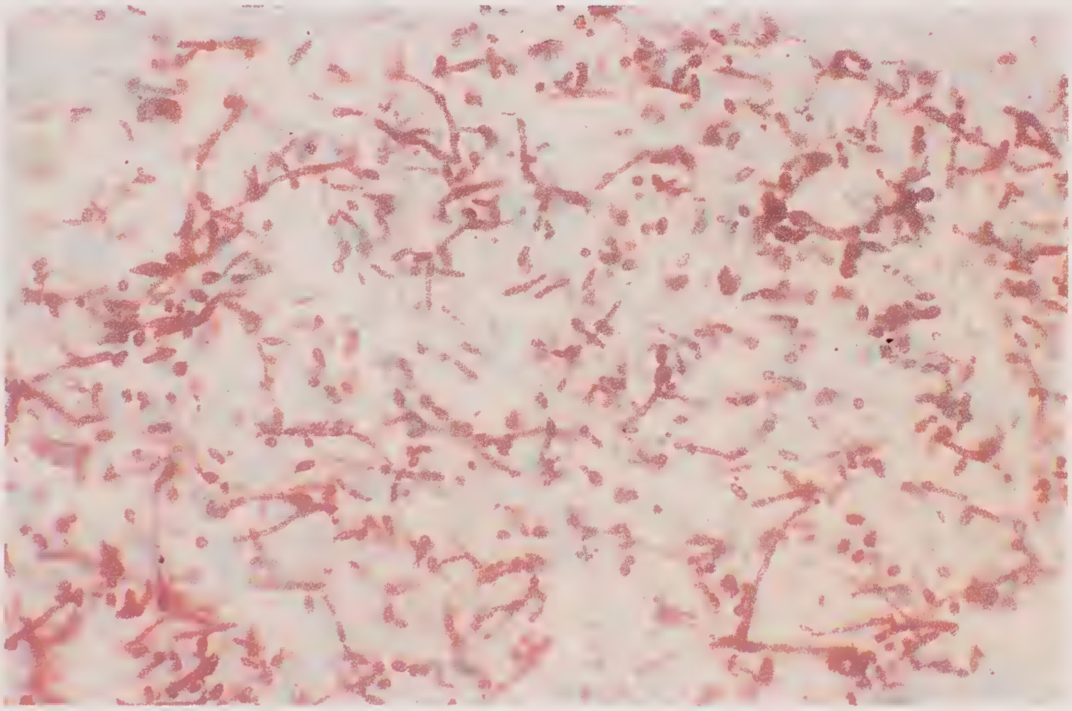

80

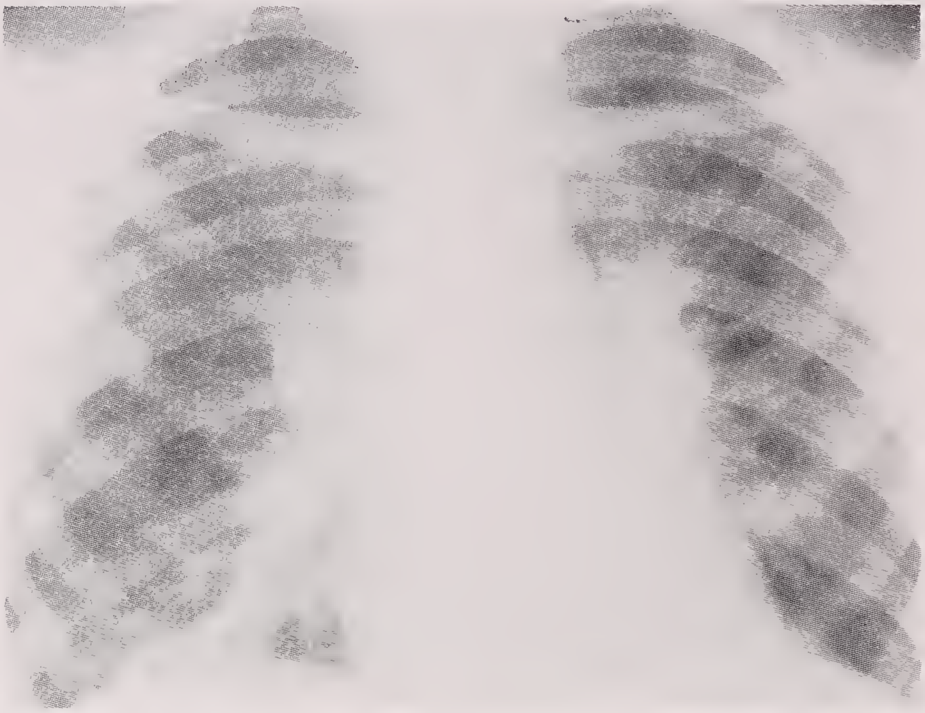

81

81 ◆ Chest radiograph of an individual with primary coccidioidomycosis, showing bilateral, multiple, thin-walled cysts with upper lung zone predominance. In general, the radiographic findings are nonspecific and may be more prominent than the clinical symptoms. In primary coccidioidomycosis, the usual findings on chest radiography are solitary peripheral nodules, single or multiple thin-walled cavities, or airspace consolidation, whereas in chronic progressive coccidioidal pneumonia, apical fibronodular cavitary lesions are usually apparent.

82 ◆ *Coccidioides immitis* spherule in lung tissue (hematoxylin-eosin stain).

83 ◆ *Coccidioides immitis* spherule in lung tissue (Grocott-Gomori stain). The *C immitis* spherule may be found in sputum or in bronchoalveolar lavage specimens.

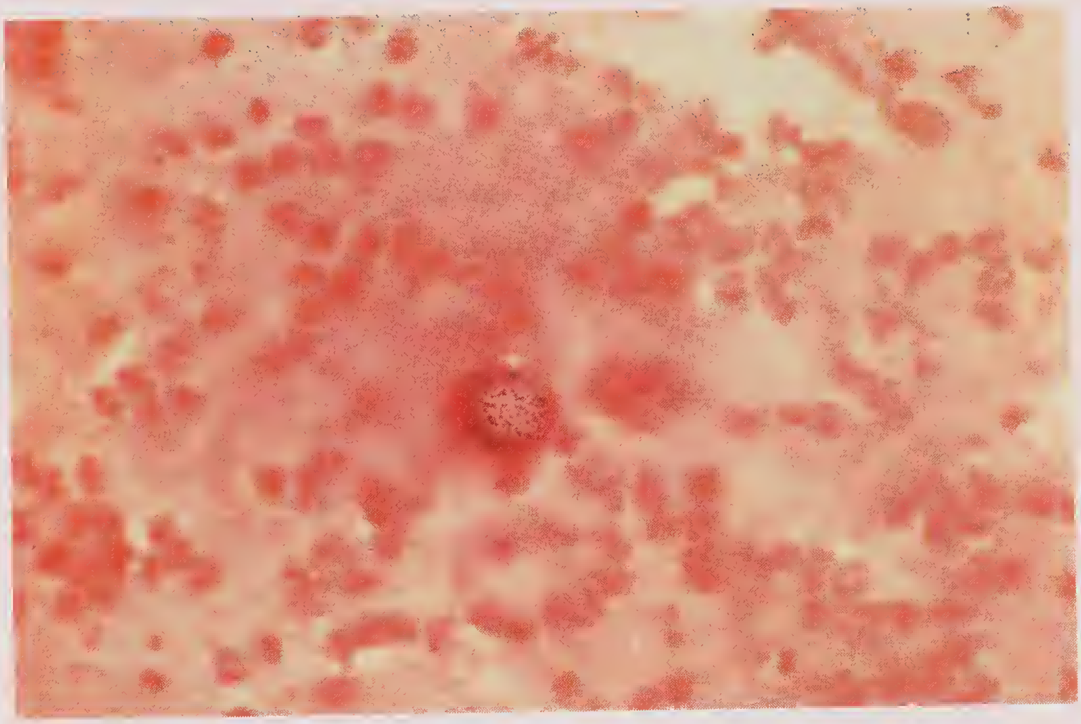

82

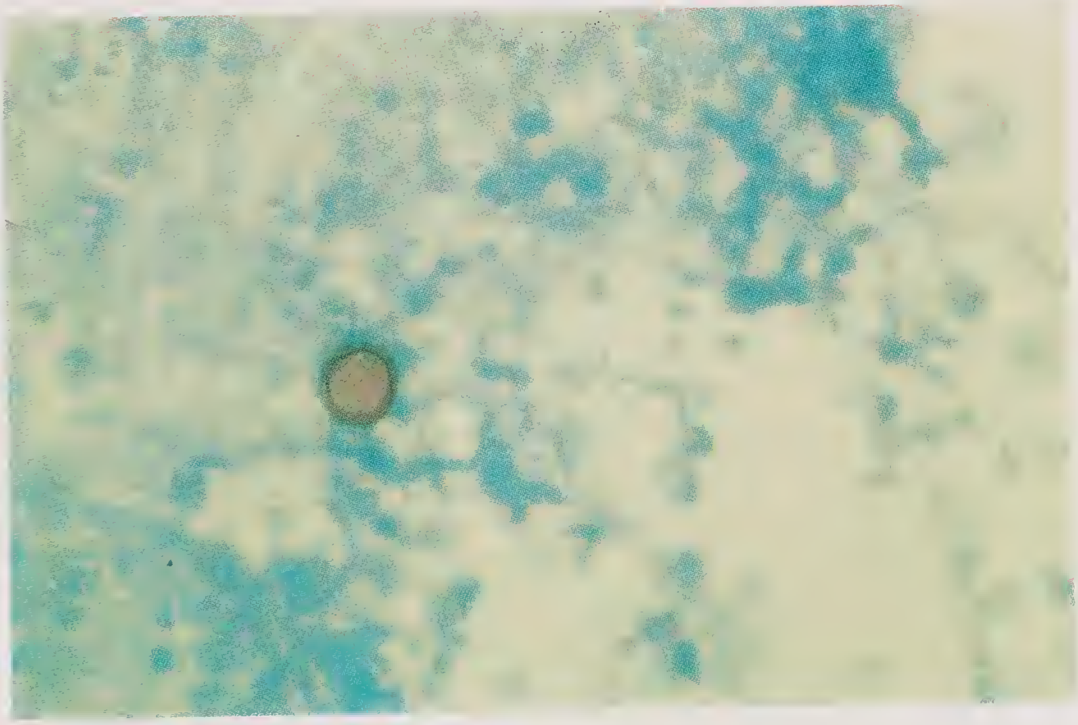

83

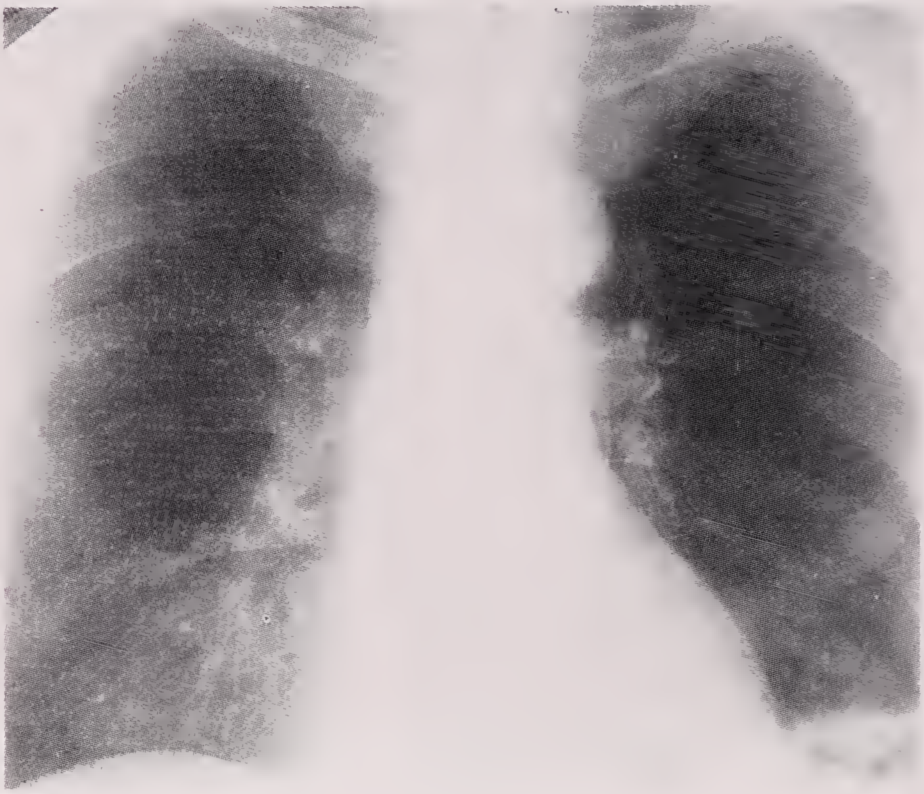

84

84 ♦ Chest radiograph in a patient with a hematologic malignancy and primary pulmonary cryptococcosis. Note the mass in the lower left lung field. A solitary, pleural-based mass is the most common finding on chest radiograph. Other presentations include solitary or multiple nodules, ill-defined areas of pulmonary consolidation, or a diffusely disseminated miliary pattern. Cavitation, hilar or mediastinal adenopathy, and pleural effusions are uncommon.

85 ♦ Computed tomography scan of the chest, showing a cavitary lesion in the left lower lobe.

86 ♦ Lung tissue with abscess formation secondary to *Cryptococcus neoformans.*

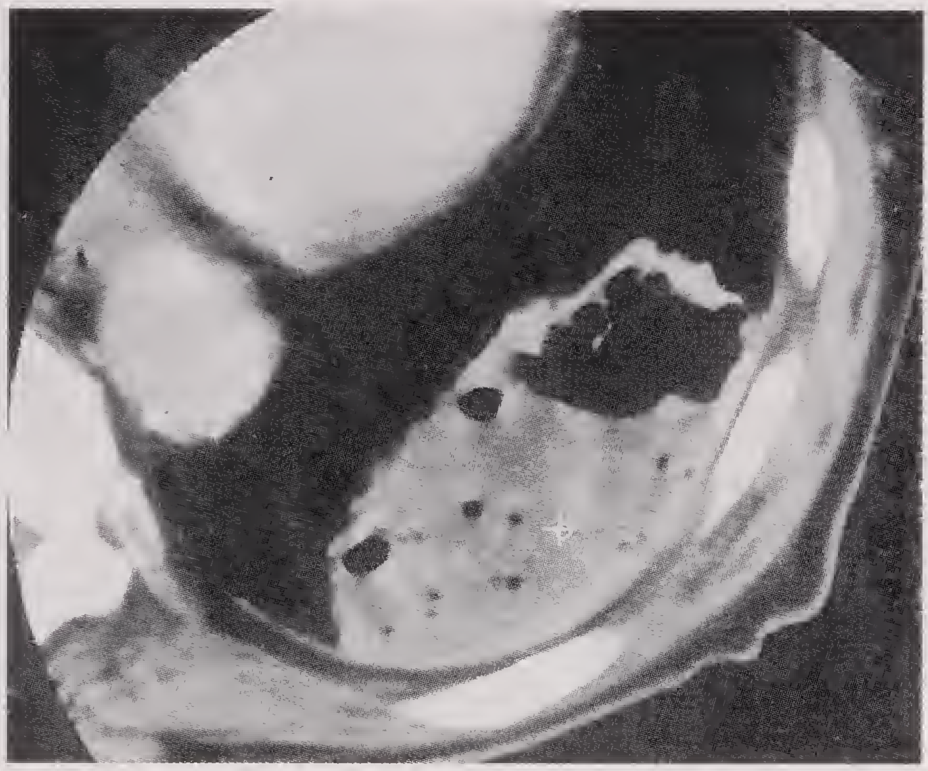

85

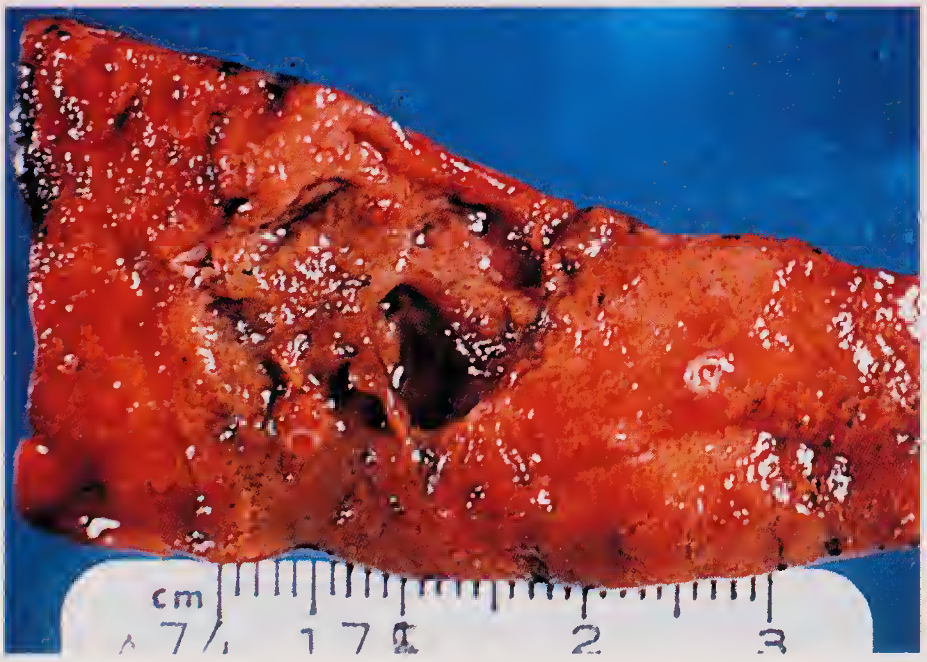

86

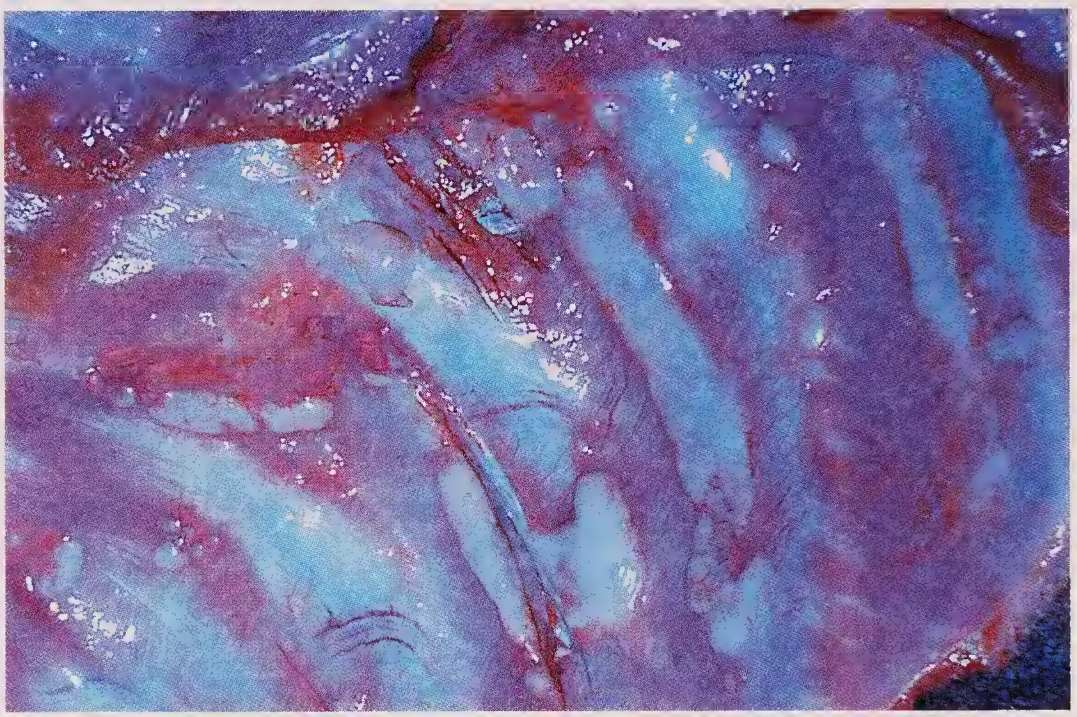

87

87 ◆ Multiple pleural plaques in a patient with disseminated cryptococcosis.

88 ◆ Encapsulated yeast of *Cryptococcus neoformans* in lung tissue (mucicarmine stain). Diagnosis can be made on the basis of cerebrospinal fluid (CSF), sputum, or urine smears with an India ink preparation. The organism is best identified on biopsy specimens using mucicarmine or silver stains. In the majority of patients with meningoencephalitis, cryptococcal antigen is detected in the CSF.

89 ◆ Encapsulated yeast of *Cryptococcus neoformans* in lung tissue (hematoxylin-eosin stain).

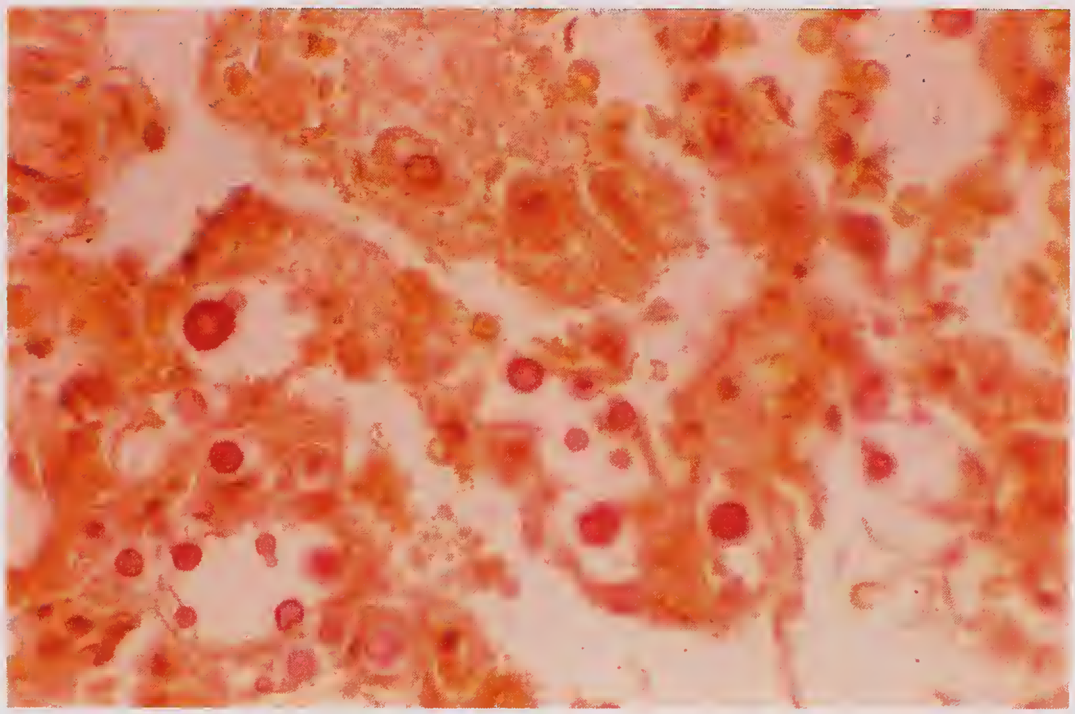

88

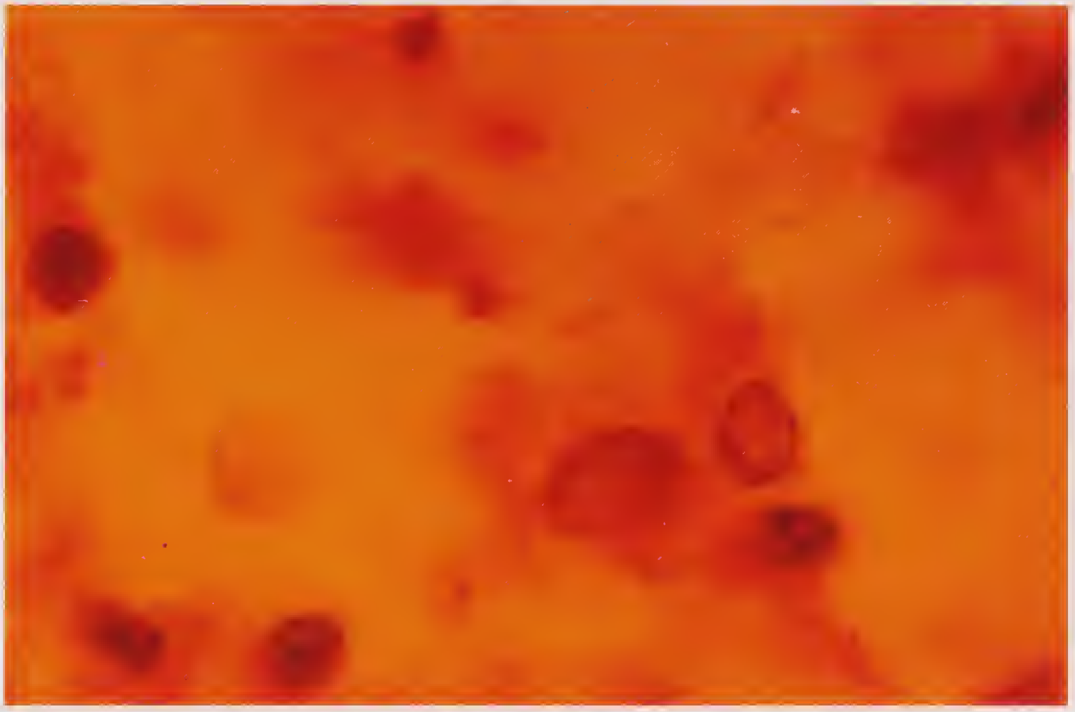

89

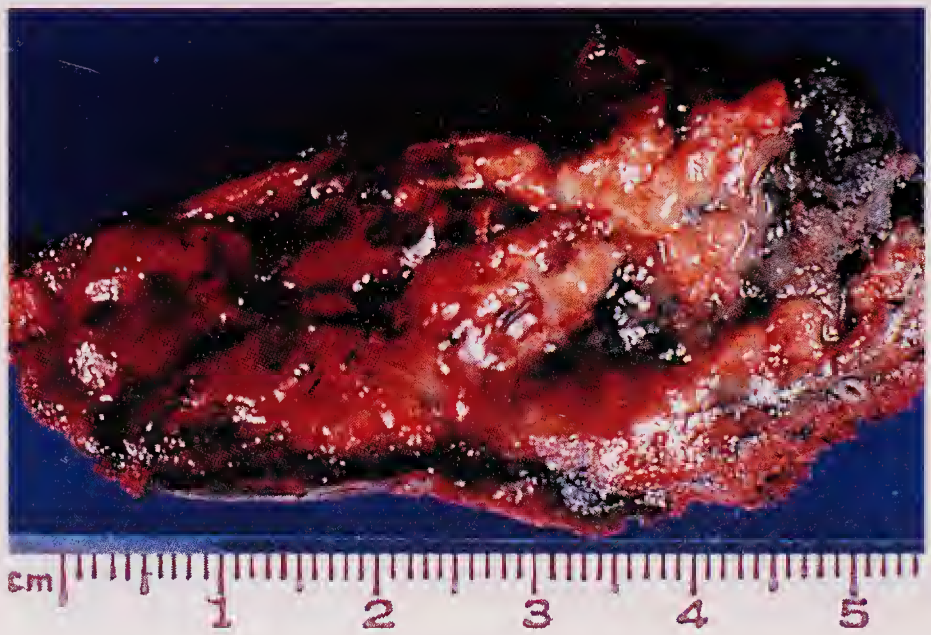

90

90 ◆ Right middle lobe of the lung with organizing bronchopneumonia and abscess formation. An individual with pulmonary mucormycosis can present with a lobar or bronchopneumonia, solitary lung nodule, lung abscess, or pulmonary infarction due to vascular invasion and thrombosis of the blood vessel. Pleural effusions are an uncommon finding. The infection can extend along tissue planes and involve the heart, diaphragm, or mediastinum.

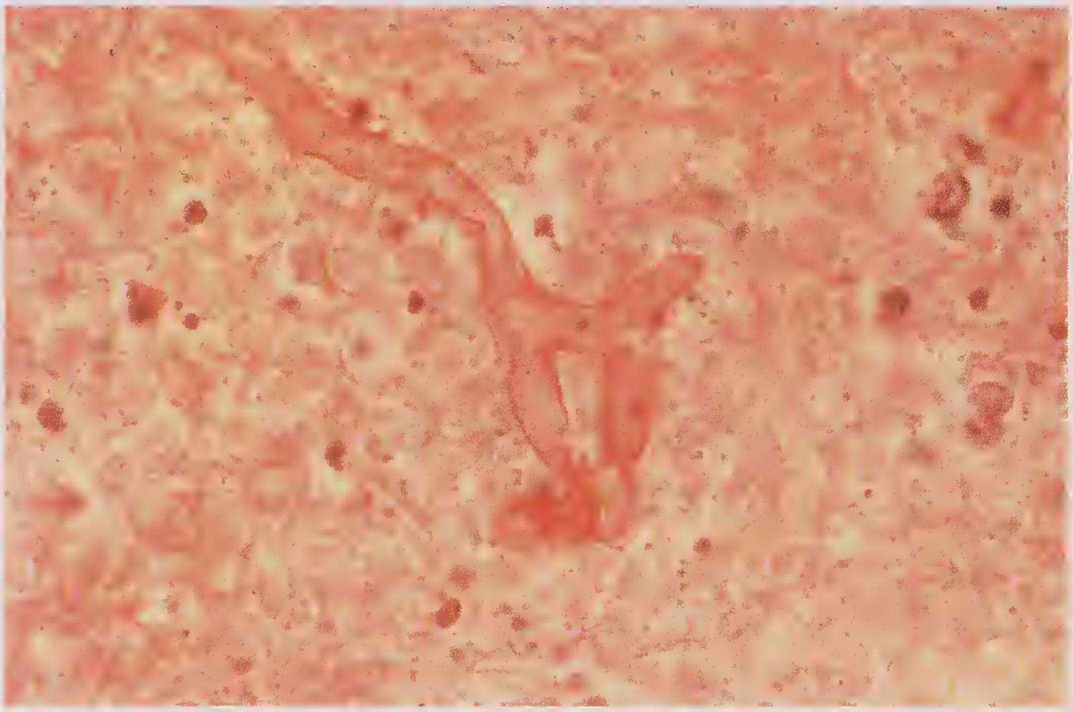

91

91 ♦ Fungal hyphae of mucormycosis in lung tissue (hematoxylin-eosin stain). Diagnosis is made by histologic examination of the affected tissue. The hyphae are characteristically broad and nonseptate, with right-angle branching. Growing hyphae can be found in both viable and necrotic tissue, invading blood vessels, or extending along tissue planes.

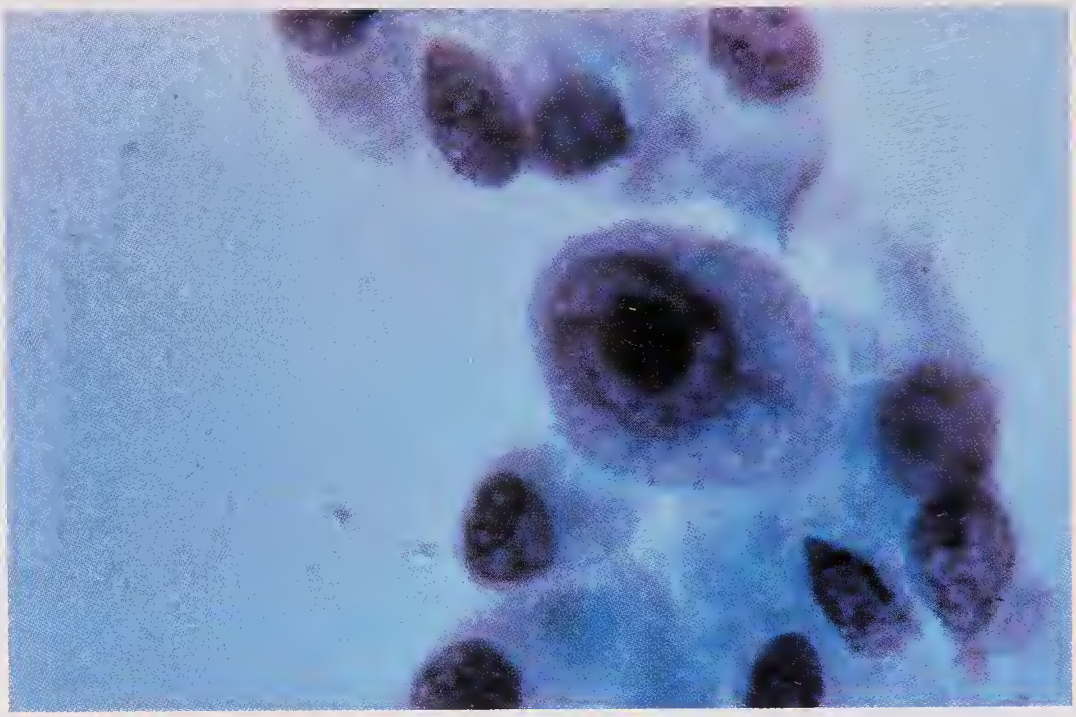

92

92 ♦ Specimen from bronchoalveolar lavage, showing an intracellular inclusion body. The cytologic appearance of a dense intranuclear inclusion body and a halo separating it from the thickened nuclear membrane, which is classic in cytomegalovirus (CMV)-infected cells, is diagnostic of CMV pneumonitis.

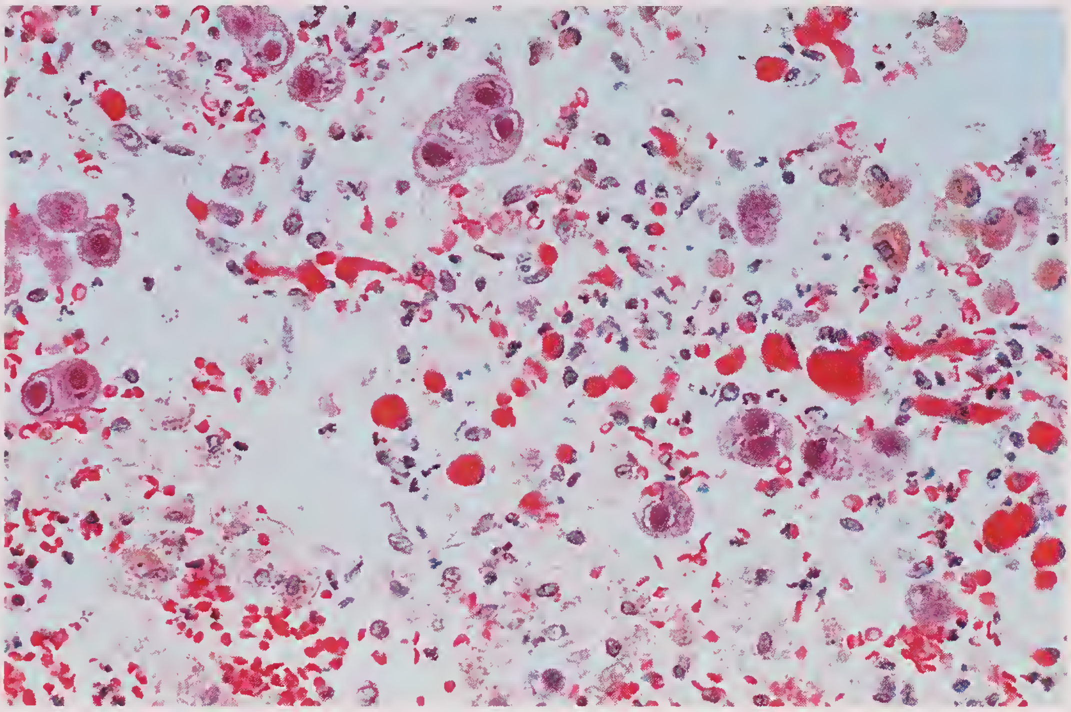

93

93 ♦ Photomicrograph showing characteristic cytomegaly, with intranuclear and intracytoplasmic inclusions of cytomegalovirus.

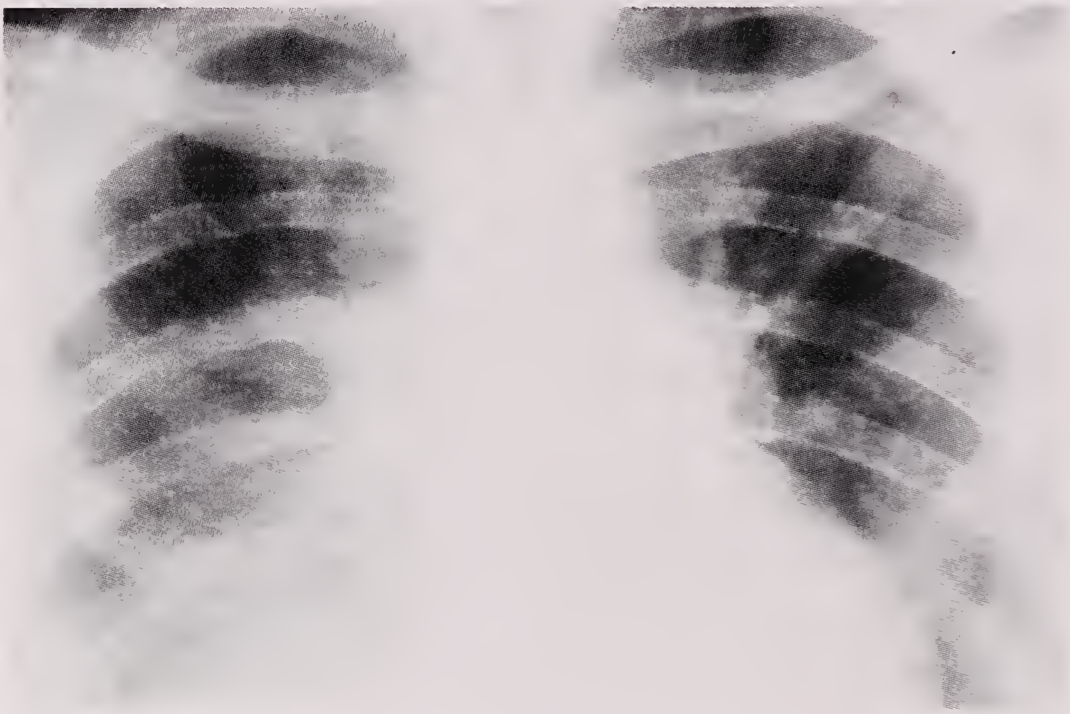

94

94 ♦ Typical radiographic appearance of cytomegalovirus pneumonitis, which involves diffuse or focal interstitial pneumonitis. Rarely, affected individuals may present with miliary infiltrate, focal areas of segmental consolidation, or discrete nodules.

95 ♦ Autopsy study depicting diffuse cytomegalovirus pneumonitis.

96 ♦ Autopsy specimen of fulminant measles pneumonia, showing diffuse pulmonary parenchymal involvement.

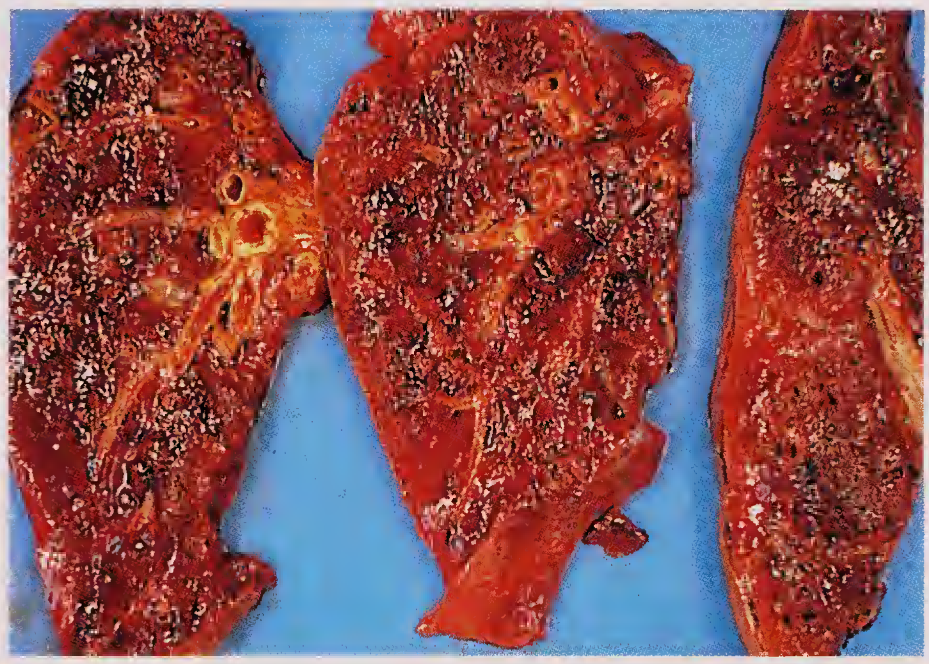

95

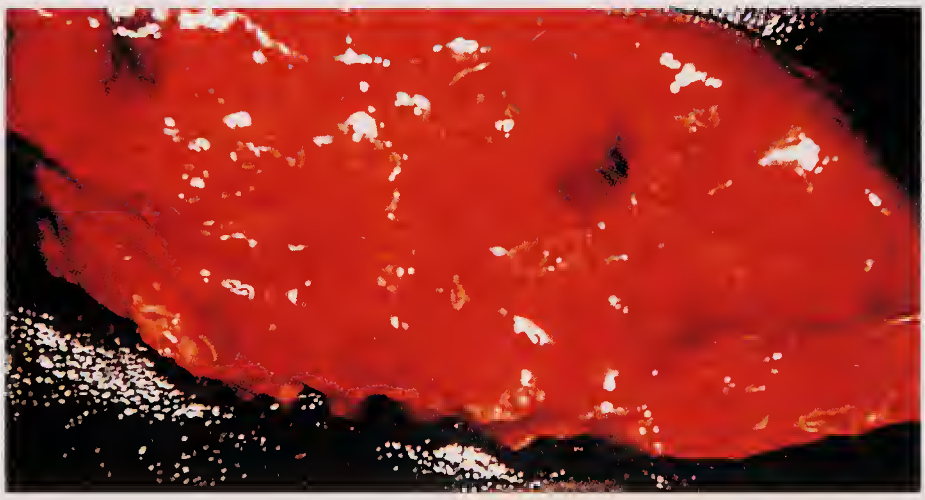

96

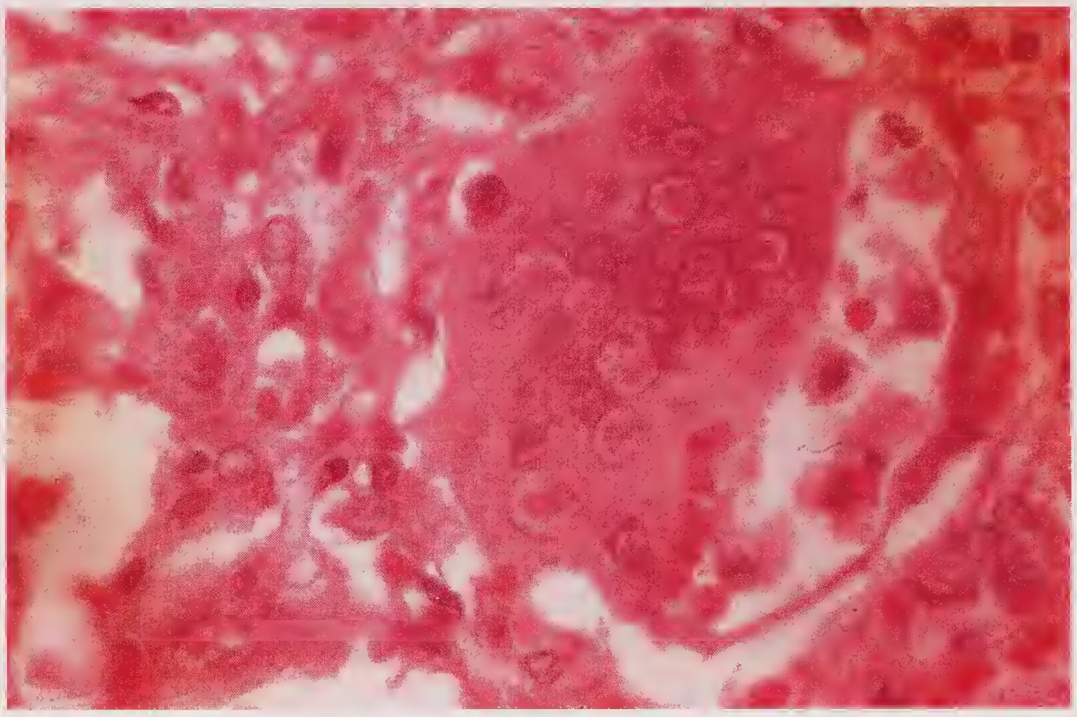

97

97 ◆ Measles pneumonitis, showing a characteristic multinucleated giant cell (hematoxylin-eosin stain). Intracytoplasmic and intranuclear inclusions have been identified within the giant cells. These have also been found in parainfluenza and respiratory syncytial virus infection.

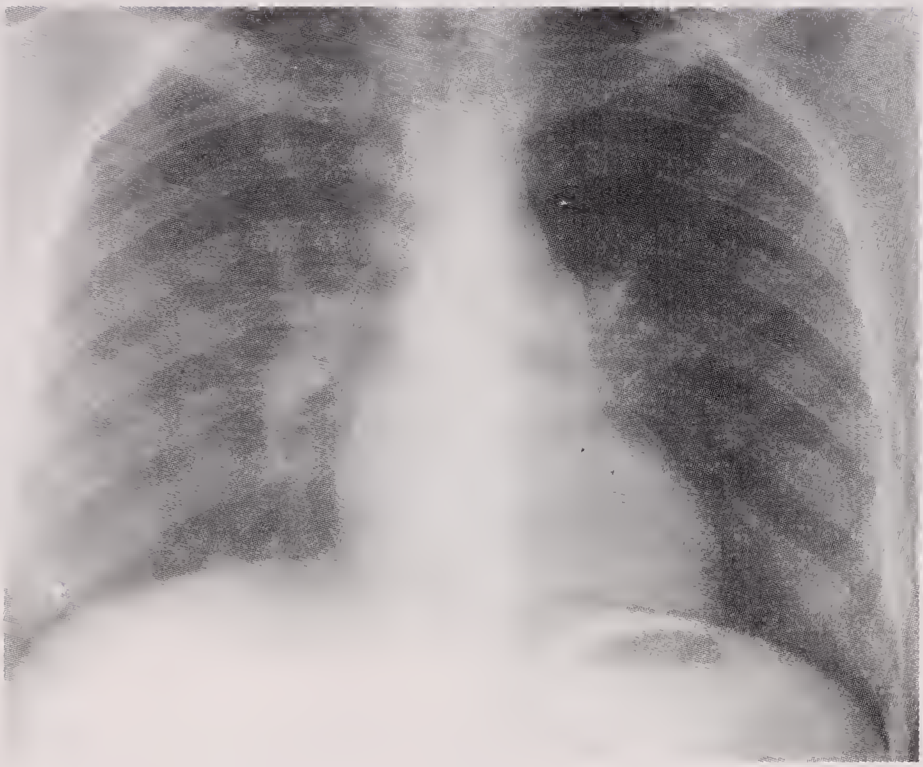

98

98 ♦ Chest radiograph (posteroanterior view) in a young man with acquired immunodeficiency syndrome, showing no significant infiltrate. The typical presentation involves bilateral, diffuse, interstitial infiltrates in a perihilar distribution. Alveolar and interstitial infiltrates usually are associated with more severe disease. Other findings include a solitary nodule, lobar consolidation, thin-walled pneumatoceles, and spontaneous pneumothorax. Some individuals present with hypoxemia and normal-appearing chest radiographs. Bilateral upper lobe involvement can occur in patients on prophylactic aerosolized pentamidine.

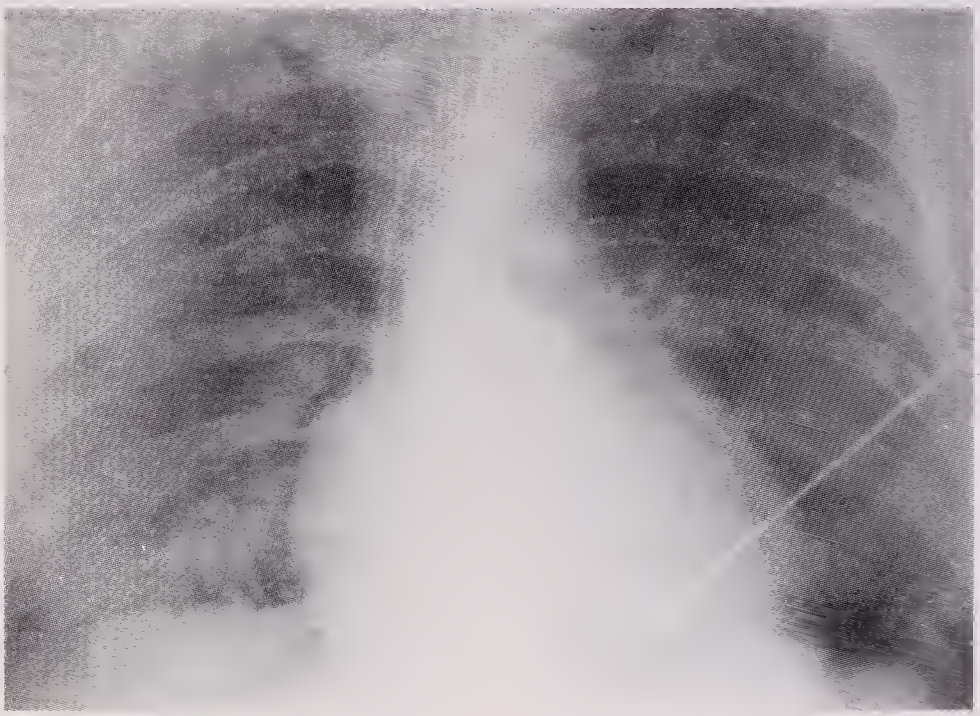

99

99 ♦ Chest radiograph in a young man with acute respiratory failure. This anteroposterior view contains bilateral, diffuse alveolar and interstitial infiltrate.

100 ♦ *Pneumocystis carinii* organisms. The diagnosis is established with the demonstration of organisms in respiratory tract secretions or lung tissue. The sputum or bronchoalveolar lavage fluid is prepared using either Giemsa, methenamine silver, or immunofluorescent staining.

101 ♦ Transbronchial lung biopsy in a patient with *Pneumocystis carinii* pneumonia. Histologically, this usually corresponds to alveoli filled with foamy, acellular, eosinophilic, intra-alveolar exudate. *Pneumocystis carinii* cysts can be seen as clusters of rounded, clear spaces within the eosinophilic material.

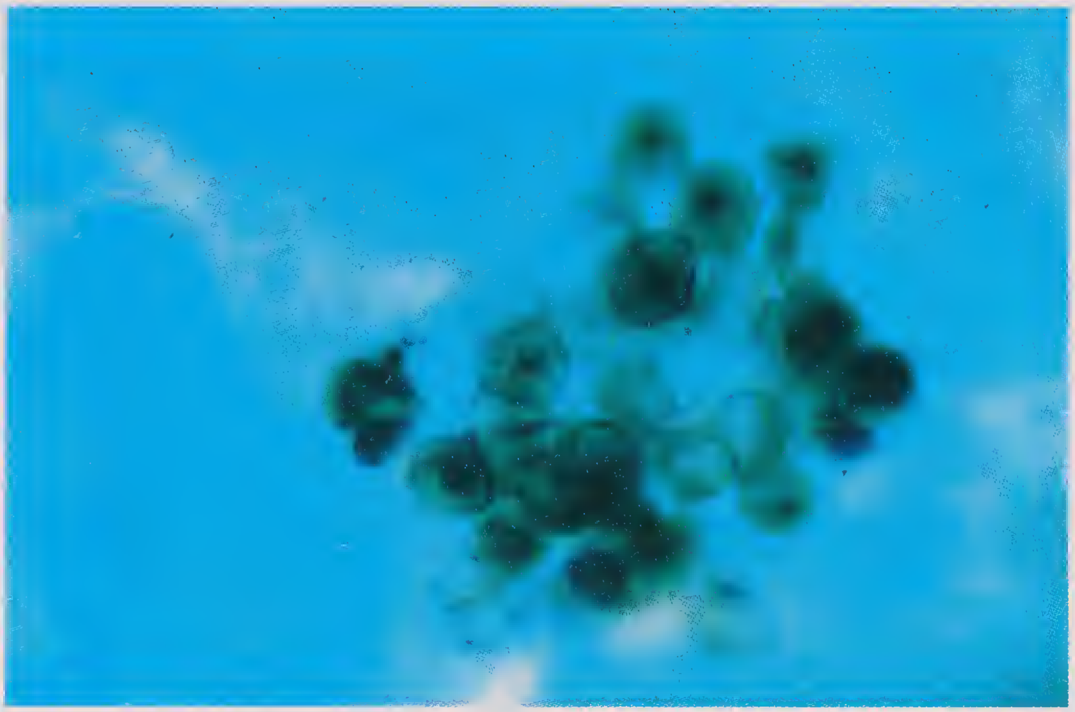

100

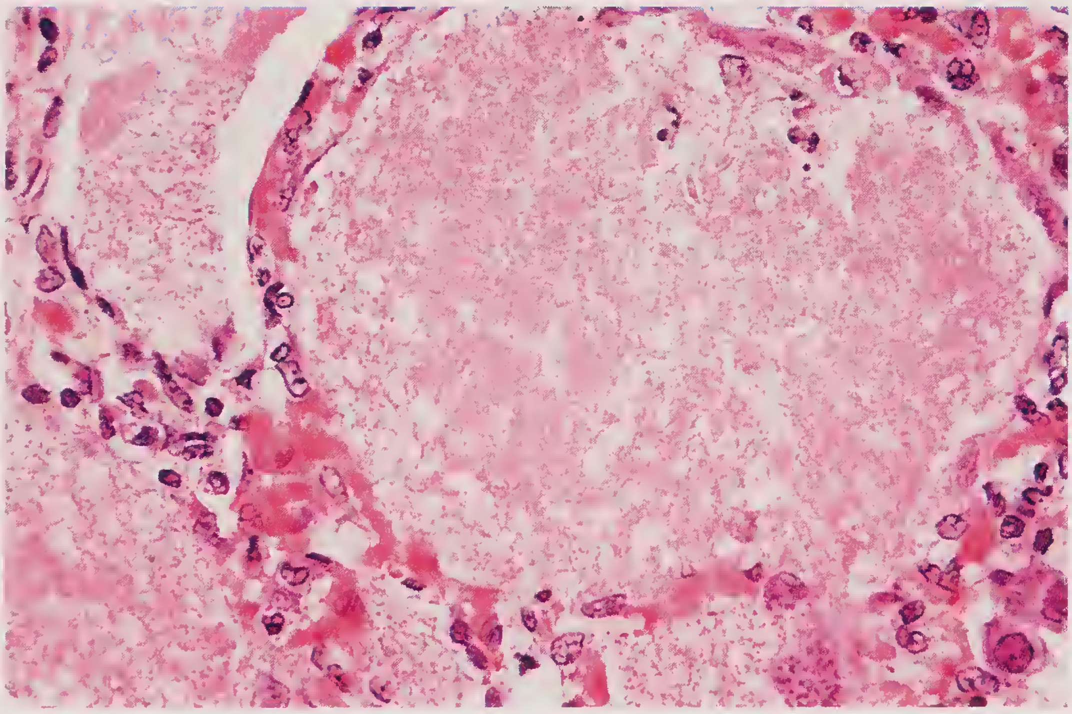

101

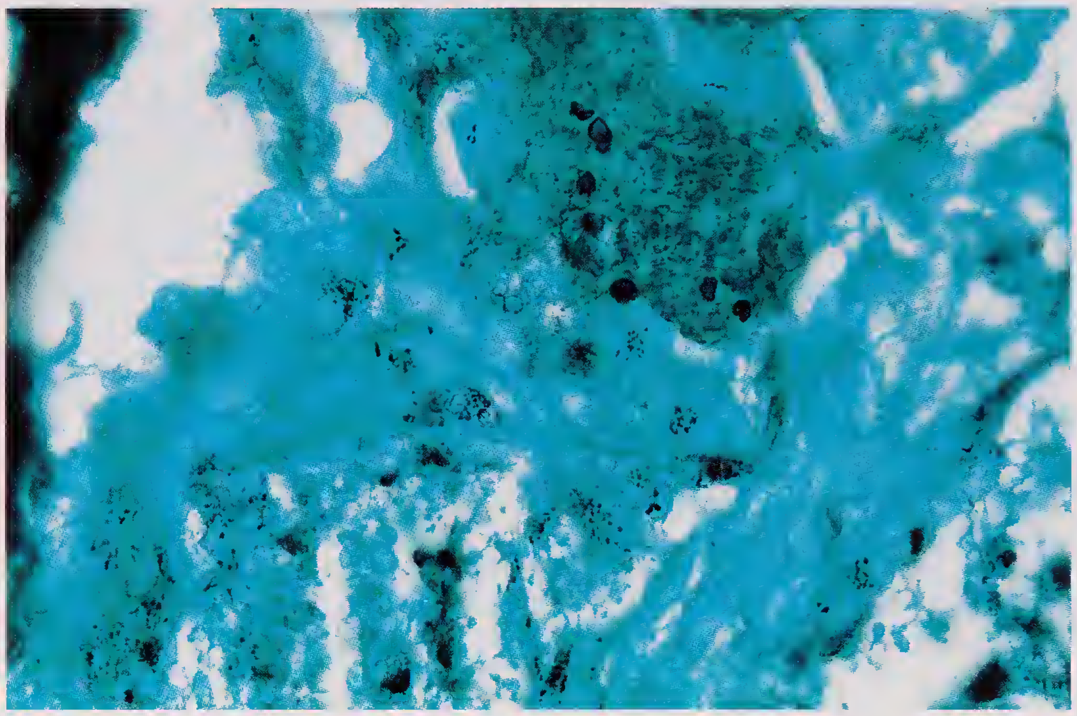

102

102 ♦ Transbronchial lung biopsy showing *Pneumocystis carinii* (silver methenamine stain). The saucer-shaped cysts, which are 5 to 7µ in size, are best identified by the methenamine silver technique, which stains the cyst wall.

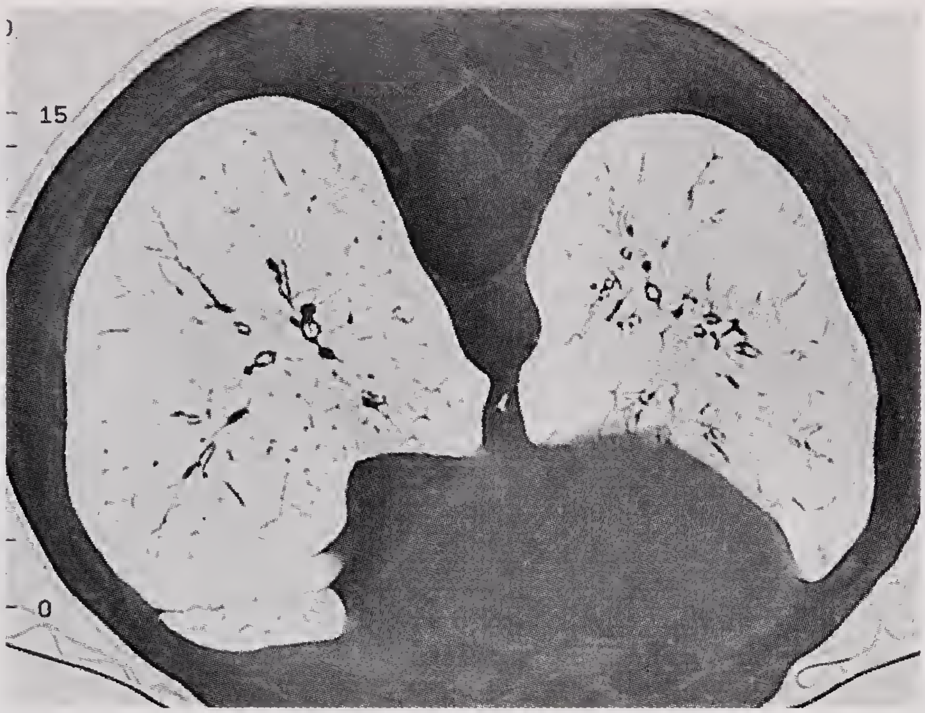

103

103 ♦ Computed tomography (CT) scan in a man with bronchiectasis, an irreversible abnormal dilation of bronchi, which is usually due to infection. Bronchiectasis may be localized or generalized. Currently, CT is the diagnostic modality of choice for identification of bronchiectasis. Thick-walled bronchi are considered dilated when they are bigger than the adjacent blood pulmonary vessels.

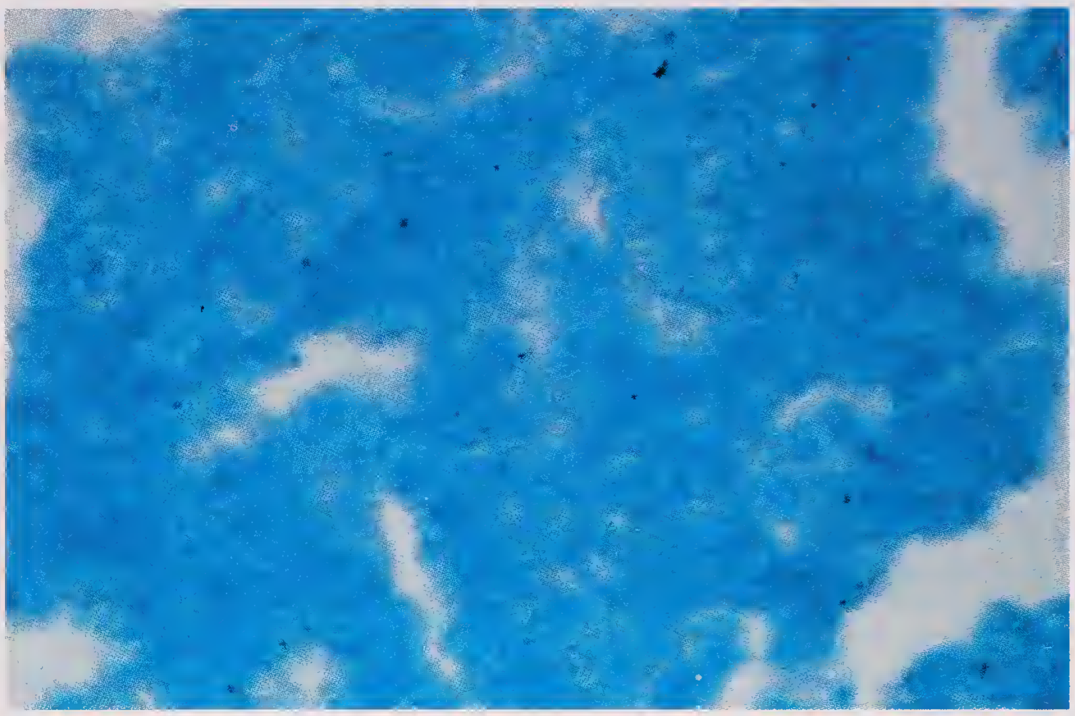

104

104 ◆ *Mycobacterium tuberculosis* (acid-fast stain). Typically, *M tuberculosis* is weakly Gram-positive or colorless.

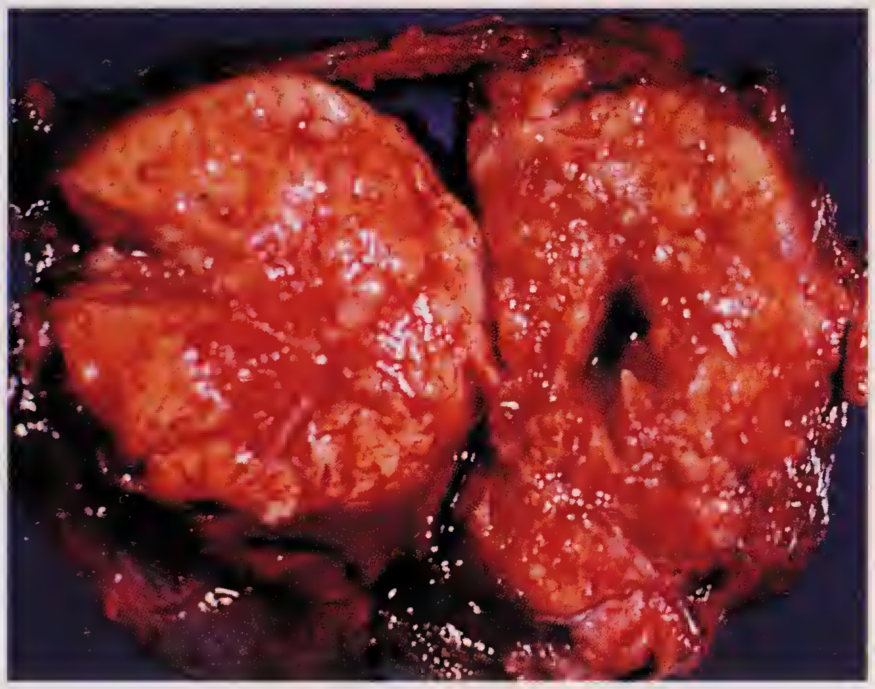

105

105 ♦ Lung biopsy showing caseating necrotic nodule of *Mycobacterium tuberculosis.*

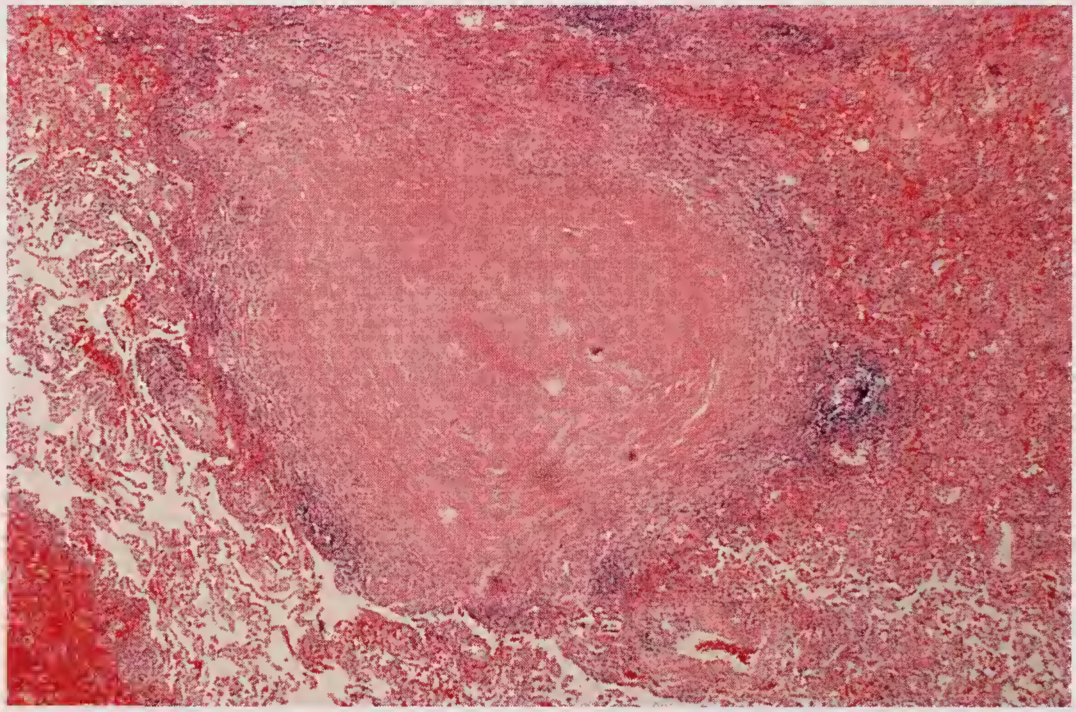

106

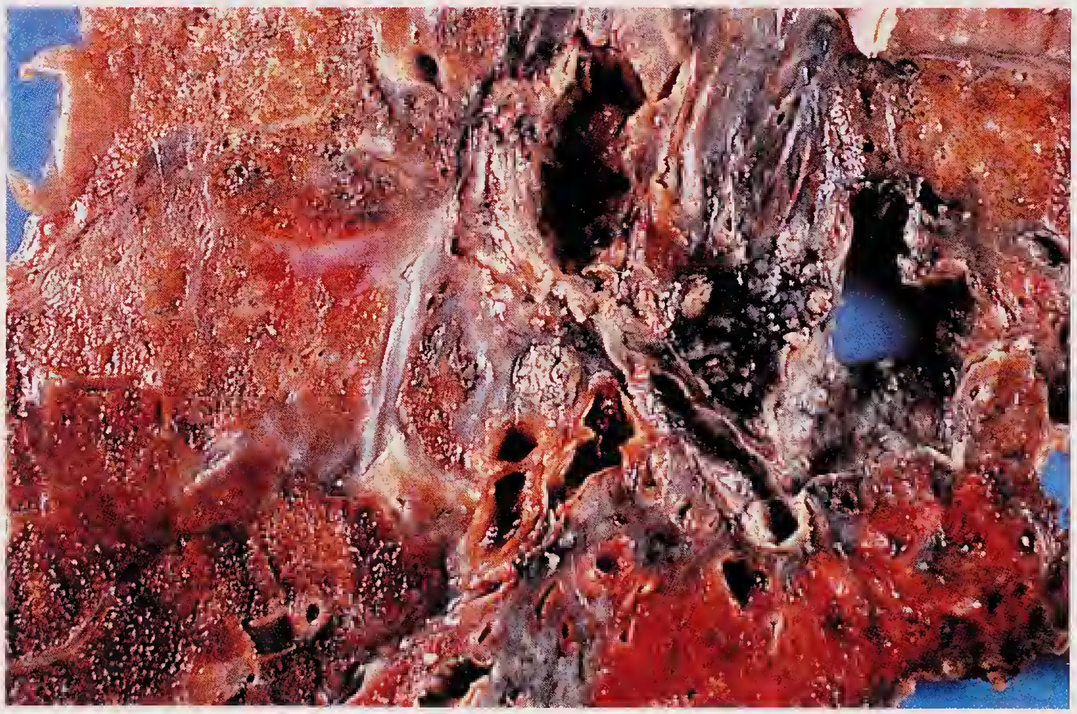

107

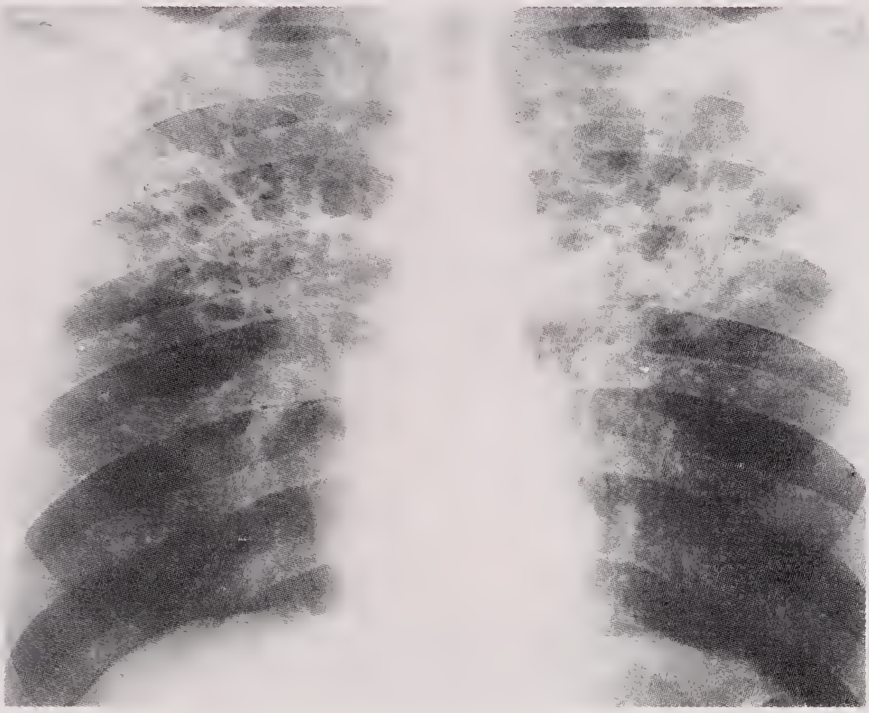

108

106 ♦ Caseating, necrotic nodule of *Mycobacterium tuberculosis* (hematoxylin-eosin stain).

107 ♦ Autopsy section showing calcified hilar lymph nodes with *Mycobacterium tuberculosis.*

108 ♦ Chest radiograph of the classic, biapical, cavitary lesions of *Mycobacterium tuberculosis.* Note that tuberculosis can affect other regions of the lung beside the apical areas. In the primary infection in adolescents and adults, any pulmonary infiltrate may represent *M tuberculosis.* Lower lobe disease can occur in older patients and in individuals with human immunodeficiency virus or endobronchial tuberculosis with distal airway obstruction.

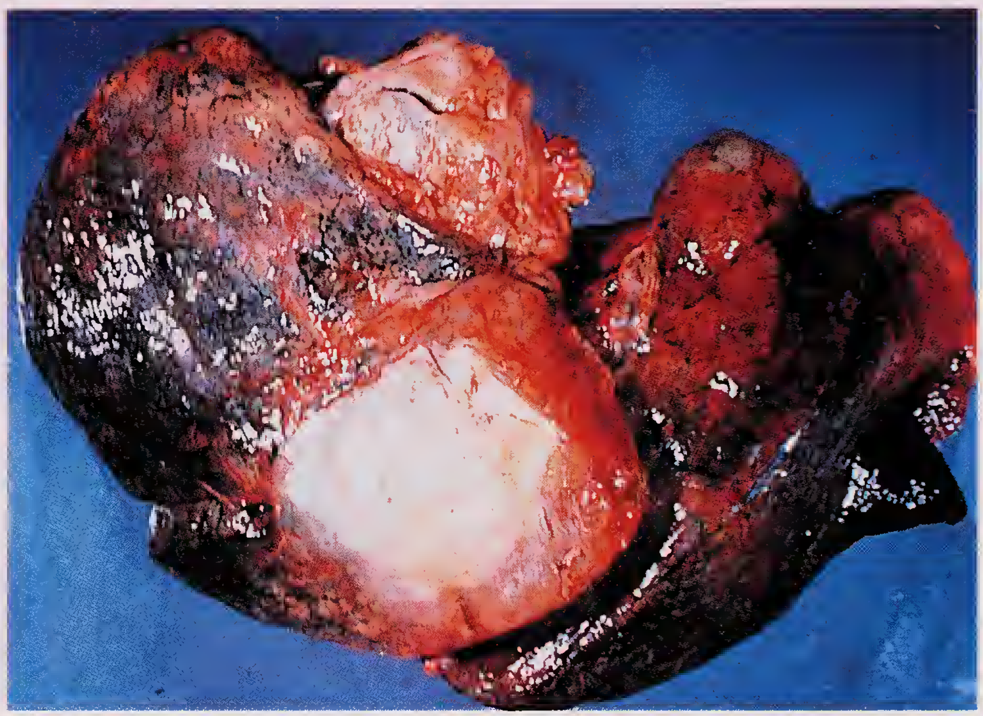

109

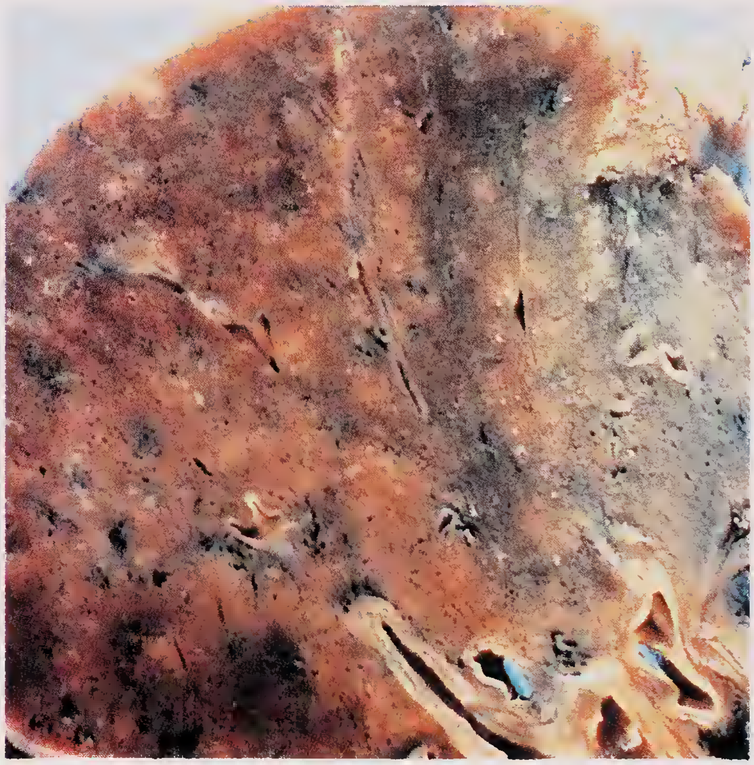

110

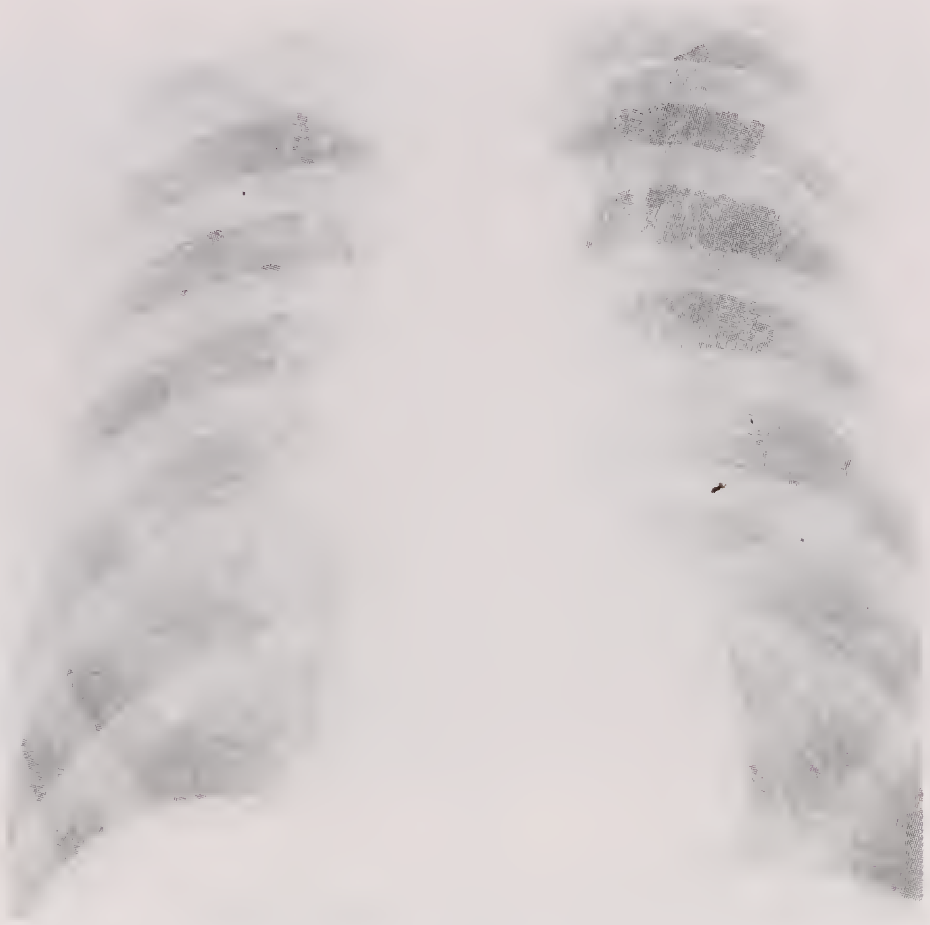

111

109 ♦ *Mycobacterium tuberculosis* pleurisy. Pleural infection by *M tuberculosis* occurs soon after primary infection, together with chronic pulmonary infection, and in association with miliary (disseminated) infection. It is accompanied by an exudative pleural effusion that usually shows a lymphocytic cell population with thoracentesis.

110 ♦ Autopsy section showing miliary tuberculosis. This is representative of hematogenously spread, progressive, disseminated mycobacterial disease.

111 ♦ Chest radiograph of an individual with miliary tuberculosis.

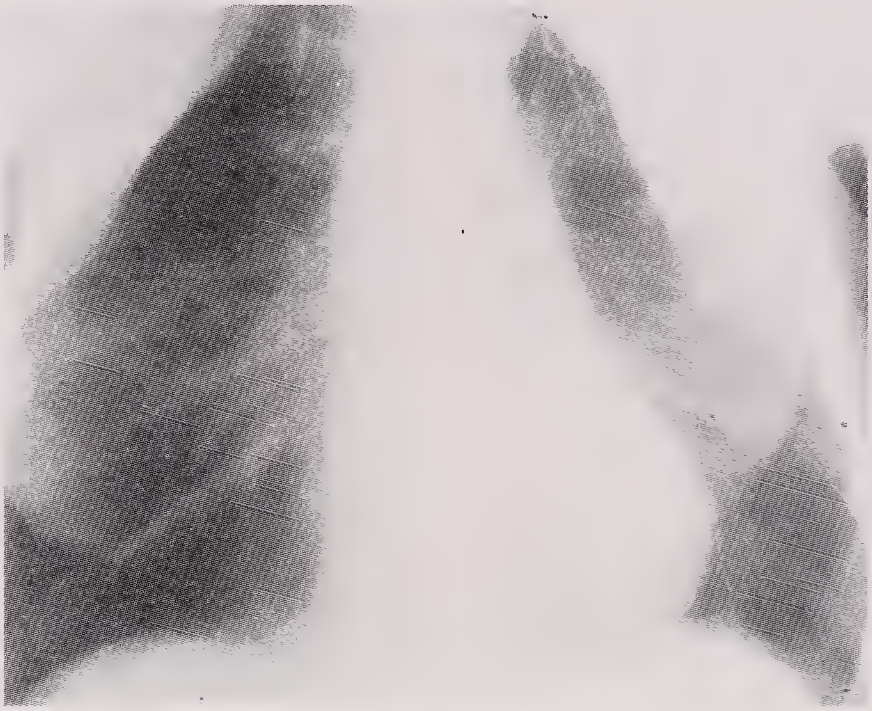

112

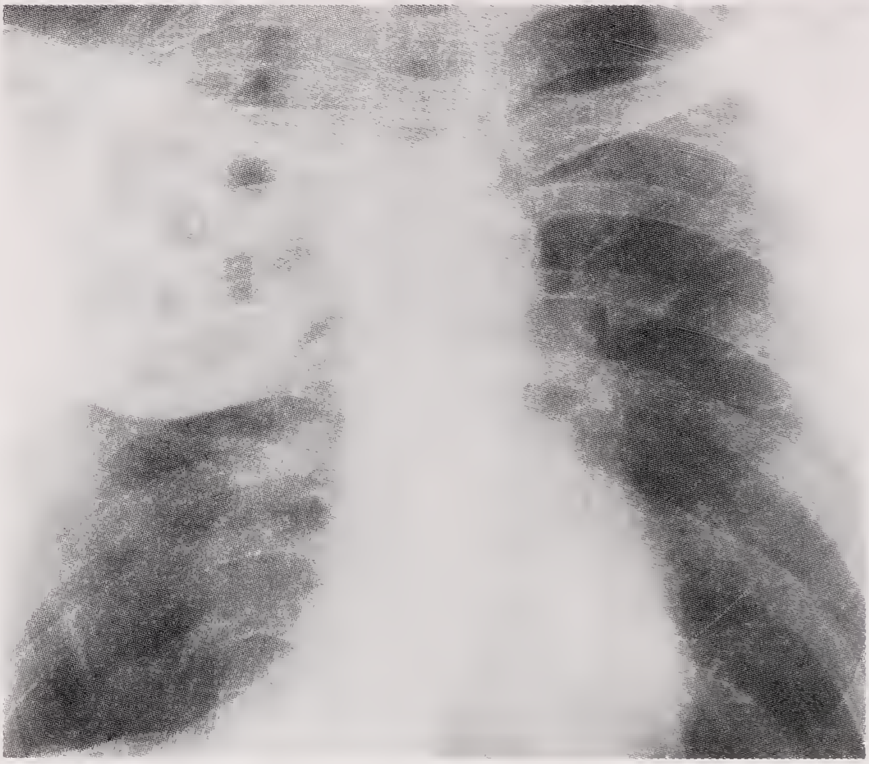

113

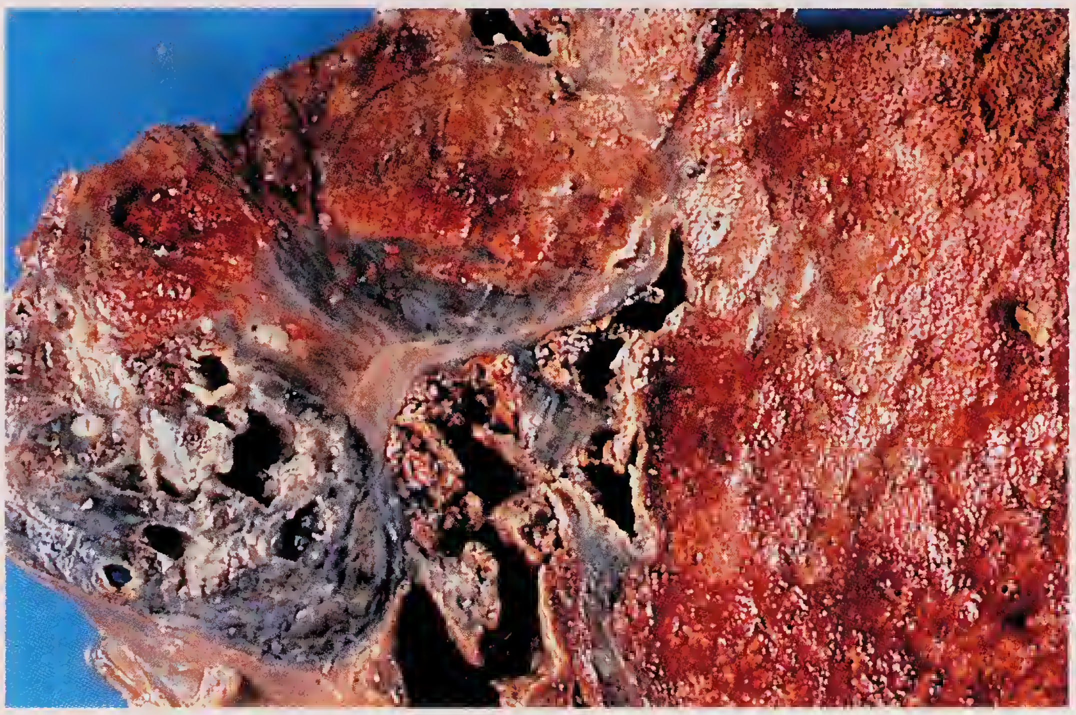

114

112-113 ♦ Chest radiographs showing previous surgical therapy for *Mycobacterium tuberculosis*. Before antituberculous drug therapy was developed, various surgical techniques, including thoracoplasty and plombage, were used to collapse the *M tuberculosis* cavities.

114 ♦ Autopsy section showing a cavitary lung lesion of *Mycobacterium tuberculosis*.

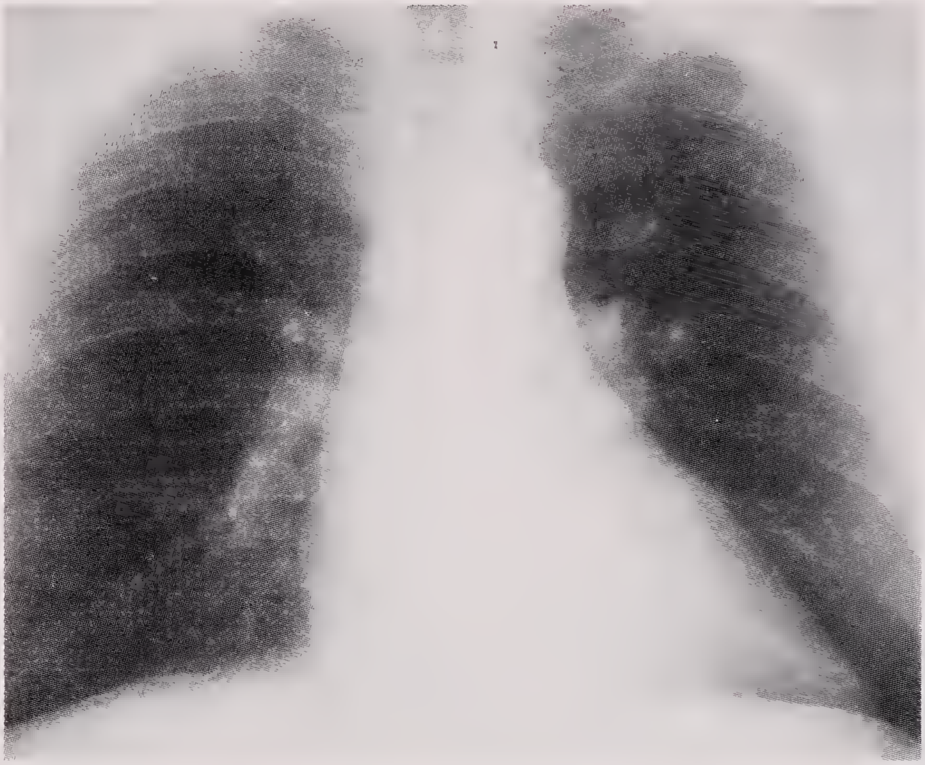

115

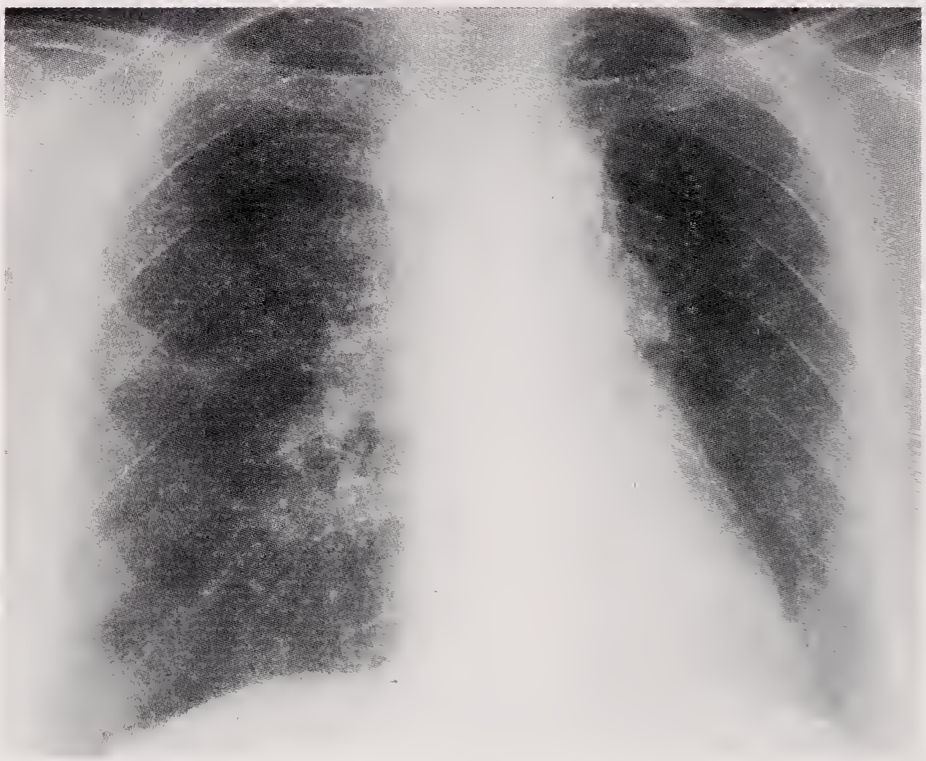

116

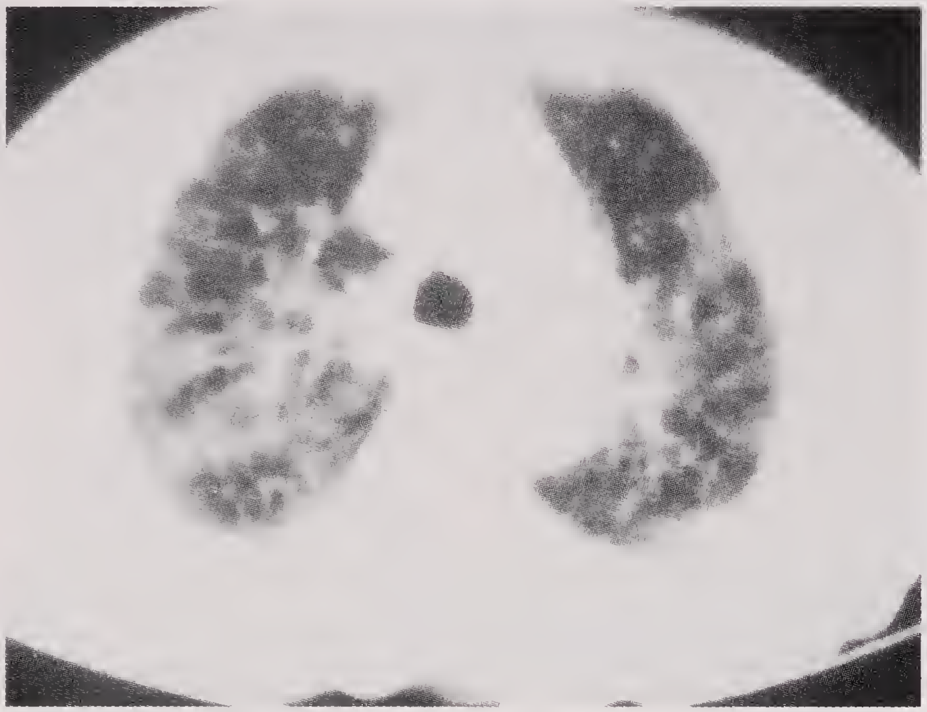

117

115-117 ♦ Radiographic progression of the primary infection of *Mycobacterium tuberculosis.* The initial infection is usually in the midlung zone. Single or multiple foci of infection occur. The Ghon complex refers to initial focus of the infection in the lung parenchyma, and the Ranke complex refers to the combination of the Ghon complex with extension of the infection to the regional hilar lymph nodes. Over time, individuals develop a right lower lobe infiltrate with progressive enlargement and calcification of the right hilar lymph nodes. In this particular patient, mycobacterial disease, with multiple cavities and fibrotic changes, is discovered on computed tomography of the chest.

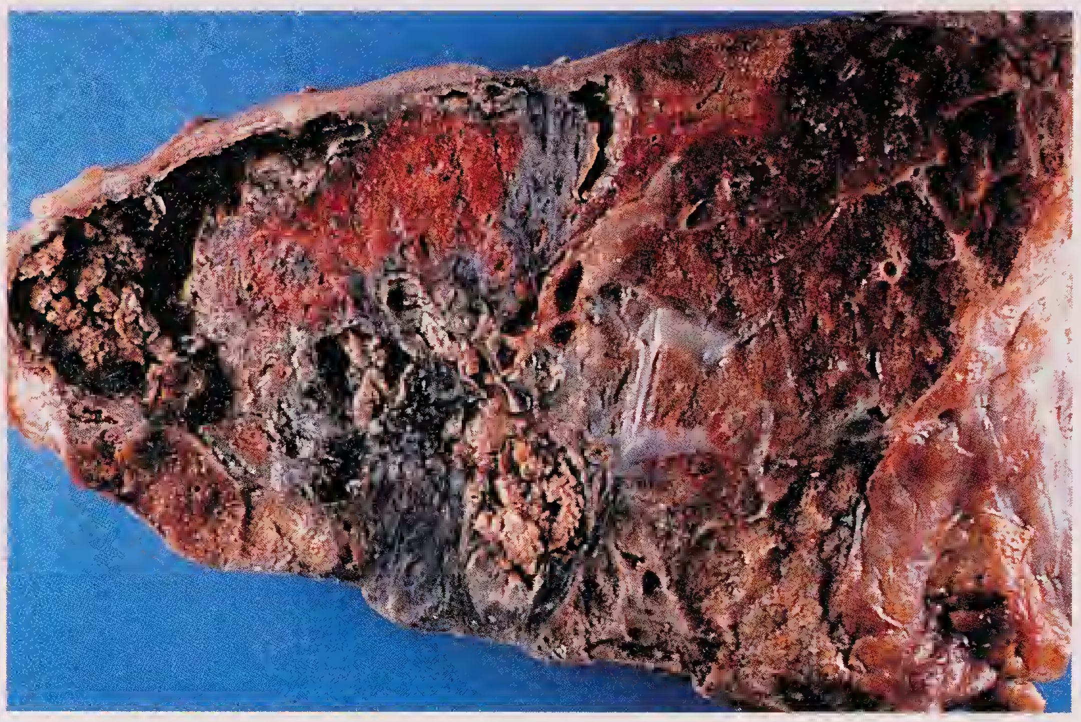

118

118 ♦ Autopsy specimen of the *Mycobacterium avium* complex (MAC), showing apical cavitary disease. This complex includes both *M avium* and *M intracellulare*. In patients without acquired immunodeficiency syndrome and disseminated disease, MAC is the most common agent responsible for nontuberculosis infection capable of producing pulmonary radiographic findings similar to *M tuberculosis*.

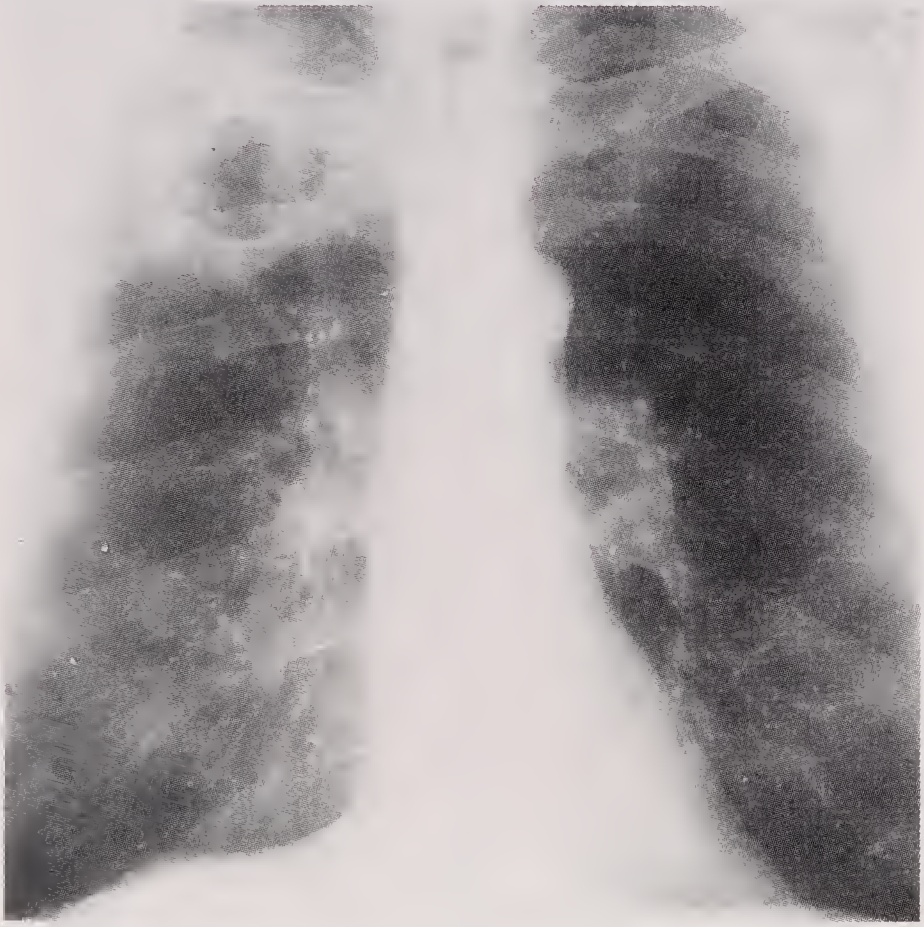

119

119 ♦ Chest radiograph of infection with *Mycobacterium avium-intracellulare*, showing a right upper lobe cavitary lesion.

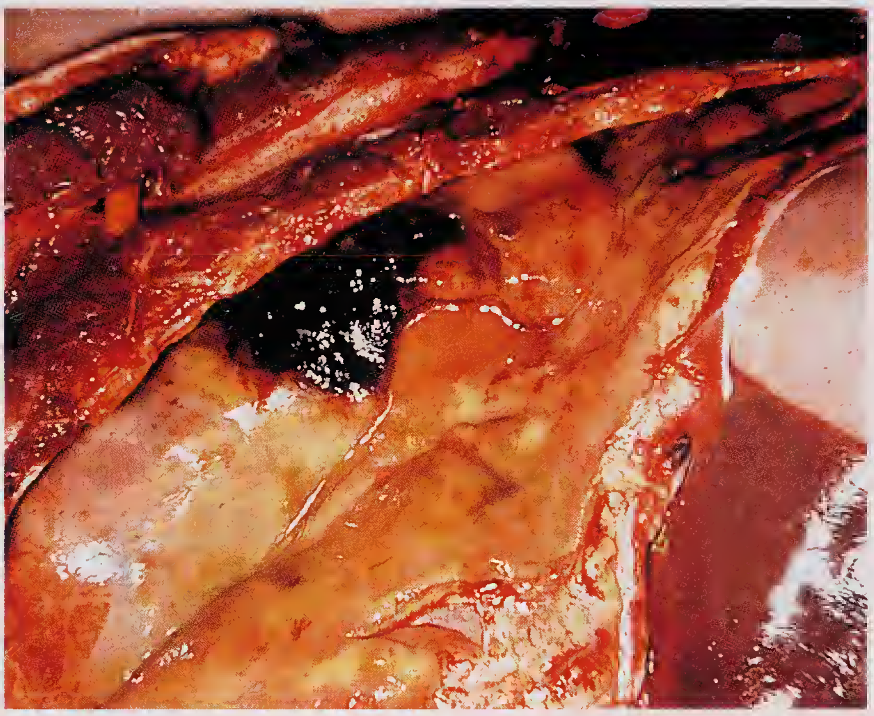

120

120 ♦ Autopsy specimen of the purulent-appearing pleural collection of an empyema, depicting the pus-containing, thick material above the diaphragm. Bacterial infection extending from an underlying pneumonia typically causes formation of this material, but it can also develop postthoracotomy. Pleural fluid that cultures positive for pathogens, often with bacteria on Gram's stain, exudative characteristics, and leukocytosis supports the diagnosis of empyema.

121-122 ♦ Chest radiographs of a hydropneumothorax with the large air-fluid level (posterior-anterior and lateral views). The effusion was consistent with an empyema.

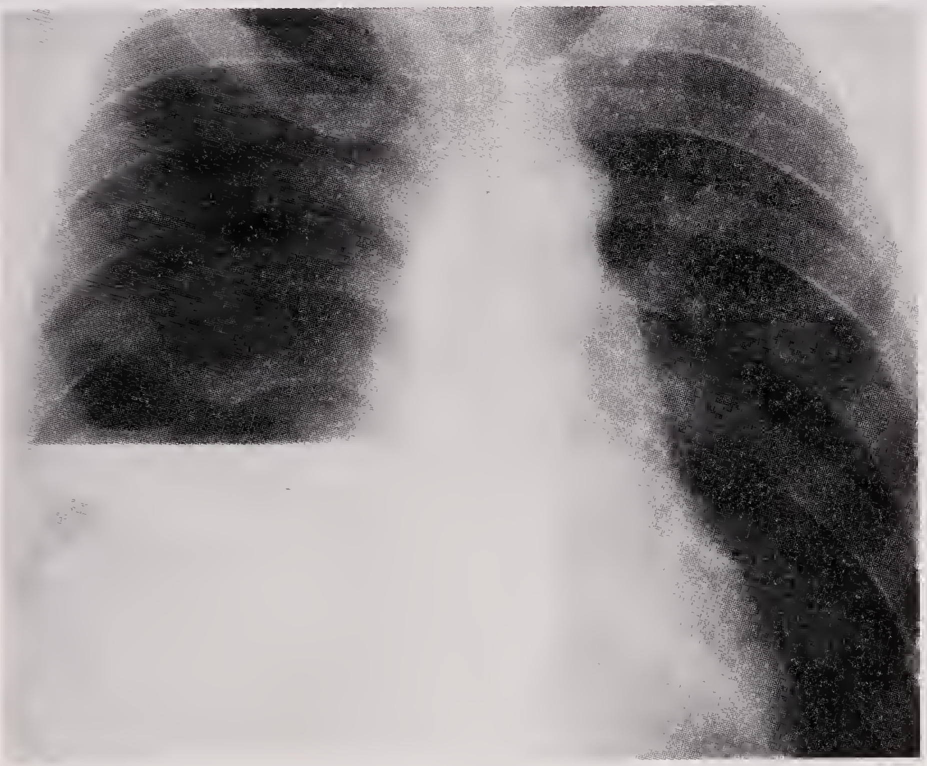

121

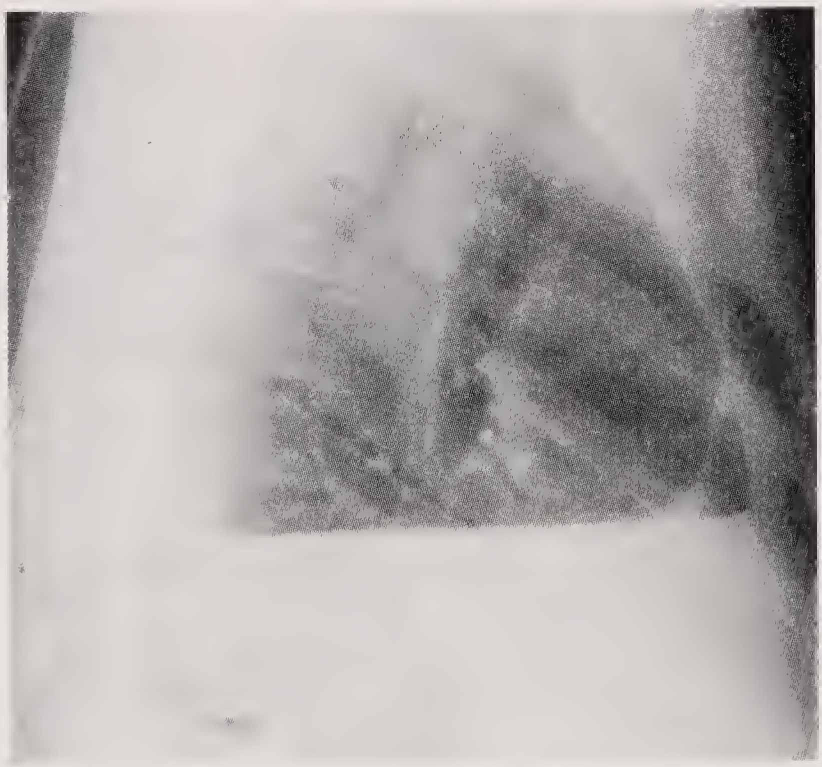

122

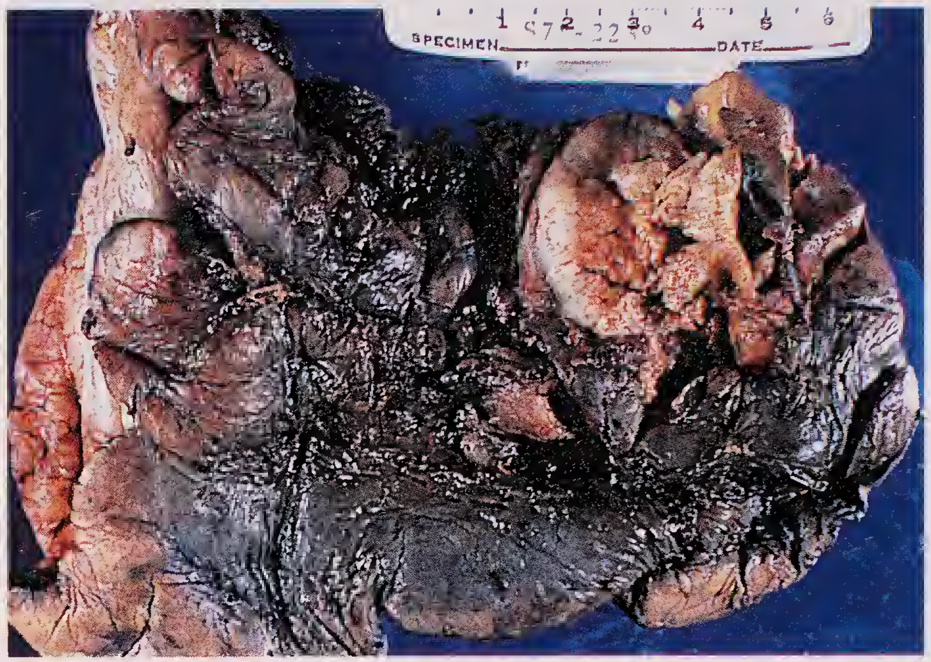

123

123 ♦ Autopsy specimen of a lung abscess, showing the well-circumscribed cavity in the upper lobe of the lung. Pathologically, this is usually a central area of necrosis within the lung parenchyma that becomes surrounded by a fibrous wall over time.

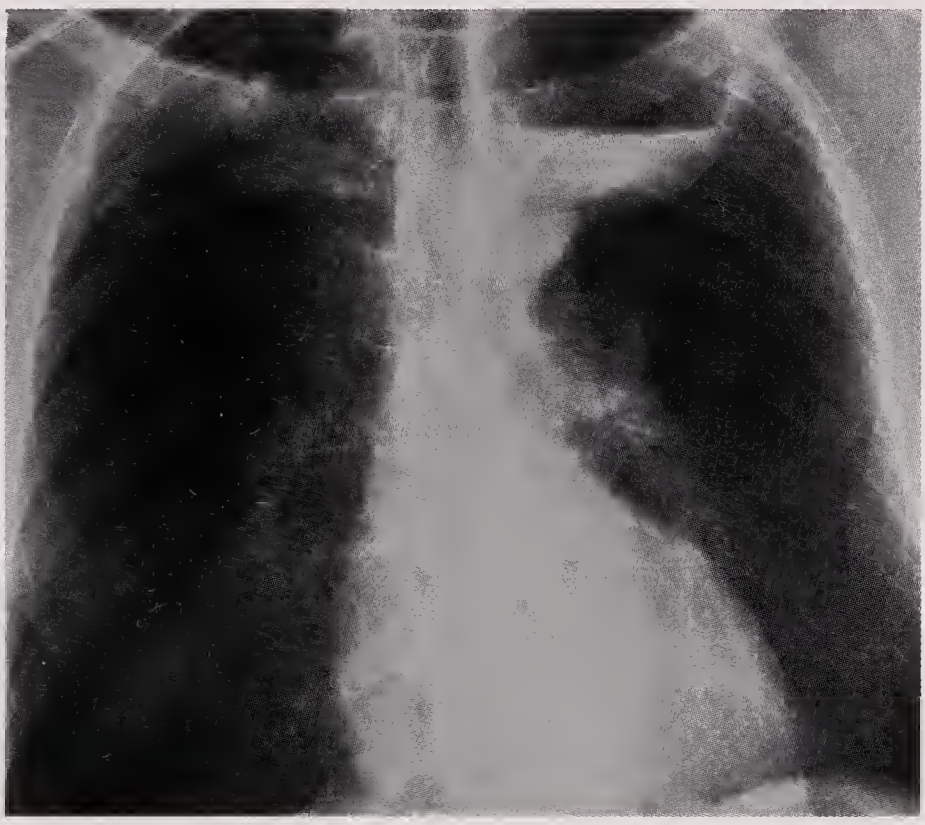

124

124 ♦ Chest radiograph showing infection in a preexisting apical bullous lesion. Air-fluid level in a preexisting bulla is rarely due to hemorrhage or development of bronchogenic carcinoma. An infection within or adjacent to the bulla is the most common cause for the development of fluid within a vesicle. Any organism capable of producing pneumonia can promote fluid development.

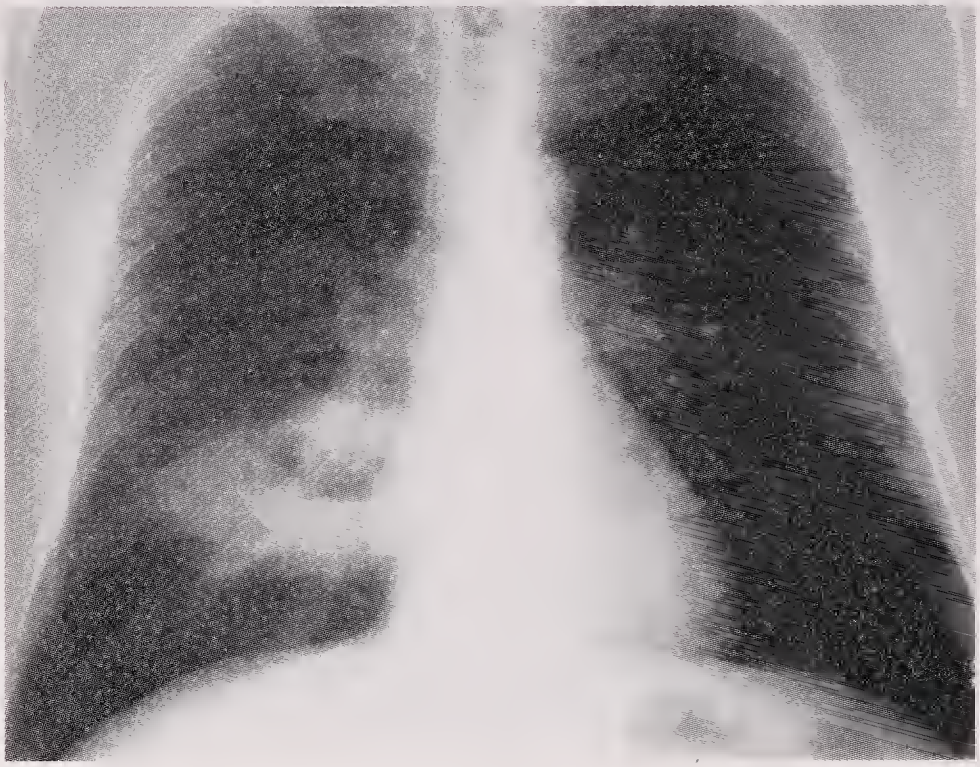

125

125 ♦ Chest radiograph of a 51-year-old nonsmoking man, which demonstrates an 8-cm cavitary lesion with an air-fluid level located in the superior segment of the right lower lobe. This finding is suggestive of a lung abscess.

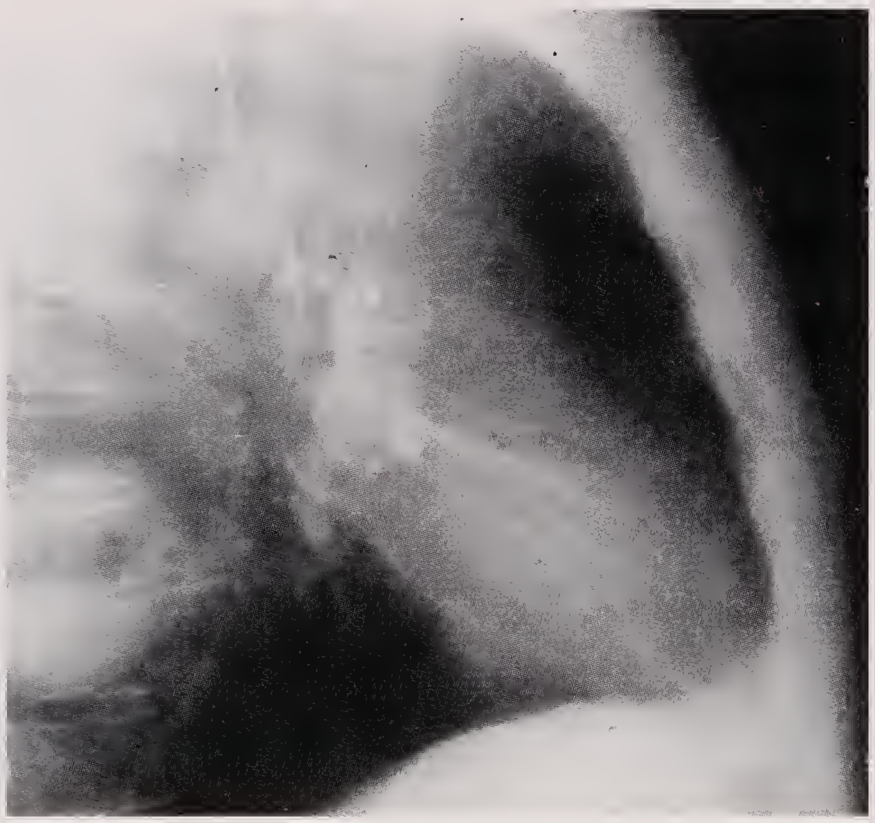

126

126 ♦ Chest radiograph of the patient in 125. The primary sites of infection include the posterior segment of the right upper lobe and the superior segment of both lower lobes.

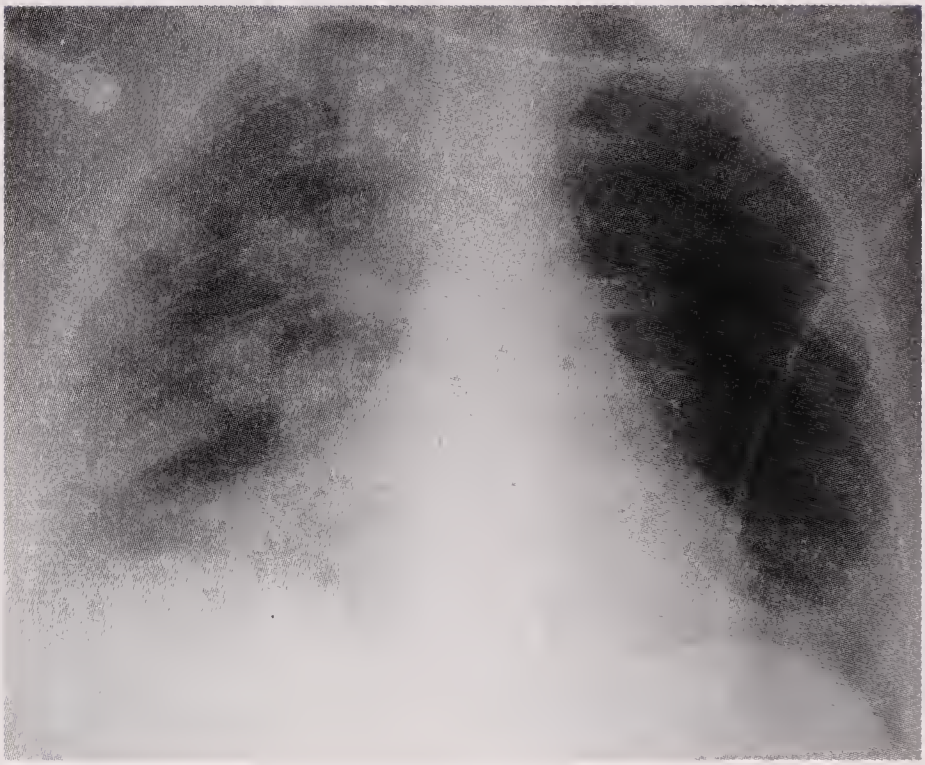

127

127 ◆ Chest radiograph showing multiple, small, nodular densities. This appearance is a highly suggestive diagnostic clue of septic pulmonary emboli. The characteristic densities have "shaggy" or "fuzzy" borders. Cavitation commonly occurs, and the number of nodules may increase as embolization continues. The septic pulmonary emboli can cause an acute necrotizing pneumonia or a purulent, hemorrhagic infarct.

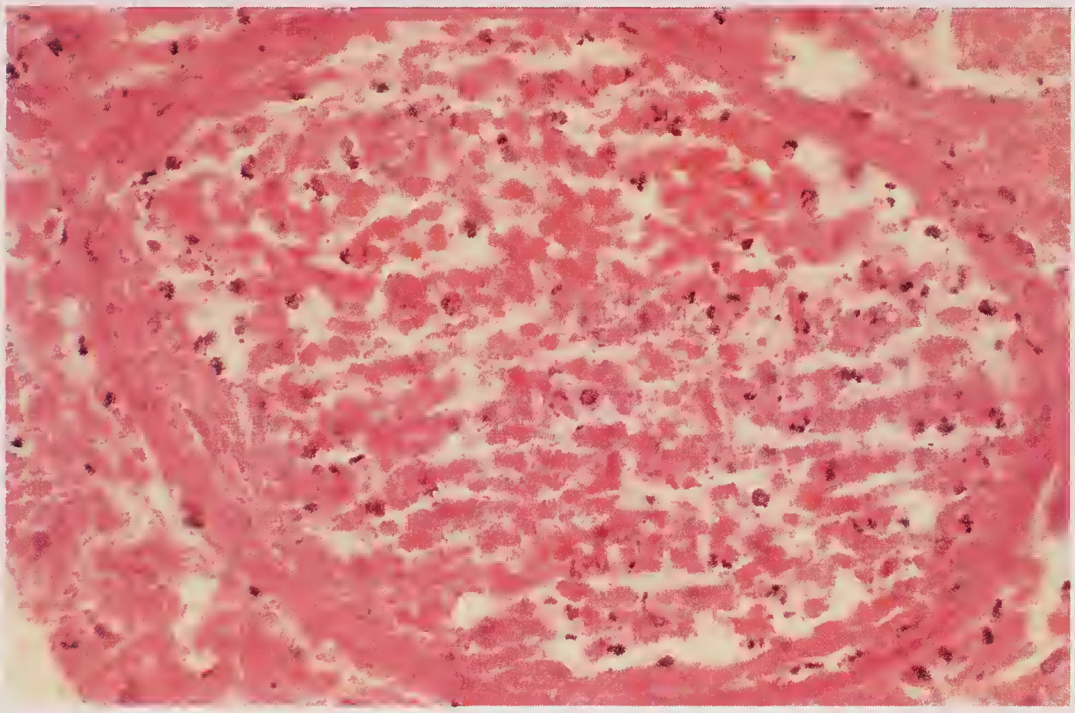

128

128 ♦ Pulmonary vessel with septic emboli (hematoxylin-eosin stain at 25×). Thrombosis occurs due to either trauma or infection of the vein, and the clot then becomes infected and friable. Small and repetitive emboli to the lung result.

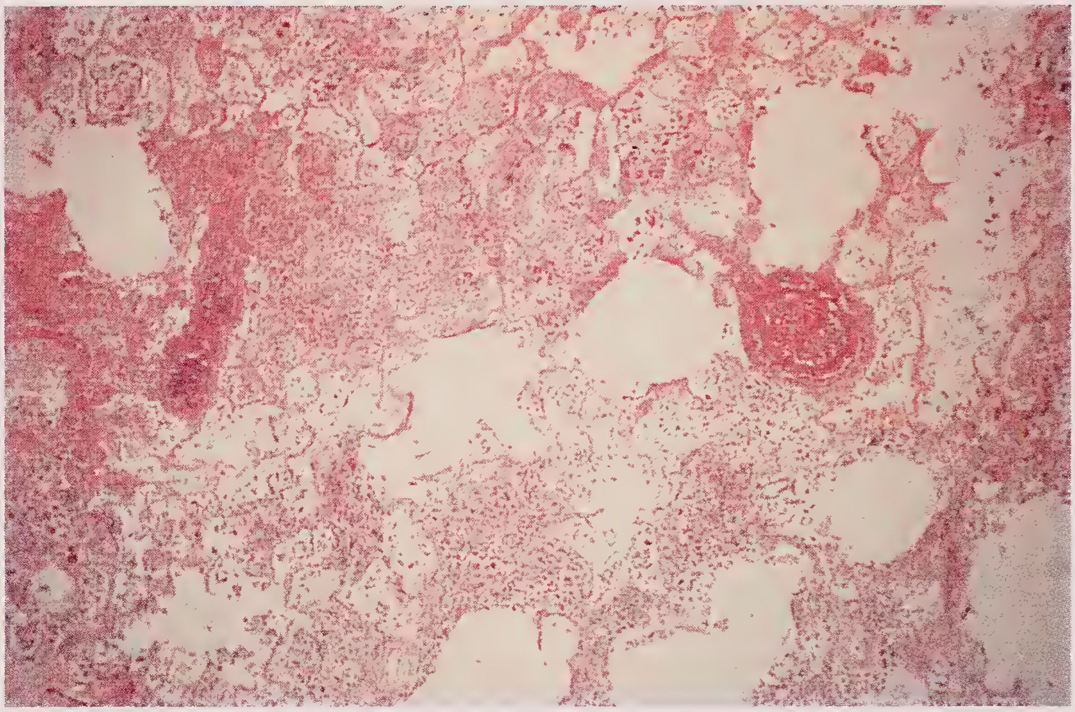

129

129 ◆ Lung tissue with acute inflammatory pneumonitis and two blood vessels with septic pulmonary emboli (hematoxylin-eosin stain).

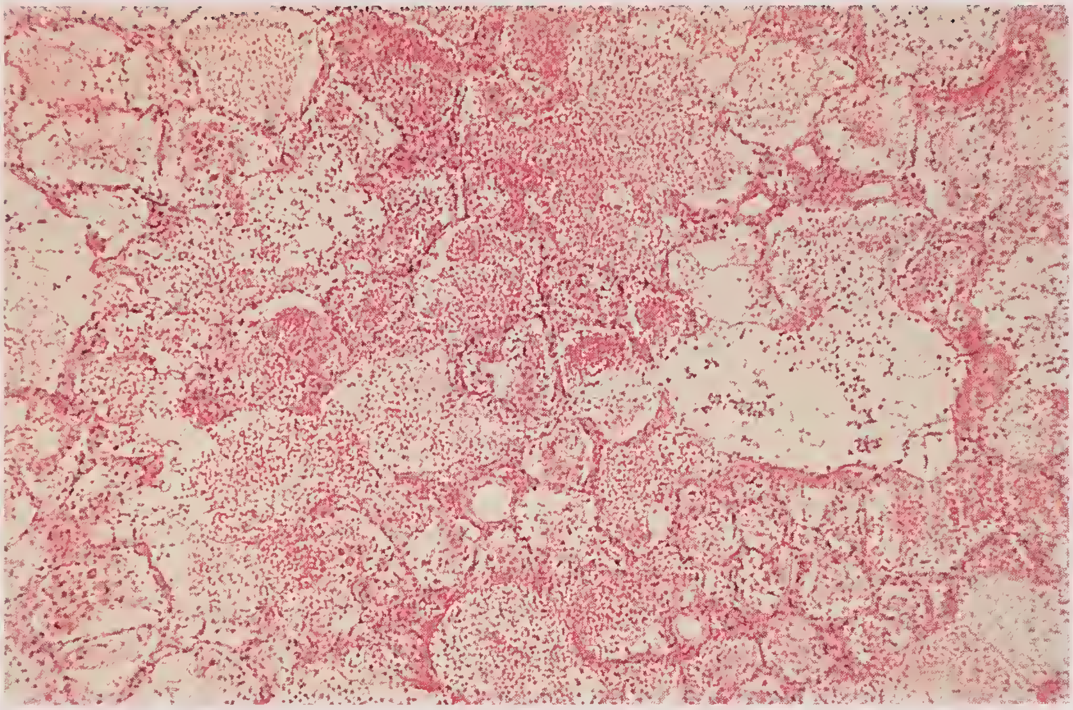

130

130 ♦ Lung tissue with acute inflammatory pneumonitis and microabscess formation (hematoxylin-eosin stain).

Skin/Soft Tissue

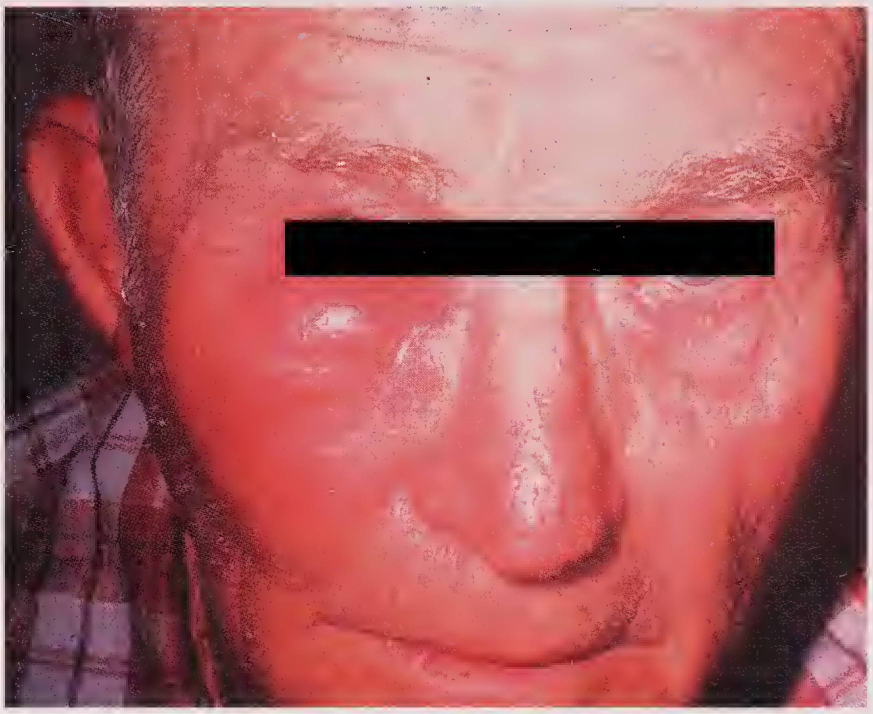

131

131 ♦ A 72-year-old man who presents with fever and a right facial rash that is sharply demarcated, raised, deeply erythematous, indurated, and painful. This patient demonstrates the classic picture of erysipelas. The infection is usually associated with a break in the skin. Group A β-hemolytic and group G streptococci are the most commonly implicated organisms.

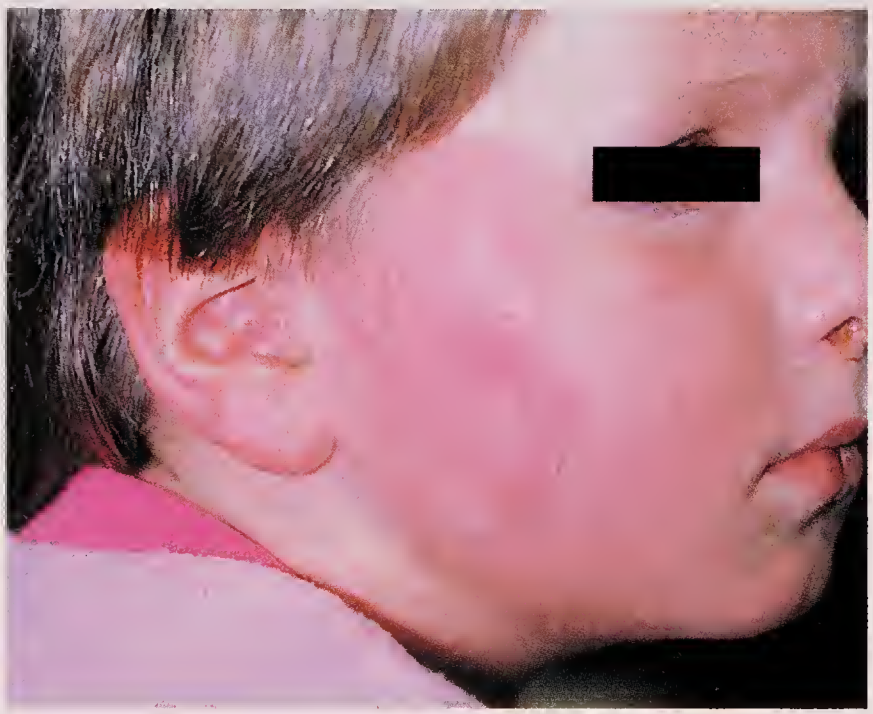
[redacted]

132

132 ♦ An 8-year-old girl who presents with fever and a facial rash, which is preauricular and violaceous with central induration. This presentation suggests facial or "buccal cellulitis," a rare but potentially life-threatening infection caused by *Haemophilus influenzae* (suggested by a purple hue to the rash), group B streptococcus, and *Streptococcus pneumoniae.*

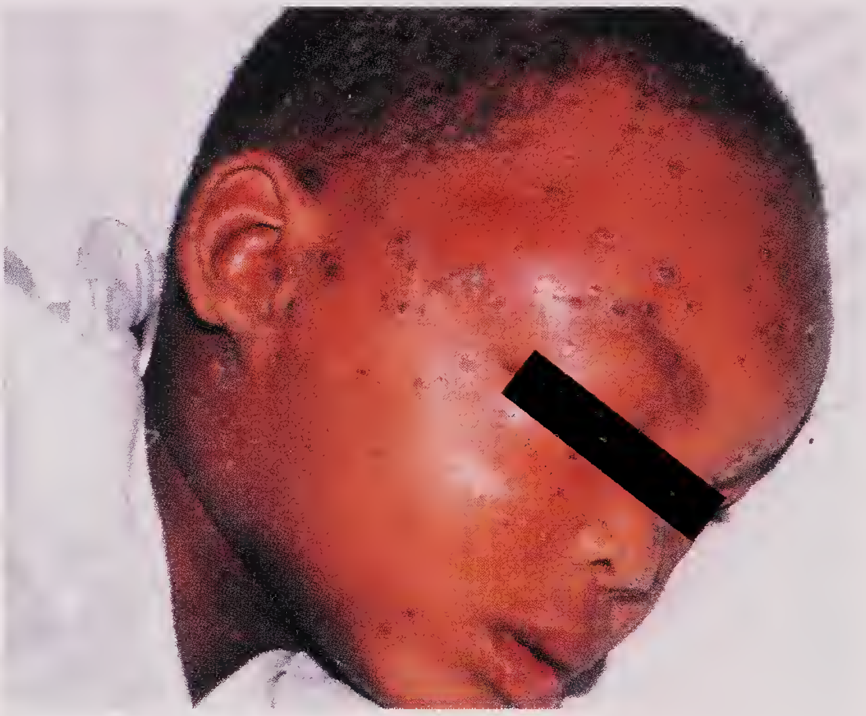

133

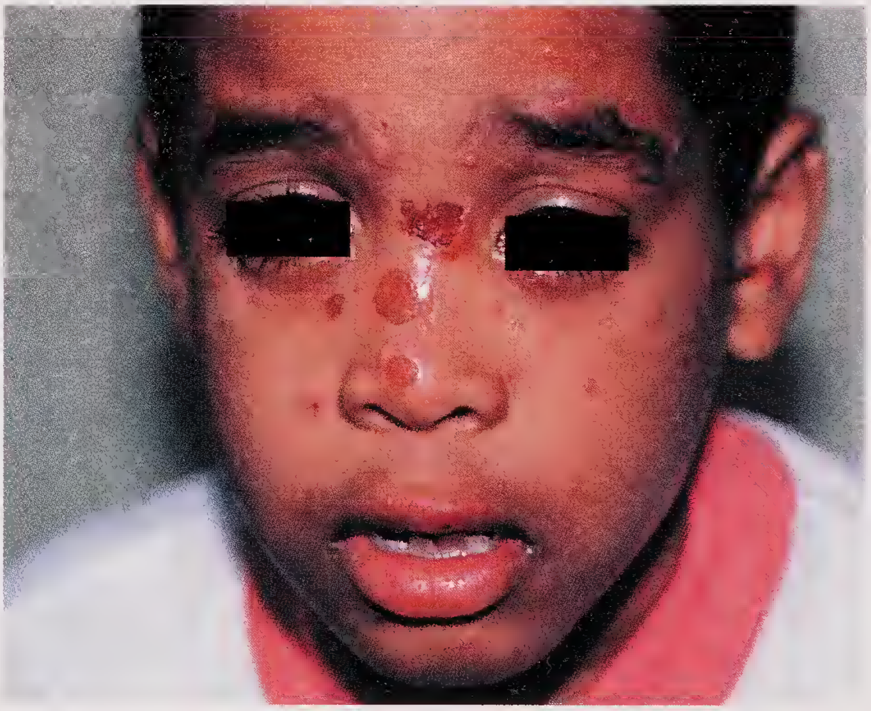

134

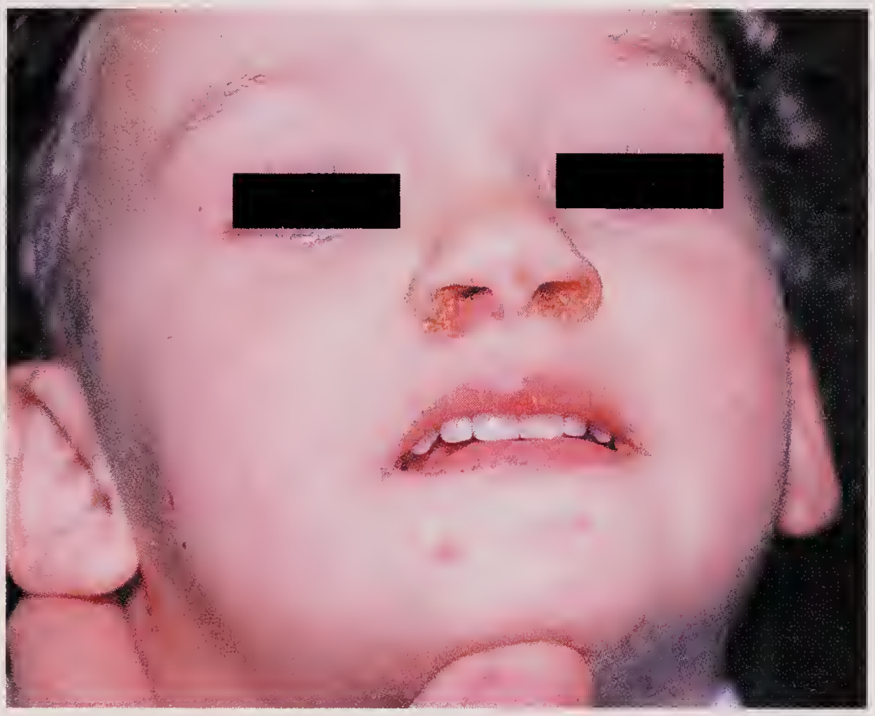

135

133 ♦ Varicella, which is complicated by a secondary group A β-hemolytic streptococcal skin infection, in a child. The cellulitis has extended across the face and has resulted in significant edema. The central lesion was unroofed, and 10 mL of pus was removed.

134 ♦ A 4-year-old boy who had been scratching several insect bites repeatedly. These clear bullous lesions appeared over 1 week and were initially treated with a steroid cream. Culture with a moistened swab showed a staphylococcal infection.

135♦ Child with a resolving upper respiratory infection and a persistent, painful nose. The cause of this infection is *Staphylococcus aureus*, as proved by culture. Satellite lesions, which are common, are seen on the chin and nose. This localized crusty lesion with an erythematous base is commonly caused by the bacteria.

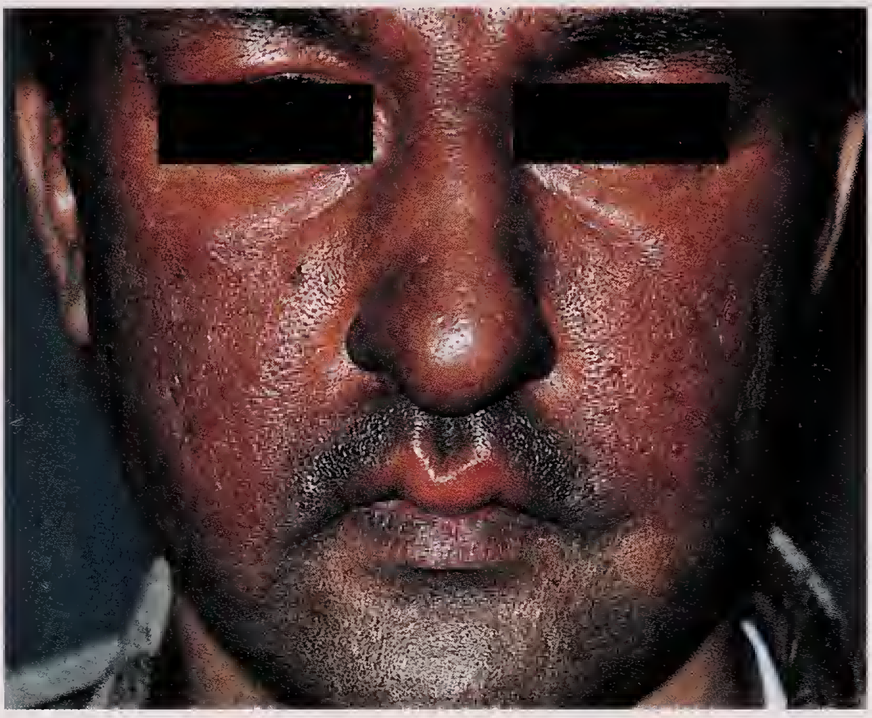

136

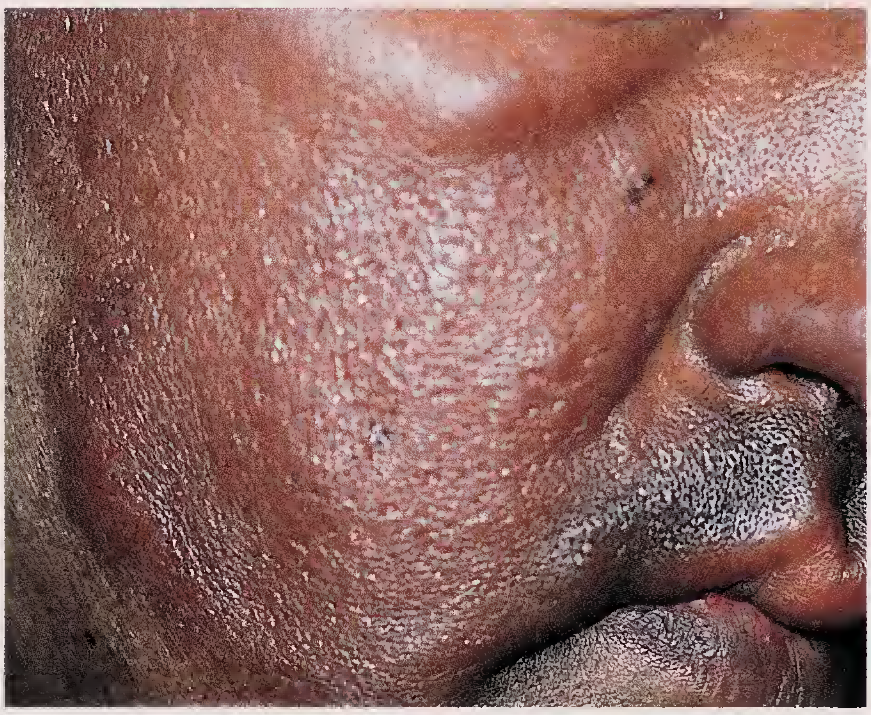

137

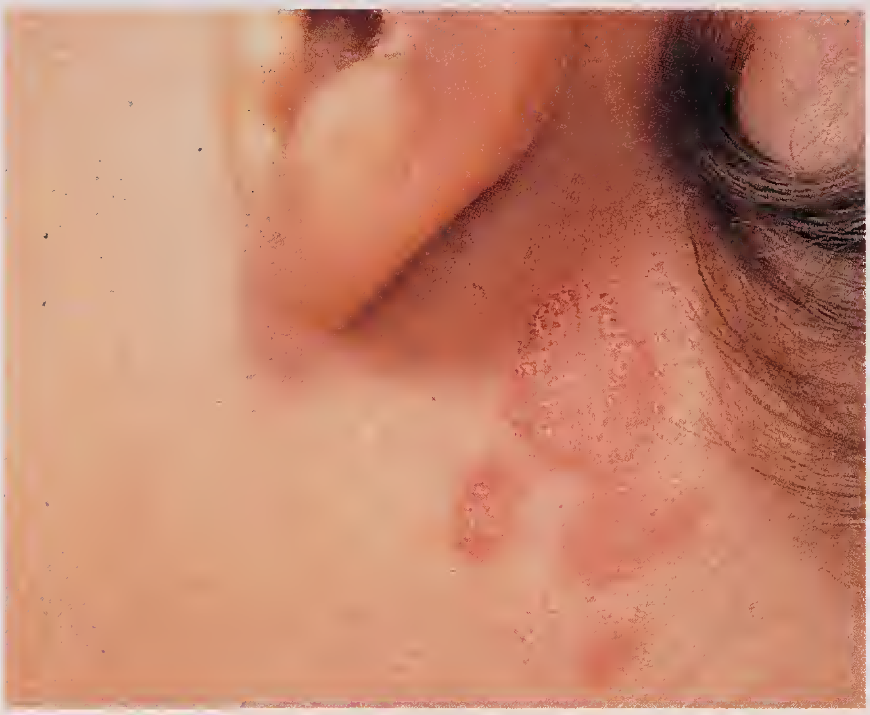

138

136-137 ♦ Classic "leonine" face of leprosy. Thickening of the facial skin deepens the line in the forehead and thickens the nose and ears. Infiltration of the dermis by the disease leads to a shiny, raised appearance.

138 ♦ Tinea corporis involving the skin inferior and posterior to the left auricle. This superficial skin infection usually manifests by circular lesions (ringworm), with slightly erythematous, well-demarcated, scaly borders.

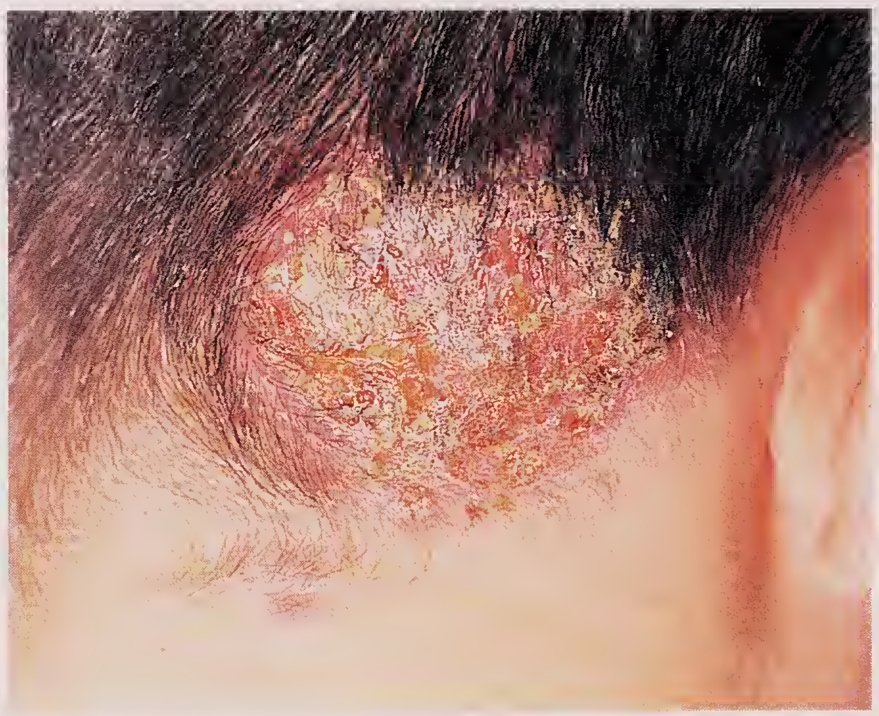

139

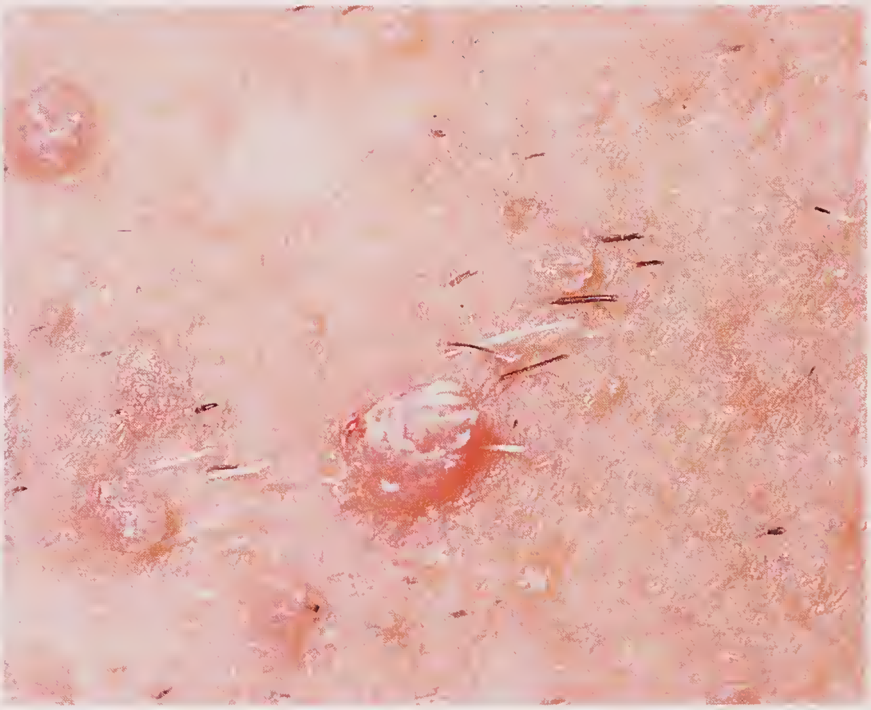

140

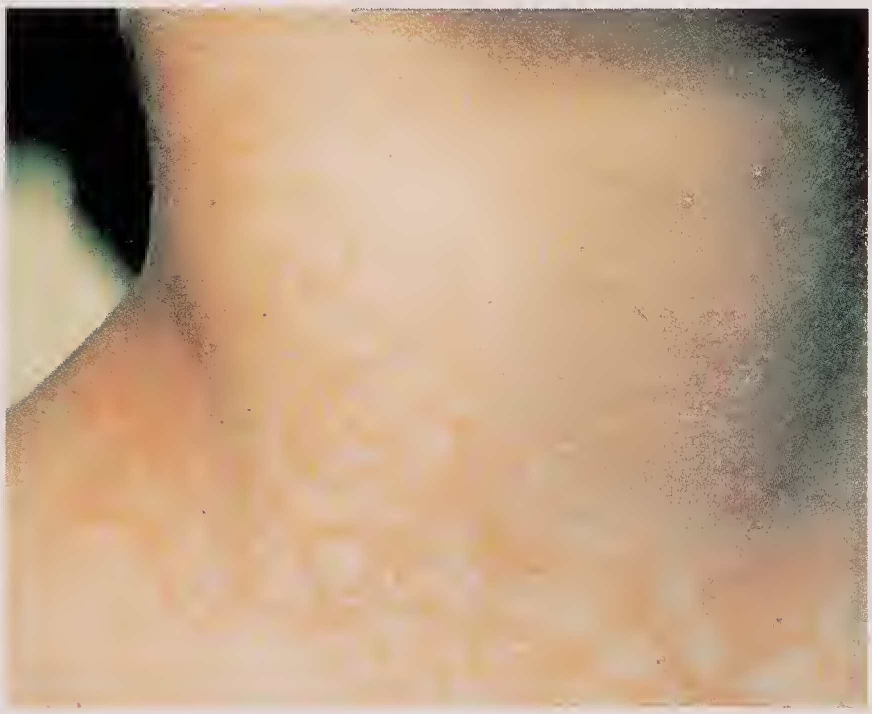

141

139 ♦ A kerion, a boggy, inflamed, purulent nodule of the scalp, which is associated with hair loss. It represents a hypersensitivity reaction to a fungal infection.

140 ♦ Brown-to-flesh–colored, flat papules on the face, which suggest flat warts; these must be differentiated from seborrheic keratoses and comedones.

141 ♦ Characteristic exanthem of erythema infectiosum, caused by the B19 parvovirus, which starts with a "slapped-cheek" erythema on the face and progresses to a more reticulated pattern on the extremities. The fishnetlike pattern of erythema shown on the patient's neck is also present on her arms.

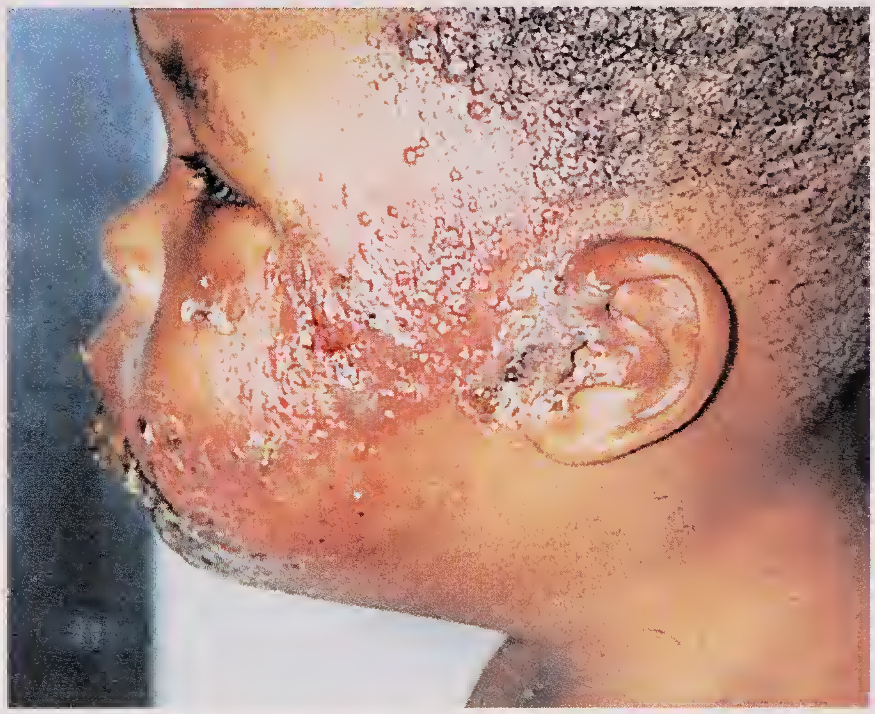

142

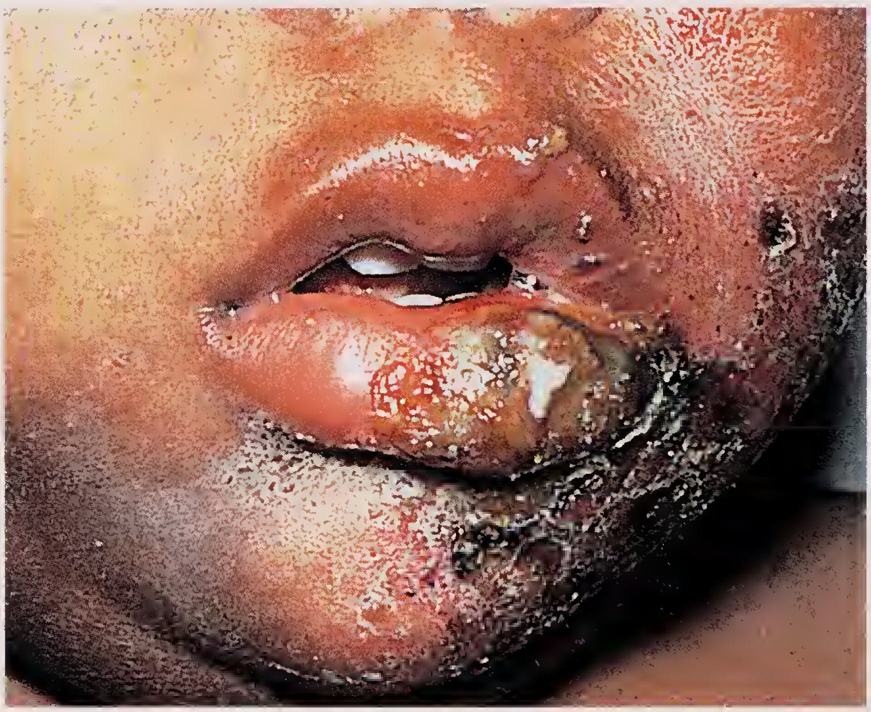

143

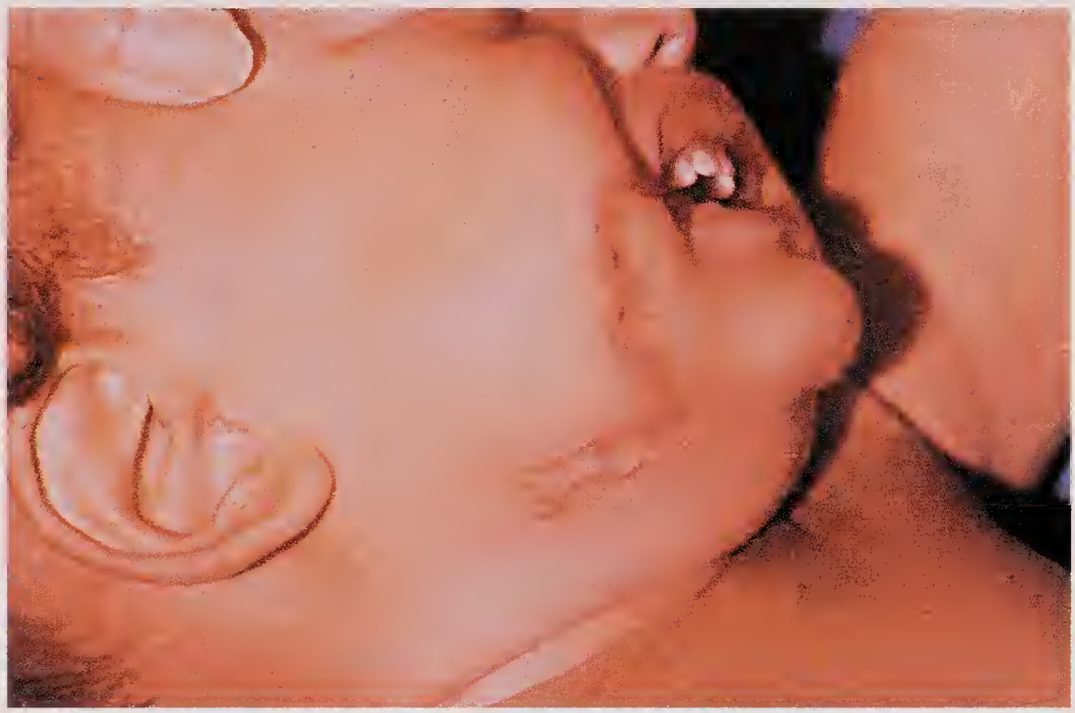

144

142-143 ♦ Acute herpes zoster infection (shingles) of the second division of the left trigeminal nerve in a 3 $^1/_2$-year-old child. Note the grouped vesicular lesions over the distribution of the left second division of the trigeminal nerve. The vesicles are surrounded by significant inflammatory changes in the skin.

144 ♦ Cutaneous larva migrans, which in humans is usually caused by the migration of cat or dog hookworm larvae. These larvae are usually trapped by the skin and cannot complete their life cycles. Secondary bacterial infection is common.

♦ Recently, it has been learned that a few such larvae may reach the human gut, causing an eosinophile enteritis.

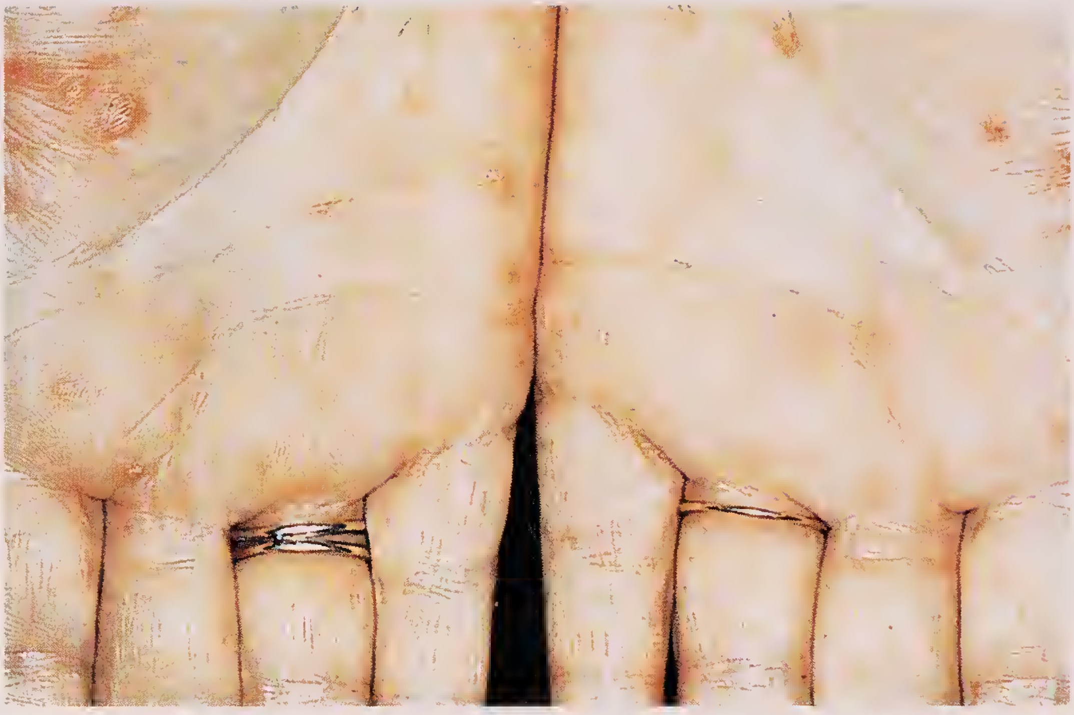

145

145 ♦ Scattered scaly papules on the palms, which are highly suggestive of secondary syphilis. The soles of the feet may also be affected. Similar lesions on the trunk can be caused by a number of unrelated conditions.

146 ♦ Skin biopsy specimen showing spirochetes, which appear as corkscrew-type bodies on tissue examination. Their presence in a patient with scaly papules on the palms and soles is diagnostic of secondary syphilis.

147 ♦ Disseminated gonococcal infection. Tender hemorrhagic necrotic pustules are located on the arm.

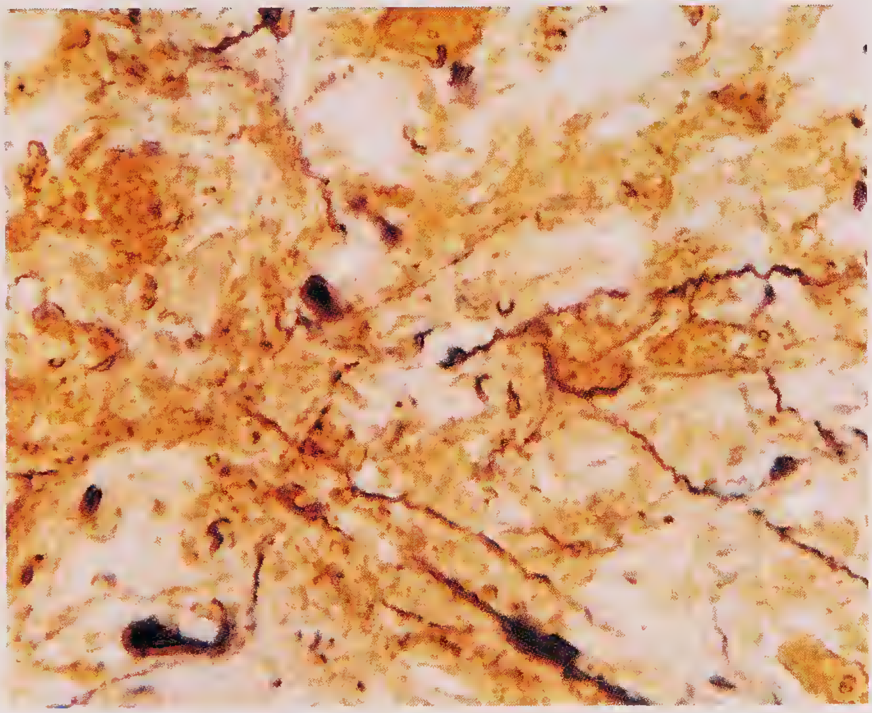

146

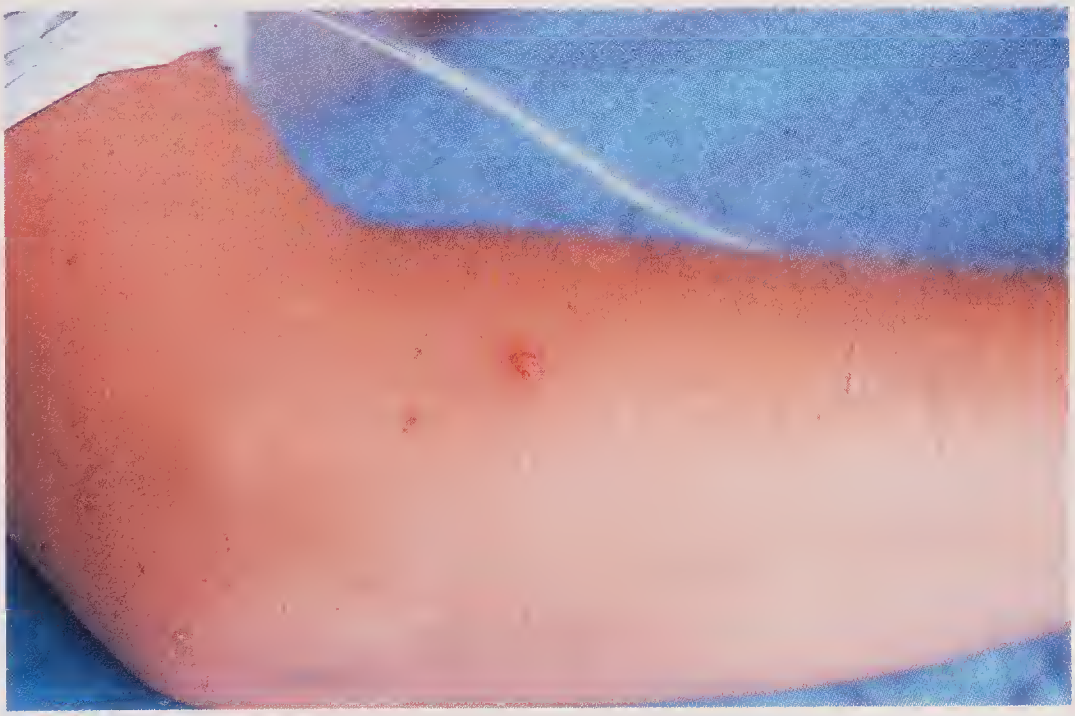

147

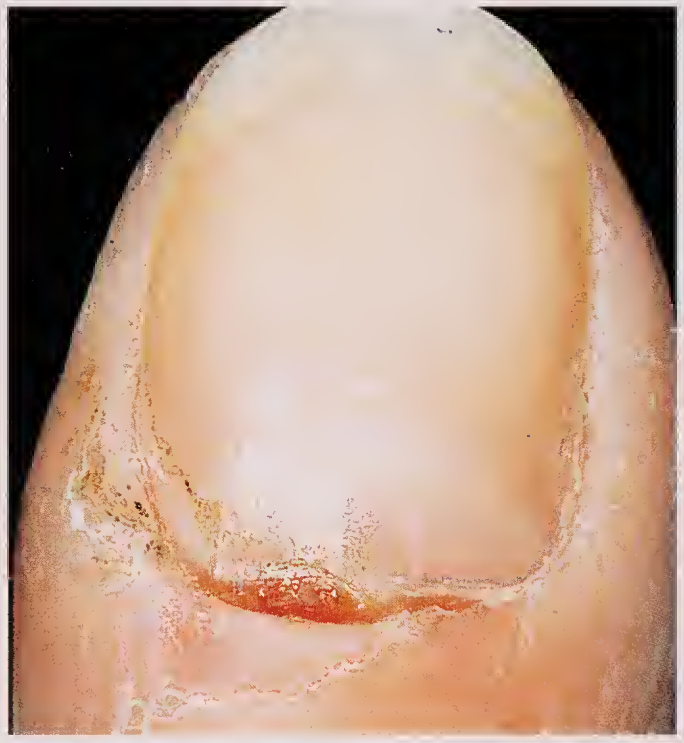

148

148 ♦ Paronychia (redness and swelling of the nail folds), which has a number of causes. Bakers, dishwashers, and dentists, whose hands are repeatedly exposed to moisture, are at greatest risk. The presence of *Pseudomonas* is suggested by a greenish discoloration of the nail and is diagnosed by bacterial culture. Many other organisms such as staphylococci and *Candida albicans* thrive in this warm, moist, intertriginous space.

149-150 ♦ Intensely pruritic eruption of scabies, which characteristically involves the interdigital areas of the hands, wrists, axillae, waistline, and genital areas. Burrows, which represent the linear migration of the infecting organism, are occasionally noted among the vesicles and crusts. "Crusted" scabies occurs in debilitated or immunosuppressed patients and appears as psoriasiform lesions of the palms and soles.

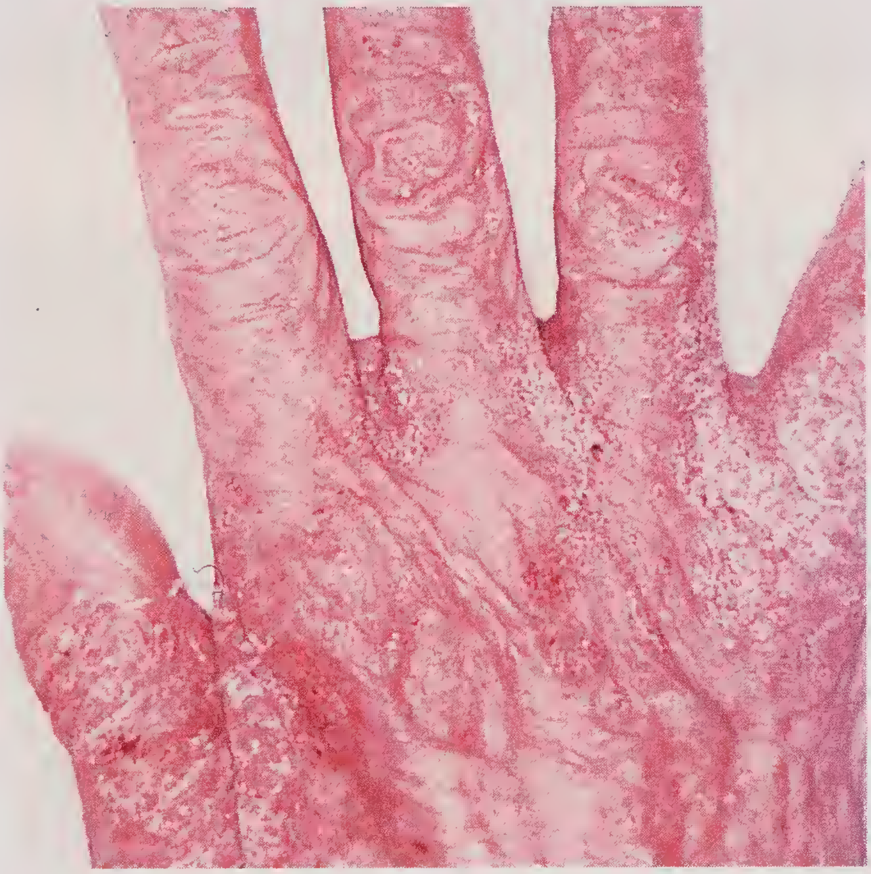

149

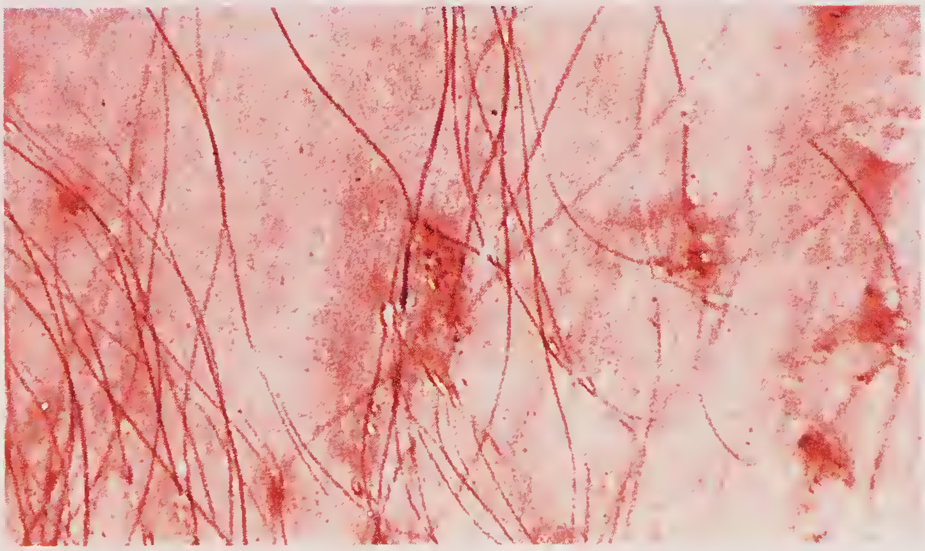

150

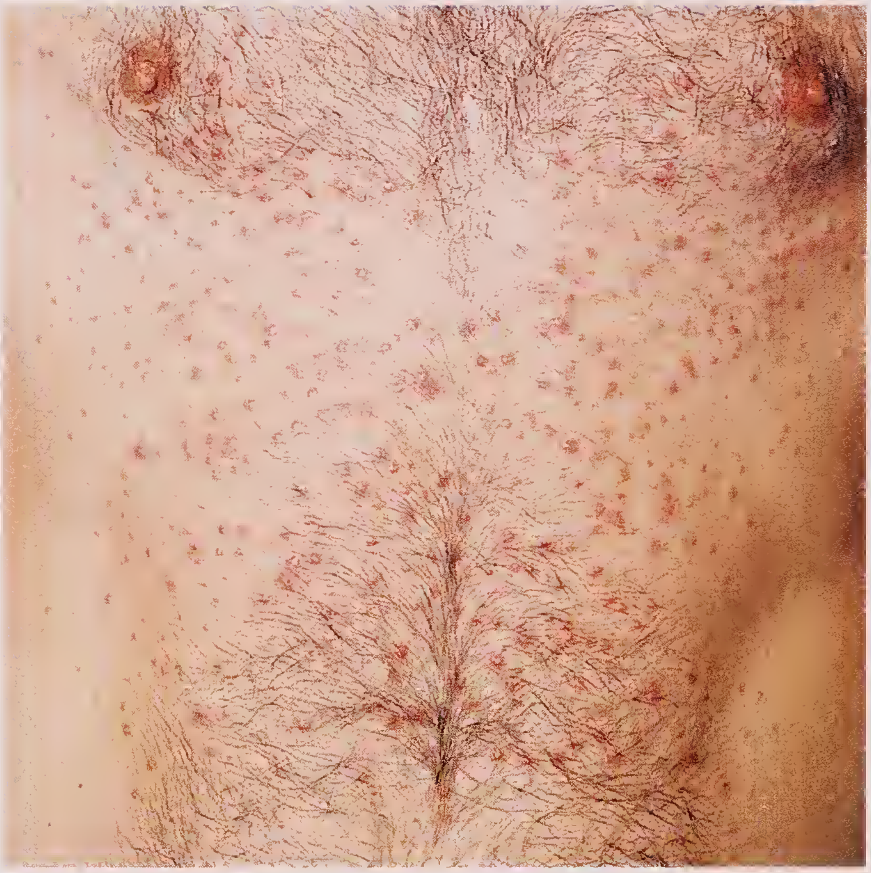

151

151 ♦ Guttate psoriasis in a patient who recently has had streptococcal pharyngitis. This condition, which is thought to represent a hypersensitivity reaction to streptococcal antigen, appears as small, droplike papules of psoriasis on the trunk and extremities.

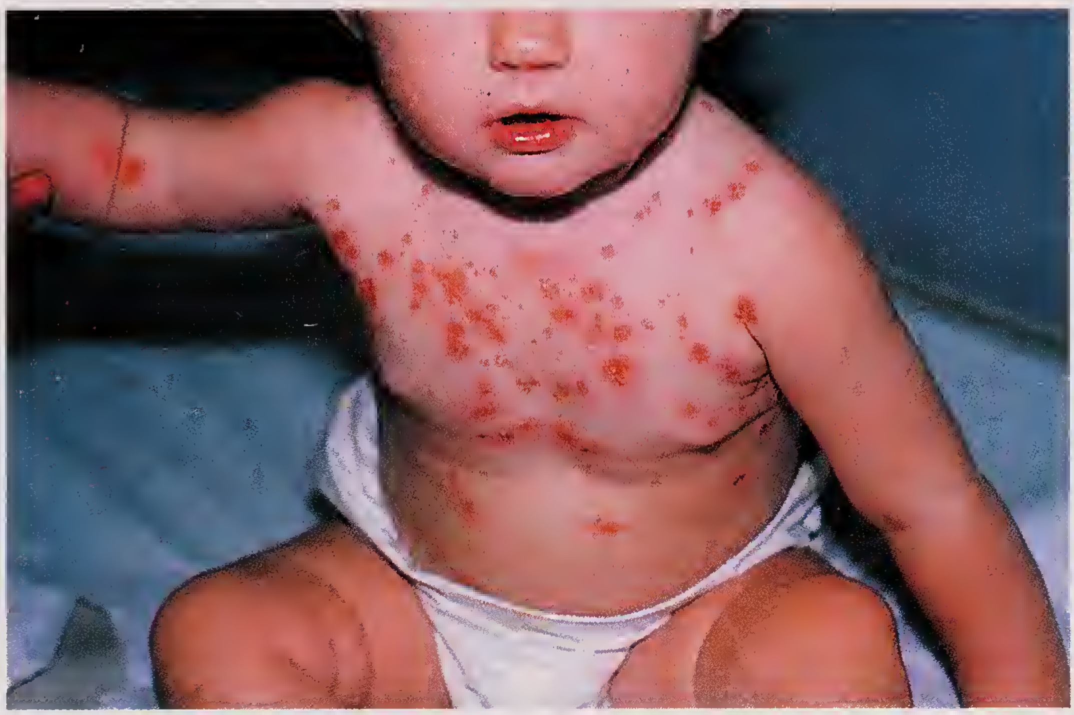

152

152 ♦ Several mosquito bites in a child, which have become secondarily infected with *Staphylococcus aureus*, resulting in bullae formation. The right antecubital fossa demonstrates what are commonly called "kissing lesions," with one part of the arm inoculating the other.

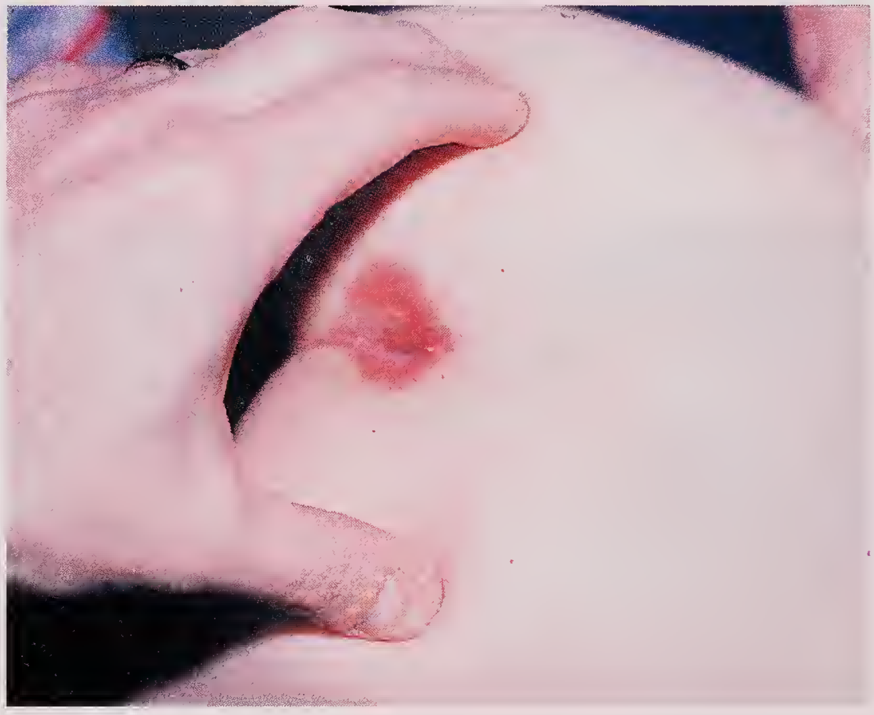

153

153 ♦ Erythema around the anus in a child, suggesting a group A β-hemolytic streptococcal infection. Proof of infection was discovered. Monilial infections are also common at this site and can be primary or secondary infections. The white material on the surface of the lesion indicates a yeast infection.

154 ♦ *Pseudomonas* folliculitis ("hot tub folliculitis"). A young woman who had been bathing 3 days previously in a hot tub contaminated with *Pseudomonas aeruginosa* has asymptomatic, perifollicular, erythematous papules and pustules in the bathing suit area.

155 ♦ Secondary monilia (yeast) dermatitis, which has occurred in the diaper area due to the antibiotic treatment this patient was receiving for otitis media and the moist "tropical jungle" nature of this region. This condition is easily diagnosed because the rash is red with a whitish discharge from the reddened area, and satellite red, macular lesions are present.

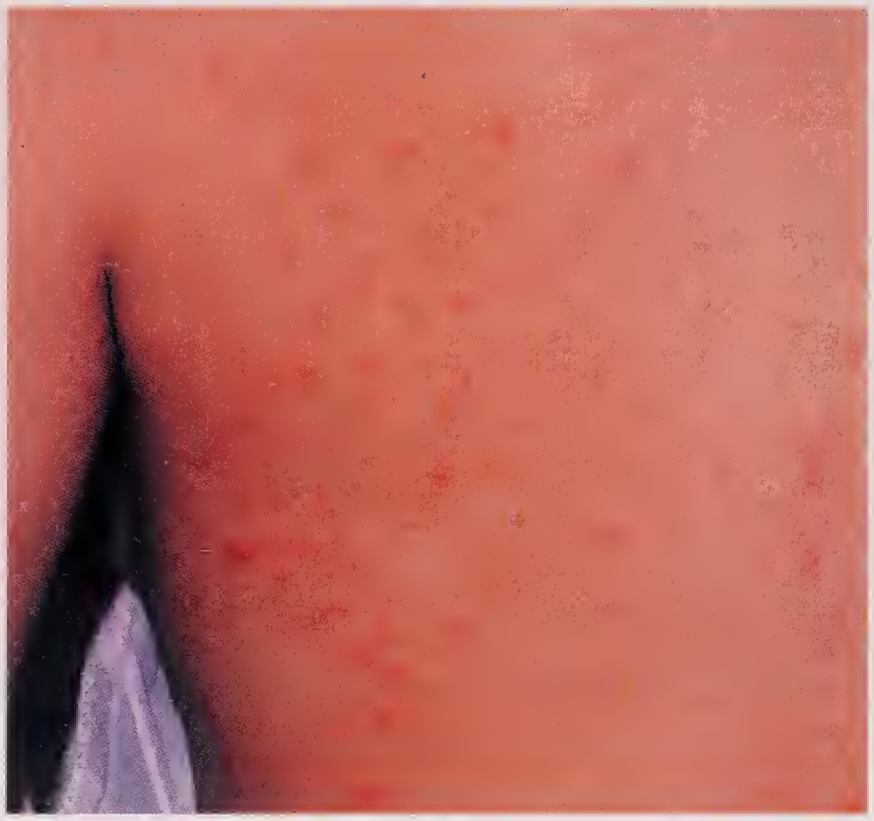

154

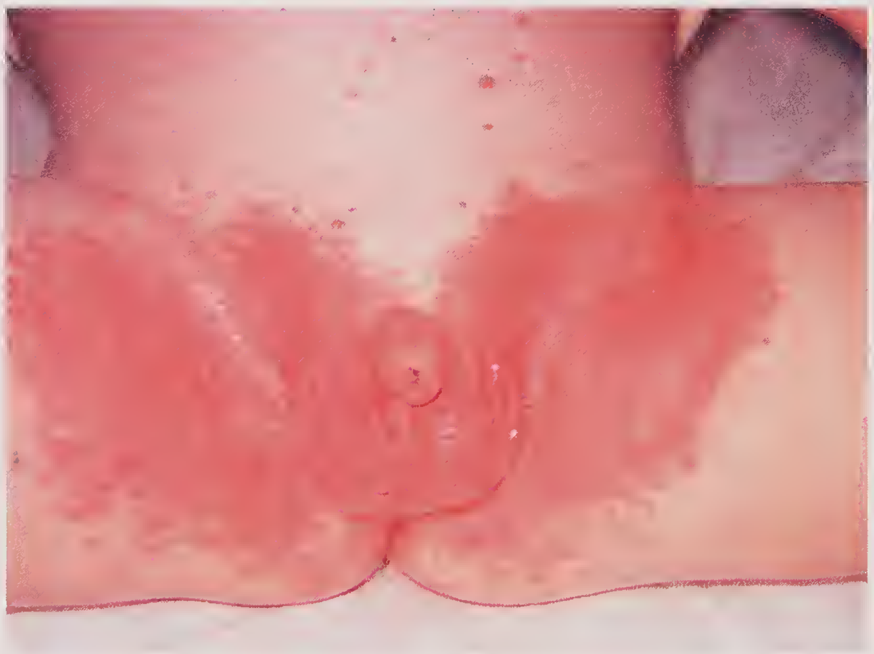

155

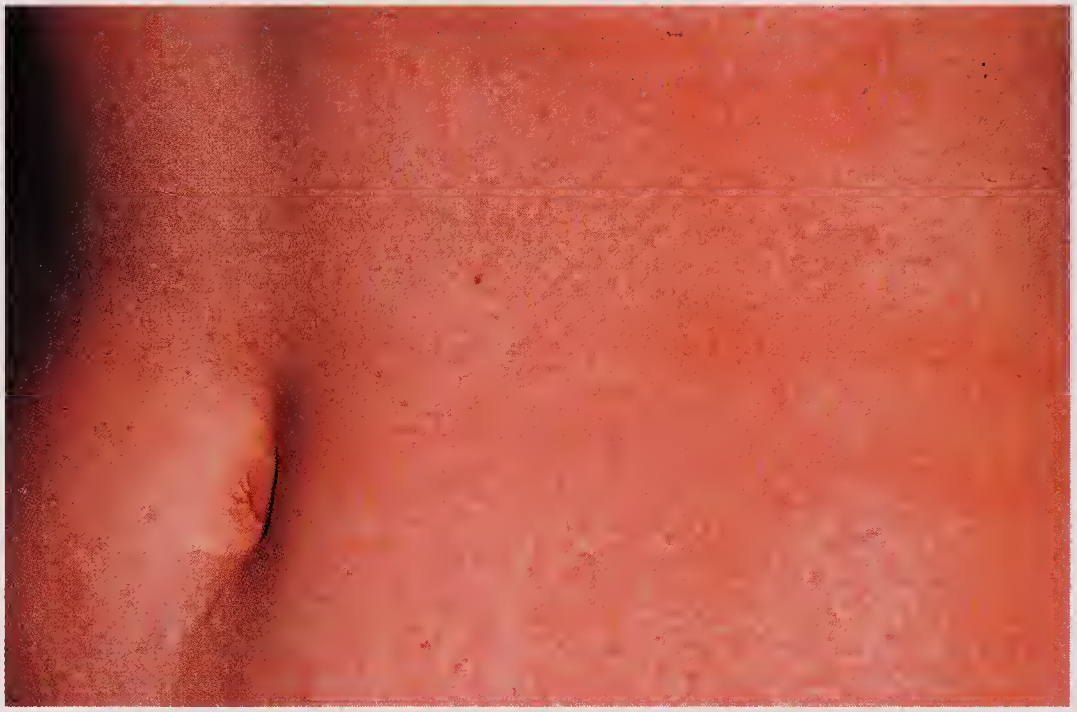

156

156 ♦ Measles eruption on the trunk, which begins as erythematous macules and papules that may become confluent, especially on the face, neck, and shoulders. A characteristic enanthem (Koplik's spots) is apparent on the buccal mucosa opposite the premolar teeth.

157 ♦ Nonspecific viral exanthem, which consists of a macular or papular erythematous eruption with or without associated pruritus.

158 ♦ Vesicular lesions, which are caused by a common viral infection (coxsackievirus), near the base of the spine in a child. The occurrence of similar lesions on the hands, feet, and in the mouth is better known.

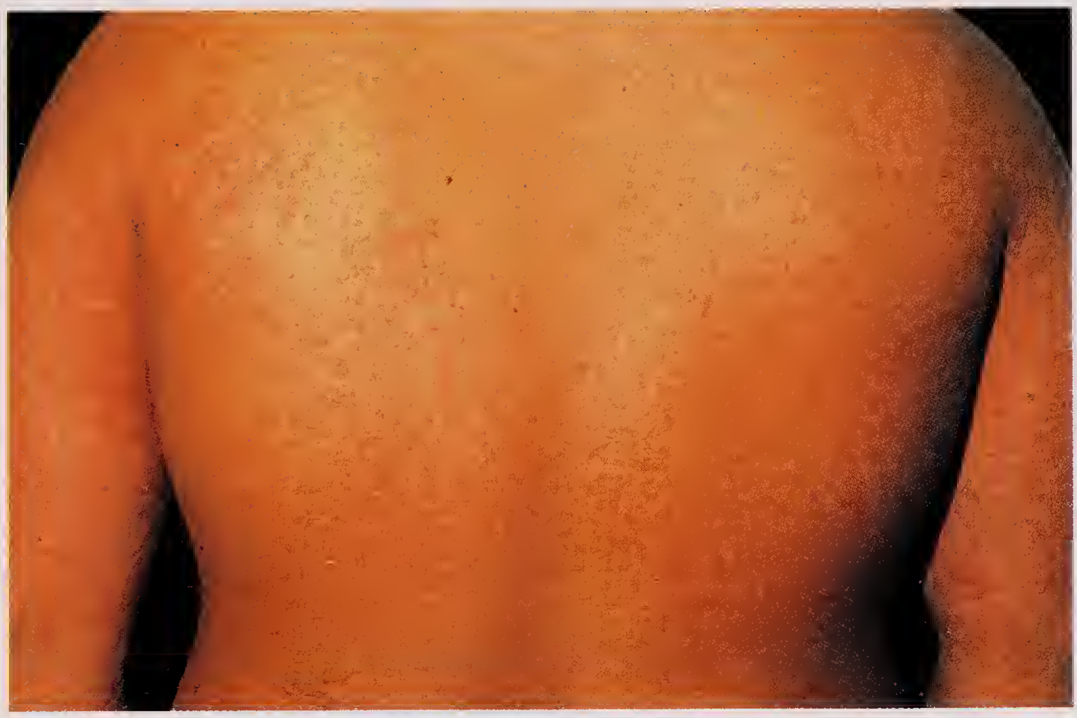

157

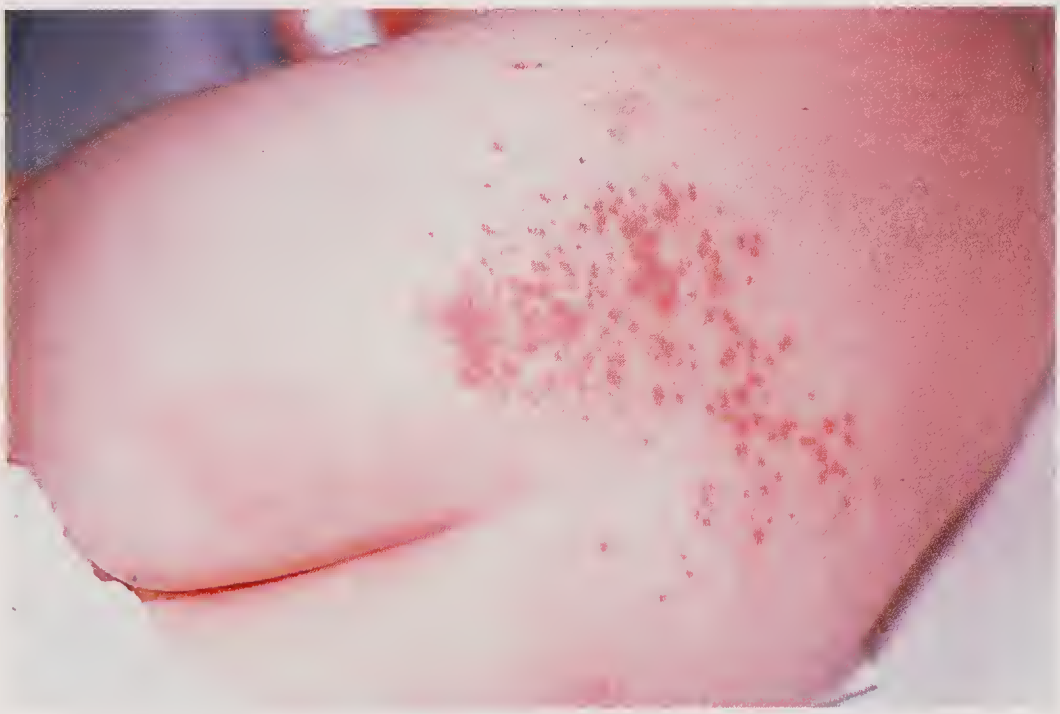

158

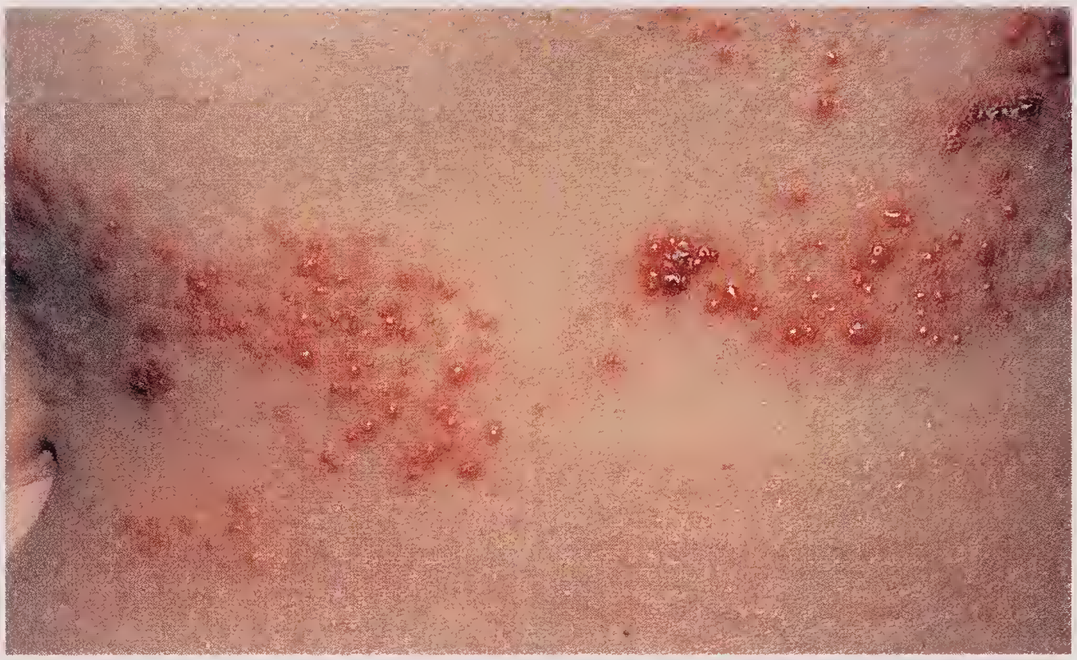

159

159 ♦ Herpes zoster, which is characterized by groups of vesicles surrounded by erythema. The eruption is painful and progresses distally along a dermatome.

160 ♦ Classic case of varicella (chickenpox), which began centrally and spread to the extremities. The lesions progress from macules, to vesicles, to crusted, healing lesions. The total number of lesions ranges from 0 to 500; the larger the number, the more common the constitutional symptoms (fever, cough, etc).

161 ♦ Rash in a young boy with a past history of a mild case of varicella (chickenpox) in the first year of life. The rash appeared over the previous 5 days. The boy reported that his skin felt strange before the rash appeared, but he was in little pain (unlike adults). The dermatomal distribution of this varicella-zoster infection is evident. A few lesions can actually be seen on the inner aspect of the left arm as well as just across the midline.

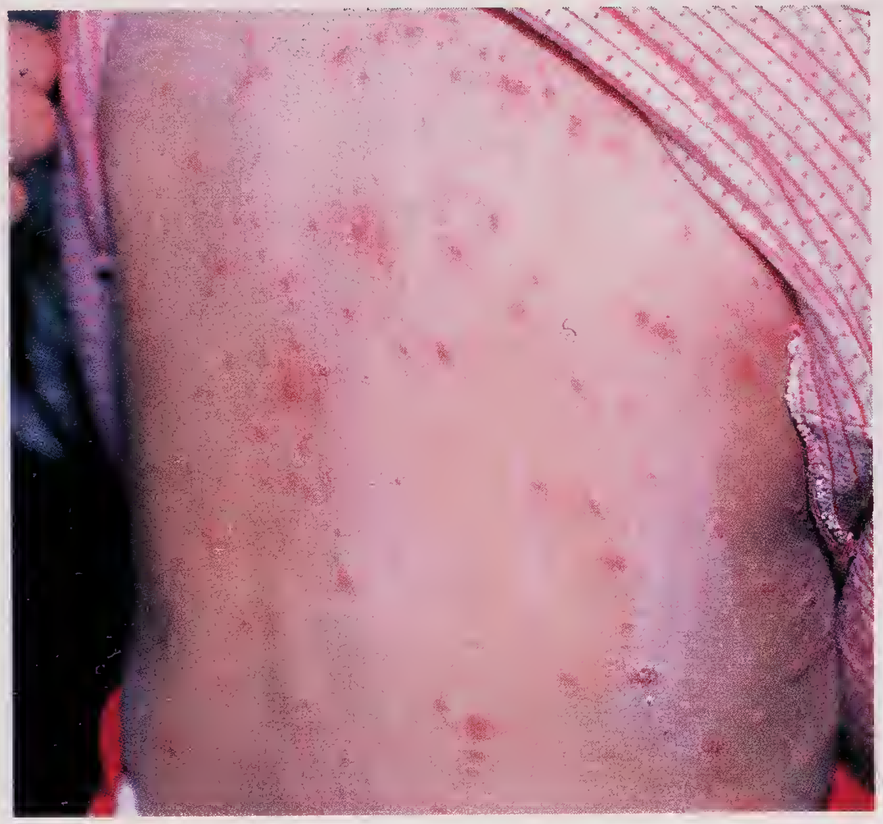

160

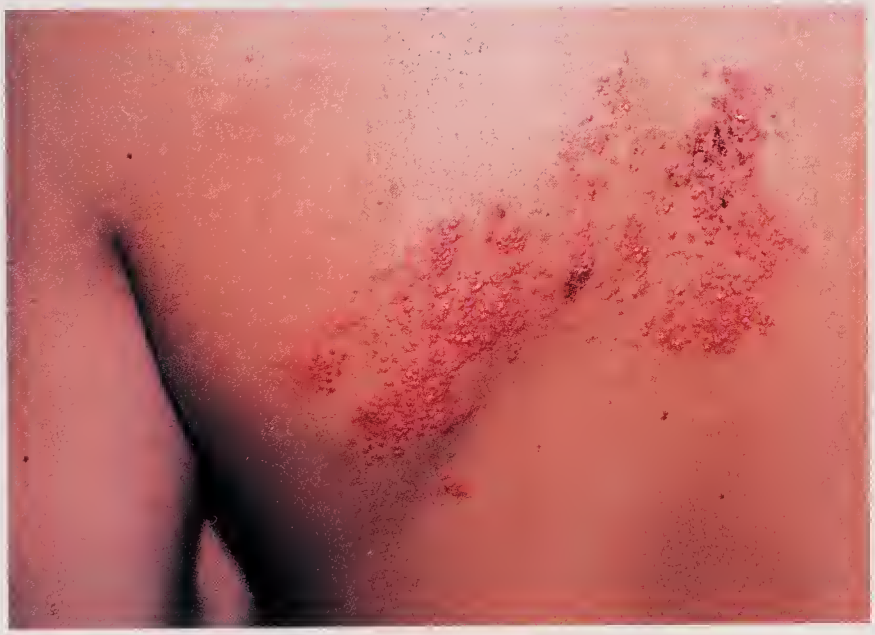

161

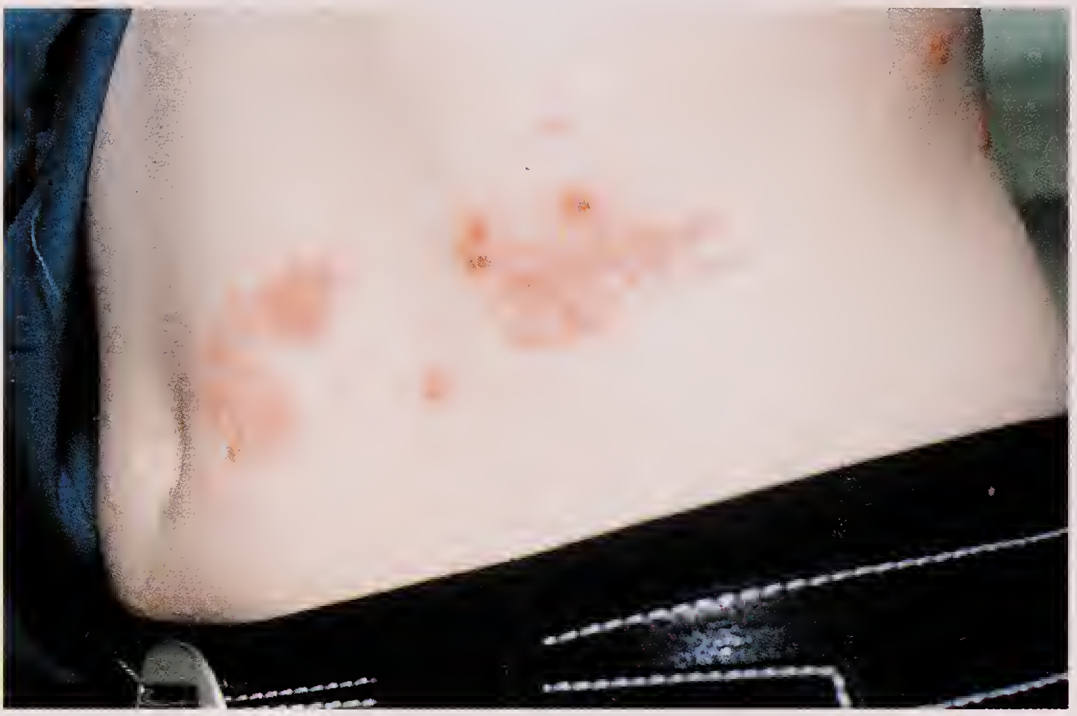

162

162 ◆ Varicella infection in a child, who experienced tingling and burning on the skin before the rash appeared. The boy had no past history of chickenpox. The dermatomal distribution of this varicella-zoster infection is evident.

163-164 ◆ Molluscum contagiosum in a 24-month-old child. This benign, asymptomatic viral disease of the skin is characterized by a relatively small number (2 to 20) discrete, papular skin lesions. Some lesions may have a central umbilication. The cause of this disorder is a poxvirus.

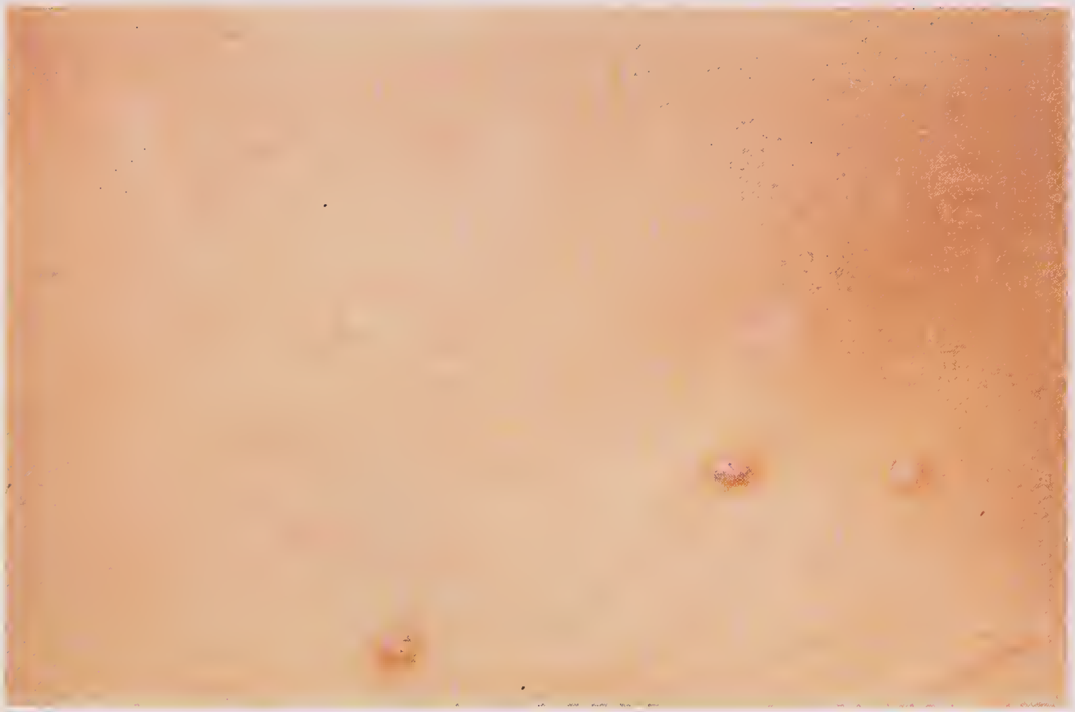

163

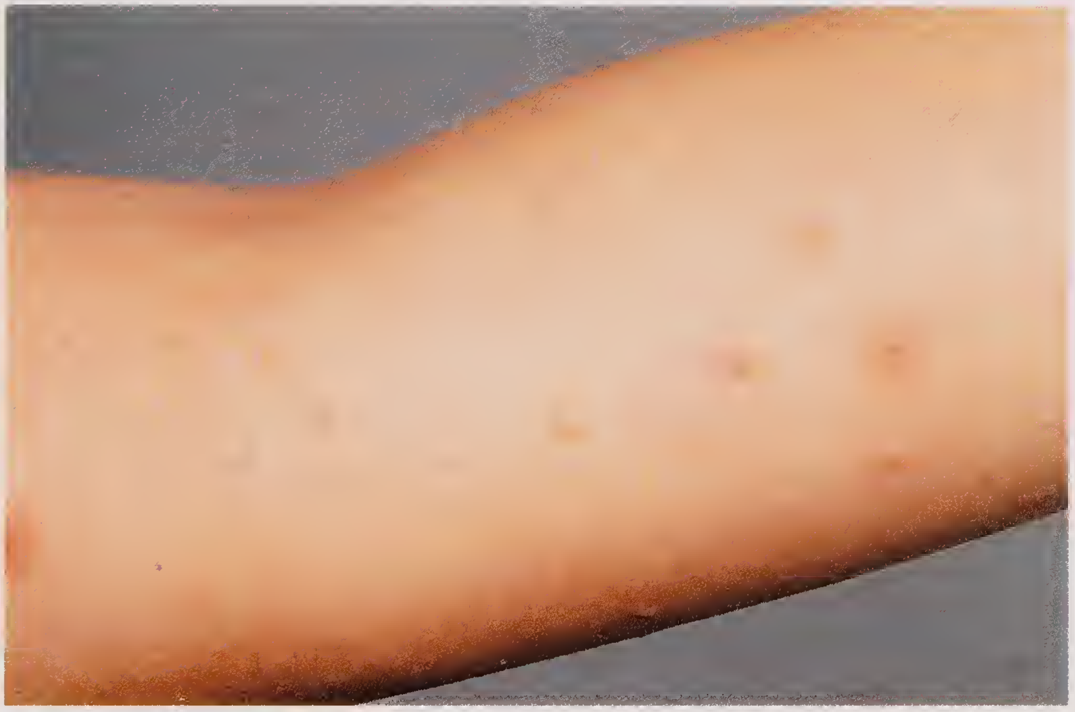

164

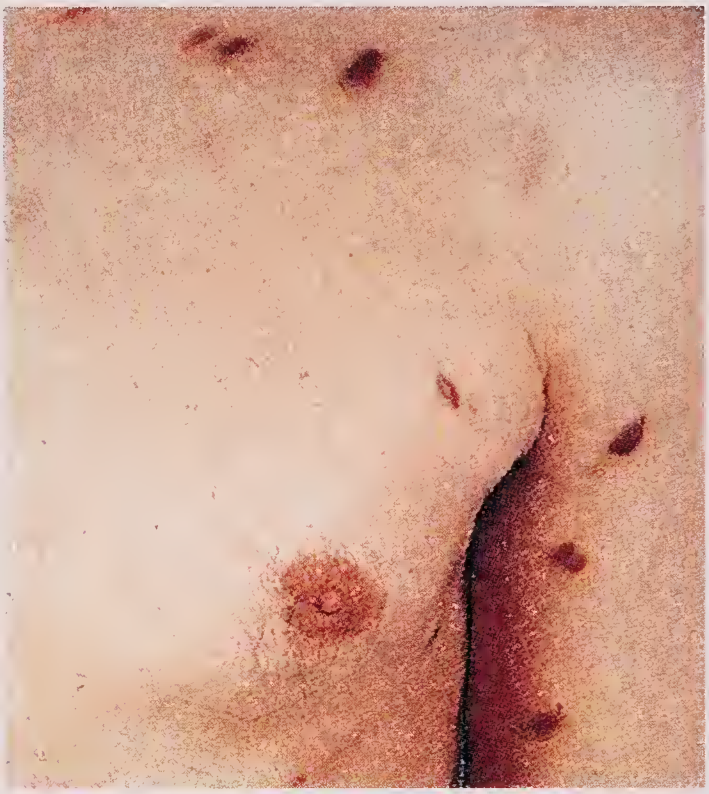

165

165 ♦ Cutaneous lesions of Kaposi's sarcoma, which are often associated with human immunodeficiency virus infection. Affected individuals present with violaceous papules and nodules that can involve the face, trunk, and extremities, as well as mucous membranes and internal organs.

166-167 ♦ Toxic epidermal necrolysis. This condition clinically begins as an exfoliative dermatitis; bullae, vesicles, and erosions may be seen in 166. Distribution is commonly perioral, perigenital, inguinal, and axillary. Proposed infectious etiologies include viral exanthems, *Streptococcus pyogenes*, and *Klebsiella*. Adverse drug reactions (predominately sulfonamides and anticonvulsants) have also been implicated. As the photomicrograph in 167 indicates, the skin has areas of denuded dermis and areas of full thickness necrosis of the epidermis.

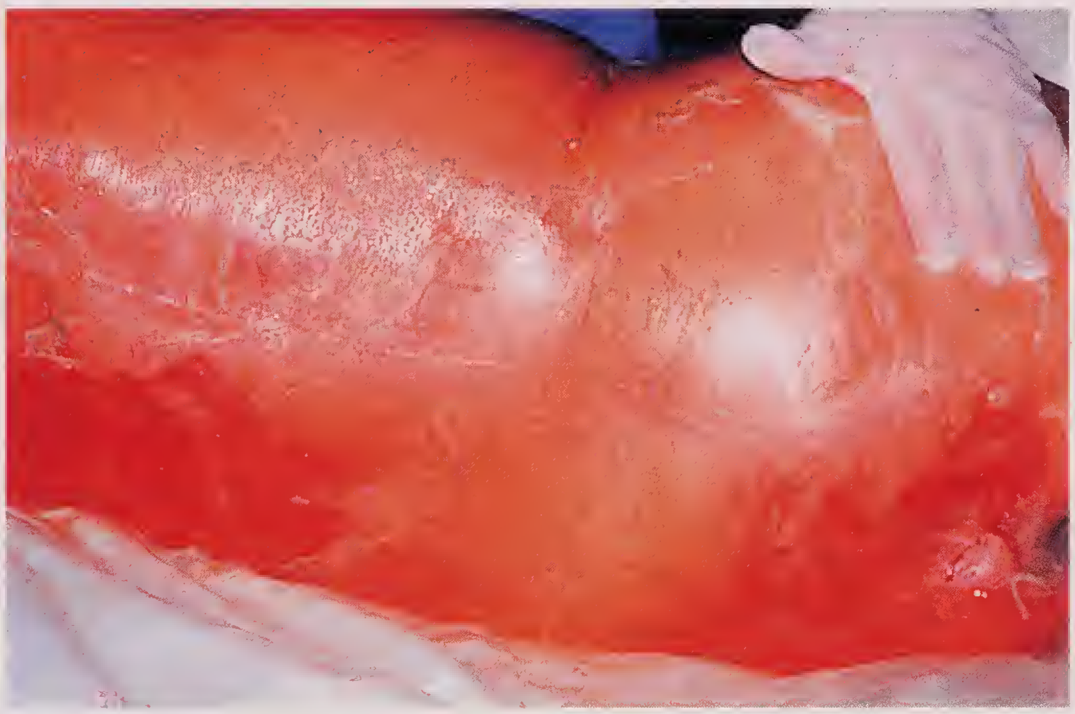

166

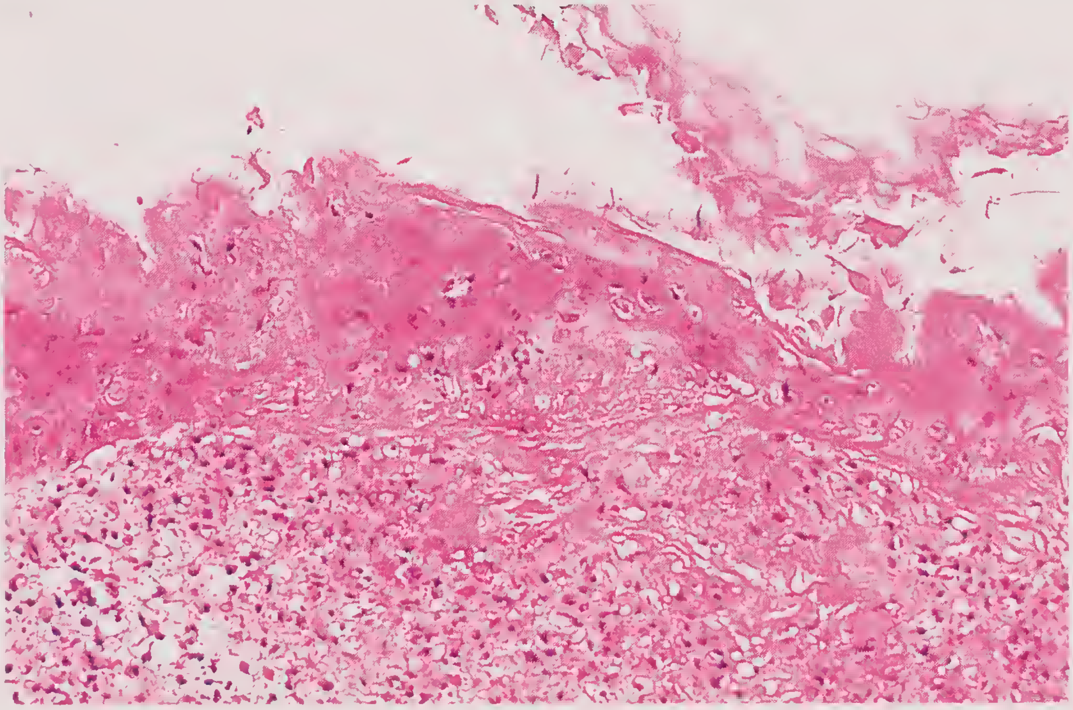

167

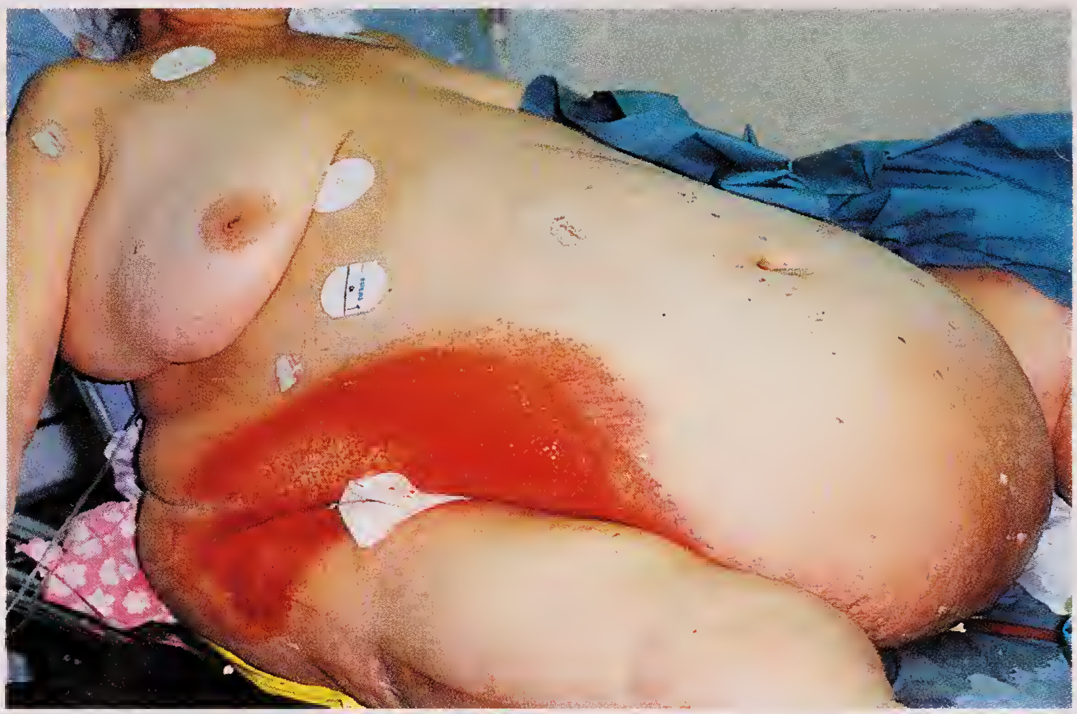

168

168 ◆ Intertriginous candidiasis in a patient who presents with the typical rash involving the infrapannus skin and fever. This condition is manifested by sharply demarcated, polycyclic, erythematous, erosive lesions with colarettelike scales and small pustular lesions at the periphery. Secondary bacterial infection is suggested, most likely due to staphylococci and streptococci.

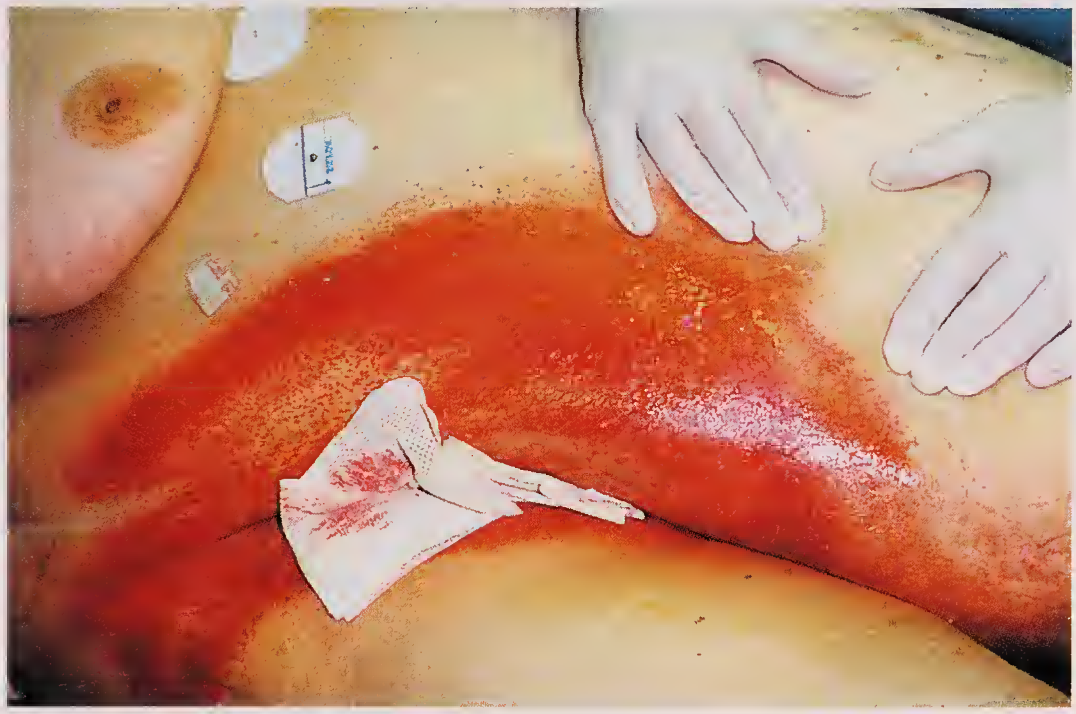

169

169 ♦ Patient in 168, with panniculus drawn back.

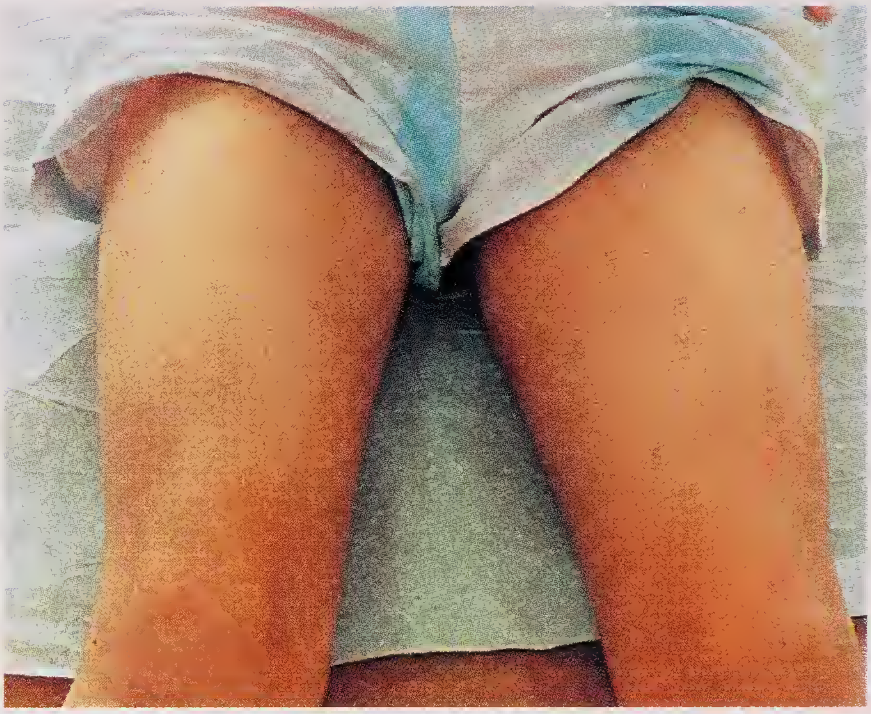

170

170 ♦ Faint migratory rash of the legs, which is seen in Lyme disease.

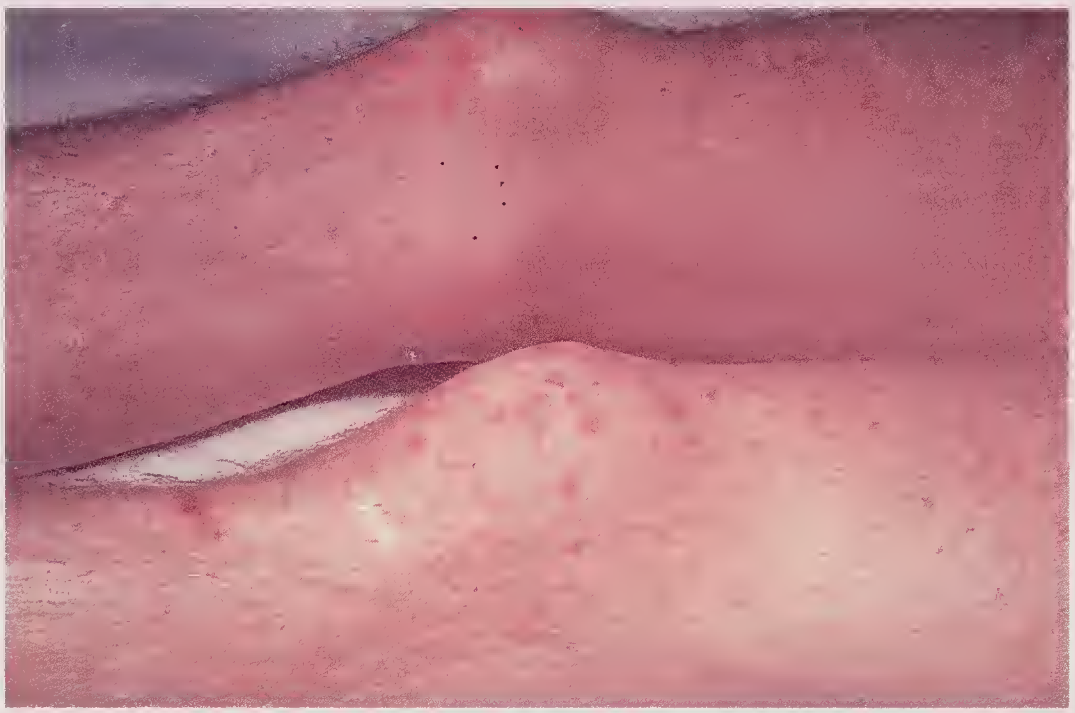

171

171 ♦ Rocky Mountain spotted fever. This disease is characterized by hemorrhagic macules and papules that begin distally and may eventually spread centripetally to involve the proximal portions of the extremities, as well as the trunk and face.

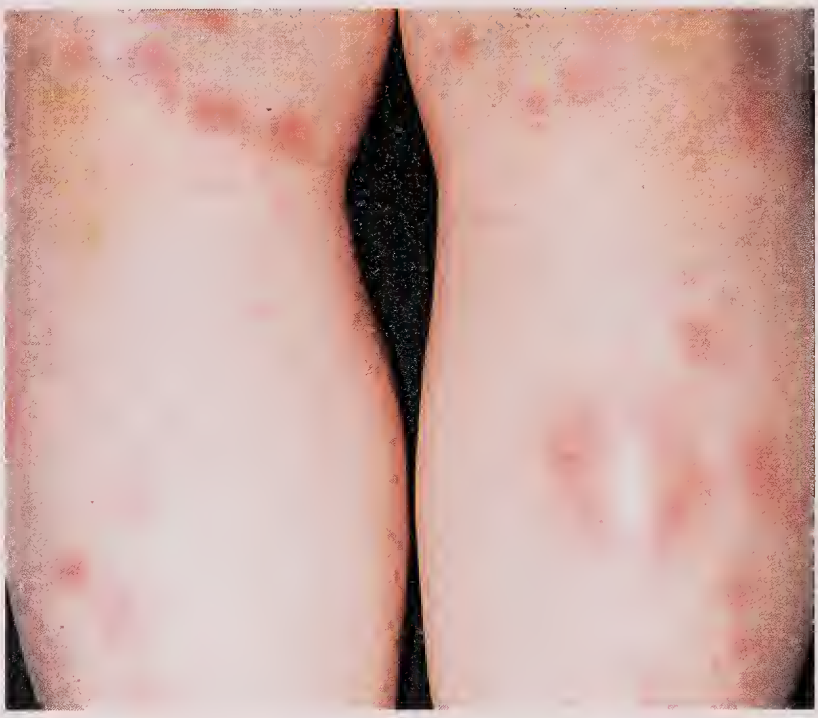

172

172 ♦ Erythema nodosum. Affected individuals present with exquisitely tender inflammatory nodules, most commonly in the pretibial area.

173 ♦ Erythema nodosum in a patient with tuberculosis. The lesions, which are tender nodules that vary in diameter from one to several centimeters, are typically located on the anterior portion of the legs. They usually heal without treatment in a few weeks. Agents such as *Streptococcus, Mycobacteria, Lymphogranuloma venereum,* and various fungi are prominent causes.

174 ♦ Tinea pedis in a patient with a severe fungal infection of the foot. This infection usually starts in the lateral interdigital spaces of the foot or on the undersurface of the toes. The main symptom is itching, with skin cracks that can become macerated. The usual causes of this infection are *Trichophyton rubrum* and *T mentagrophytes.*

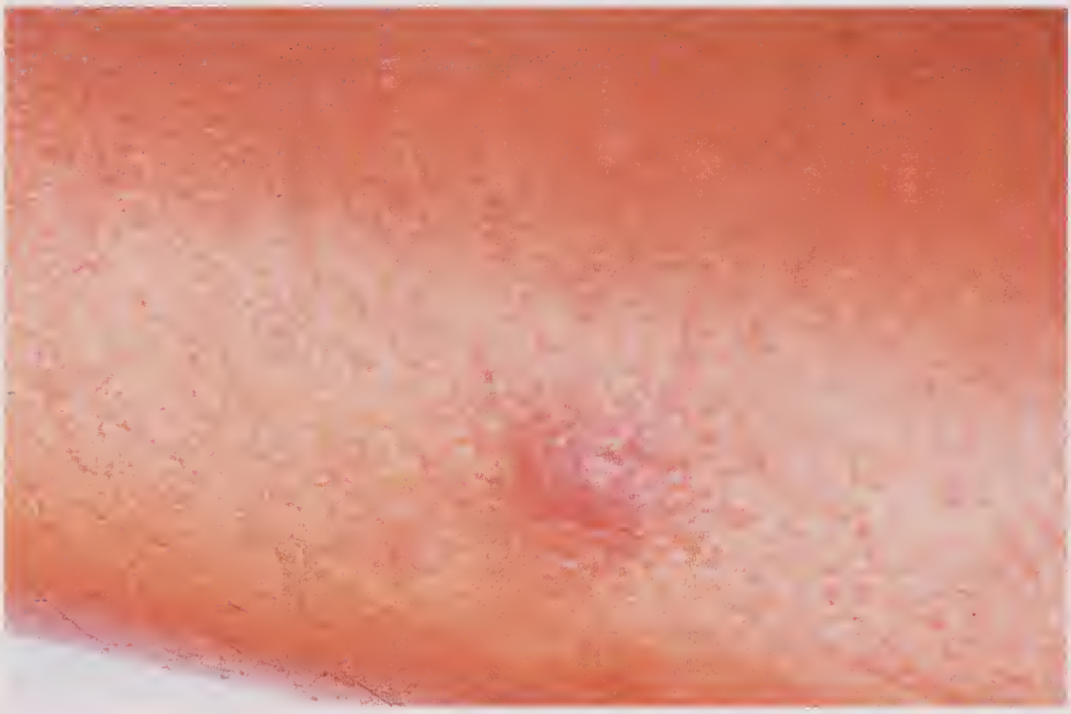

173

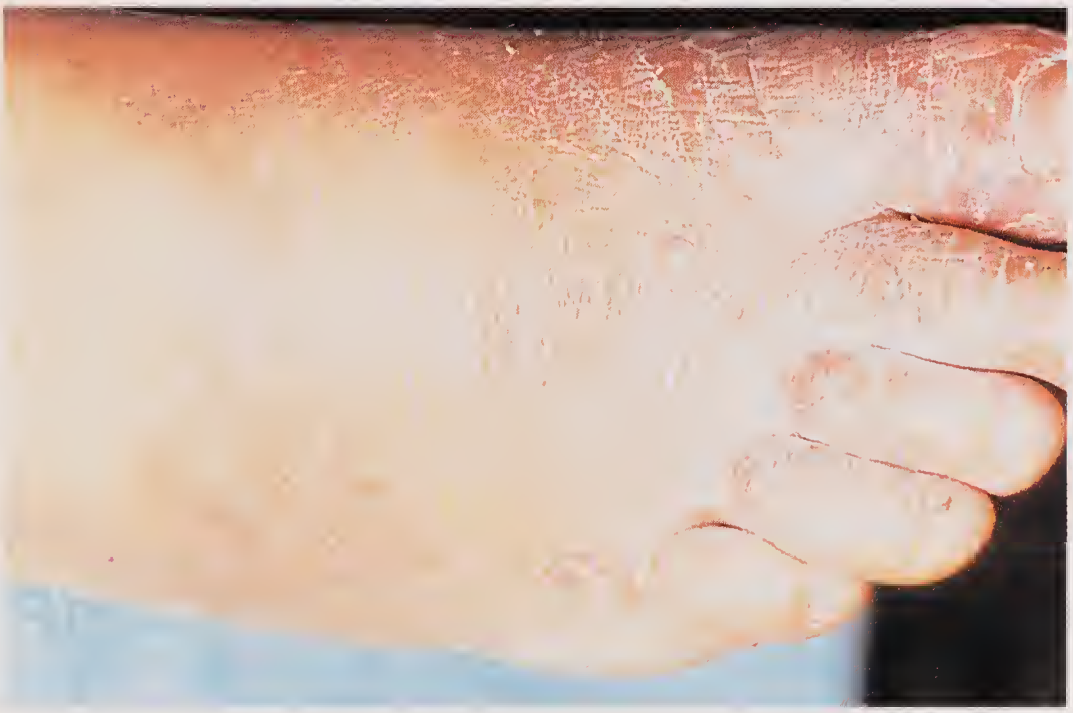

174

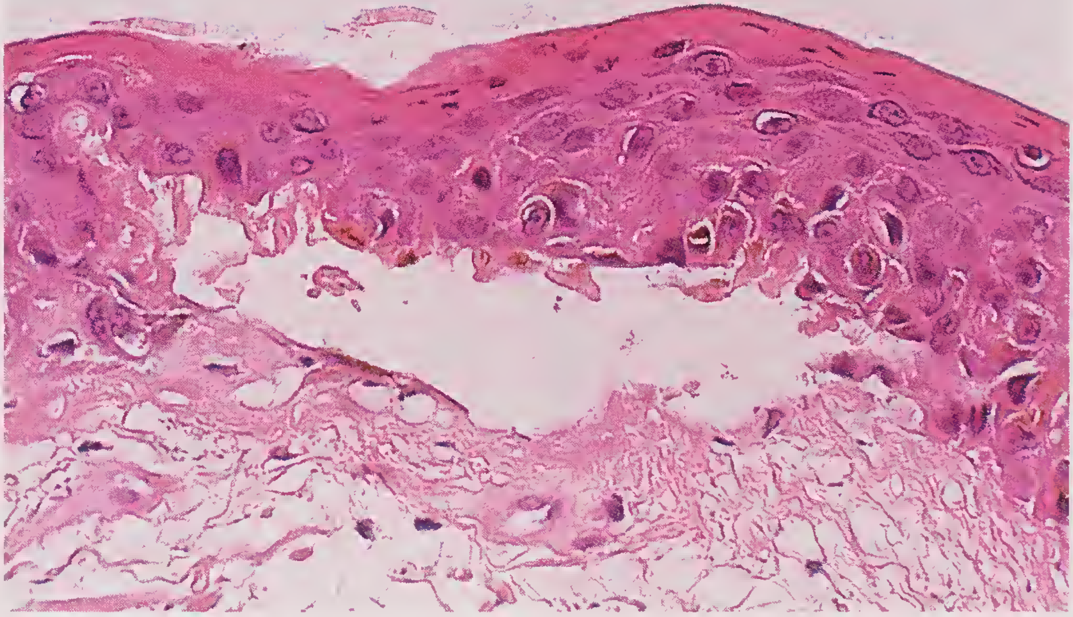

175

175 ♦ Erythema multiforme, which is clinically characterized by a papular rash with target lesions in a generalized symmetric distribution; microscopically, dermatitis with dyskeratotic cells and subepidermal bullae are seen. Proposed infectious etiologies include herpes simplex virus, primary atypical pneumonia, streptococcal infection, adverse drug reactions, and systemic lupus erythematosus.

176-177 ♦ Scarlet fever in a 4-year-old child. Note the fine, red, scarlatiniform rash covering the face and trunk; this rash is also found on the extremities. The child also has the classic flushing of the cheeks with circumoral pallor.

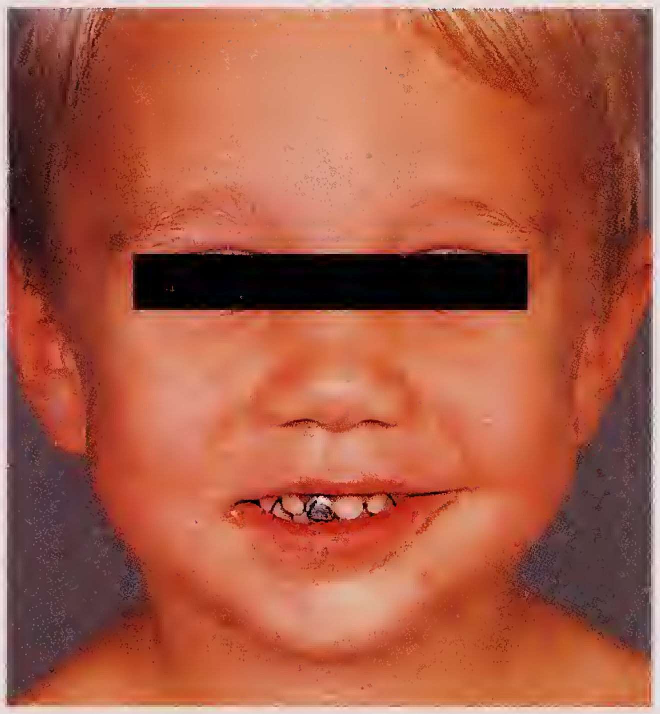

176

177

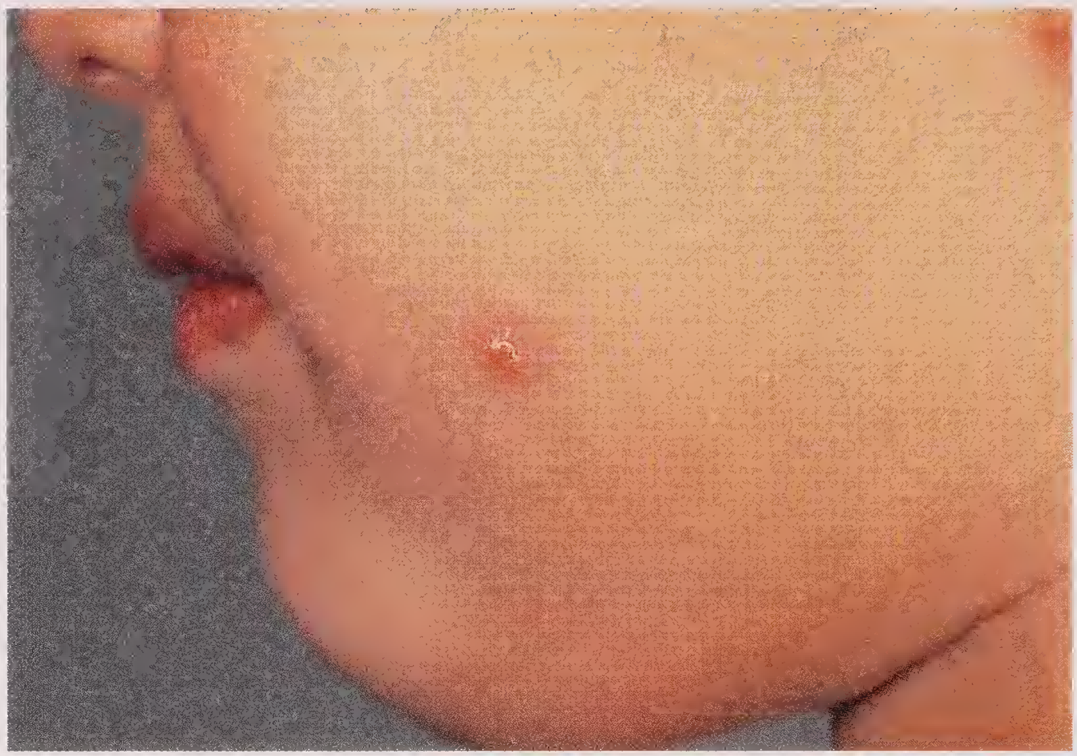

178

178 ♦ Cat-scratch disease in a 4-year-old girl. A primary lesion is located on the left cheek, with obvious swelling of the submental lymph node.

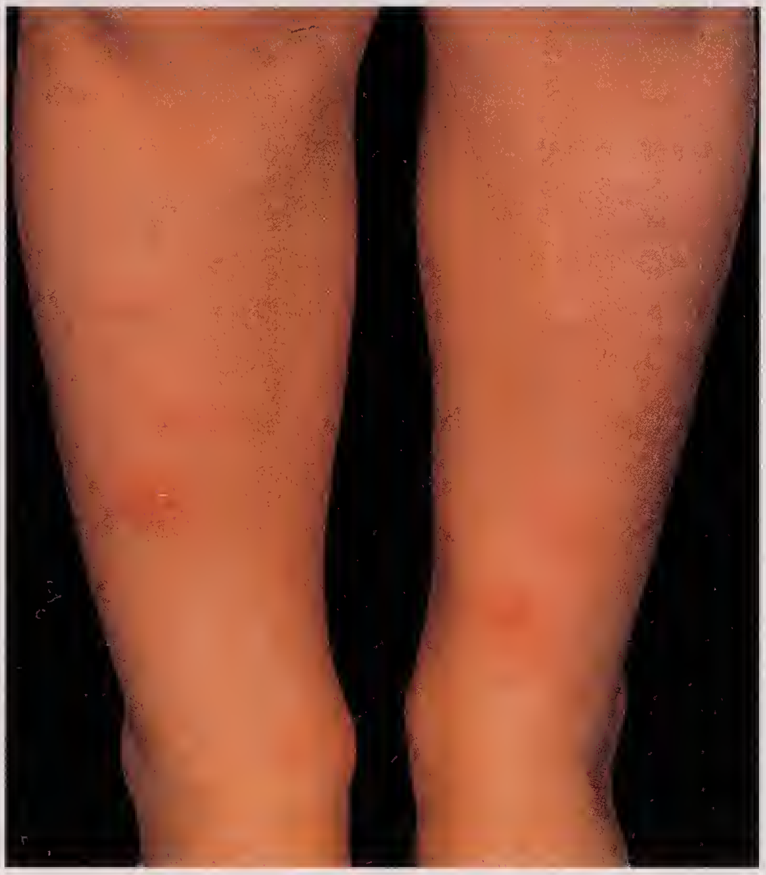

179

179 ♦ Patient in 178 with associated erythema nodosum. This rash, which is occasionally seen in children who suffer from cat-scratch disease, is characterized by multiple nodules covered by bright red, smooth, shiny skin. The rash usually involves the shins, as seen in this child.

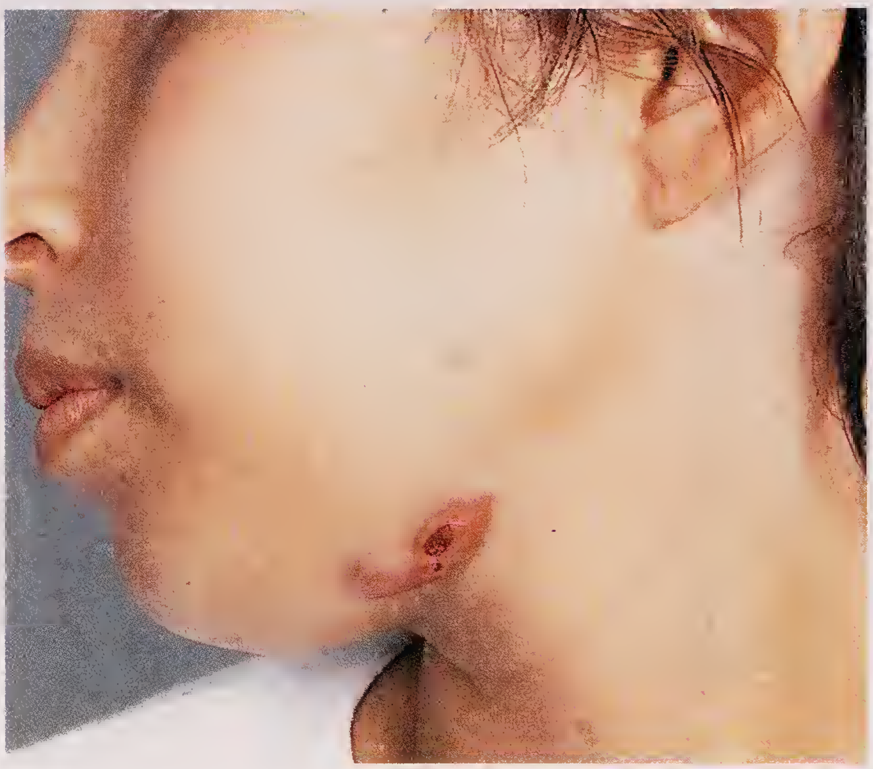

180

180 ♦ Cervical adenitis and cutaneous involvement due to *Mycobacterium kansasii* in an 11-year-old girl.

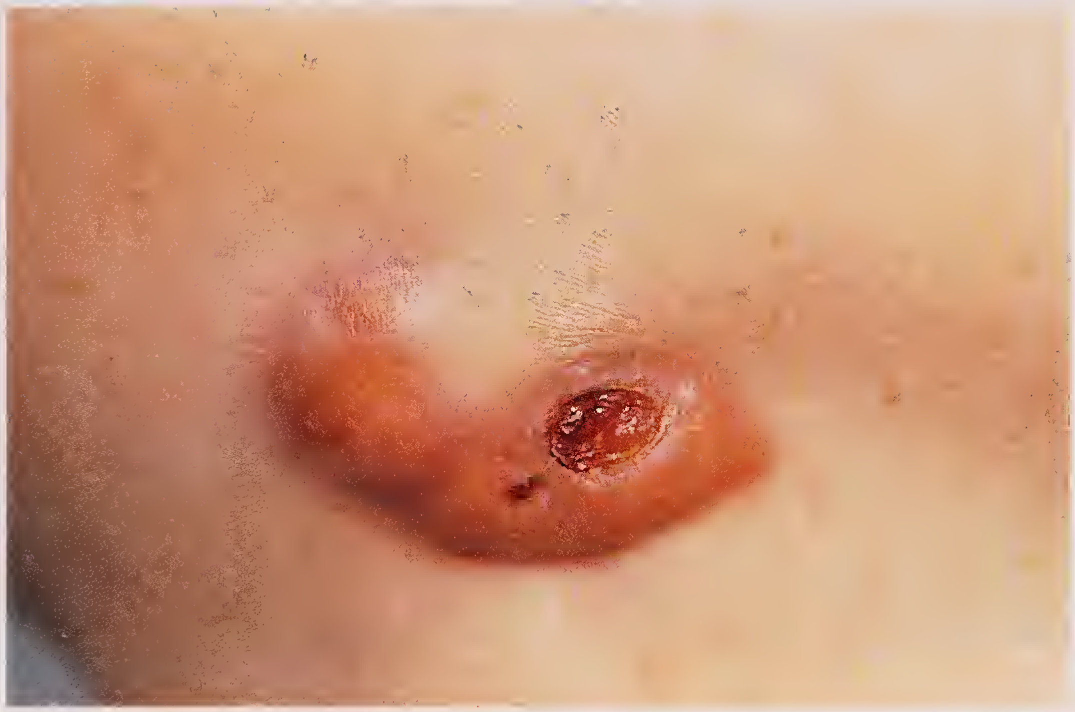

181

181 ♦ Close-up view of the patient in 180. Note the violaceous ulcerative lesion overlying the enlarged nodes beneath the body of the mandible.

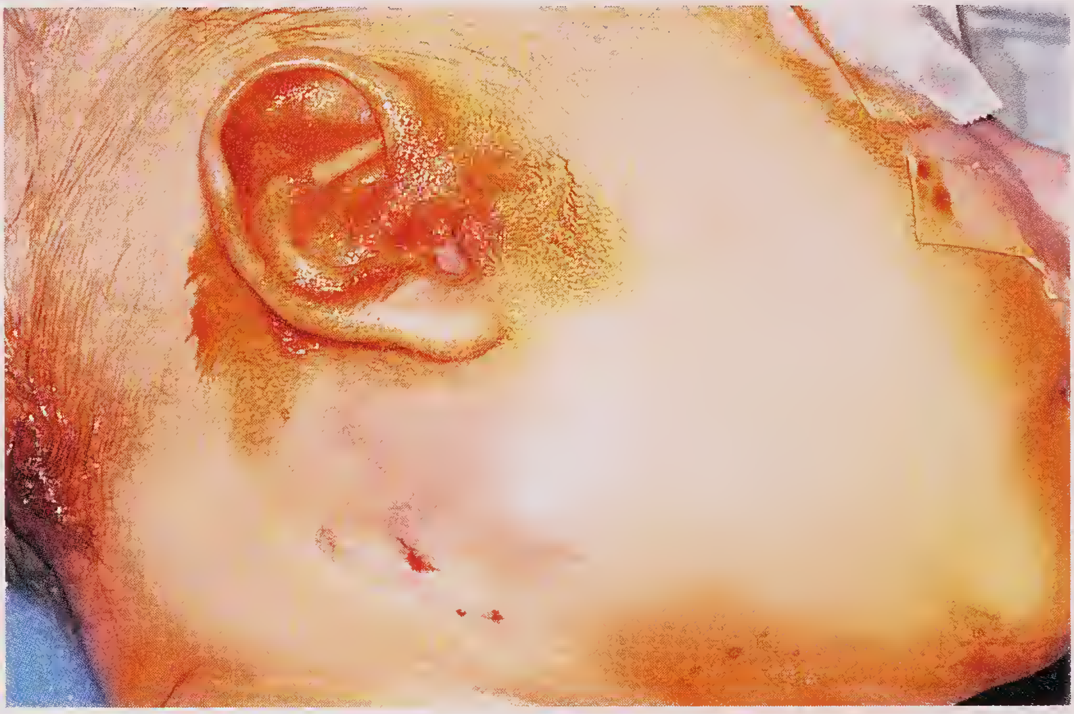

182

182 ♦ Acute right-sided cervical abscess in a child. This disorder, which is usually due to *Staphylococcus aureus*, involves suppuration of a cervical lymph node. The swollen, red, tender mass is clearly seen posterior to the angle of the mandible.

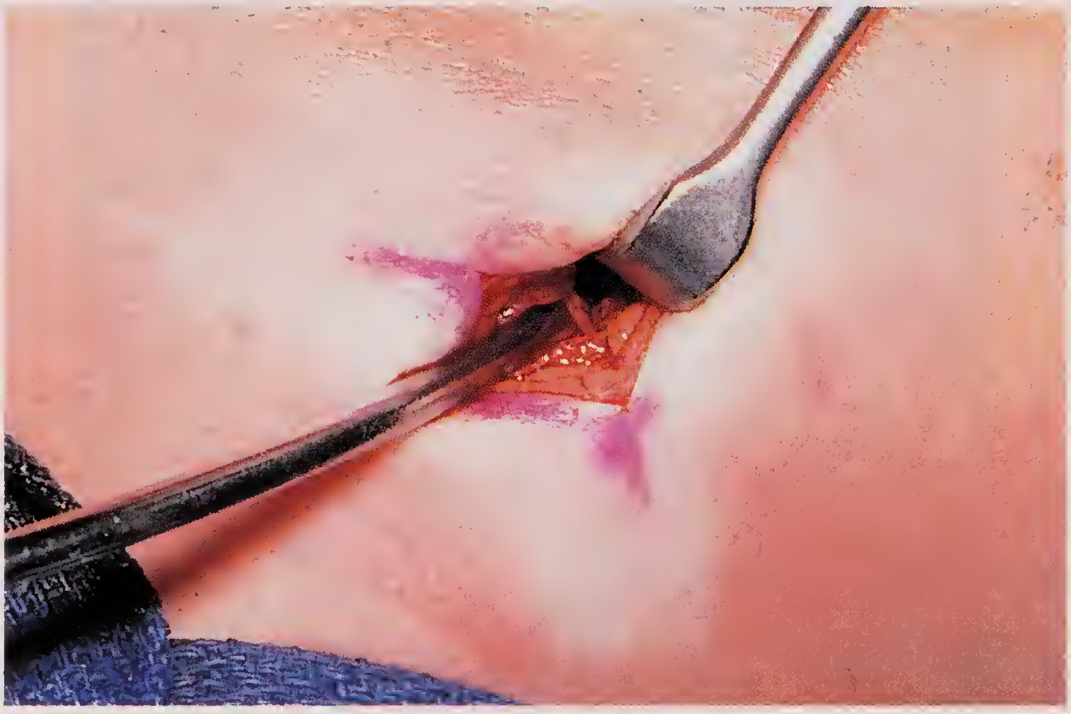

183

183 ♦ Treatment of the mass in 182, which involves surgical incision and drainage with irrigation of the abscess cavity. This photograph shows the interior of the abscess cavity following removal of all the purulent contents.

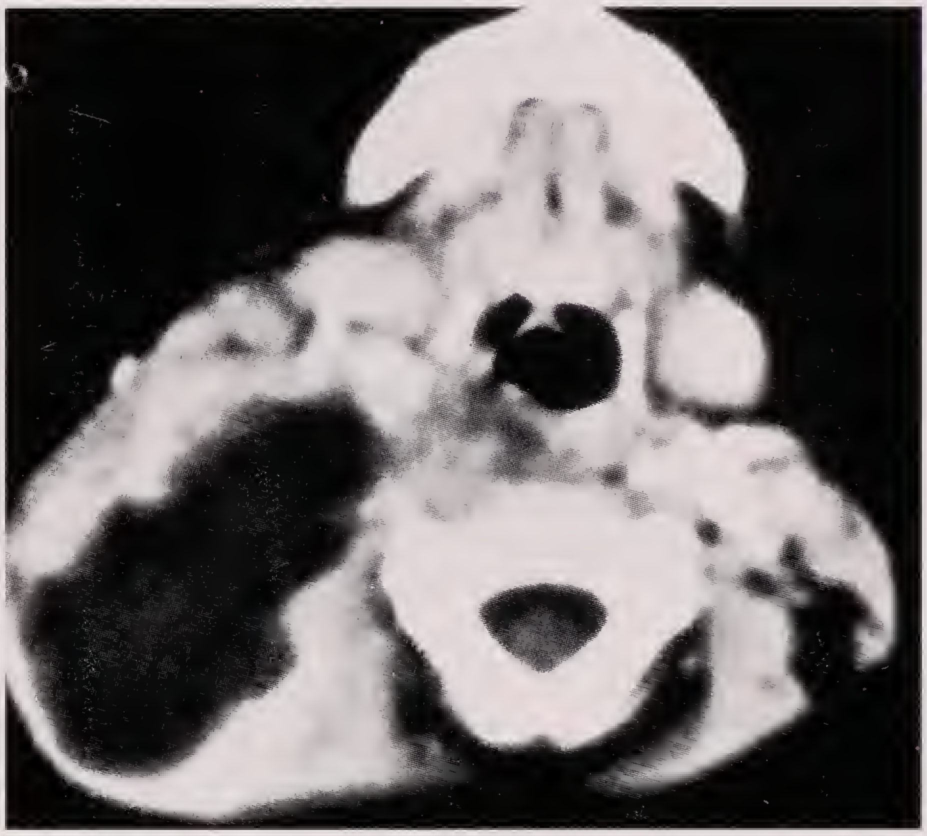

184

184 ♦ Axial computed tomography scan of a young child with a right-sided cervical abscess. Note the accumulation of a large amount of a radiolucent material in the right cervical area.

185-186 ♦ Acute right-sided cervical abscess in a 13-month-old child. Note the significant inflammatory changes on the right side of the patient's neck. The outline of the mandible is illustrated on the lateral photograph.

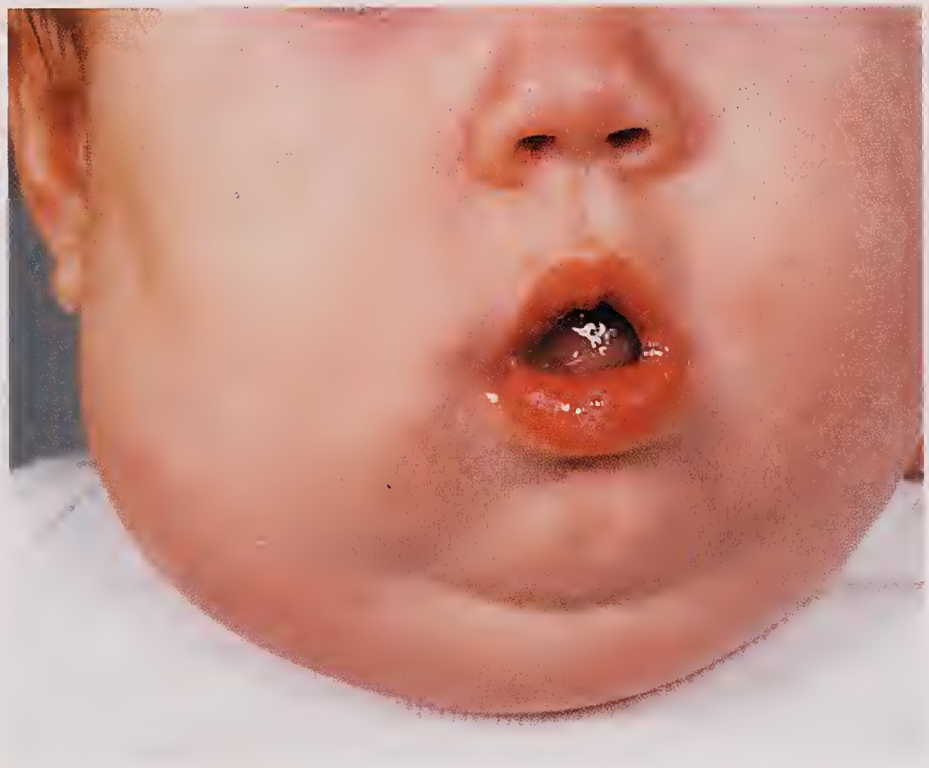

185

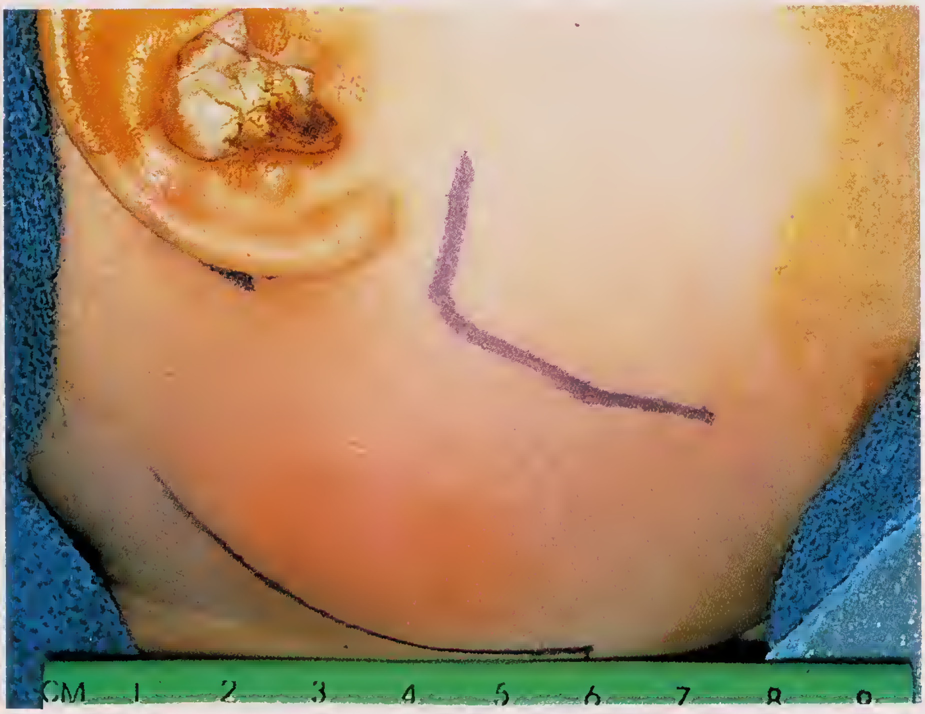
CM 1 2 3 4 5 6 7 8 9

186

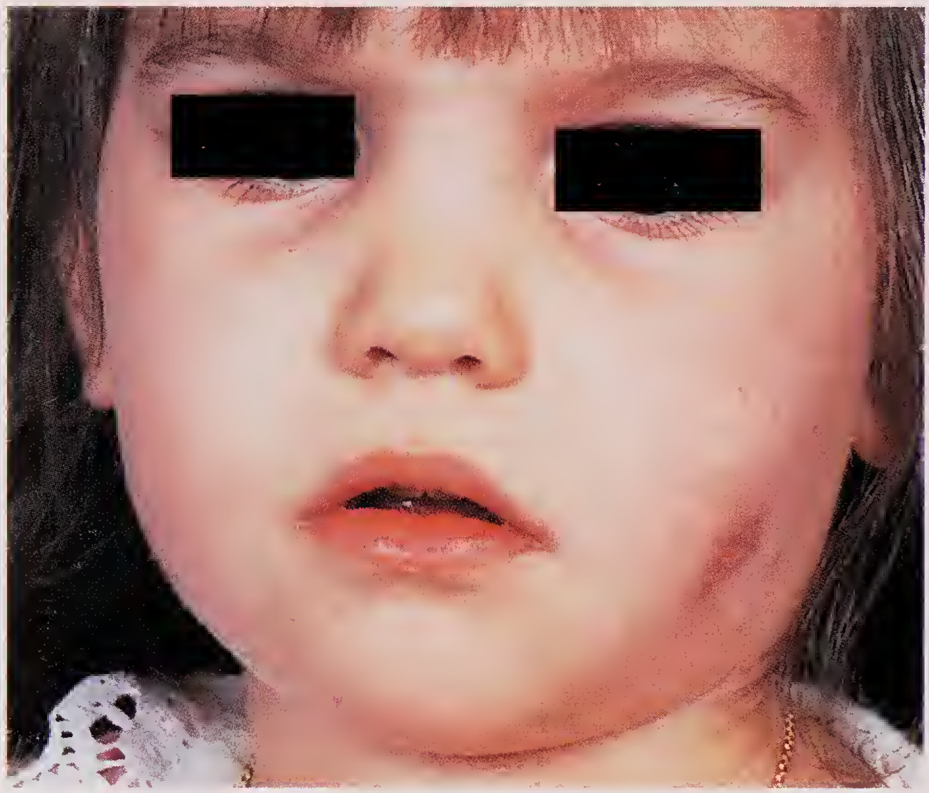

187

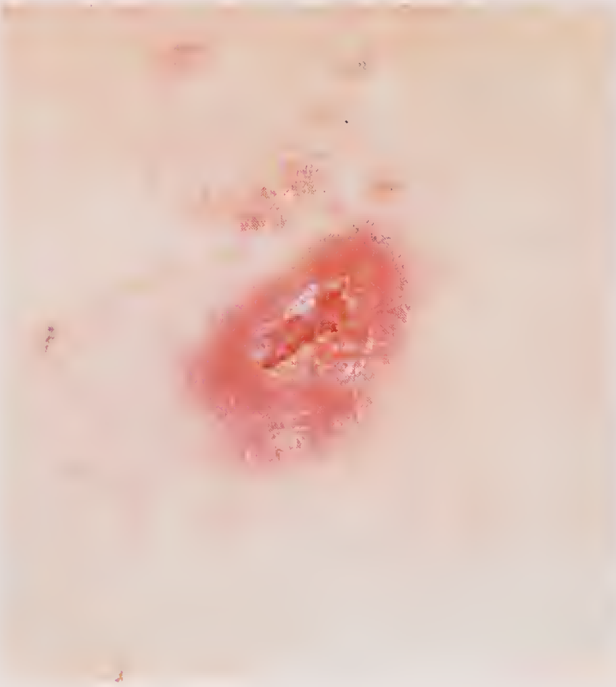

188

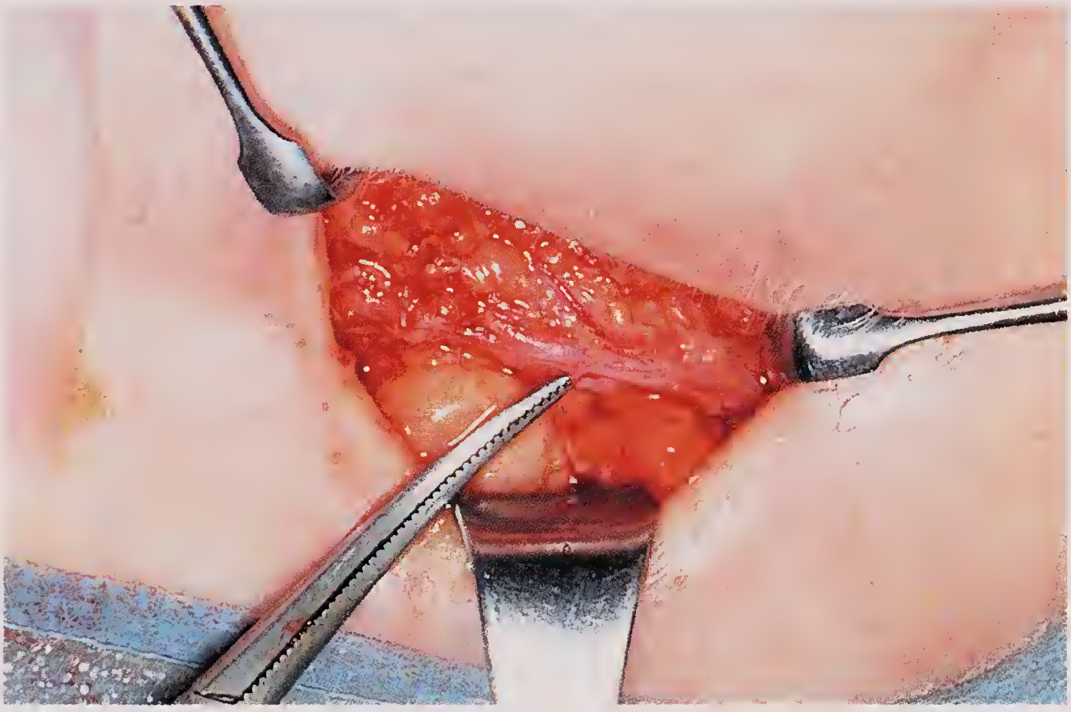

189

187-188 ♦ Cervical facial adenitis and skin involvement due to *Mycobacterium avium* complex in an 18-month old girl. This atypical mycobacterium responds poorly to chemotherapy, and surgical excision is necessary.

189 ♦ Patient in 188. The surgical excision required exposure of the buccal branch of the facial nerve, as illustrated in this photograph. The infected lymph node and skin can then be safely excised.

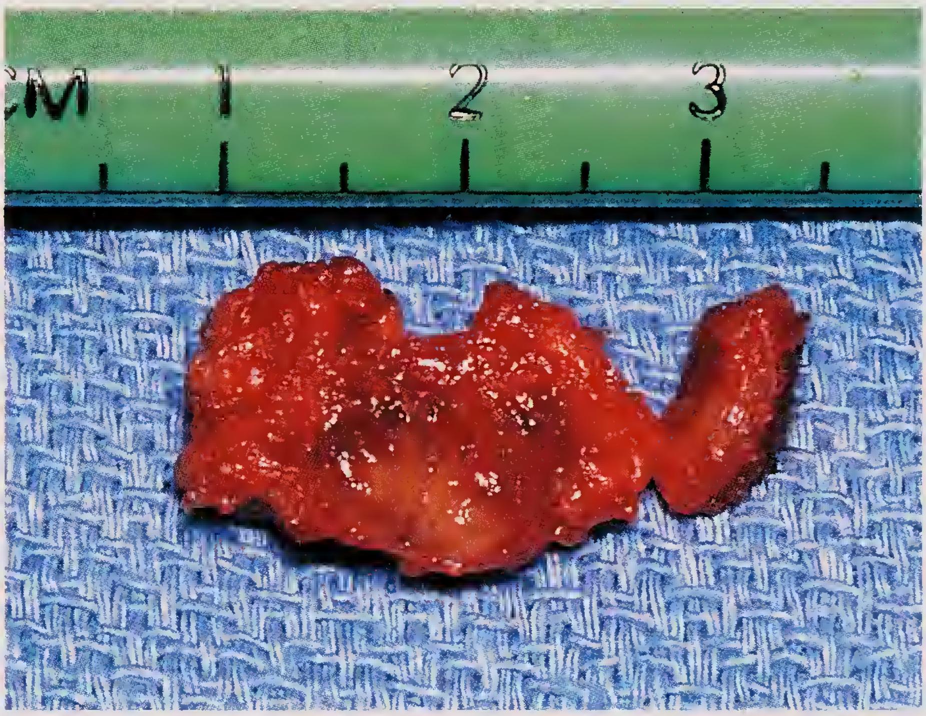

190

190 ♦ Surgical specimen from the patient in 188, including the involved node, surrounding soft tissue, and overlying skin.

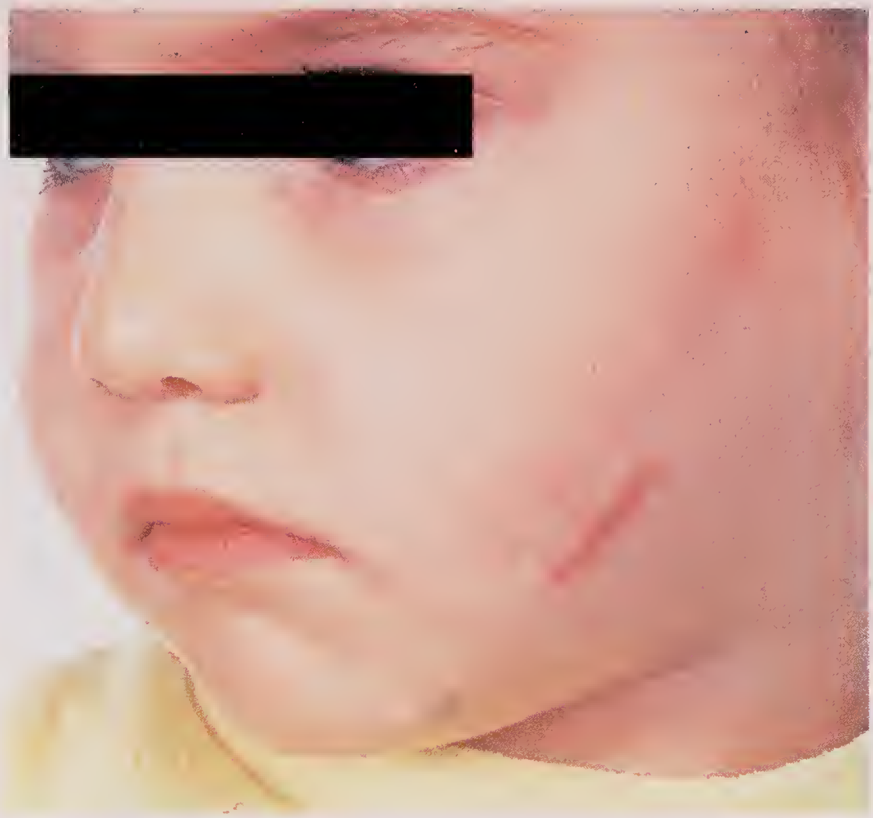

[redacted]

191

191 ♦ Patient in 190 seen 4 months postoperatively. There has been no recurrence.

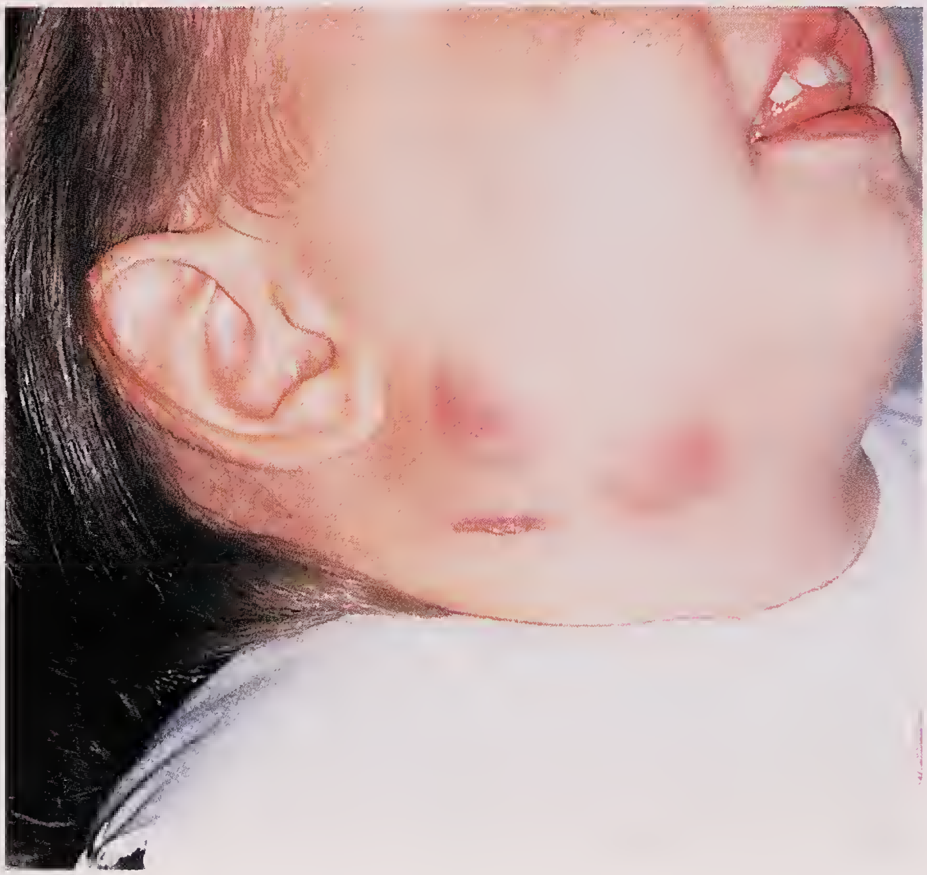

192

192-194 ♦ Atypical *Mycobacterium scrofulaceum* in a 15-month-old child. Note the biopsy site on the neck. Incisional biopsy is not recommended, because it usually leads to a chronic draining skin lesion and possible extension of the disease. This child did develop these complications. Note the extension to the preauricular and submandibular area. Treatment involved exposure of the parotid gland and complete dissection of the facial nerve, with removal of all of the infected lymph nodes and skin.

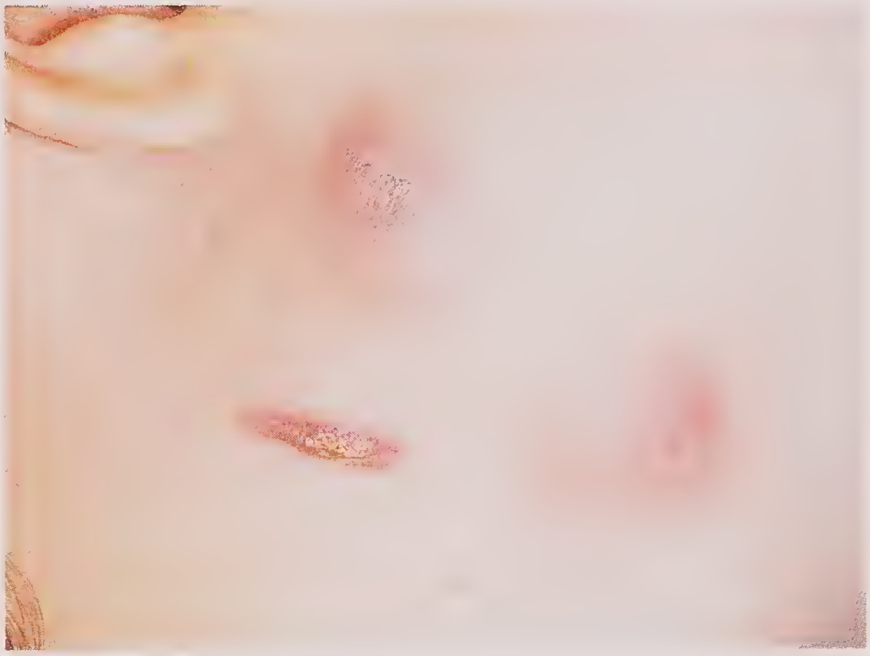

193

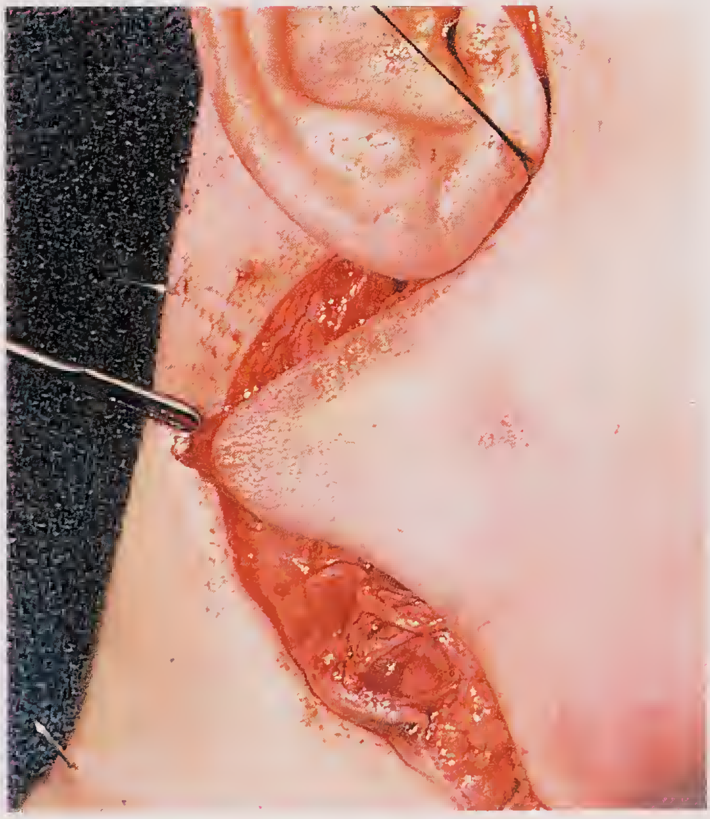

194

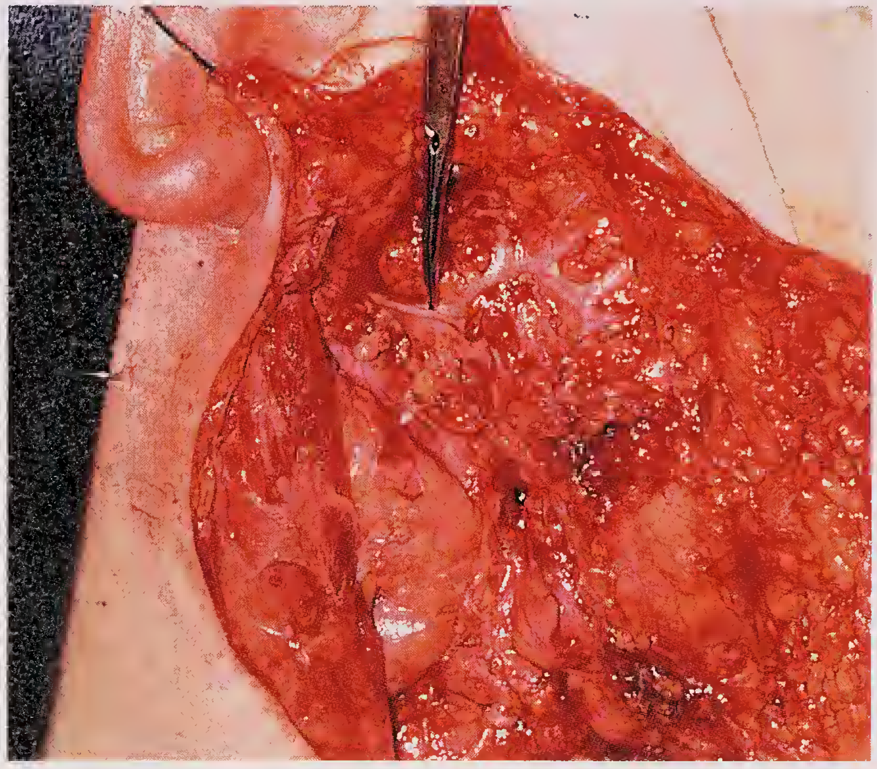

195

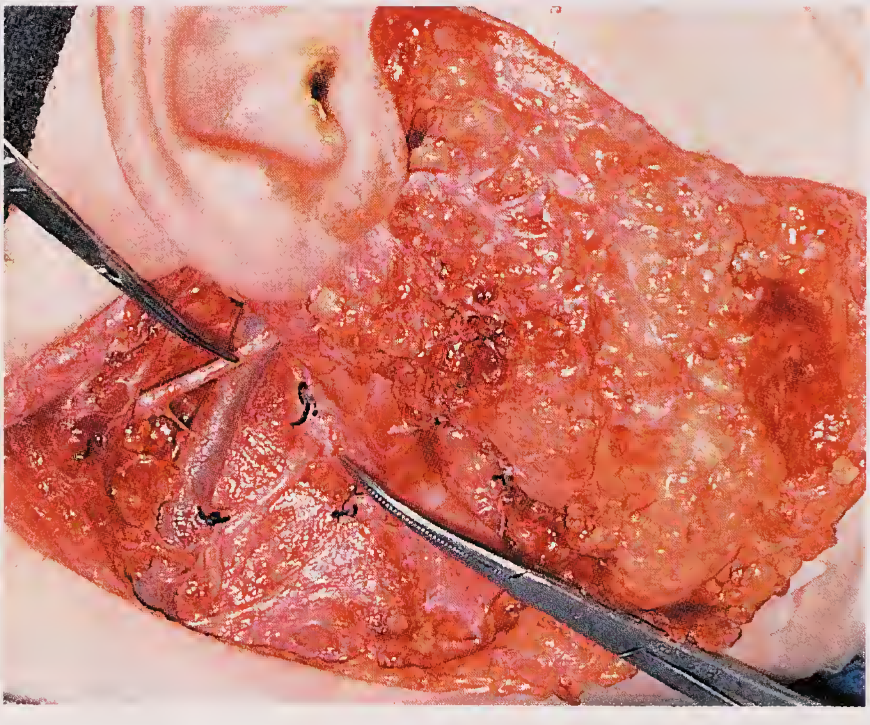

196

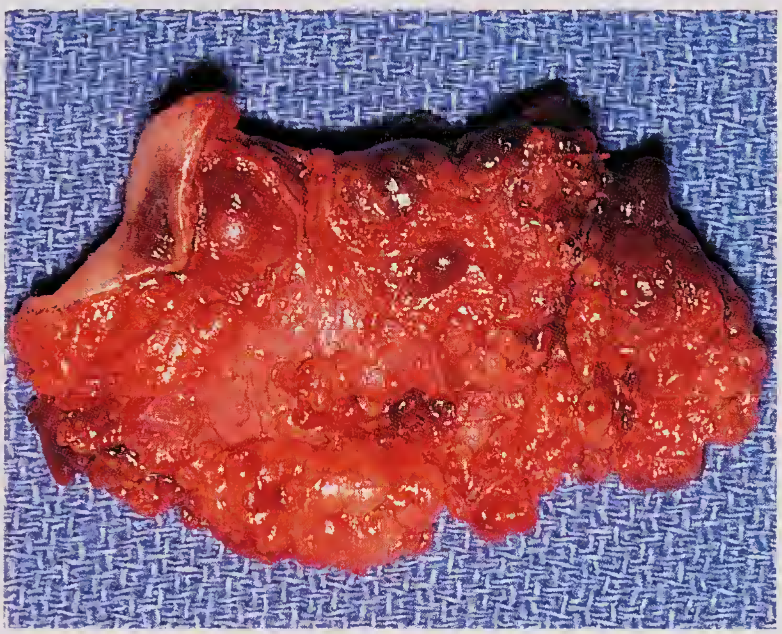

197

195-197 ♦ Treatment of atypical *Mycobacterium scrofulaceum*, which involves exposure of the parotid gland and complete dissection of the facial nerve, with removal of all of the infected lymph nodes and skin. The view in 196 shows exposure of the spinal accessory nerve, internal jugular vein, and hypoglossal nerve. The complete surgical specimen in 197 includes the infected skin lesions and all subcutaneous lymph nodes.

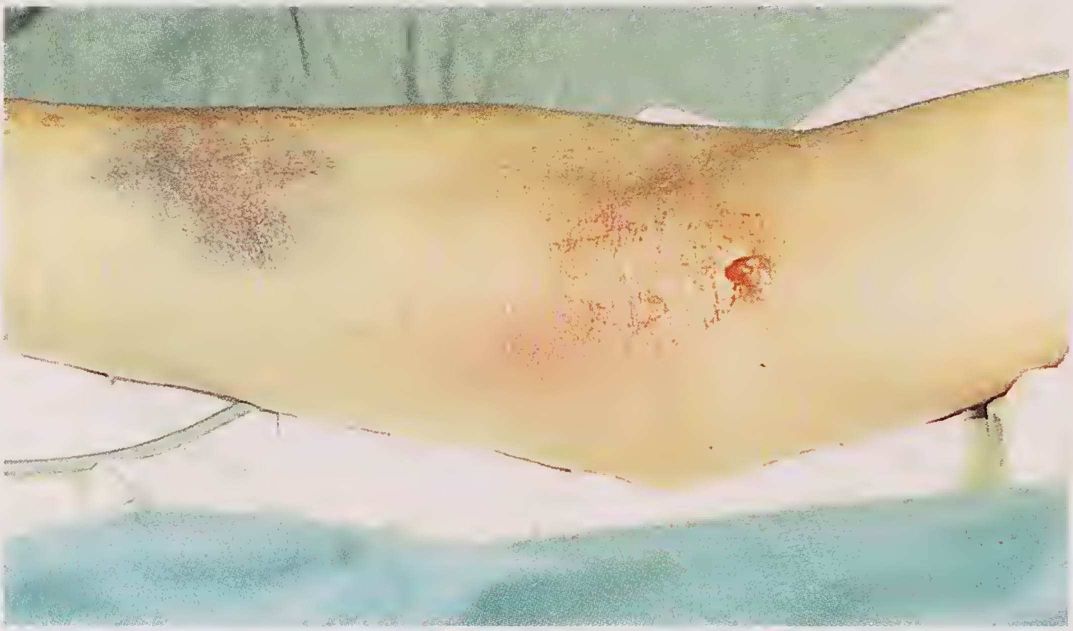

198

198 ♦ A 73-year-old woman who presents with fever as well as right arm pain and redness. She was recently hospitalized with an intravenous line at the area of pain. The presence of fever, erythema, a palpable cord, and pus exuding from the prior intravenous site, as seen here, suggests septic thrombophlebitis.

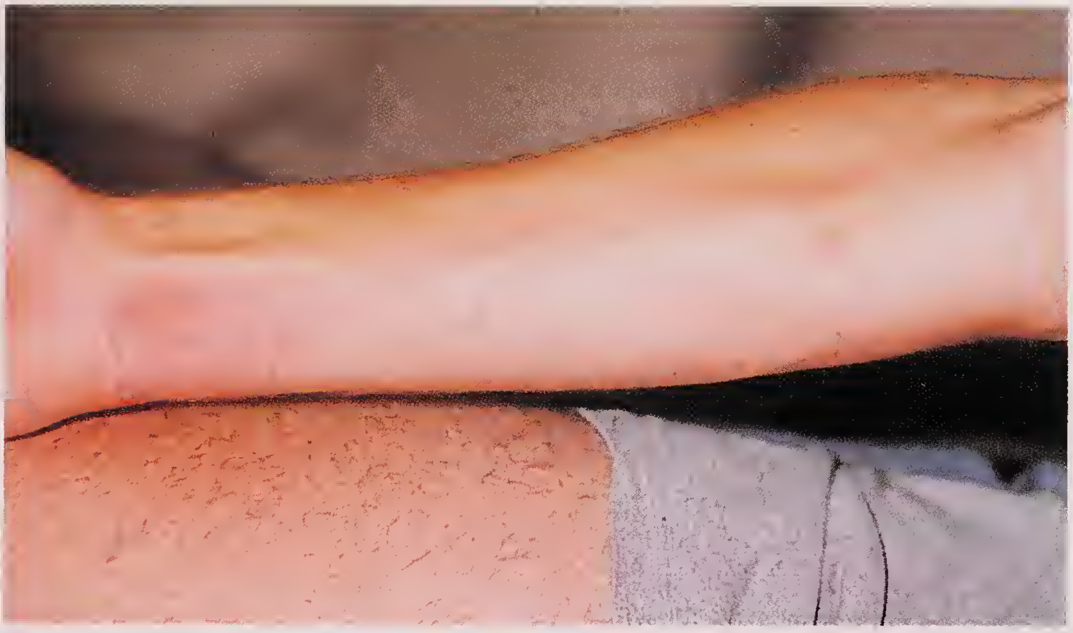

199

199 ♦ Lymphangitis, which may extend from a distal site of infection (cellulitis) to the trunk, as seen here. The disease is manifest by a cutaneous erythematous streak along the course of a lymphatic vein. The bacteriology usually reflects the original infection and often is *Staphylococcus aureus* or group A β-hemolytic streptococcus.

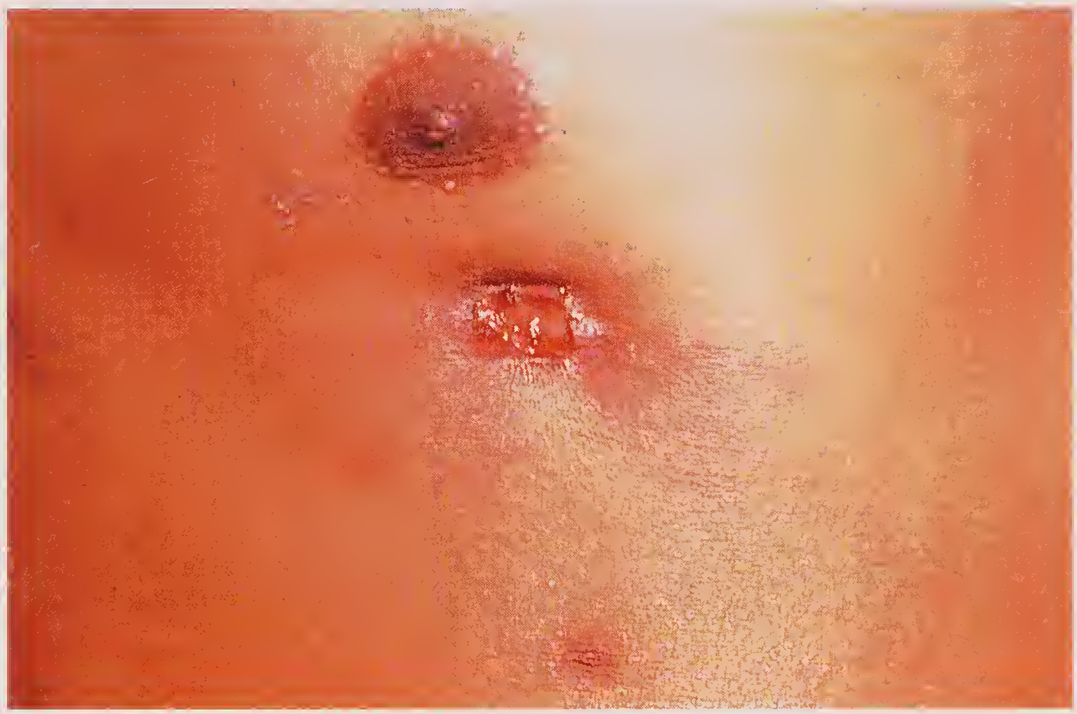

200

200 ♦ Ulcerative lesion in the right inframammary area, which was found to be positive for acid-fast bacilli and later identified as *Mycobacterium tuberculosis*. Rarely, individuals with tuberculosis present with single or multiple abscesses with subsequent rupture, causing ulceration with granulation tissue. This condition may be associated with osteolytic rib tuberculosis or dissection of pus from underlying caseous foci.

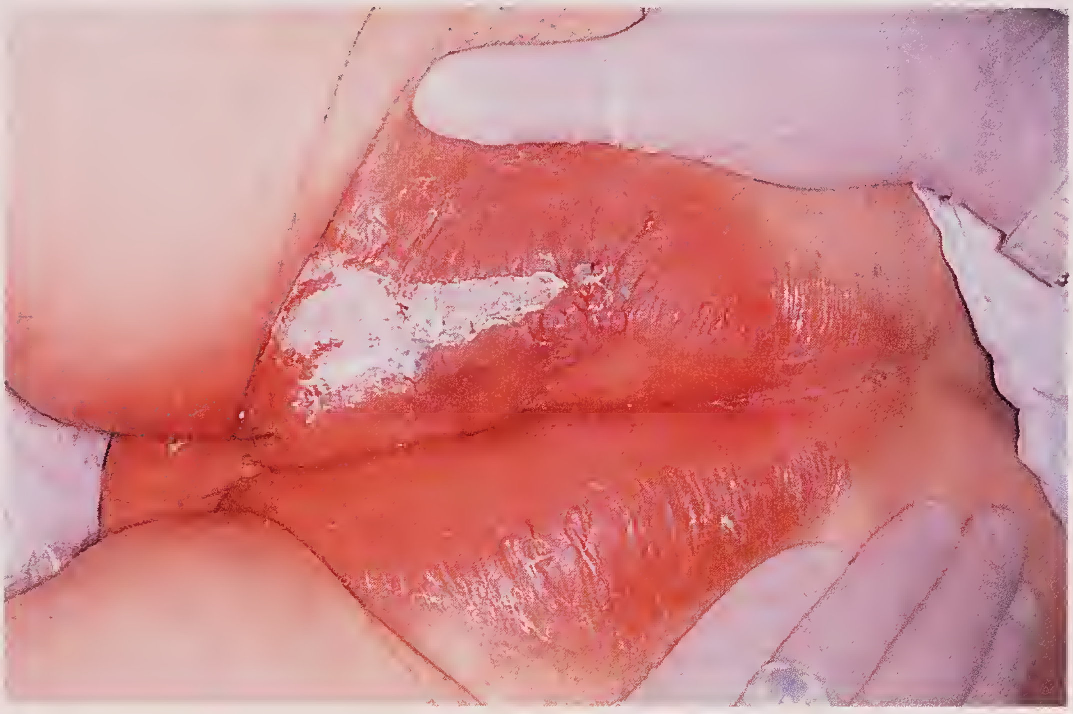

201

201 ♦ Intertriginous candidiasis of the gluteal cleft in a 66-year-old man who presents with a 2-day history of fever and throbbing perianal pain. The pain is worse with sitting, coughing, and straining. Fluctuance is present around the left perianal area, with a large area of erythema that extends beyond the gluteal cleft. The perianal abscess and cellulitis are a secondary infection of the candidiasis.

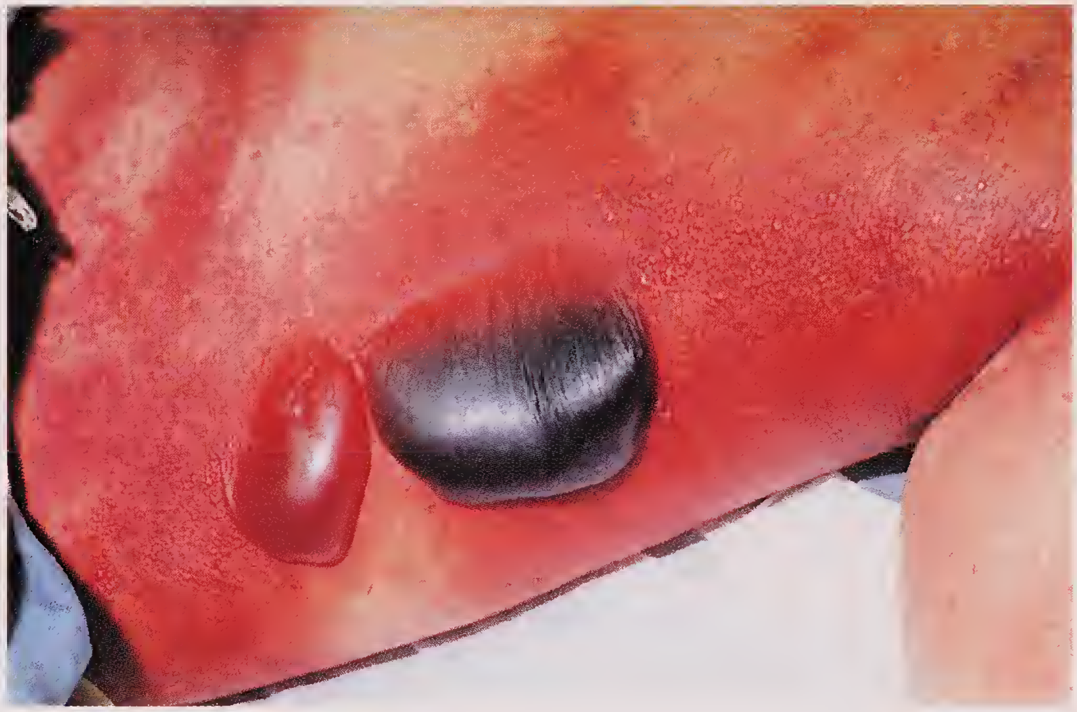

202

202 ◆ A 76-year-old woman who presents with fever, proximal left leg swelling, and erythema. During the 4-hour examination, the erythema seen here extends to involve the entire thigh, and hemorrhagic bullae develop and coalesce. The woman also becomes hypotensive. The aggressive nature of these symptoms, including rash, suggest necrotizing fasciitis. The causative organisms are most commonly polymicrobial; however, β-hemolytic streptococci, *Staphylococcus aureus*, anaerobes, and Gram-negative rods alone may cause this syndrome.

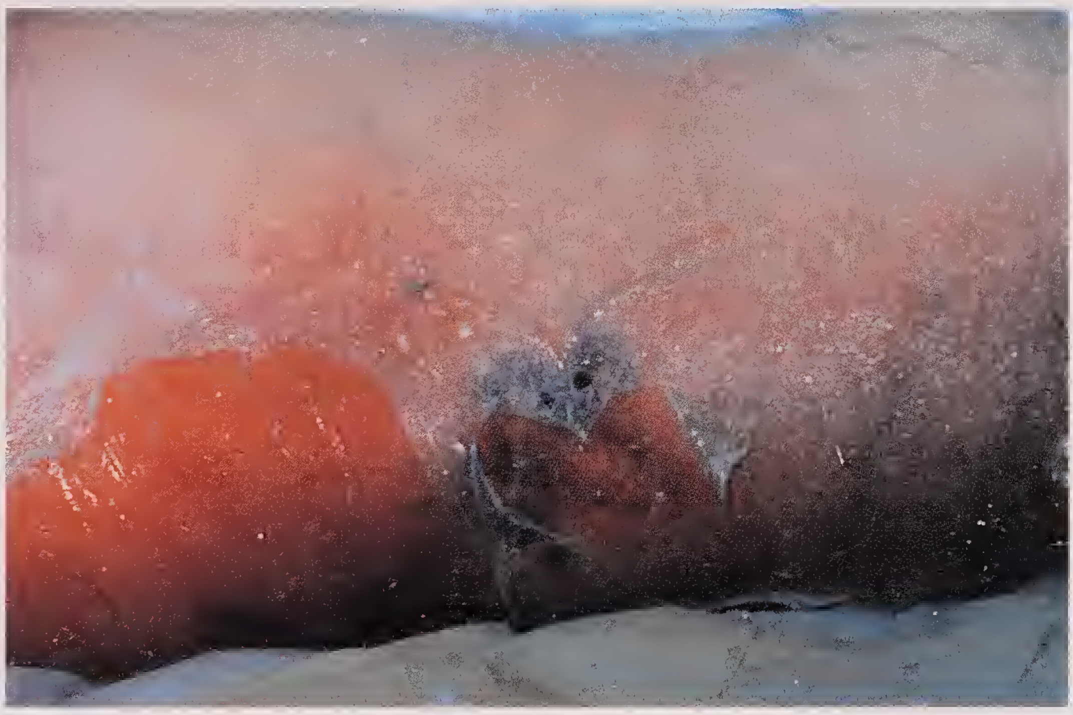

203

203 ♦ Patient in 202 twenty-four hours after admission.

Bone/Joint

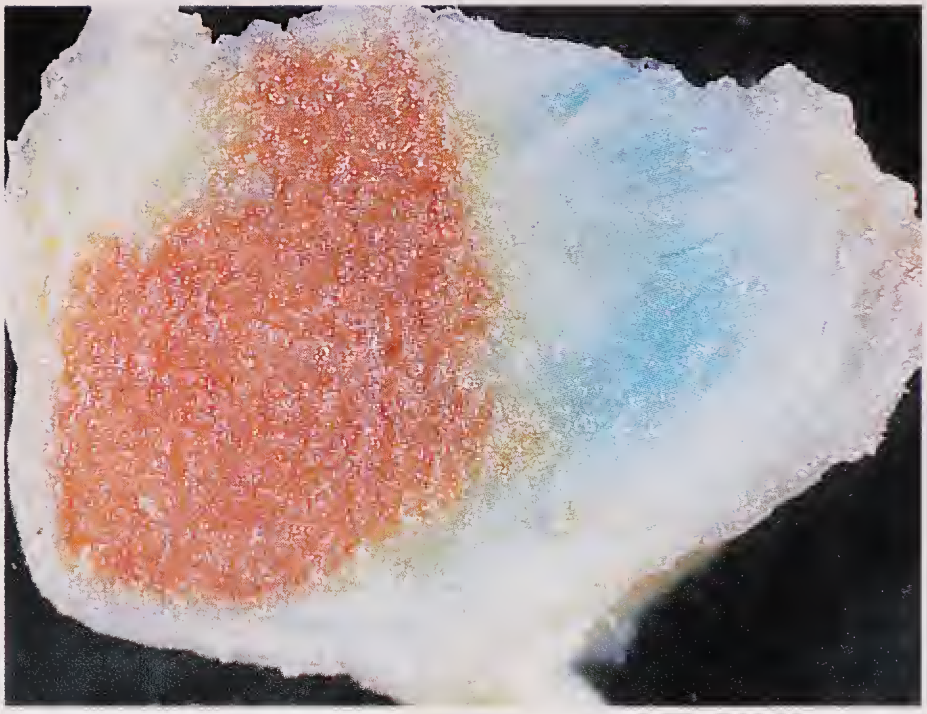

204

204 ♦ Sternoclavicular cartilage showing blue-green pigmentation due to *Pseudomonas* sepsis. Gangrenous skin lesions are also present (ecthyma gangrenosum).

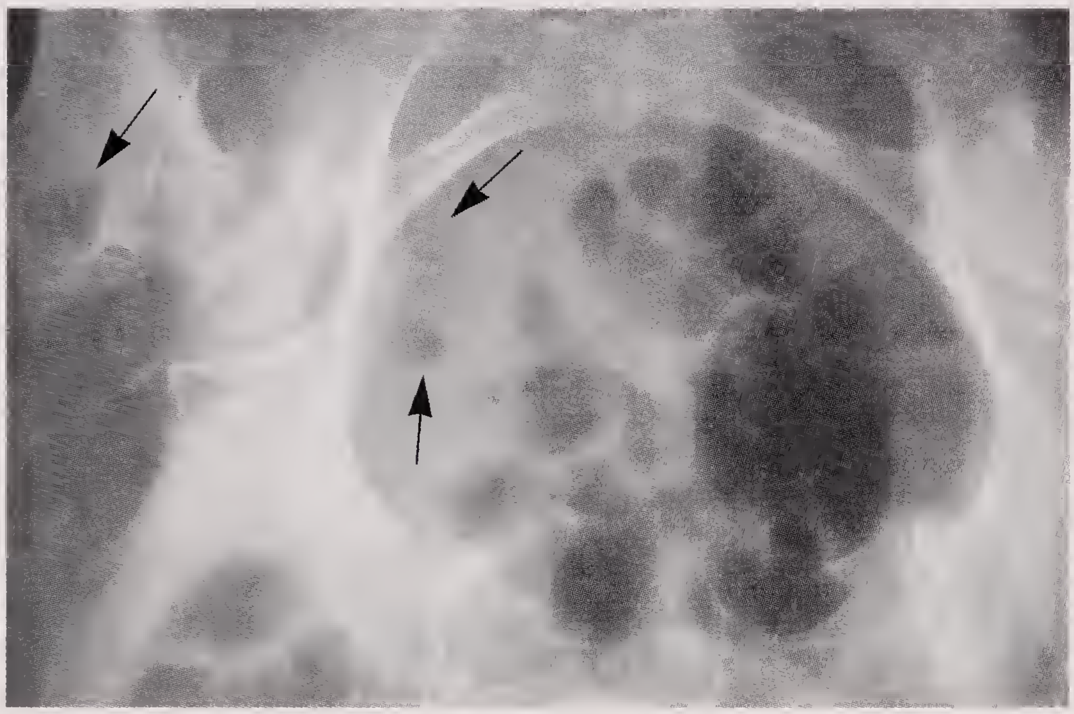

205

205 ♦ Radiograph with gas bubbles in and about left hip joint (arrows), which are beginning to invade the pelvic bone, due to severely infected left colon carcinoma.

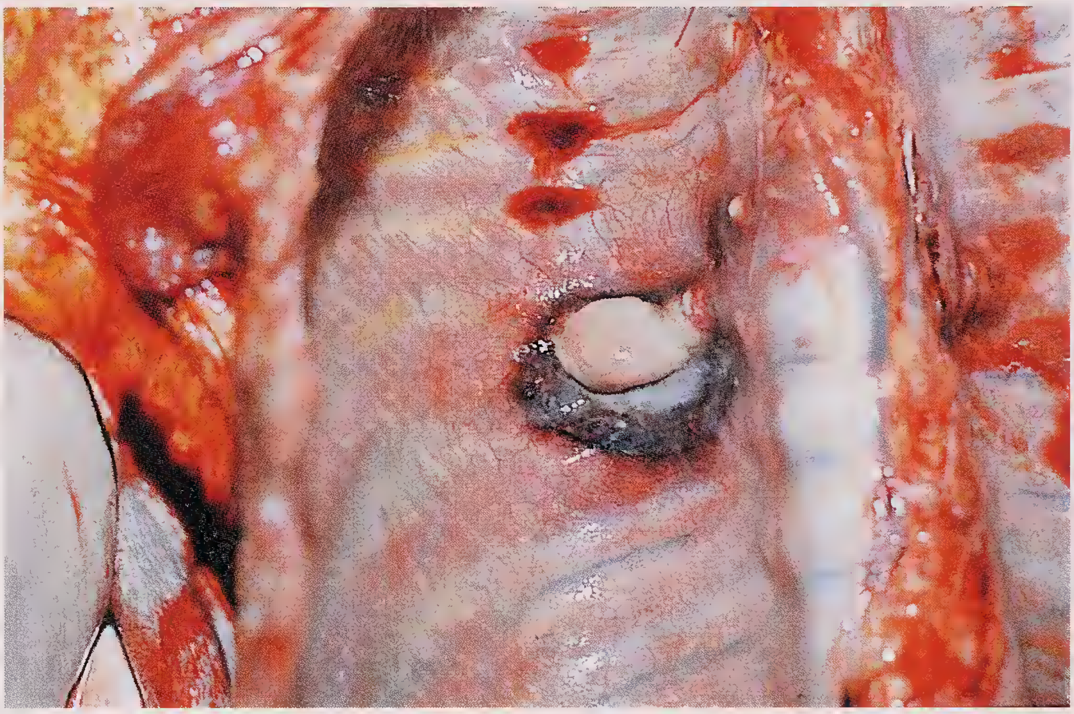

206

206 ♦ Metastatic abscess in thorax, beginning in a rib. *Pseudomonas* species are cultured.

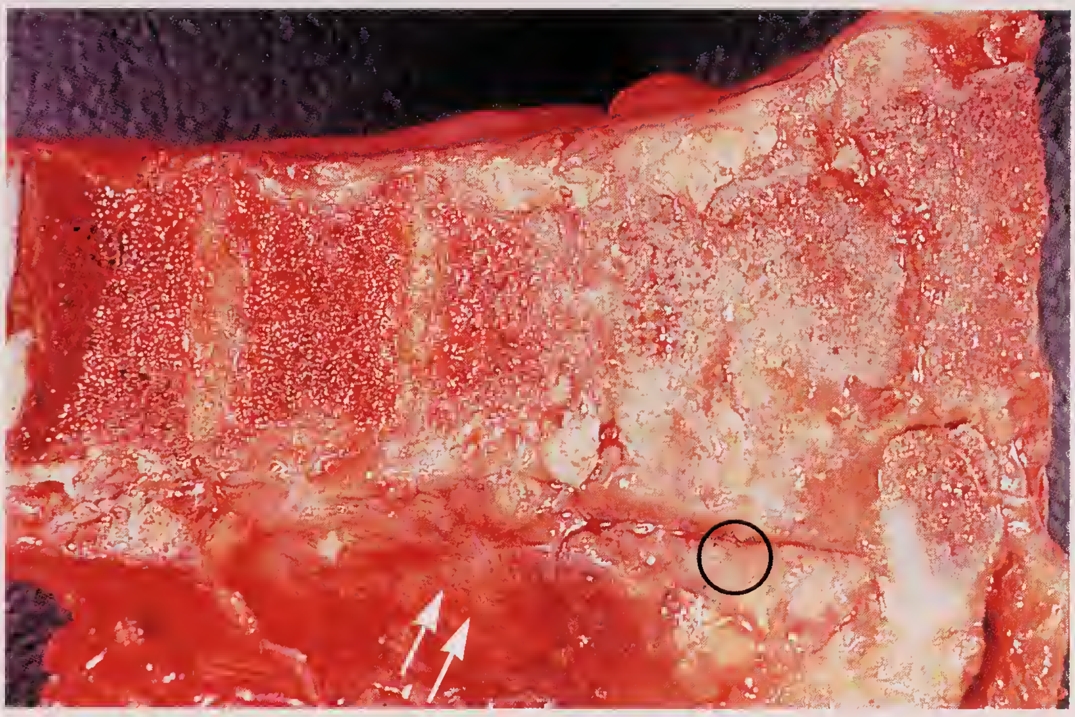

207

207 ♦ Tuberculosis: Lower spine showing complete disappearance of intervertebral disk, with replacement by creamy mass (circle) that extends beyond the periosteum into psoas muscle, forming a psoas abscess (double arrow). The abscess can travel downward and appear at the femoral triangle or even the knee.

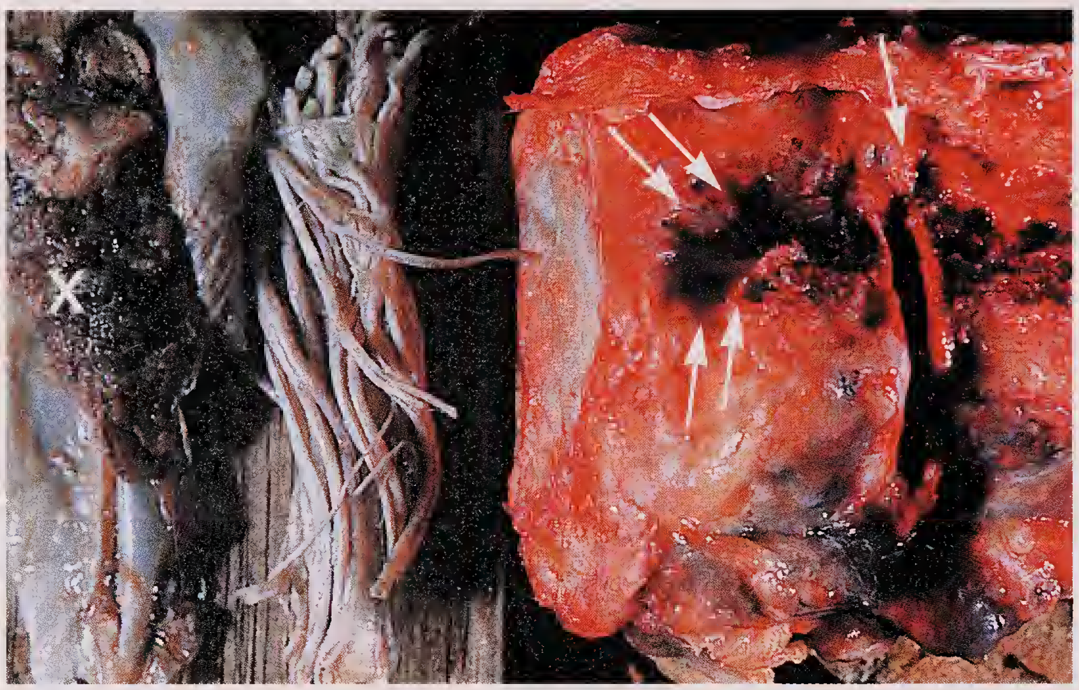

208

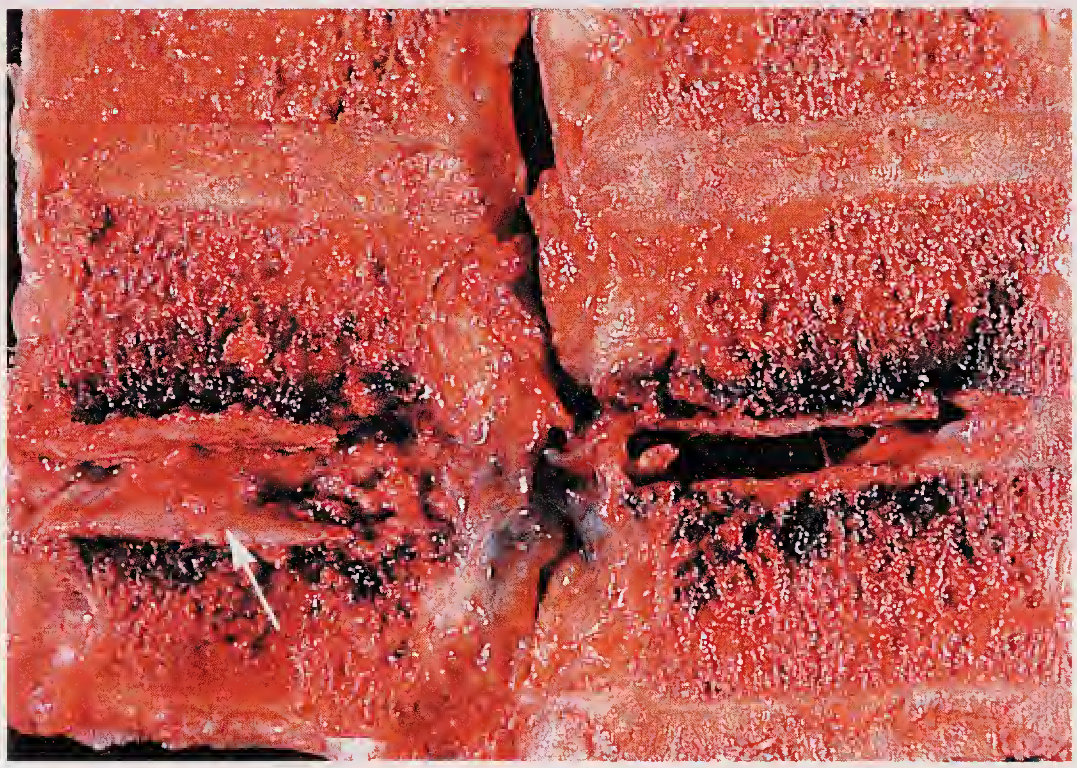

209

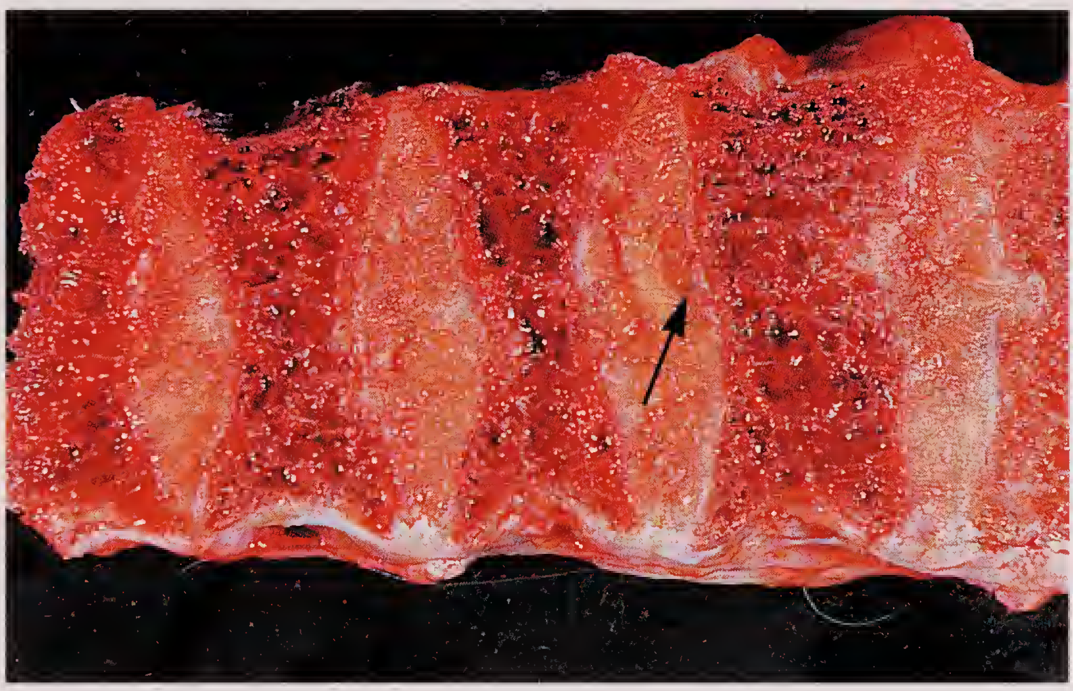

210

208 ♦ Spinal tuberculosis, with selective disk destruction (arrow). Early bone destruction is also evident (double arrow). The lower cord and cauda equina are present, with tuberculous inflammation of the meninges (cross).

209 ♦ Spinal tuberculosis with softening of cartilaginous disk by tuberculous abscess (arrow).

210 ♦ Early upper spinal tuberculosis (Pott's disease) in a patient with Huntington's chorea. The involved disk can be identified (arrow). Severe osteoporosis is also present.

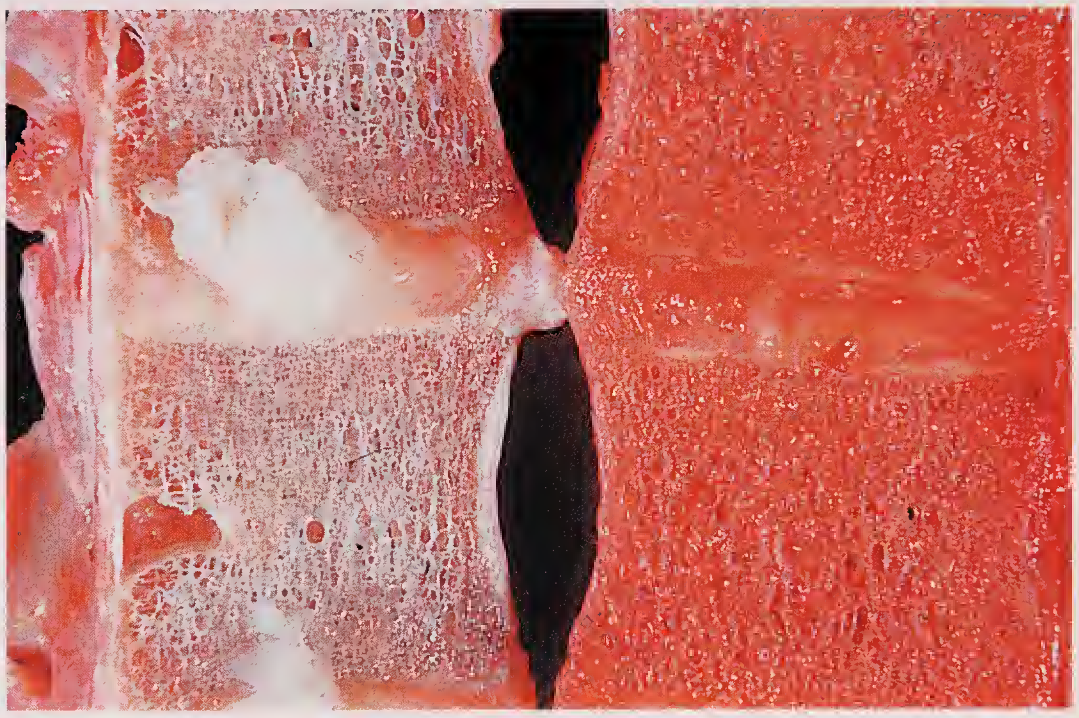

211

211 ♦ Seemingly normal lumbar vertebrae, which are known to be heavily seeded with early miliary tubercles.

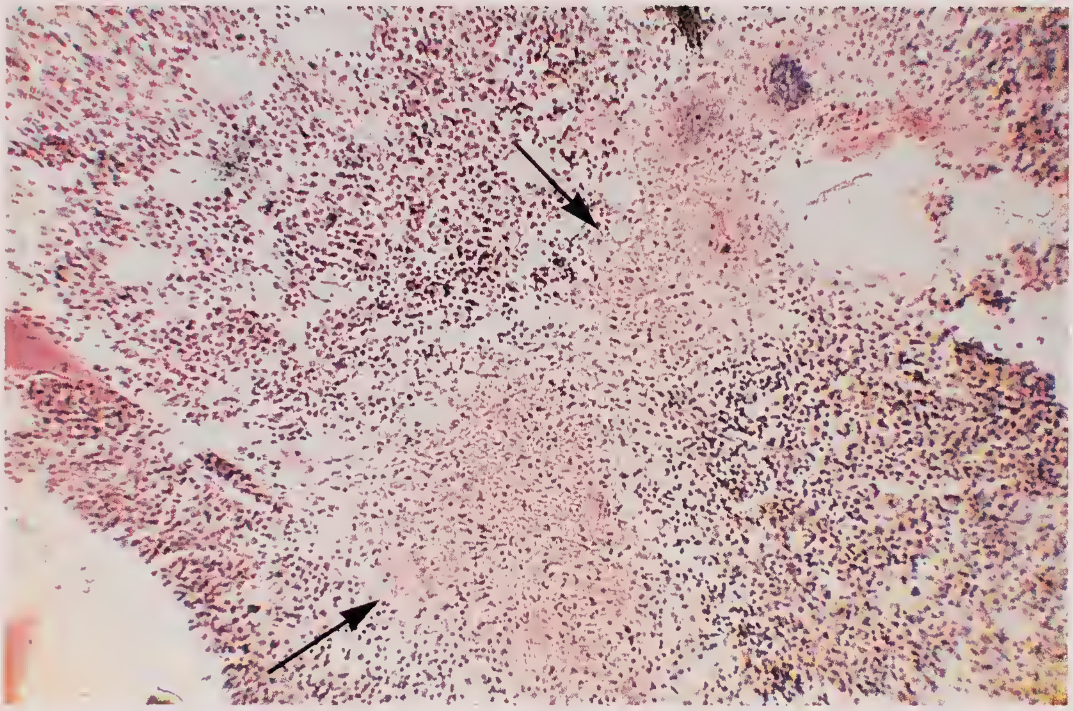

212

212 ♦ Low-power photomicrograph of vertebra with two miliary tubercles (arrows) in widespread miliary tuberculosis (see 211).

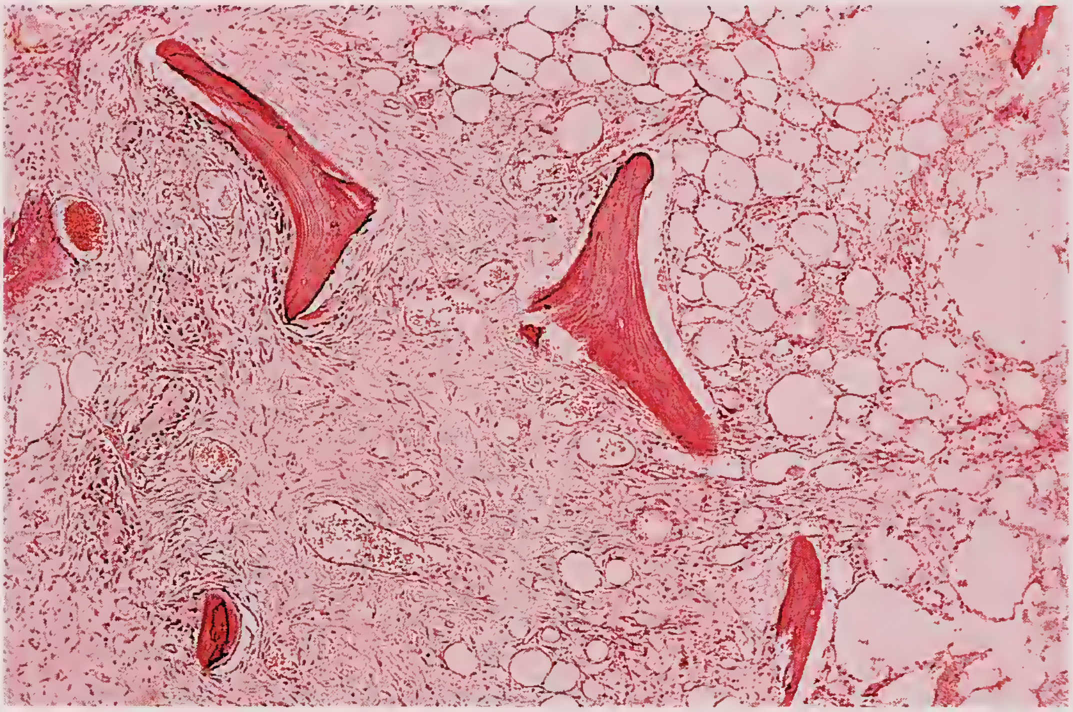

213

213 ◆ Photomicrograph of extensive, healed infarct of vertebra due to embolism from subacute bacterial endocarditis. The healed infarct encompasses the left half of the field, and a fibrous scar replaces the marrow.

214 ◆ Thoracic vertebrae with many small abscesses, caused by infected chordoma of the lumbosacral area.

215 ◆ Photomicrograph of vertebral marrow with venous thrombus that fills most of the photograph. This was due to advanced pyelonephritis.

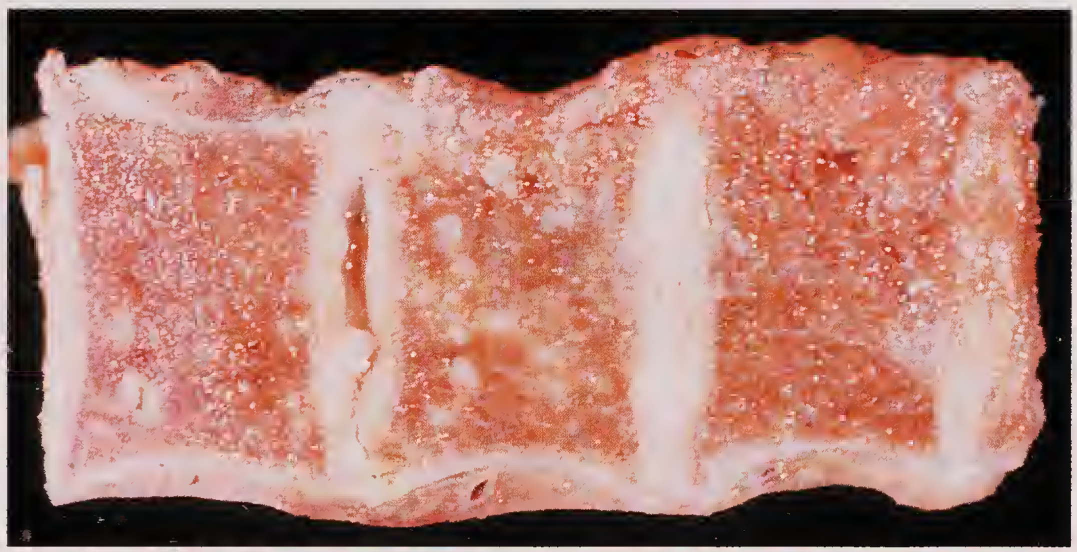

214

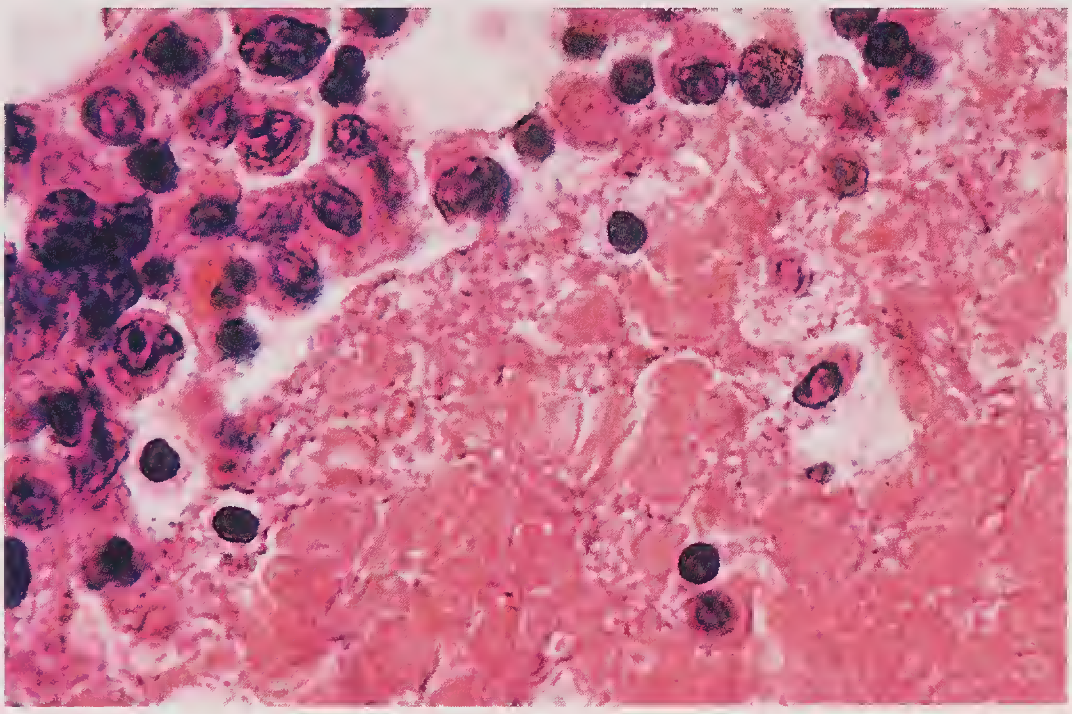

215

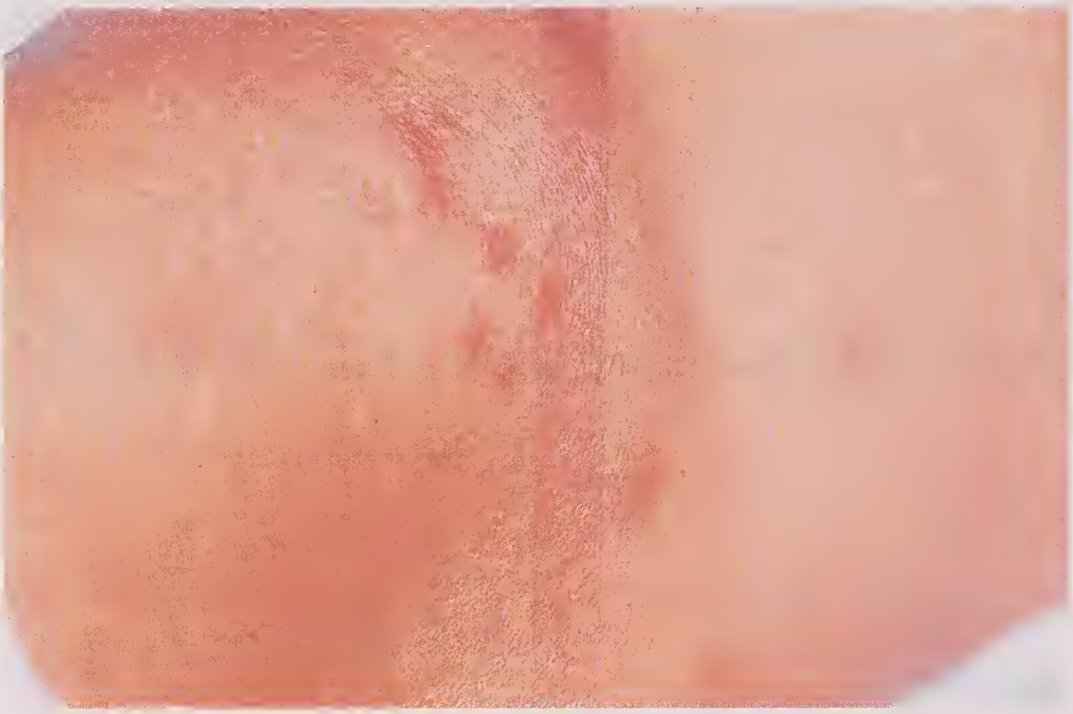

216

216 ◆ Synovitis with a definite joint effusion of the knee in a patient with disseminated gonococcal infection.

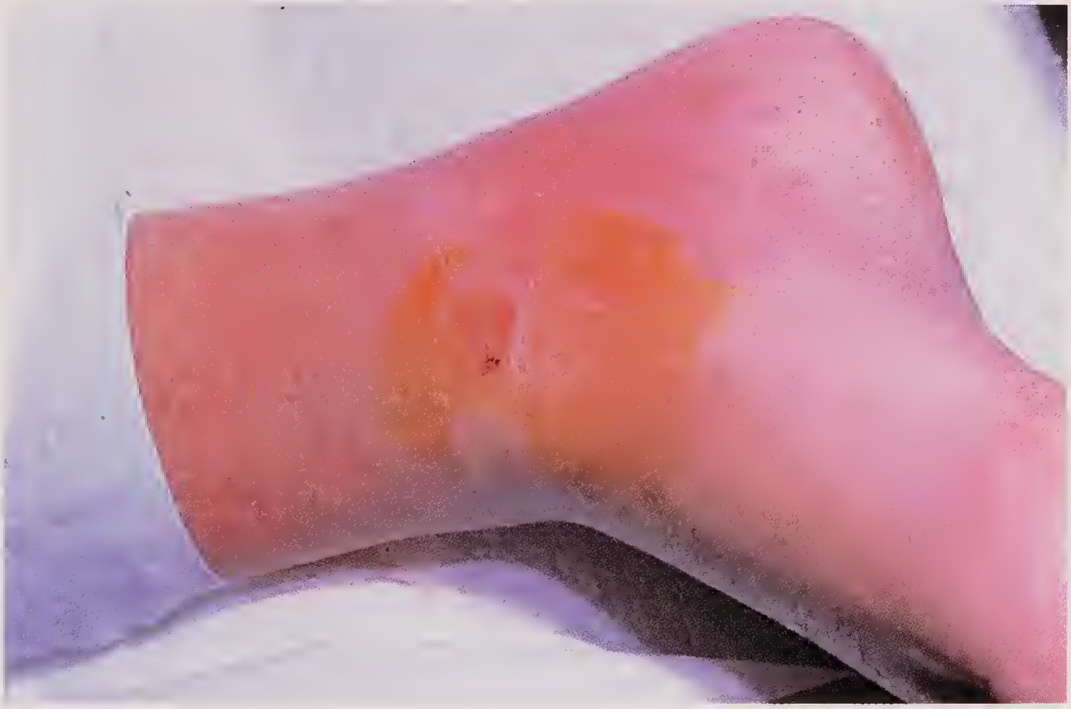

217

217 ♦ Swollen, red, warm, tender ankle, with range of motion markedly diminished. In adults, *Staphylococcus aureus* is responsible for 60% of cases, and streptococcus, which was isolated from this lesion, is the next most common cause.

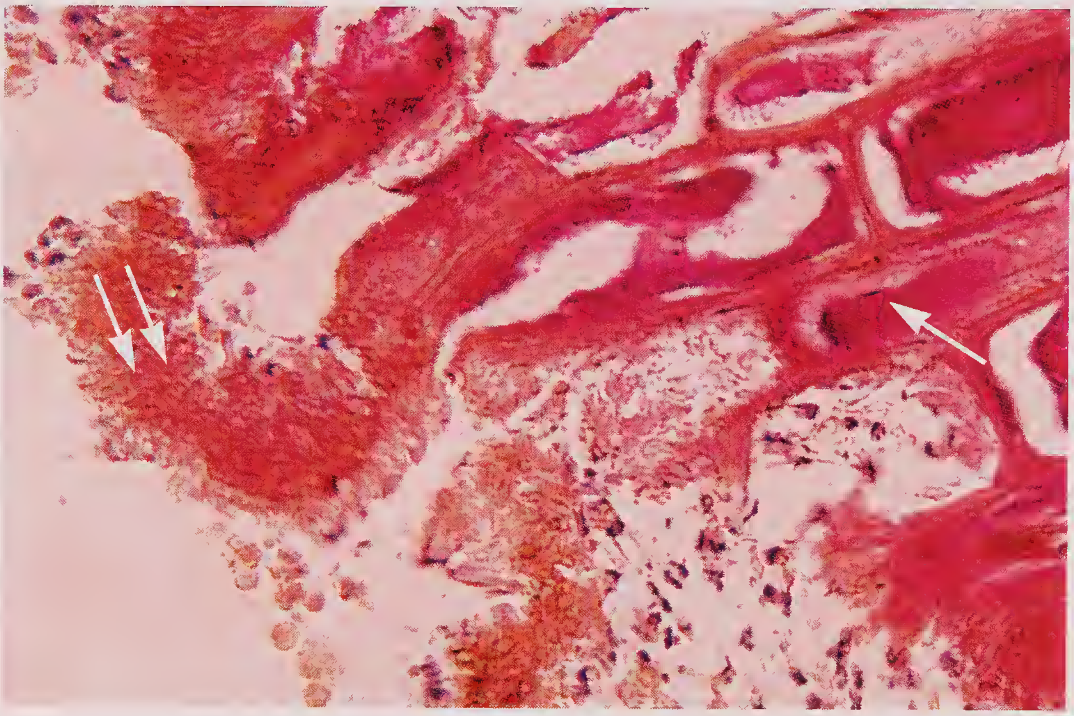

218

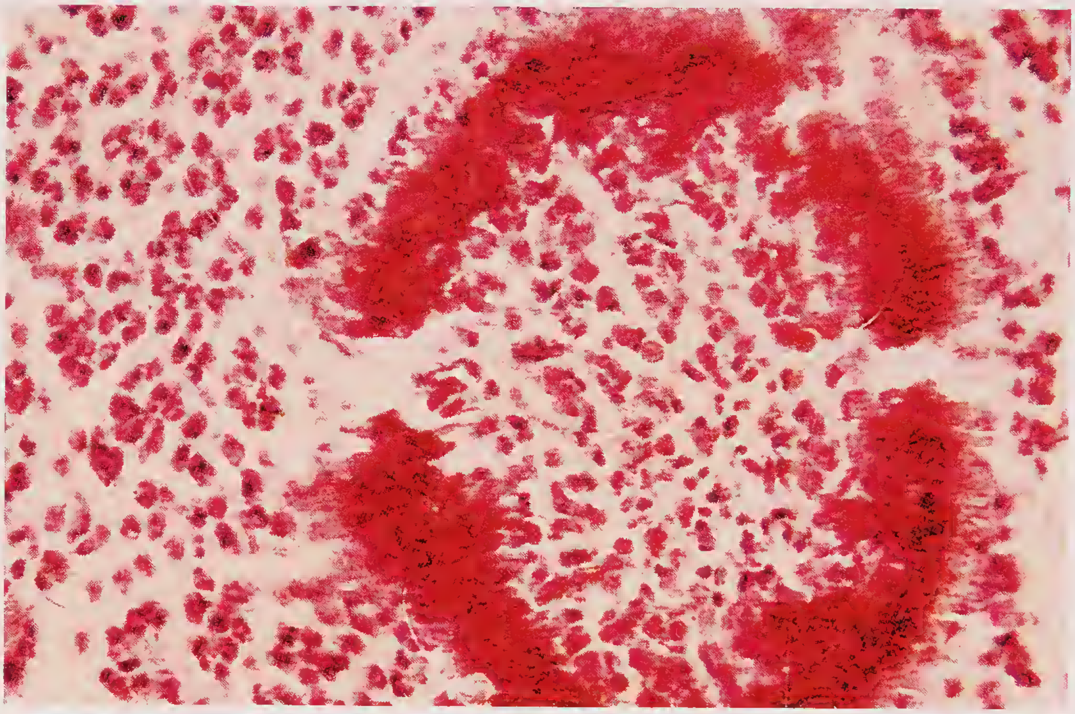

219

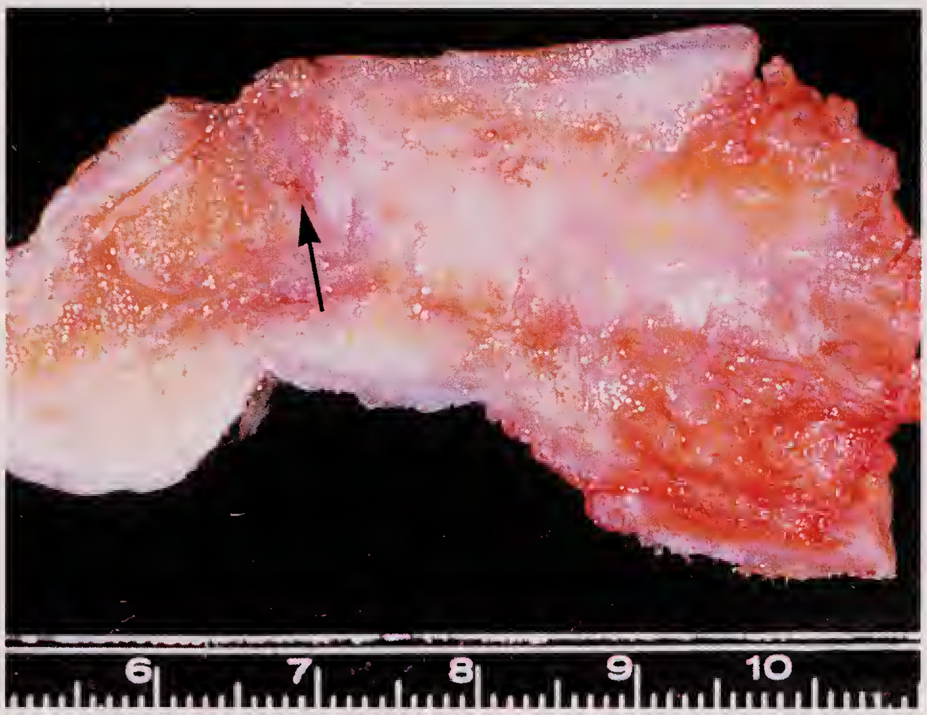

220

218-219 ♦ Maduromycosis osteomyelitis. 218 is a low-power view of a large woody fiber (thorn, marked by an arrow) from a nodule of the right leg, embedded in bone (from an accident many years before in India). A fungal colony (double arrow) is present at edge of thorn. Mycetoma, a progressive fungal infection, eventually destroys the afflicted limb.

219 is a higher power view of the fungus, showing radiating hyphae and specks of pigment surrounded by inflammatory cells.

220 ♦ Chronic osteomyelitis of the second toe, with marrow and joint destruction in diabetes mellitus. Note the joint destruction (arrow).

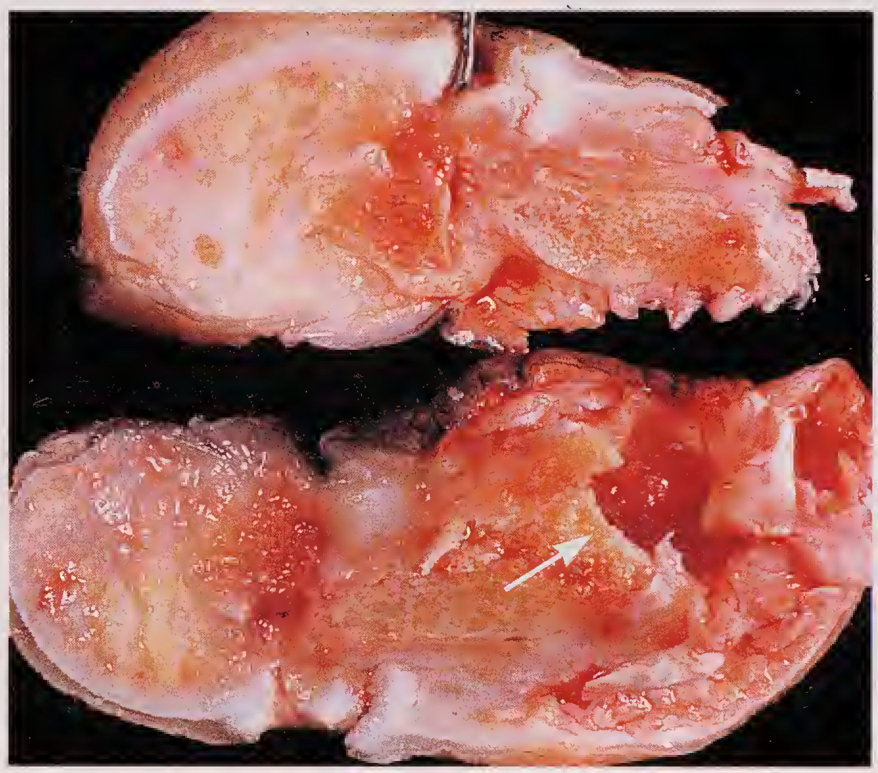

221

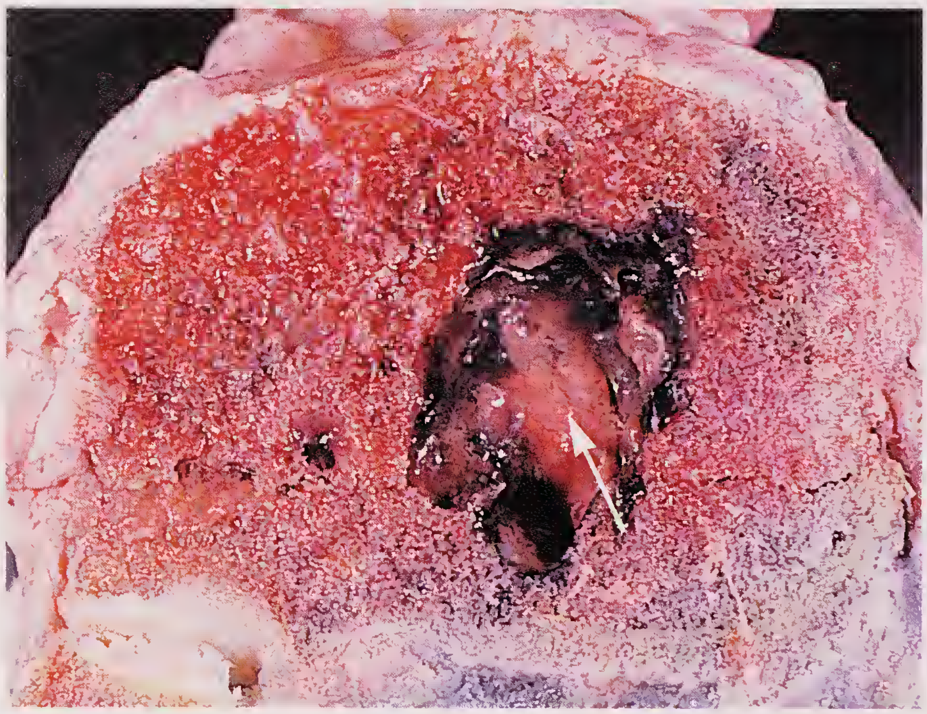

222

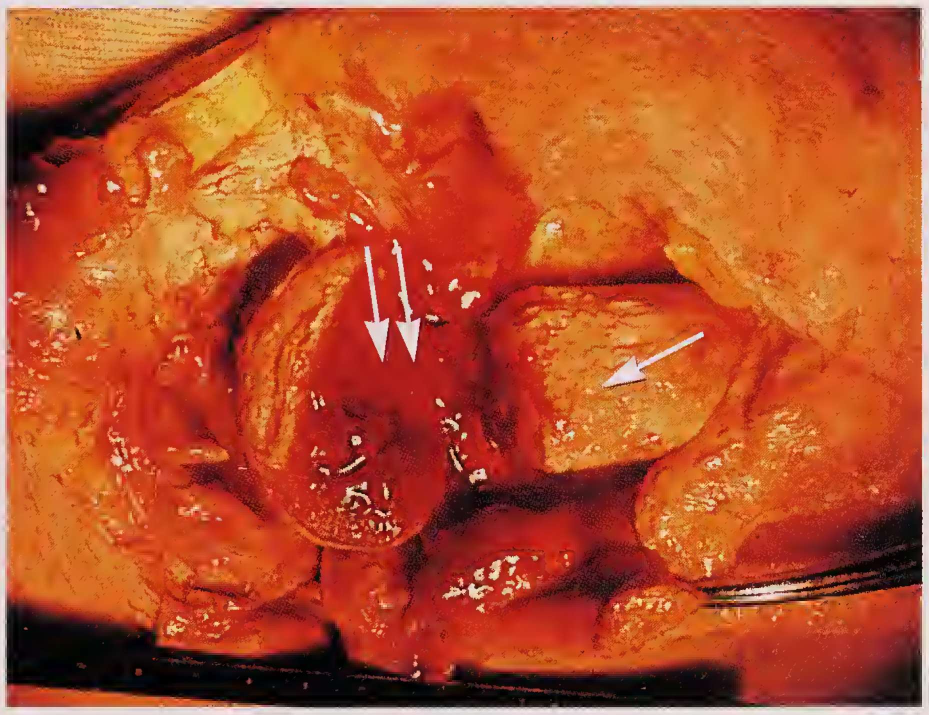

223

221 ♦ Widespread chronic osteomyelitis and abscess of toe in diabetes mellitus (arrow).

222 ♦ Cross section of upper tibia, with chronic osteomyelitis and central sequestrum (arrow) in diabetes mellitus.

223 ♦ Head of femur (arrow) at autopsy, with suppuration and liquefaction (double arrow) following fracture.

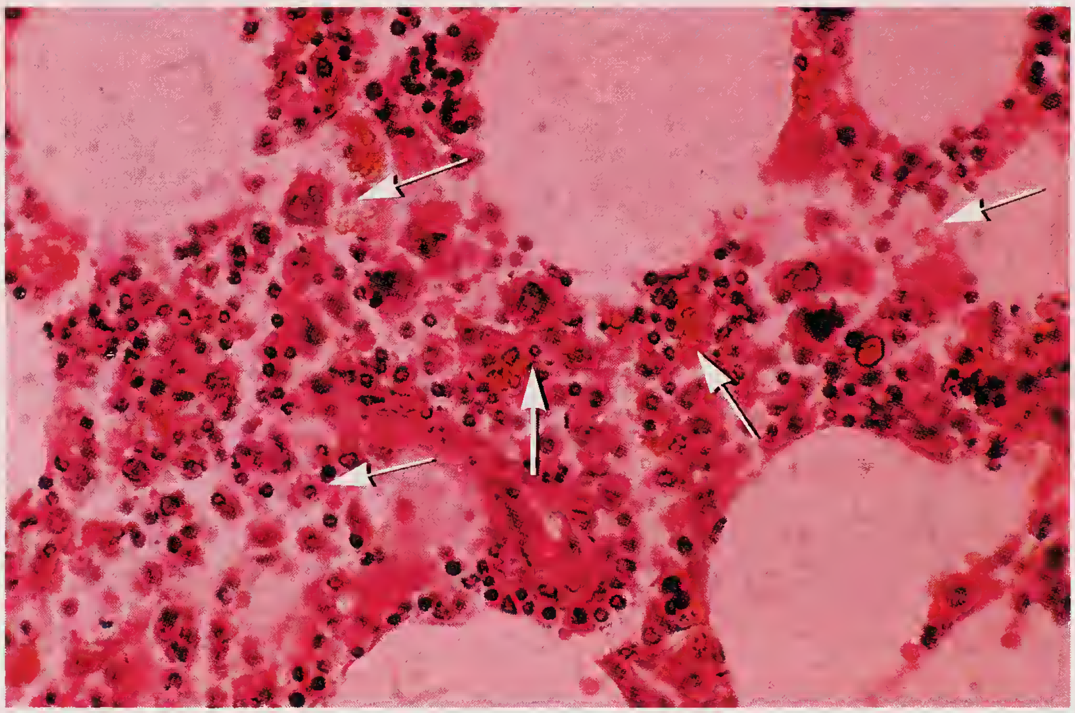

224

224 ♦ Marrow with cross sections of fungi in an individual with diabetes mellitus and sepsis. Both *Mucor* and *Aspergillus* were identified by culture (arrows).

EXPERIENCE THE POWER EXPERIENCE THE POWER EXPERIENCE THE POWER

EXPERIENCE THE POWER.

Power You Can Trust In Lower Respiratory Infections.

- Proven efficacy and safety.
- Well-tolerated, convenient q12h regimen.

In Vitro

- Excellent penetration into respiratory tissue.*
- Active against ß-lactamase-producing respiratory pathogens.†

Cipro® I.V. (ciprofloxacin) / Cipro® (ciprofloxacin HCl) Tablets

Cipro I.V. and Cipro Tablets are indicated for mild to moderate LRIs caused by *Escherichia coli, Klebsiella pneumoniae, Enterobacter cloacae, Proteus mirabilis, Pseudomonas aeruginosa, Haemophilus influenzae, Haemophilus parainfluenzae, Streptococcus pneumoniae.*

Cipro Tablets also are indicated for severe/complicated infections caused by the above-mentioned organisms.

NOTE: SERIOUS AND FATAL REACTIONS HAVE BEEN REPORTED IN PATIENTS RECEIVING CONCURRENT ADMINISTRATION OF CIPROFLOXACIN AND THEOPHYLLINE. If con-comitant use cann of theophylline sho dosage adjustment

Most frequently rep without regard to drug relationship:

Cipro I.V.: nausea; diarrhea; CNS disturbance; local iv site reactions; abnormalities of hepatic enzymes; eosinophilia; headache; restlessness; rash.

Cipro Tablets: nausea; diarrhea; vomiting; abdominal pain/discomfort; headache; rash; restlessness.

*Tissue/fluid penetration is regarded as essential to therapeutic efficacy, but penetration levels have not been correlated with specific therapeutic results.

7089

EXPERIENCE THE POWER EXPERIENCE THE POWER EXPERIENCE THE POWER EXPERIENCE THE POWER

EXPERIENCE THE POWER EXPERIENCE THE POWER EXPERIENCE THE POWER EXPERIENCE THE POWER

EXPERIENCE THE OWER

1570130418 22
07/11/2018 22:49-3